

Resilient Coastal Sites for Conservation in the Northeast and Mid-Atlantic US



The Nature Conservancy

Eastern Conservation Science

Mark G. Anderson and Analie Barnett



May 15, 2017

Please cite as: Anderson, M.G. and Barnett, A. 2017. Resilient Coastal Sites for Conservation in the Northeast and Mid-Atlantic US. The Nature Conservancy, Eastern Conservation Science.

View the interactive map, download the data, and read the report at:
<https://www.nature.org/resilientcoasts>

Funding: This research was funded by a grant from the US Fish and Wildlife Service's North Atlantic Landscape Conservation Cooperative.



Acknowledgements

Thanks to Melissa Clark, John Prince, and Arlene Olivero-Sheldon who developed the web page, interactive tools, story maps and graphics that accompany this report. Special thanks to Charles Ferree who developed early models of migration space that helped put this project on the right track. Most of all, thanks to our steering committee who attended regular calls, constructively argued the concepts, checked details of the data sets, and thoroughly reviewed the draft results. Their engagement and feedback ensured that the results of this project are as scientifically sound and spatially robust as possible.

Steering committee members included:

Agencies and Academic Institutions

NOAA: Nate Herold, Darlene Finch, Jamie Carter

EPA: Regina Lyons

USFW NALCC: Andrew Milliken, Bartholomew Wilson, Megan Tyrrell, Scott Schwenk

USFW: Aimee Weldon, Laura Mitchell, Susan Adamowicz, Tim Jones

UMASS: Brad Compton

Maine NHP: Justin Schlawin, Kirsten Puryear

Delaware NHP/DNR: Anthony Gonzon

Connecticut DEEP: David Kozak

Rhode Island DEM: Jay Osenkowski

Massachusetts CZM: Marc Carullo

Maryland DNR: Nicole Carlozo

The Nature Conservancy

Connecticut: Adam Whelchel

Regional: Lise Hanners, Marta Ribera, Sally McGee, Mary Conley, Jay Odell

Florida: Kristina Serbesoff-King, Laura Geselbracht

Georgia: Sara Gottlieb

Global Marine: Zach Ferdana

Maryland: Michelle Canick

Massachusetts: Alison Bowden, Christopher McGuire

Maine: Jeremy Bell, Geoffrey Smith

New Jersey: Bob Allen, Metthea Yepsen, Moses Katkowski, Patricia Doerr

New York: George Schuler, Marci Bortman, Becca Benner

North and South Carolina: Brian Boutin, Jodie LaPoint, Colette Degarady

Rhode Island: John Torgan, Kevin Ruddock

Virginia: Gwynn Crichton, Angela Watland, Chris Bruce

Table of Contents

INTRODUCTION	1
Objective.....	1
Abstract	1
Study Area	2
Approach	3
Steering Committee	3
BACKGROUND	4
DEFINING AND MAPPING COASTAL SITES	7
Tidal Complex	7
Tidal marsh:.....	7
Brackish marsh:	8
Tidal flat:.....	8
Sandy beach and dune:.....	8
Seagrass bed:.....	8
Mapping Tidal Complexes	8
Buffer Area.....	12
Mapping Buffer Area.....	12
Migration space	14
Mapping Migration Space	15
Migration Space Scenarios.....	19
COASTAL SHORELINE REGIONS	22
Maine Drowned River Valley (650 sites).....	22
Northeast River Dominated (1566 sites)	23
Southern New England Coastal Embayment (2110 sites).....	23
Mid-Atlantic Coastal Lagoon (1275 sites)	23
ESTIMATING SITE RESILIENCE	25
Tidal Complex and Migration Space	26
Physical Characteristics.....	28
Physical Characteristics of the Migration Space	29
Size of Migration Space (Weight = 5):	29

Tidal Height Classes Variety and Evenness (Weight = 3):	31
Shared Edge (Weight = 3):	33
Physical Characteristics of the Existing Tidal Complex	34
Shoreline Complexity (Weight = 2):	34
Size of Existing Tidal Complex (Weight = 2):	35
Current Condition	38
Current Condition Characteristics of the Existing Tidal Complex.....	38
Hardened Shoreline (Weight = 5):	38
Current Condition Characteristics of the Migration Space	39
Water Quality / Nitrogen Inputs (Weight = 5):.....	39
Freshwater Flow (Weight = 4, River-Dominated CSRs only):	43
Sediment Input (Weight = 3):	46
Integration of Physical and Condition Characteristics:	48
Buffer Area	49
Physical Options:	50
Size of the Buffer Area (Weight = 5):	50
Landform Diversity (Weight = 4):	51
Soil Diversity (Weight = 2):	53
Wetland Connectedness (Weight = 5):	54
Percent Natural Cover (Weight = 5):.....	57
Integration of Physical and Condition Characteristics	58
Integration	59
ADDITIONAL CHARATERISTICS TO INFORM MANAGEMENT STRATEGIES	62
Securement.....	62
Migration Space Development.....	62
Migration Space Future Development	63
RESULTS	64
Maine Drowned River Valleys CSR: Results.....	65
Physical and Condition Scores.....	70
Estimated Resilience Score	77
Trends in Migration Space Size.....	82
Migration Space Securement.....	87
Migration Space Development and Future Development	88

Northeast River-Dominated CSR: Results	90
Physical and Condition Scores	95
Estimated Resilience Score	102
Trends in Migration Space Size.....	107
Migration Space Securement.....	112
Migration Space Development and Future Development	113
Southern New England Coastal Embayment CSR: Results	115
Physical and Condition Scores	120
Estimated Resilience Score	127
Trends in Migration Space Size.....	132
Migration Space Securement.....	137
Migration Space Development and Future Development	138
Mid-Atlantic Coastal Lagoon CSR: Results	140
Physical and Condition Scores	145
Estimated Resilience Score	152
Trends in Migration Space Size.....	157
Migration Space Securement.....	162
Migration Space Development and Future Development	163
Chesapeake Bay and Piedmont River-Dominated CSR: Results	165
Physical and Condition Scores	170
Estimated Resilience Score	177
Trends in Migration Space Size.....	182
Migration Space Securement.....	187
Migration Space Development and Future Development	188
Full Region: Results	190
Full Region.....	191
Tidal Complex Units	191
Migration Space Units	195
Buffer Area Units	197
Physical and Condition Scores	198
Estimated Resilience Score	207
Trends in Migration Space Size.....	213
Migration Space Securement.....	219

Migration Space Development and Future Development	220
DISCUSSION	222
References	228
APPENDIX I SCORING METHODS	236
APPENDIX II DETAILED DATA SOURCES AND METHODS	238

Figures

Figure 3.1. Tidal complexes.....	10
Figure 3.2. Unconsolidated shore complexes.....	11
Figure 3.3. Buffer area.	13
Figure 3.4. Migration space.	14
Figure 3.5. Migration space model comparisons.....	18
Figure 3.6. Migration space scenarios.....	20
Figure 3.7. Migration space scenario illustration	21
Figure 4.1. Coastal Shoreline Regions.....	24
Figure 5.1. Tidal complex and migration space characteristics that increase resilience.	28
Figure 5.2. Tidal complex and migration space association.	30
Figure 5.3. Tidal classes and habitats.....	31
Figure 5.4. Tidal class diversity and evenness.....	32
Figure 5.5. Shared edge between migration space and tidal complex.....	33
Figure 5.6. Tidal complex shoreline complexity.	35
Figure 5.7. 2080 Dynamic response model (Lentz et al. 2016).....	37
Figure 5.8. Tidal complex hardened shoreline.....	39
Figure 5.9. Water quality model results for the project area.....	41
Figure 5.10. Drainage-area weighted average approach.....	42
Figure 5.11. Mean annual flow and cumulative drainage area.	44
Figure 5.12. Estimated flow alteration for the project area.	45
Figure 5.13. Estimated sediment inputs for the project area.....	47
Figure 5.14. Buffer area characteristics that increase resilience	50
Figure 5.15. Landform variety in first 1-km of buffer area.....	52
Figure 5.16. Soil variety in first 1-km of buffer area.....	53
Figure 5.17. Local connectedness components.....	56
Figure 5.18. Natural land cover in the first 1-km of the buffer area.....	58
Figure 5.19. Calculating estimated resilience.....	60
Figure 5.20. Approach to calculate physical and condition attribute values for the tidal complex unit.	61
Figure 7.1. Distribution of tidal complex size (acres) by ten size classes in the Maine Drowned River Valleys CSR.	66
Figure 7.2. Tidal complex, migration space, and buffer area units in the Maine Drowned River Valleys CSR.....	67
Figure 7.3. Migration space class distribution by tidal complex size class for the 6-foot sea level rise scenario.	68
Figure 7.4. Buffer area class distribution by tidal complex size class for the 6-foot sea level rise scenario.....	69
Figure 7.5. Estimated physical score for the Maine Drowned River Valleys CSR.	71
Figure 7.6. Estimated condition score for the Maine Drowned River Valleys CSR	72

Figure 7.7. Relationship between the tidal complex units' physical and condition z-scores for the 6-foot sea level rise scenario, after removing complexes with no migration space.	73
Figure 7.8. Distribution of the physical scores for each condition class at a sea level rise of 6 feet.	74
Figure 7.9. Tidal complex (n=1) with high physical score but in poor condition	76
Figure 7.10. Estimated resilience score.	78
Figure 7.11. Relationship between condition and physical components for each estimated resilience class at a sea level rise of 6 feet.	79
Figure 7.12. The top ten highest scoring tidal complexes in the Maine CSR.	80
Figure 7.13. Vulnerable tidal complexes	81
Figure 7.14. Estimated resilience score with migration space trend.	84
Figure 7.15. Estimated resilience class changes after incorporating migration space trend.....	86
Figure 7.16. Amount (%) of migration space in permanent protection by estimated resilience class	87
Figure 7.17. Amount (%) of migration space comprised of developed land, by estimated resilience class.	88
Figure 7.18. Distribution of tidal complex size (acres) by ten size classes in the Northeast River-Dominated CSR.	91
Figure 7.19. Tidal complex, migration space, and buffer area units in the Northeast River-Dominated CSR.	92
Figure 7.20. Migration space class distribution by tidal complex size class for the 6-foot sea level rise scenario.	93
Figure 7.21. Buffer area class distribution by tidal complex size class for the 6-foot sea level rise scenario.....	94
Figure 7.22. Estimated physical score for the Northeast River-Dominated CSR.....	96
Figure 7.23. Estimated condition score for the Northeast River-Dominated CSR.....	97
Figure 7.24. Relationship between the tidal complex units' physical and condition z-scores for the 6-foot sea level rise scenario, after removing units with no migration space.....	98
Figure 7.25. Distribution of the physical scores for each condition class at a sea level rise of 6 feet.	99
Figure 7.26. Tidal complexes (n=7) with high physical scores but in poor condition..	101
Figure 7.27. Estimated resilience score.	103
Figure 7.28. Relationship between condition and physical components for each estimated resilience class at a sea level rise of 6 feet.	104
Figure 7.29. The top ten highest scoring tidal complexes in the Northeast River-Dominated CSR.	105
Figure 7.30. Vulnerable tidal complexes.	106
Figure 7.31. Estimated resilience score with migration space trend.	109
Figure 7.32. Estimated resilience class changes after incorporating migration space trend.....	111
Figure 7.33. Amount (%) of migration space in permanent protection by estimated resilience class.	112

Figure 7.34. Amount (%) of migration space comprised of developed land, by estimated resilience class.	114
Figure 7.35. Distribution of tidal complex size (acres) by ten size classes in the Southern New England Coastal Embayment CSR.	116
Figure 7.36. Tidal complex, migration space, and buffer area units in the Southern New England Coastal Embayment CSR.....	117
Figure 7.37. Migration space class distribution by tidal complex size class for the 6-foot sea level rise scenario.	118
Figure 7.38. Buffer area class distribution by tidal complex size class for the 6-foot sea level rise scenario.....	119
Figure 7.39. Estimated physical score for the Southern New England Coastal Embayment CSR.....	121
Figure 7.40. Estimated condition score for the Southern New England Coastal Embayment CSR.....	122
Figure 7.41. Relationship between the tidal complex units' physical and condition z-scores for the 6-foot sea level rise scenario, after removing complexes with no migration space.	123
Figure 7.42. Distribution of the physical scores for each condition class at a sea level rise of 6 feet.	124
Figure 7.43. Tidal complexes (n=2) with high physical scores but in poor condition..	126
Figure 7.44. Estimated resilience score.....	128
Figure 7.45. Relationship between condition and physical components for each estimated resilience class at a sea level rise of 6 feet.	129
Figure 7.46. The top ten highest scoring tidal complexes in the Southern New England Coastal Embayment CSR.	130
Figure 7.47. Vulnerable tidal complexes.	131
Figure 7.48. Estimated resilience score with migration space trend.	134
Figure 7.49. Estimated resilience class changes after incorporating migration space trend.....	136
Figure 7.50. Amount (%) of migration space in permanent protection by estimated resilience class.	137
Figure 7.51. Amount (%) of migration space comprised of developed land, by estimated resilience class.	139
Figure 7.52. Distribution of tidal complex size (acres) by ten size classes in the Mid-Atlantic Coastal Lagoon CSR.	141
Figure 7.53. Tidal complex, migration space, and buffer area units in the Mid-Atlantic Coastal Lagoon CSR.....	142
Figure 7.54. Migration space class distribution by tidal complex size class for the 6-foot sea level rise scenario.	143
Figure 7.55. Buffer area class distribution by tidal complex size class for the 6-foot sea level rise scenario.....	144
Figure 7.56. Estimated physical score for the Mid-Atlantic Coastal Lagoon CSR	146
Figure 7.57. Estimated condition score for the Mid-Atlantic Coastal Lagoon CSR.	147

Figure 7.58. Relationship between the tidal complex units' physical and condition z-scores for the 6-foot sea level rise scenario, after removing unit with no migration space.....	148
Figure 7.59. Distribution of the physical scores for each condition class at a sea level rise of 6 feet.	149
Figure 7.60. Tidal complex with high physical score but in poor condition.	151
Figure 7.61. Estimated resilience score	153
Figure 7.62. Relationship between condition and physical components for each estimated resilience class at a sea level rise of 6 feet.	154
Figure 7.63. The top ten highest scoring tidal complexes in the Mid-Atlantic Coastal Lagoon CSR.	155
Figure 7.64. Vulnerable tidal complexes.	156
Figure 7.65. Estimated resilience score with migration space trend.	159
Figure 7.66. Estimated resilience class changes after incorporating migration space trend.....	161
Figure 7.67. Amount (%) of migration space in permanent protection by estimated resilience class. The	162
Figure 7.68. Amount (%) of migration space comprised of developed land, by estimated resilience class.	163
Figure 7.69. Distribution of tidal complex size (acres) by ten size classes in the Chesapeake Bay and Piedmont River-Dominated CSR.	166
Figure 7.70. Tidal complex, migration space, and buffer area units in the Chesapeake Bay and Piedmont River-Dominated CSR.	167
Figure 7.71. Migration space class distribution by tidal complex size class for the 6-foot sea level rise scenario.	168
Figure 7.72. Buffer area class distribution by tidal complex size class for the 6-foot sea level rise scenario.....	169
Figure 7.73. Estimated physical score for the Chesapeake Bay and Piedmont River-Dominated CSR.	171
Figure 7.74. Estimated condition score for the Chesapeake Bay and Piedmont River-Dominated CSR.	172
Figure 7.75. Relationship between the tidal complex units' physical and condition z-scores for the six- foot sea level rise scenario, after removing units with no migration space.....	173
Figure 7.76. Distribution of the physical scores for each condition class at a sea level rise of 6 feet.	174
Figure 7.77. Tidal complexes (n=18) with high physical scores but in poor condition.....	176
Figure 7.78. Estimated resilience score.	178
Figure 7.79. Relationship between condition and physical components for each estimated resilience class at a sea level rise of 6 feet.	179
Figure 7.80. The top ten highest scoring tidal complexes in the Chesapeake Bay and Piedmont River-Dominated CSR.....	180
Figure 7.81. Vulnerable tidal complexes.	181
Figure 7.82. Estimated resilience score with migration space trend.	184

Figure 7.83. Estimated resilience class changes after incorporating migration space trend.....	186
Figure 7.84. Amount (%) of migration space in permanent protection by estimated resilience class.	187
Figure 7.85. Amount (%) of migration space comprised of developed land, by estimated resilience class.	188
Figure 7.86. Frequency of tidal complex size class by CSR.	192
Figure 7.87. Physical settings and land use characteristics of the full region.....	193
Figure 7.88. Tidal complex, migration space, and buffer area units.	194
Figure 7.89. Frequency of migration space size class by CSR.	195
Figure 7.90. Percent of tidal complex units with migration space by CSR.	196
Figure 7.91. Frequency of buffer area size class by CSR.	197
Figure 7.92. Estimated physical score, not stratified by shoreline region.	200
Figure 7.93. Top ten highest scoring sites for physical characteristics, not stratified by shoreline region.	201
Figure 7.94. Estimated physical score, stratified by shoreline type.....	202
Figure 7.95. Estimated condition score, not stratified by shoreline region.....	203
Figure 7.96. Top eleven highest scoring sites for condition characteristics, not stratified by shoreline region.....	204
Figure 7.97. Estimated condition score, stratified by shoreline region.....	205
Figure 7.98. Estimated resilience score, not stratified by shoreline region.	209
Figure 7.99. The top ten highest scoring tidal complexes in the full region, not stratified by shoreline region.....	210
Figure 7.100. Estimated resilience score, stratified by shoreline region.	212
Figure 7.101. Mean migration space size by sea level rise scenario for each shoreline region.	214
Figure 7.102. Migration space size trend by shoreline region	215
Figure 7.103. Estimated resilience score with migration space trend.	217
Figure 7.104. Estimated resilience class changes after incorporating migration space trend.....	218
Figure 7.105. Amount (%) of migration space in permanent protection for each CSR by estimated resilience class.	219
Figure 7.106. Amount (%) of migration space comprised of developed land for each CSR by estimated resilience class.	221
Figure 8.1. Priority migration corridors for the Blackwater National Wildlife Refuge. .	223

Tables

Table 3.1. Migration space data.	17
Box 5.1. Physical and condition attributes used to estimate resilience of coastal sites	26
Table 5.1 IPCC probability classes (Mastrandrea et al. 2010) used to classify the 2080 Dynamic Response model probabilities (Lentz et al. 2016).	36
Table 5.2. Water quality model classes	40
Table 5.3. Resistance weights used in the local connectedness model.....	55
Table 7.1. Frequency of physical and condition scores in the Maine Drowned River Valleys CSR for the 6-foot sea level rise scenario.	73
Table 7.2. The number of tidal complex units in each physical and condition score category.	75
Table 7.3. Distribution of estimated resilience scores in the Maine Drowned River Valleys CSR for the 6-foot sea level rise scenario.	79
Table 7.4. Relationship between resilience components and analysis unit size.....	82
Table 7.5. Summary statistics for migration space size by sea level rise scenario.....	83
Table 7.6 Summary of regression coefficients	83
Table 7.7. The change in resilience class after incorporating the trend in migration space size.....	85
Table 7.8. Amount (%) of migration space estimated to be developed in 2100, by estimated resilience class.	89
Table 7.9. Frequency of physical and condition scores in the Northeast River- Dominated CSR for the 6-foot sea level rise scenario.	98
Table 7.10. The number of tidal complex units in each physical and condition score category.	100
Table 7.11. Distribution of estimated resilience scores in the Northeast River- Dominated CSR for the 6-foot sea level rise scenario.	104
Table 7.12. Relationship between resilience components and analysis unit size.....	107
Table 7.13. Summary statistics for migration space size by sea level rise scenario....	108
Table 7.14. Summary of regression coefficients	108
Table 7.15. The change in resilience class after incorporating the trend in migration space size.....	110
Table 7.16. Amount (%) of migration space estimated to be developed in 2100, by estimated resilience class.	114
Table 7.17. Frequency of physical and condition scores in the Southern New England Coastal Embayment CSR for the 6-foot sea level rise scenario.	123
Table 7.18. The number of tidal complex units in each physical and condition score category.	125
Table 7.19. Distribution of estimated resilience scores in the Southern New England Coastal Embayment CSR for the 6-foot sea level rise scenario.	129
Table 7.20. Relationship between resilience components and analysis unit size.....	132
Table 7.21. Summary statistics for migration space size by sea level rise scenario....	133

Table 7.22 Summary of regression coefficients	133
Table 7.23. The change in resilience class after incorporating the trend in migration space size.....	135
Table 7.24. Amount (%) of migration space estimated to be developed in 2100, by estimated resilience class.	139
Table 7.25. Frequency of physical and condition scores in the Mid-Atlantic Coastal Lagoon CSR for the 6-foot sea level rise scenario.....	148
Table 7.26. The number of tidal complex units in each physical and condition score category.	150
Table 7.27. Distribution of estimated resilience scores in the Mid-Atlantic Coastal Lagoon CSR for the 6-foot sea level rise scenario.....	154
Table 7.28. Relationship between resilience components and analysis unit size.....	157
Table 7.29. Summary statistics for migration space size by sea level rise scenario....	158
Table 7.30. Summary of regression coefficients	158
Table 7.31. The change in resilience class after incorporating the trend in migration space size.....	160
Table 7.32. Amount (%) of migration space estimated to be developed in 2100, by estimated resilience class.	164
Table 7.33. Frequency of physical and condition scores in the Chesapeake Bay and Piedmont River-Dominated CSR for the 6-foot sea level rise scenario.....	173
Table 7.34. The number of tidal complex units in each physical and condition score category.	175
Table 7.35. Distribution of estimated resilience scores in the Chesapeake Bay and Piedmont River-Dominated CSR for the 6-foot sea level rise scenario.....	179
Table 7.36. Relationship between resilience components and analysis unit size.....	182
Table 7.37. Summary statistics for migration space size by sea level rise scenario....	183
Table 7.38. Summary of regression coefficients	183
Table 7.39. The change in resilience class after incorporating the trend in migration space size.....	185
Table 7.40. Amount (%) of migration space estimated to be developed in 2100, by estimated resilience class.	189
Table 7.41. Summary statistics for tidal complex size by CSR.	192
Table 7.42. Summary statistics for migration space size by CSR.	196
Table 7.43. Summary statistics for buffer area size by CSR.....	198
Table 7.44. Frequency of stratified physical scores for the 6-foot sea level rise scenario.	206
Table 7.45. Frequency of stratified condition scores for the 6-foot sea level rise scenario.....	206
Table 7.46. The number of tidal complex units in each physical and condition score category, stratified.....	207
Table 7.47. Frequency of stratified resilience scores for the 6-foot sea level rise scenario.....	211
Table 7.48. Relationship between resilience components and analysis unit size.....	211
Table 7.49. Significant migration space trend by CSR.	215

Table 7.50. The change in resilience class after incorporating the trend in migration space size.....	216
Table 7.51. Frequency of stratified resilience scores with migration trend for the six-foot sea level rise scenario.....	216
Table 8.1. Physical and condition scores for the Blackwater River tidal complex	223
Table AI-1. Z-score classes with corresponding abbreviations and colors used in the report and accompanying spatial data.....	237

INTRODUCTION

Objective

We assessed the coastal region of nine Northeast states, estimated the relative resilience or vulnerability of over 10,000 coastal sites, and identified the ones most likely to support biological diversity and ecological functions under multiple scenarios of sea level rise. The results are summarized in this report and available via the accompanying data, web site, and map service.

Abstract

Coastal wetlands are critical to the productivity and diversity of marine ecosystems and to the human economies they support. The Northeast and Mid-Atlantic regions of the US include thousands of coastal wetlands, with the shoreline characterized by salt marshes, tidal flats, beaches and dunes, and a wide variety of river deltas, sounds, inlets, and estuaries. Yet many coastal counties are experiencing significant population growth, and with estimates of sea level rise projected up to six feet by the next century, it is likely that many wetland habitats and their ecosystem services will be lost. The characteristics of some coastal wetlands make them more likely to be resilient and remain diverse and productive even as they adjust to climate-induced changes. In this project, we mapped these characteristics and estimated the relative resilience or vulnerability of 10,736 coastal sites from Maine to Virginia.

Technical methods for mapping and estimating coastal resilience were developed in concert with a steering committee of 35 coastal experts that included members of the U.S. Fish and Wildlife Service (USFWS), representatives from the National Oceanic and Atmospheric Association (NOAA) and other federal, state and NGO staff from both Northeastern and Southeastern states. We divided the coast into 10,736 individual sites centered around each tidal marsh or complex of tidal habitats over two acres. For each site, we estimated the amount of migration space available under six sea-level rise scenarios and we identified the amount of buffer area surrounding the tidal complex. We then examined the physical properties and condition characteristics of the site using newly developed analyses as well as previously published and peer-reviewed datasets. For tidal complexes, the physical factors assessed included the size and tidal zone diversity of the migration space, the size and shoreline intricacy of the existing tidal complex, and the amount of shared edge between the tidal complex and

its migration space. Condition factors included the amount of hardened shoreline, as well as the magnitude of nitrogen inputs, and the quantity of sediment and freshwater inputs. For the buffer area, we assessed its size and variety of compatible landforms and soils, the connectedness of its wetlands, and the amount of natural cover. A score was calculated for each site based 80% on the tidal complex and 20% on the buffer, with equal weight given to physical and condition characteristics. Scores were calculated for each of six sea-level rise scenarios (1 to 6 ft.). Our final maps were based on the 6-foot scenario because this scenario reveals the sites with the greatest long-term potential for adaptive response. We made the 6-foot results even more robust by slightly boosting or penalizing the score based on whether the size of the migration space showed a significant increasing or decreasing trend over the 3-6 foot scenarios.

The scores are presented relative to other complexes within one of five coastal shoreline regions. Coastal shoreline regions are geographic areas where the coasts and estuaries are dominated by a common set of processes and geomorphology (e.g., drowned river valleys, lagoons, embayments). The scores are presented in standardized normalized values (z-scores), which are units of standard deviations above or below the mean score of all sites in the coastal shoreline region. For example, a z-score of 3 SD for a site in the lagoon shoreline region indicates that the site score is three standard deviations higher than the average score for all lagoon sites.

Study Area

The study area included the entire Northeast Atlantic coastline from Maine to Virginia, and specifically the coastal zone from the intertidal region landward to the 6-foot elevation zone. States included were: CT, DE, ME, MA, MD, NH, NY, RI, and VA.

The region's coastline is well known for its hundreds of productive estuaries that provide juvenile nursery and spawning grounds for fish, mollusks, seabirds, and crabs. The coastline is a critical ecological transition area, and although it forms a sharp natural boundary, it is very dynamic over geologic time. Over millennia, it has advanced and retreated thousands of kilometers inland and seaward in cycles, and it is now once again retreating as the sea level is rising at an unprecedented rate.

This study focuses on the ecological resilience of coasts and estuaries in this region to sea level rise (SLR). The focal area of this study is the zone of intertidal habitats and low elevation landforms that is sculpted by waves and tides and by the continuous flow of new sediments carried by freshwater in coastal watersheds. This shallow, well-lit, and productive area gives rise to salt marshes, tidal flats, oyster reefs, and seagrasses that directly and indirectly support an abundance of uniquely adapted species.

Coasts and estuaries are also of great importance to humans. Tremendous material and aesthetic resources associated with shorelines have attracted and sustained

humans for thousands of years. Coastal ecosystems help support the economy and sustain us by providing places to live, opportunities for tourism, shipping and transportation routes, commercial fishing, and seafood processing. The malfunctioning of these systems either due to sea level rise or from pollution, habitat destruction, hypoxia, harmful algal blooms, fishery collapses, and increased coastal erosion can have devastating social and financial impacts for coastal communities.

Approach

This two-year project aimed to estimate and map the ecological resilience of 10,736 coastal sites. To estimate resilience, we compiled and analyzed region-wide data on factors that influence a site's vulnerability or resilience to SLR and other climate-driven changes. Physical and condition attributes were assessed and integrated into a spatially-explicit dataset. Using these attributes, we evaluated each site's tidal habitats and estimated their ability to migrate landward with SLR based on the size, shape, condition and context of their available migration space. The relative resilience of each site was determined by comparing it to other sites within the same coastal shoreline region. We hope the resulting maps and web tools will provide local communities, policy makers, resource managers, and conservationists with clear and objective information for understanding the vulnerable and resilient areas of their coasts.

Steering Committee

We convened a steering committee of 35 coastal experts from state and federal agencies, conservation organizations, regional coalitions, and subject matter experts representing each of the states covered by this study. The role of committee participants was to join in bi-monthly discussions focusing on the review of approaches, methods, datasets, interim products, and results. Engaged participation of the steering committee was essential to ensure that the final products were rigorous and accurate, and that they will be useful to the stakeholders. The list of steering committee members appears in the acknowledgments.

BACKGROUND

CHAPTER 2

As sea levels rise, intense storms become more frequent, and other impacts of climate change are felt by coastal communities, there is an urgent and growing interest in understanding coastal resilience. Cities and towns are being forced to reconsider how and where to invest their coastal resources, and these decisions affect millions of people, important infrastructure, and coastal-based economies and livelihoods. Since 2007, TNC has led the development of an online decision support tool, “Coastal Resilience” (<http://coastalresilience.org/>), to help address the devastating effects of climate change and natural disasters. The aim of the tool and the approach is to help coastal communities increase their resilience to climate change by identifying nature-based or green infrastructure solutions that will enable communities to effectively protect, restore, and sustainably manage their natural resources while also strengthening local capacity for climate adaptation.

The challenge of identifying the places where nature and people could succeed in sustaining diverse and productive ecosystems is the topic of this study. The tools and products arising from this study can be used in conjunction with the Coastal Resilience tool or independently, depending on the needs of the user. While the former is focused on facilitating decisions about green infrastructure, it is predicated on the need for diverse and productive coastal habitats which is addressed in depth here.

Identifying resilient coastal sites where salt marshes can migrate landward and the ecological conditions favor stable and productive habitats has given rise to numerous studies, and several excellent ones are underway, or have been completed, in the study region. In Maine, the Natural Areas Program led a state-wide “coastal resiliency” assessment that included an evaluation of current tidal marshes, potential tidal marsh migration areas, and adjacent undeveloped blocks of land. In Massachusetts, the UMASS/USFWS project to design sustainable landscapes coupled a landscape change model with a sea level rise model, and developed an approach for integrating the results of the landscape change assessment into decision support for landscape design. In New Jersey, the Resilient Coastlines Initiative developed tools to support the identification, implementation, and monitoring of nature-based solutions to coastal risks, and a key outcome was a “future habitat” application that helps users visualize how salt marshes will be affected by sea level rise. Users can enter scenarios of 1, 2, or 3 feet of sea level rise and see whether the marshes will likely migrate inland or

succumb to inundation. In Virginia, TNC worked with leading coastal scientists and community partners to explore and document the resilience inherent in natural systems of the Eastern Shore (Warren Pinnacle Consulting Inc. 2015). The approach and methods developed in these studies had a large influence on our own approach and methods, and many of the authors served on our steering committee. Although these very recent projects have not yet been published in the peer reviewed literature, many have excellent web sites and mapping tools where users can explore the results or download the data:

Maine: http://www.maine.gov/dacf/mnap/assistance/coastal_resiliency.html

Massachusetts: <http://www.umass.edu/landeco/research/dsl/dsl.html>

New Jersey: <http://maps.coastalresilience.org/newjersey/>

Virginia: <http://maps.coastalresilience.org/virginia/>

At the scale of the whole Eastern Seaboard, NOAA has sponsored a website, Digital Coast (<https://coast.noaa.gov/digitalcoast/>) that is focused on helping communities address coastal issues, and it has become one of the most-used resources in the coastal management community. The web mapping tool allows users to visualize community-level impacts from coastal flooding or sea level rise and maintains data related to water depth, connectivity, flood frequency, socio-economic vulnerability, wetland loss and migration, and mapping confidence. We adapted the underlying marsh migration data in NOAA's Sea Level Rise Viewer (Marcy et al. 2011) as the basis of our migration space models.

Our approach to mapping resilience focuses on the characteristics of the underlying geophysical stage rather than on the dynamics of the biotic systems. We assume that the biotic systems will change in concert with the changing climate, but that sites with certain enduring physical characteristics will have a larger capacity to support diversity, productivity, and ecological function into the future (Anderson et al. 2014). This approach, which has been called "conserving nature's stage," is supported by current and historical evidence (Lawler et al. 2015, Beier et al. 2015, Gill et al. 2015, Anderson and Ferree 2010). In the case of coastal sites, the elevation, landforms, and parent material that underlie a site, as well as the tidal heights and shoreline complexity can determine whether the site has space and options for adaptation.

We use the term "site resilience" to distinguish this approach from "ecosystem resilience" as the latter implies that an ecosystem is rebounding back to a previous state. Site resilience, in contrast, refers to the capacity of a physical site to maintain species diversity and ecological function even as the composition and proportion of habitats change in response to climate change. A resilient site is characterized as an area with sufficient options to sustain species and ecosystems in the face of stress and uncertainty. Such options, or characteristics that foster resilience, may include topographic and elevation diversity that provides a range of habitat types and

microclimates, and space for adaptive movements with minimal barriers that restrict the movement of species or ecosystems. A site without such options would be considered vulnerable in the face of climate change.

Prior to this study, we developed a method for estimating the resilience of terrestrial sites (Anderson et al. 2014) by evaluating a site's landscape diversity (microclimates created by a site's topography, elevation gradients, and wetlands) and local connectedness (the degree to which the land cover is conducive to the movement of organisms and the flow of ecological processes). We mapped areas with higher microclimate diversity and local connectedness across 61 different geophysical sites to identify resilient sites throughout the entire Eastern US region except for the coastal shoreline region (<http://maps.tnc.org/resilientland/>). The terrestrial study has been used successfully to inform conservation decisions and we hope that this counterpart study addressing the coastal shoreline will be equally useful.

Our approach has similarities to the USGS Coastal Vulnerabilities Index (Thieler and Hammar-Klose 1999), Natural Capital Coastal Vulnerability Model (Sharpe et al. 2016), the National Estuarine Research Reserve multi-metric approach (Raposa et al. 2016), and other models that estimate the vulnerability of coastal regions to long-term sea level rise, erosion and inundation. In the terminology of the Intergovernmental Panel on Climate Change (IPCC), ecosystem vulnerability is a combination of sensitivity and exposure. The primary difference between this study and the vulnerability studies is that we do not estimate exposure, surge potential, or buffering by natural habitats, because the amount and condition of those factors are dependent on climate and not stable over time. Instead, we simply assume high exposure by running multiple SLR scenarios and scaling our results to the extreme 6-foot SLR scenario. This allows us to focus solely on the sensitivity of the sites and identify the sites with more options for adaptation under an uncertain future. Thus, in our model a site is not considered more vulnerable if it has more exposure to risk, rather it is considered more vulnerable only if it has no options for adapting to, or accommodating, risk.

DEFINING AND MAPPING COASTAL SITES

We defined a coastal site as an area of land that is regularly flooded by saline waters and contains tidal and estuarine habitats. Our focus was on the physical features - the landforms, soils, and tidal inundation zones - that define the site and regulate local processes. These features set the stage for a mix of biotic and abiotic habitats such as salt marsh and tidal flats that are constantly in flux. We mapped each tidal complex as an individual “site” and our analysis centered on the characteristics and processes that influence each site’s ability to accommodate sea level rise (SLR). Specifically, we examined the space and conditions that would allow the tidal complex to migrate inland and adapt to new conditions. Below we discuss the approaches we used to map the tidal complex, its buffer area, and its migration space.



Tidal Complex

We used the term “tidal complex” to refer to a set of interconnected tidal and estuarine habitats that were spatially grouped into a contiguous area. The habitats included:

Tidal marsh: Intertidal wetlands of low energy environments that form expansive meadows or narrow shoreline fringes dominated by *Spartina patens* or *S. alterniflora* (i.e., salt marsh). Tidal marshes are one of the most productive ecosystems in the world, providing shoreline stabilization, nutrient cycling and critical wildlife habitat for many species of plants, invertebrates, mammals and birds, including the rare New England endemic Saltmarsh Sparrow. Salt marshes also provide breeding, refuge, nursery, and forage habitats for marine fauna.

Brackish marsh: Brackish marshes are transitional between freshwater and salt marsh, and form along the upland edge of salt marshes where freshwater runoff or groundwater dilutes the salinity of the marsh surface. Dominated by bulrushes and sedges, the species vary depending on local hydrology and salinity levels.

Tidal flat: Non-vegetated sand and mud flats are the central habitat for blue mussel, eastern oyster, hard clam, soft shell clam, horseshoe crab, marine annelids and many other invertebrates. At high tide, they are productive foraging grounds for fish, eels, crabs, and snails. At low tide, many shorebird species depend on them for grazing and foraging. Tidal flats have historically been undervalued by coastal managers and are poorly mapped for this region.

Sandy beach and dune: Beaches are highly dynamic systems that form where sand is deposited as waves lose energy near the mainland. They can form extensive barrier islands or small pocket beaches and are constantly shaped and reshaped by winds, storms, and ocean currents. Sandy beaches are breeding grounds for rare species such as piping plover, least tern, Arctic tern, roseate tern, and several species of sea turtles. Beaches also provide habitat for a wide variety of invertebrates and are critical roost sites for migrant shorebirds.

Seagrass bed: Seagrasses are rooted vascular plants found in shallow coastal waters with soft substrate. Eelgrass (*Zostera marina*) and Widgeon grass (*Ruppia maritima*) are the dominant species in the Northeast and Mid-Atlantic regions. Eelgrasses form extensive beds that serve as shelter and nursery grounds for hundreds of species, including juvenile and adult fishes, shellfish, and other invertebrates.

Mapping Tidal Complexes

To identify and map tidal complexes, we used the 2010 C-CAP 30-m land cover data (NOAA 2010) which had been incorporated into NOAA's 10-m Sea Level Rise Viewer (Marcy et al. 2011) for the project area (Figure 3.1). First, we selected all pixels coded as estuarine forested wetland, estuarine scrub/shrub wetland, estuarine emergent wetland, and unconsolidated shoreline from the land cover dataset. Then, to create individual polygons, the selected pixels were expanded by one 30-m pixel and region-grouped into clusters using a four-neighbor rule (connectivity between pixels was defined as pixels immediately to the left, right, above, or below each of the four nearest neighbors). This had the effect of grouping closely adjacent cells of the various tidal habitats into a single unit. The units were then converted to discrete polygons using the unique region IDs, and the acreage and perimeter of each tidal complex polygon was calculated.

The mapping method resulted in 51,930 polygons of which most were single pixel sites. To reduce noise in the dataset and focus on sites that were likely to be ecologically meaningful, we identified a subset of the tidal complex units that had at least two acres of estuarine emergent wetland (salt marsh). This decision reduced the number of polygons to 10,736 that became the set of sites assessed in this study.

We initially had included tidal complexes composed solely of unconsolidated substrate (i.e., beach and tidal flats). However, after review internally and by steering committee members, we excluded these sites as they were often erroneously and inconsistently mapped across the region (Figure 3.2). We tried different approaches to identify real complexes, but were unable to develop a successful technique due to variations in tide levels when the underlying imagery was taken.

To provide more information about each tidal complex, we intersected the 10,736 tidal complex polygons with National Wetland Inventory (NWI) data (USFWS 2012) and assigned the dominant NWI wetland type code to each polygon (e.g., E2US3N = estuarine intertidal, unconsolidated mud shore). We also calculated the number of different NWI wetland types captured by each tidal complex unit (mean = 3.4 types).

Figure 3.1. Tidal complexes. The map shows the original 2010 C-CAP map of Tuckahoe, New Jersey on the left, and the mapped tidal complex on the right. The migration space and buffer area are explained below.

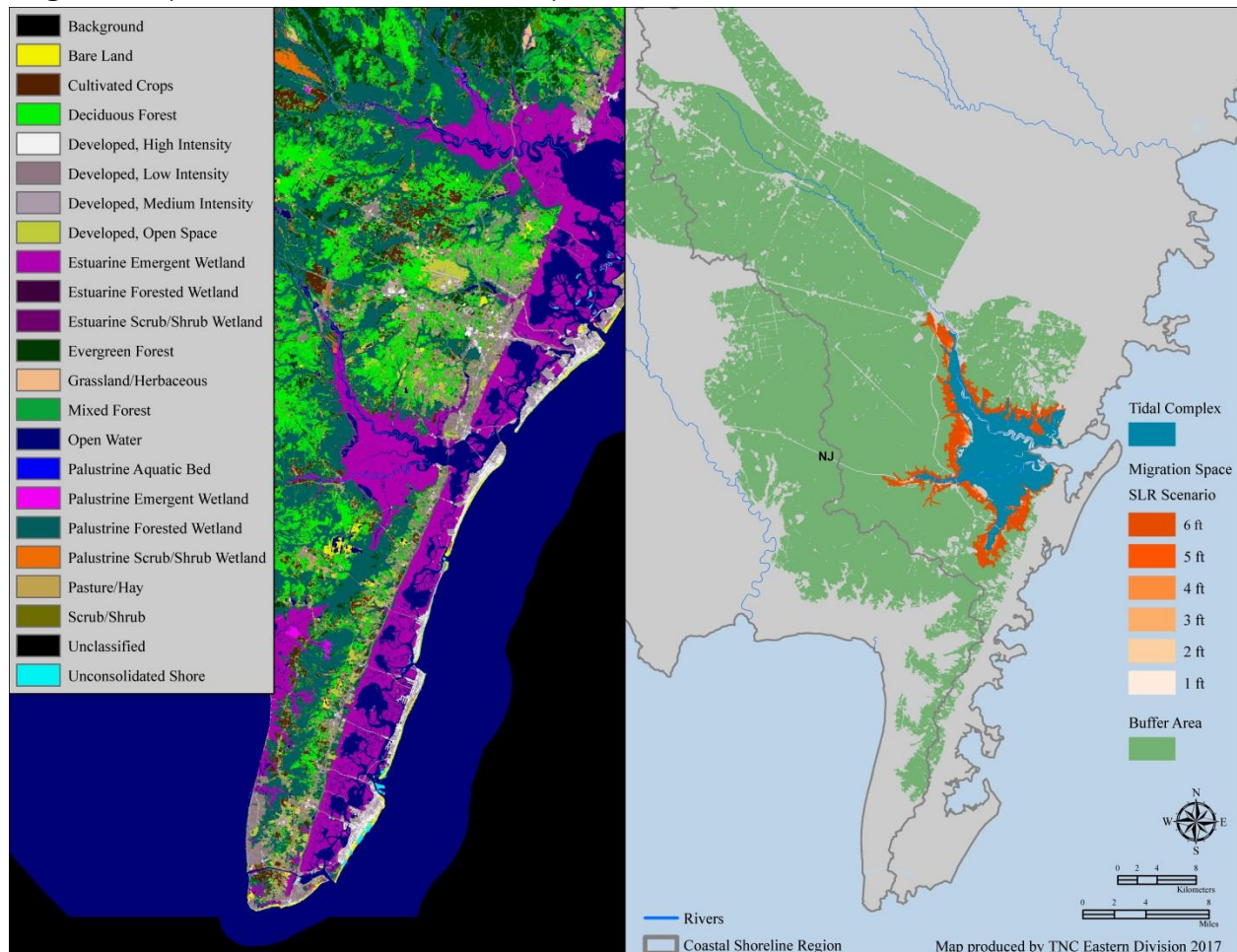
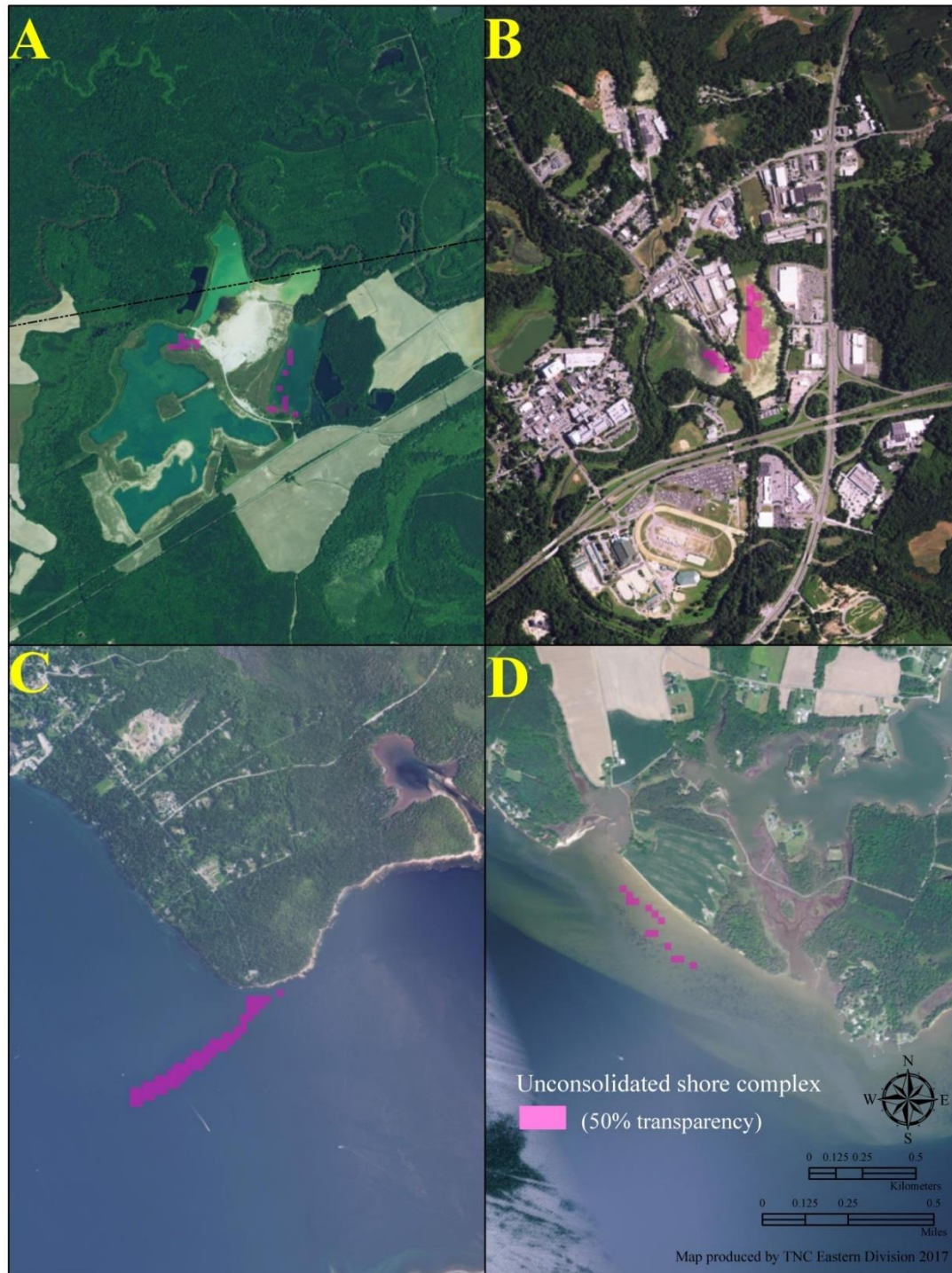


Figure 3.2. Unconsolidated shore complexes. These four examples illustrate the problems with including complexes comprised solely of unconsolidated shore. In panels A and B, the unconsolidated shore complex is actually part of an industrial site. In B and C, the unconsolidated substrate is not visible in satellite imagery, likely due to when the imagery was captured.



Buffer Area

The natural and agricultural land immediately surrounding the tidal complex is an important component of a site, because it influences the condition and ecological processes occurring in the tidal complex and its migration space. We referred to these lands as “buffer area” and we measured their extent, quality, and naturalness. A large intact buffer area allows coastal systems to interact with surrounding terrestrial and freshwater systems, and the condition of the buffer influences the water quality, sediment transport, species migrations, and dynamic processes within the migration space and tidal complex. A tidal complex hemmed in by development and having a small, degraded, homogenous buffer area is presumably less resilient than a complex with a large, natural, and ecologically heterogeneous buffer, because the complex has limited options for rearrangement and interactions. The buffer area also represents potential migration space beyond a sea level rise scenario of 6 feet. Initially, we focused solely on natural land cover, however, discussion and input from the steering committee highlighted the importance of agricultural lands, particularly poorly drained farm land, as a potential influence on marsh migration patterns in the future.

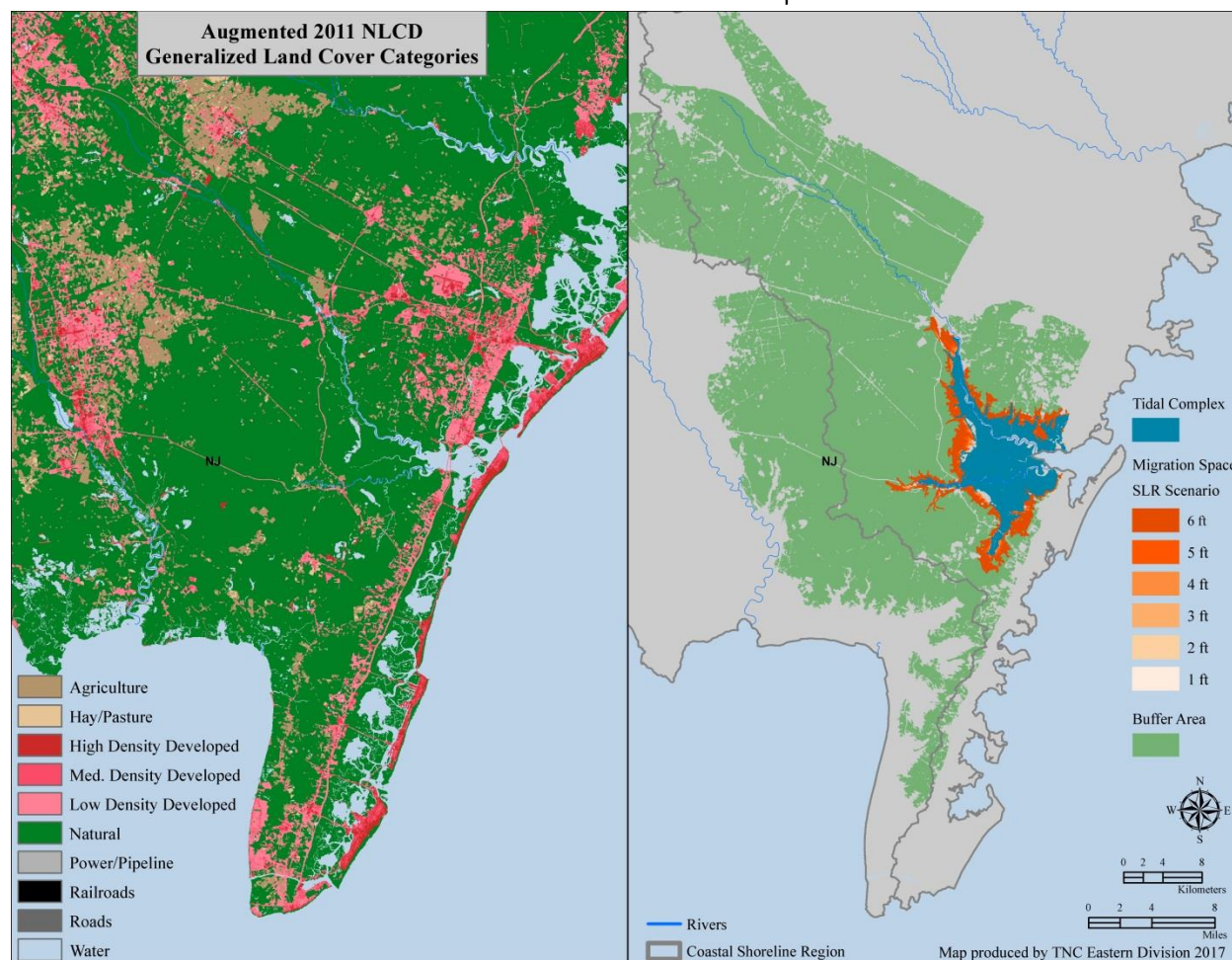
Mapping Buffer Area

To delineate the buffer area for each tidal complex and its migration space, we selected natural cover and agricultural land cover, including hay and pasture, from an augmented version of the NLCD 2011 land use/land cover grid (Homer et al. 2015; Figure 3.3). The augmented NLCD had more information on minor roads, railroads and transmission lines than the standard version (Anderson et al. 2016). We then used a series of masks to remove all pixels likely to be underwater in each of the six SLR scenarios, and we also removed any cells in the buffer area that had been mapped as tidal complex or migration space. The remaining pixels of natural and agricultural land cover were region-grouped using an eight-neighbor rule and converted to a polygon.

For each SLR scenario, discrete buffer polygons that intersected marsh migration space polygons were selected and then attributed with a unique ID, acreage, and perimeter. Next, the output from a one-to-many spatial join in ArcGIS was restructured and aggregated in R (R Core Team, 2016) to link each buffer area polygon with the migration space unit that it intersected. As some of the buffer area polygons were quite large, there were cases where a tidal complex had no migration space but did have buffer area. To account for this, the spatial linkage was repeated between the buffer area units and the tidal complex units. Both linkages were done for each of the SLR scenarios.

With the buffer area units linked to the migration space and tidal complex units, several cumulative attributes were then calculated for each buffer area. These included the total tidal complex acreage, count of tidal complexes, total migration space acreage, migration space count, and the shared edge with the migration space and tidal complex units.

Figure 3.3. Buffer area. The map on the left shows the augmented NLCD 2011 land use (Anderson et al. 2016) around Tuckahoe, New Jersey, where green is natural cover and brown is agricultural land. The map on the right shows how the land cover data translated to the buffer area around the Tuckahoe complex.

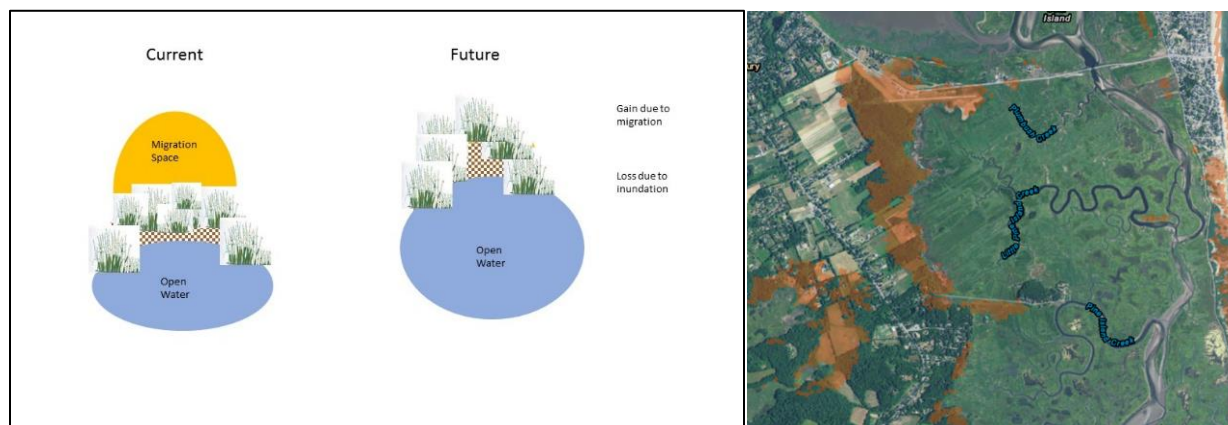


Migration space

Migration space is defined as the area of adjacent low-lying land that is potentially suitable for supporting tidal habitats in the future as sea levels rise, and into which the current habitats could migrate. For example, as sea levels rose over the last century, Maryland's Blackwater National Wildlife Refuge gained 2,949 acres of new salt marsh at the existing marsh's upland edge (i.e., in the migration space, Lerner et al. 2013). The concept of migration space appears in many coastal resilience studies where it has been variously called "marsh migration opportunity areas," "migration pathways," and "potential marsh zone" (Maine Natural Areas Program. 2016, C. Chaffee, pers. comm., K. Lucey, pers. comm.). The transition process works like this: tidal marshes exist in a narrow zone between the mean high tide and the mean high water line. As the tide rises, existing marshes become increasingly inundated, creating unsuitable conditions for vegetation growth and converting the marsh to unconsolidated substrate or open water. Meanwhile, new land suitable for habitat development may become available in the immediately adjacent lowlands as they start receiving regular tidal inundation. If conditions are right, the marsh may be able to migrate onto this land (Figure 3.4).

Sites vary widely in the amount and suitability of migration space they provide. This is determined by the physical structure of the site and the intactness of processes that facilitate migration. A marsh hemmed in by rocky cliffs will eventually convert to open water, whereas a marsh bordered by low lying floodplain with ample migration space and a sufficient sediment supply will have the option of moving inland. As existing tidal marshes degrade or disappear, the amount of available high-quality migration space becomes an indicator of a site's potential to support estuarine habitats in the future.

Figure 3.4. Migration space. Diagram illustrating how current tidal marsh is expected to move into its migration space, while the existing marsh is mostly lost to inundation. The image on the right shows the current marsh and migration space (orange) for a section of Great Marsh, MA.



The size and shape of a site's migration space is dependent on the elevation, slope, and substrate of the adjacent land. The condition of the migration space also varies substantially among sites. For some tidal complexes, the migration space contains roads, houses, and other forms of hardened shoreline that resist conversion to tidal habitats, while the migration space of other complexes consists of intact and connected freshwater wetlands that could easily convert to tidal habitats.

Our aim was to estimate site resilience but not predict future composition. Towards this end, we measured characteristics of the migration space related to its size, shape, volume, and condition, and we evaluated the options available to the tidal complex to rearrange and adjust to sea level rise. We made no predictions about exactly what habitats will be in the migration space in the future because nature's transitions are often non-linear and facilitated by pulses of disturbance and internal competition. For instance, in response to a 1.4 mm increase in the rate of SLR, the landward migration of low marsh cordgrass in some New York marshes appears to be displacing high marsh (Donnelly and Bertness 2001). Thus, our assumption was simply that a tidal complex with a large amount of high quality and heterogeneous migration space will have more options for adaptation, and will be more resilient, than a tidal complex with a small amount of degraded and homogenous migration space.

Mapping Migration Space

Given the importance of migration space in our analysis, we evaluated several potential approaches to delineate it by reviewing existing work. Specifically, we compared:

- (1) a logistic regression model to predict new salt marsh areas for the state of Massachusetts using a 1-m SLR scenario. The regression model used non-marsh and marsh points extracted from currently mapped Massachusetts salt marsh data (MassDEP 2015), a 30-m digital elevation model, and an estimated tidal range grid developed using an interpolation of 120 NOAA tide gauges.
- (2) the results from a coastal resilience analysis of Virginia's Eastern Shore conducted by Warren Pinnacle Consulting, Inc. for TNC's Virginia Chapter using the Sea-Level Affecting Marshes Model (SLAMM) (Warren Pinnacle Consulting, Inc. 2015).
- (3) draft results from an analysis to prioritize Maine's existing and future tidal marsh completed by Maine's Natural Heritage Program (2017). The Maine project examined a 1-m SLR scenario using a bathtub model.
- (4) the results from the NOAA SLR Viewer marsh migration data, which covers the entire US coast and uses a modified bathtub approach that considers local and regional tidal variability for six SLR scenarios from 1 to 6 feet in 1-foot increments.

The NOAA model does not map migration space per se, but instead predicts the distribution of future habitat types based on the SLR scenario and tidal class thresholds. To convert the results to migration space, we combined the area of four predicted habitat classes: brackish marsh, tidal marsh, tidal flat, and open water into a single spatial extent. This simplified and strengthened the results because it eliminated error in habitat class predictions and focused only on the spatial extent of the migration space. We compared the results of the simplified NOAA model with the three geographically focused models described above (Figure 3.5). The comparison showed substantial agreement and overlap between the NOAA migration space and the migration space delineated in the other projects. Areas of disagreement were mostly the result of spatial resolution differences between the datasets or differences in the base land cover. After an in-depth comparison and review with the steering committee, the team unanimously agreed to the use of the NOAA SLR Viewer data for this project due to its high consistency and relative accuracy across the study area.

To delineate migration space for the full project area, we downloaded the latest SLR Viewer marsh data, with no accretion rate, for the eight NOAA geographic units within the project area (Table 3.1). As accretion is very location-dependent, we chose not to use one of the three SLR Viewer accretion rates because they were flat rates applied across each geographic unit. For each geography, we combined the six SLR scenarios (1 to 6 feet by 1 foot increments) with the baseline scenario to identify pixels that changed from baseline. We only selected cells that transitioned to tidal habitats (unconsolidated shoreline, salt marsh, and transitional / brackish marsh) and not to open water or upland habitat. We combined the results from each of the geographies and projected to NAD83 Albers. The resultant migration space was then resampled to 30 m and snapped to the 2010 NOAA C-CAP land cover grid.

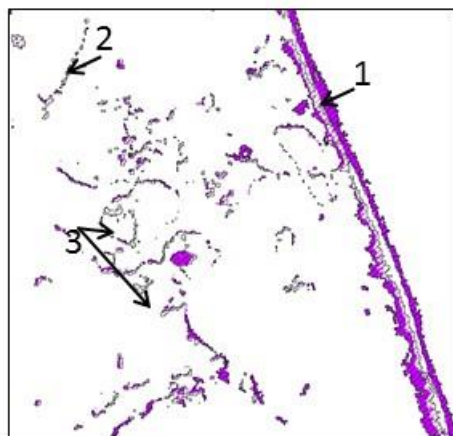
The tidal complex grid and the migration space grid were combined to ensure that there were no overlapping pixels. The remaining migration space was then spatially grouped into contiguous regions using an eight-neighbor rule that defined connected cells as those immediately to the right, left, above, or diagonal to each other. The region-grouped grid was converted to a polygon, and the SLR scenario represented by each migration space footprint was assigned to each polygon. Finally, the migration space scenario polygons that intersected any of the 10,736 tidal complexes were selected. Because a single migration space polygon could be adjacent to and accessible to more than one tidal complex unit, each migration space polygon was linked to their respective tidal complex units with a unique ID by restructuring and aggregating the output from a one-to-many spatial join in ArcGIS. This linkage enabled the calculation of attributes for each tidal complex such as total migration space acreage, total number of migration space units, and the percent of the tidal complex perimeter that was immediately adjacent to migration space. Similar attributes were calculated for

each migration space unit including total tidal complex acreage, number of tidal complex units, and shared edge with tidal complex unit.

Table 3.1. Migration space data. NOAA SLR Viewer marsh data used to develop migration space for the six SLR scenarios (1-6 ft. in 1-foot increments). A star indicates revised data that incorporated new digital elevation model data.

NOAA SLR Geography	Data Link
New England*	ftp://coast.noaa.gov/temp/ccap/SLR_wetlands_revised/NewEngland/
CT	ftp://coast.noaa.gov/temp/ccap/SLR_wetlands/CT/
NY	ftp://coast.noaa.gov/temp/ccap/SLR_wetlands/NY/
DE, NJ, PA	ftp://coast.noaa.gov/temp/ccap/SLR_wetlands/DE-NJ-PA/
MD, VA	ftp://coast.noaa.gov/temp/ccap/SLR_wetlands/MD-VA/
VA North	ftp://coast.noaa.gov/temp/ccap/SLR_wetlands/MD-VA/
VA South	ftp://coast.noaa.gov/temp/ccap/SLR_wetlands/MD-VA/
NC*	ftp://coast.noaa.gov/temp/ccap/SLR_wetlands_revised/NC/

Figure 3.5. Migration space model comparisons. Comparisons of the migration space derived from the NOAA model with those from a (A) 30-m logistic regression model in Massachusetts, (B) an enhanced SLAMM model in Virginia using lidar data, and (C) a 1-m lidar-based model in Maine.



1. Agreement

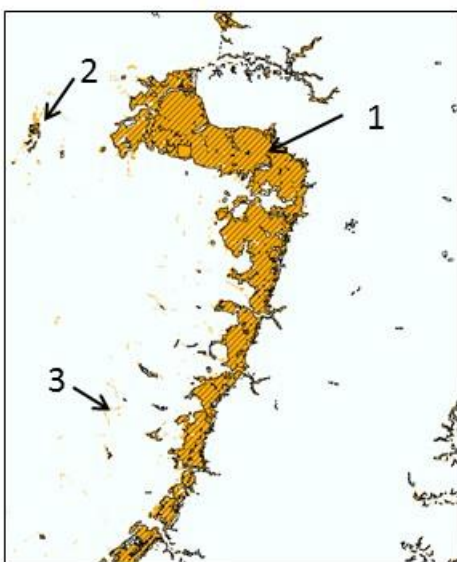
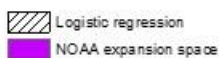
2. Class Inclusion Problem

Transitional marsh in NOAA model but we did not include this category in our original model.

2. Classification Problem

Salt marsh in MA DEP data

Freshwater wetland in current and future NOAA



1. Agreement

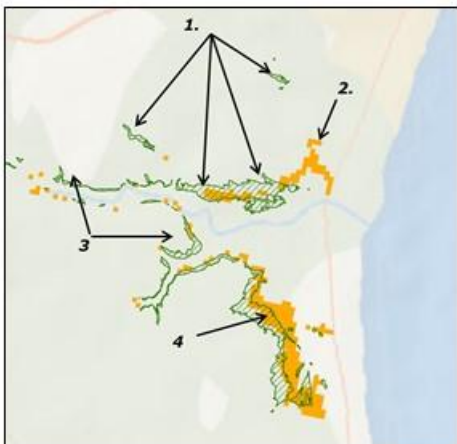
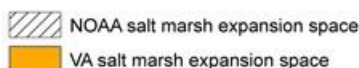
Most of this area shows strong agreement

2. Classification Problem

These cells are "Developed Open Space" in NOAA land cover so no transition

3. Classification Problem

These cells were already classified as salt marsh or open water in the NOAA land cover – so no expansion



1. Class Inclusion Problem

Transitional marsh in NOAA

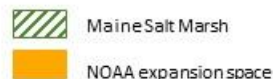
2. NOAA only

3. Maine Only

No change from current to future in NOAA

4. Resolution Mismatch

NOAA data offset from Maine data



Migration Space Scenarios

The amount of migration space available to a tidal complex is partially a function of the amount of sea level rise, since tidal complexes require periodic inundation. Initial estimates of global sea level rise over the next century suggested a range from 1.6 to 4.6 feet (Rahmstorf 2007, IPPC 2013) and have recently increased by up to 3 feet based on the volatility of the Antarctic ice sheet (DeConto and Pollard 2016). In the US, the National Climate Assessment synthesized past and projected sea level rise from 1800 to 2100, and estimated a currently projected range of sea level rise of 1 to 4 feet by 2100 with a wider range of 0.6 feet to 6.6 feet reflecting the uncertainty about how glaciers and ice sheets will react to climate change (NCA 2014).

We estimated migration space for six SLR scenarios: 1 to 6 feet in 1-foot increments (Figure 3.6). All scenarios are available to users of this project (see spatial datasets). However, after studying the patterns across all scenarios, we scaled our results to the 6-foot scenario because we wanted to identify sites that were robust to the most extreme events. Many sites have ample migration space up to the 3-foot scenario, but the space quickly decreases or disappears with more inundation. In our results, these sites are scored as more vulnerable than sites that continue to have migration space even at 6 feet.

We examined the trend of the migration space size across the 3, 4, 5, and 6-foot scenarios to identify sites where the migrations space was decreasing each year and separated them from sites where it was continuing to increase in size (Figure 3.7). This was done by fitting a regression line to the size of the new migration space across all three scenarios (3, 4, 5, and 6 -foot). Sites where the regression showed a significant trend ($p \leq 0.05$) were scored as increasing or decreasing depending on its trend sign (positive or negative), and the final score was increased or decreased slightly (by 0.5 SD) to reflect the trend.

Figure 3.6. Migration space scenarios. This map shows the 1- 6-foot migration space scenarios for Tuckahoe, New Jersey. The amount of migration space accumulates for each scenario, but at scenarios 5 and 6 some migration space is lost as it converts to open water (arrows).

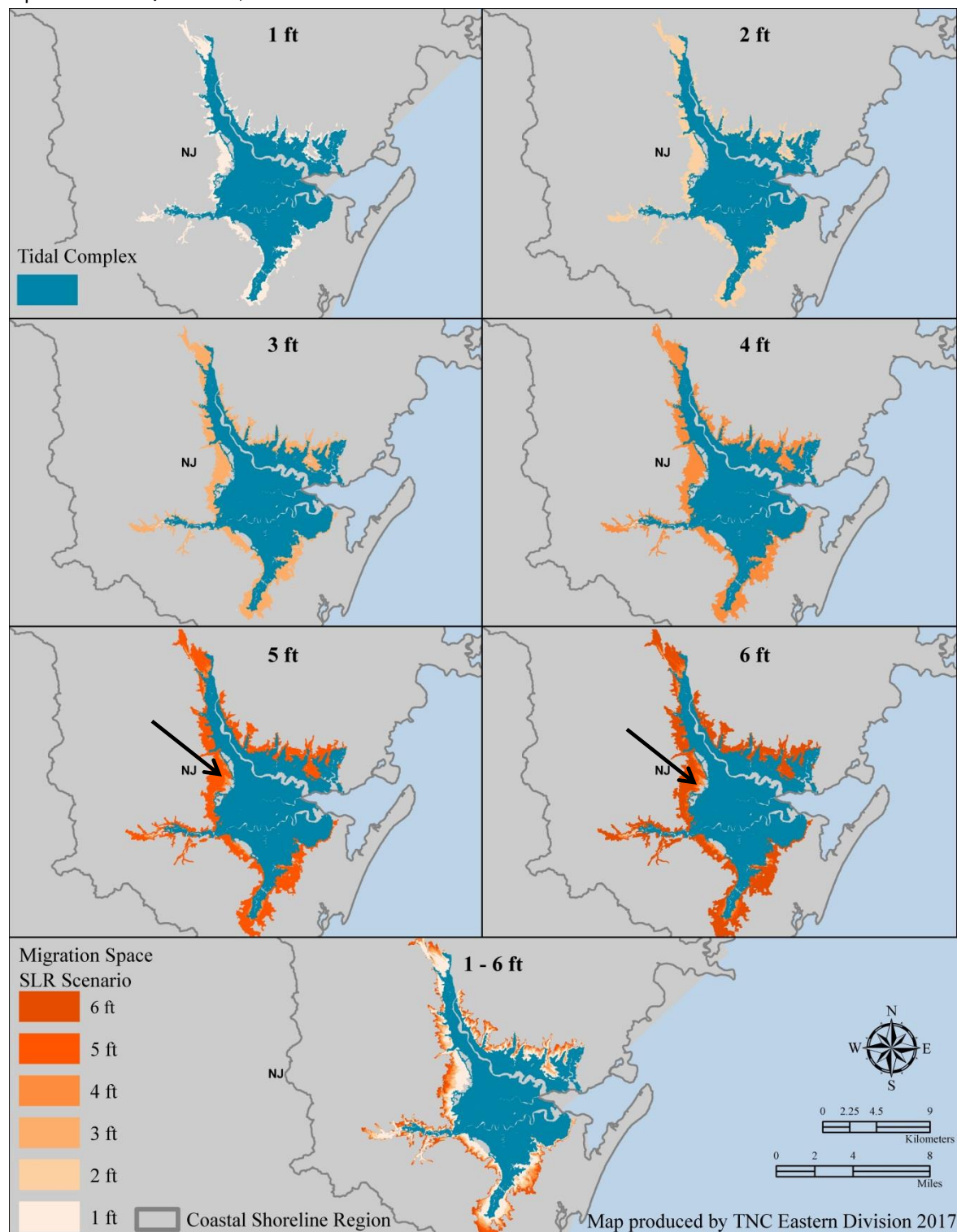
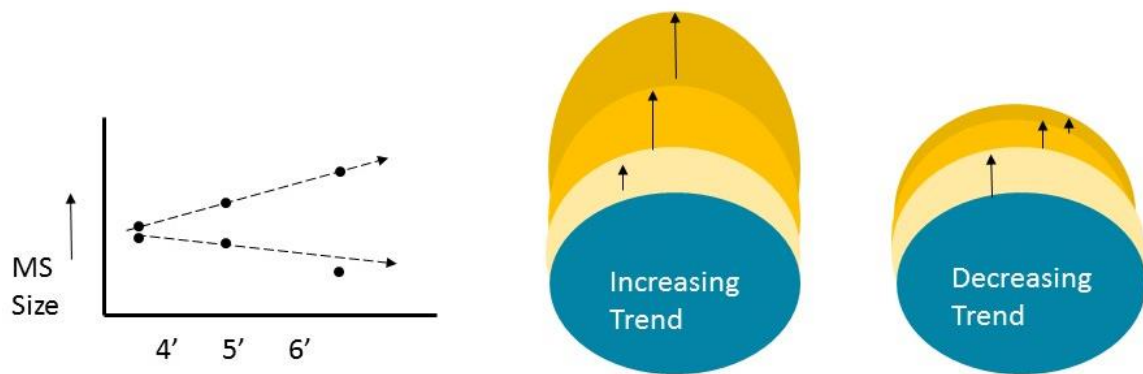


Figure 3.7. Migration space scenario illustration. The diagram shows the 4-6 foot scenarios for two sites. The left site has a small migration space under the 4-foot scenario but it increases markedly over later scenarios. The site on the right has the same size migration space under the 4-foot scenario but it decreases with each scenario. The chart shows how the trend would appear in the regression analysis.



COASTAL SHORELINE REGIONS

To facilitate comparisons between similar types of ecosystems and estuaries, we divided the study area into five coastal shoreline regions associated with discrete geographic stretches of shoreline that share similar processes and dominant estuary types (Figure 4.1). Stratifying the results within the shoreline regions allowed us to account for systematic variation in processes, geomorphology, habitat types, and species use, and thus make fair comparisons of resilience characteristics within regions of similar estuary types as opposed to comparing across types. For example, we compared Mid-Atlantic Coastal Lagoons to each other and not to the rocky Southern New England Embayments because we wanted to identify the most resilient areas for each type of shoreline. Estuary types were adopted from Madden et al. (2009) in the national Coastal Marine Ecological Classification Standard types (CMECS). The CMECS classification focuses on estuary size, shape, and flushing in dictating processes within an estuary and the adjacent coastal area.

The coastal shoreline regions, from north to south were:

Maine Drowned River Valley (650 sites)

This shoreline region consists of rocky, glacially-carved, drowned river valleys and embayments in Maine. Estuaries tend to be deep with seasonally cold-water with low to moderate riverine inputs, except around the Kennebec, Penobscot, and other large rivers. The rocky shoreline can be relatively complex and is sometimes partially enclosed by mountainous landforms. Kelly et al. (1988) divided this stretch of shoreline into an “Indented Shoreline” region in the south, a wide “Island-Bay Complex” region in the middle, and a narrow “Cliffed Shoreline” region in the north. We previously referred to this shoreline as “fjords” (small fjords) but recent research suggests there is only one true fjord on the Maine coast: Somes Sound on Mount Desert Island.

Northeast River Dominated (1566 sites)

This shoreline region contains channels, deltas and estuaries associated with large northern rivers (Merrimac, Connecticut, Providence, Hudson, Delaware), as well as associated small river valleys, arcuate embayments, and salt-wedge estuaries. River-dominated estuaries tend to be linear and seasonally turbid, especially in upper reaches, and can be subjected to high current speeds. Harbors and estuaries of the larger rivers are depositional environments and typically have deltas, spits, and sand bars. These estuaries also tend to be highly flushed, with a wide and variable salinity range, and seasonally stratified. They have moderate surface to volume ratios, high watershed to water area ratios, and have very high wetland to water area ratios.

Southern New England Coastal Embayment (2110 sites)

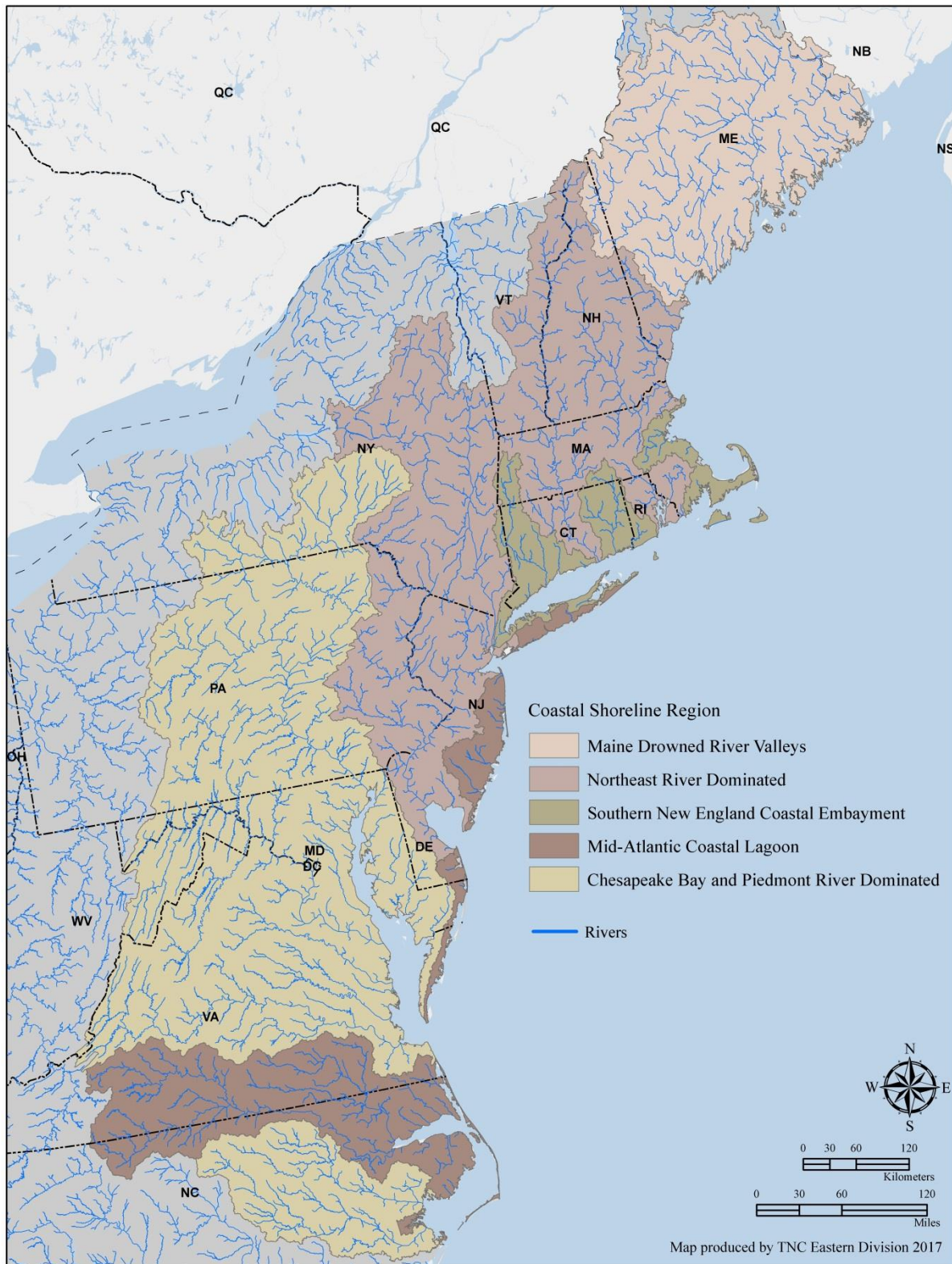
This shoreline region includes the bays, sounds, and coastal bights from Gloucester, Massachusetts to the north shore of Long Island Sound. The region includes many examples of the typical open bay loosely bounded by landforms, deep, well-flushed, and open to marine exchange, but there is much variation. Smaller sites include drowned river valleys along the Connecticut shore and sandy lagoon-like environments on Cape Cod. Bays in this region receive high energy input from tides, winds, waves, and currents, and estuaries range from very low to very high in terms of watershed to water area, and wetland to water ratio.

Mid-Atlantic Coastal Lagoon (1275 sites)

This shoreline region includes lagoons, sloughs, barrier island estuaries, and tidal inlets from Long Island south to Albemarle Sound. Lagoons tend to be shallow and highly enclosed, and have reduced exchange with the ocean. They are quiescent in terms of wind, current, and wave energy, and tend to have a very high surface to volume ratio. River inlets are small and coastal with restricted watersheds. Lagoons can have a high wetland to water ratio. This shoreline region consists of the drowned valleys of the Susquehanna, Potomac, and James rivers, plus tributaries and other small rivers associated with Chesapeake Bay. The region is characterized by a large deltaic estuary flanked with small river channels and freshwater tidal marshes. The many estuaries tend to be highly flushed, with a wide and variable salinity range, and seasonally stratified waters. They have moderate surface to volume ratios, high watershed to water area ratios, and can have very high wetland to water area ratios as well.

The shoreline regions are geographic areas where the coasts and estuaries are dominated by a set of processes and geomorphology, but not every site within the geography necessarily reflects the dominant type. The regions typically include a range of variation including small river-dominated sites and a few lagoon-like sites where sand accumulates.

Figure 4.1. Coastal Shoreline Regions.



ESTIMATING SITE RESILIENCE

In this section, we develop the concepts and methods to estimate the resilience of a coastal site. We defined “site resilience” as the ability of a site to support biological diversity and ecological functions even as it changes in response to climate change and SLR (Anderson et al. 2016). We expect all the coastal sites to change dramatically over the next century with new tidal habitats forming and migrating into the adjacent low lands where suitable migration space is available, and most of the existing marsh converting to open water. Identifying places where conservation can succeed and restoration actions could help sites adapt to change is a necessary step in sustaining the diversity and functions of coastal habitats.

We estimated site resilience based on physical site characteristics and the condition of processes that facilitate growth and migration. Physical characteristics change slowly and are expected to endure under both current and future climates making them a useful template for conservation planning. By evaluating the physical and condition characteristics of each site, we can identify the sites with relatively more options for migration and rearrangement. For example, a site with extensive high-quality migration space, supplied with adequate sediment and freshwater, and surrounded by natural buffer area offers more chances for rearrangement and change than a site with little migration space, degraded in quality, starved for sediment, and flanked by roads and development. We can reasonably call the first site more “resilient” and the second site more “vulnerable” based on the measurable differences in available options for adaptation. We do not know exactly how natural changes will play out at either site, because predicting the exact amount and spatial arrangement of each individual component in the future depends on thousands of specific climatic, hydrologic, and biotic changes, and there are large uncertainties about each of these.

To identify the measurable factors with the greatest influence on site resilience, we examined over 25 potential attributes. For each attribute, we clarified the mechanism by which it increased options for adaptation, and we tested whether we could consistently measure the attribute across the study area with the precision needed to

make realistic judgment about the site. We narrowed the attribute list down to 15 physical and condition characteristics that have a quantifiable effect on the resilience of a site and could be adequately mapped at a regional scale. Some of these factors apply directly to the migration space and some to the buffer area, and they are not all equal in influence. We present the 15 attributes in the next section, focusing first on the tidal complex and migration space, and second on the buffer area. The total list of attributes is in Box 5.1.

Box 5.1. Physical and condition attributes used to estimate resilience of coastal sites. *Condition attributes are shown in italics.*

Tidal Complex and Migration Space	Buffer Area
<ul style="list-style-type: none"> • Amount of migration space • Number of tidal height classes • Amount of shared edge • Complexity of current shoreline • Size of current tidal complex • Dynamic coastal response • <i>Percent hardened shoreline</i> • <i>Amount of nitrogen (water quality)</i> • <i>Amount of sediment inputs</i> • <i>Amount of freshwater inputs</i> 	<ul style="list-style-type: none"> • Amount of buffer area • Diversity of relevant landforms • Diversity of soil types • <i>Connectedness of wetlands</i> • <i>Percent natural cover</i>

Tidal Complex and Migration Space

This section focuses on identifying and mapping those characteristics of the tidal complex and its migration space that increase a site's ability to adapt to SLR and other climate-driven changes. Characteristics of the migration space are particularly critical to resilience because it represents the future distribution of the tidal complex, whereas characteristics of the current tidal complex are less influential because under most SLR scenarios the current complexes are unstable and expected to degrade or convert entirely to open water. Our model of site resilience addresses both the physical structure of the site and the condition of the components that could sustain the tidal complex and facilitate movement into a site's migration space. Because the factors are unequal in their degree of influence, we used a weighting scheme to give more weight to factors that have a large influence on site resilience and less weight to factors with less influence when we combined factors into a single index (Box on following page and Figure 5.1).

Tidal Complex and Migration Space: Summary of Attributes and Data Sources

Physical Characteristics

Size of Migration Space (Weight = 5): A large migration space is an essential condition for a large tidal complex in the future that supports robust species populations, allows for ecological processes, and is less susceptible to degradation. Data source: NOAA SLR Viewer 2016.

Tidal Height Classes Variety and Evenness (Weight = 3): Future estuarine habitats in the migration space are a function of the tidal classes that the space encompasses. Many tidal classes with relatively similar abundances offer options for a variety of habitats. Data source: NOAA SLR Viewer 2016

Shared Edge between Migration Space and Tidal Complex (Weight = 3): The migration of tidal habitats into the adjacent lowlands is facilitated by migration space directly adjacent to the existing habitats. Data sources: C-CAP 2010, NOAA SLR viewer 2016

Shoreline Complexity (Weight = 2): An intricate shoreline with lots of inlets and variable physical characteristics provides diverse habitat options and harbors greater ecological diversity than a smooth simple shoreline. Data source: NOAA ESI

Size of Existing Tidal Complex (Weight = 2): The size of the tidal complex is likely to influence its ability to migrate as large complexes provide large sources of biotic material. Data source: C-CAP 2010

Static Coastal Response (Weight = 5): A set of 148 static sites that were strongly hemmed-in and unable to respond dynamically. Data source: USGS Coastal Response Model (CRM).

Condition Characteristics

Hardened Shoreline (Weight = 5): Tidal complexes with their shorelines hardened by anthropogenic barriers are less adaptable as barriers prevent migration. Data source: NOAA ESI

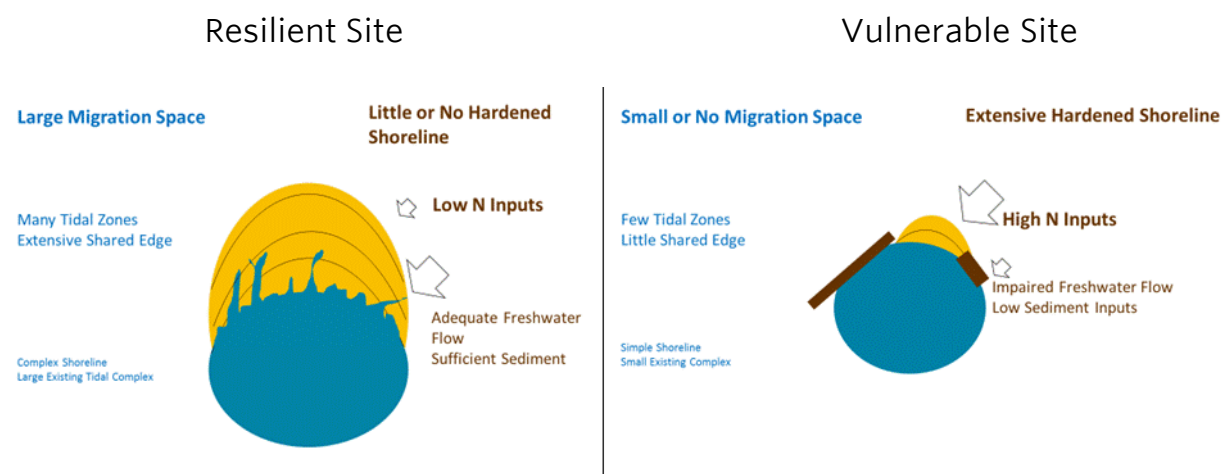
Water Quality / Nitrogen Inputs (Weight = 5): Excessive nutrient inputs can reduce sediment and organic matter accumulation and weaken root systems, reducing resilience. Data sources: USGS SPARROW 2002 Total Nitrogen Model (TNM), NLCD 2011.

Freshwater Flow (Weight = 4): Freshwater inflow is necessary for healthy and productive coastal estuaries and influences plant composition. Data source: NHDPlus v2

Sediment Input (Weight = 3): Watershed-derived sediment is a key source of tidal wetland accretion and declines have resulted in tidal wetland declines. Data sources: NHDPlus v2, NLCD 2011, SSURGO, InVEST Sediment Delivery Ratio (SDR) model.

Data Source References: **NOAA SLR** (Marcy et al. 2011), **C-CAP 2010** (NOAA 2010), **NOAA ESI** (Peterson et al. 2002), **USGS CRM** (Lentz et al. 2016), **USGS SPARROW 2002 TNM** (Moore et al. 2011), **NLCD 2011** (Homer et al. 2015, Anderson et al. 2016), **NHDPlus v2** (USEPA& USGS 2012), **SSURGO** (gSSURGO 2014), **InVEST SDR** (Sharp et al. 2016).

Figure 5.1. Tidal complex and migration space characteristics that increase resilience. Characteristics of a resilient site are shown on the left, and contrasted with a vulnerable site on the right. Physical factors are listed in blue and condition factors in brown. Factors with a strong influence are listed in bold and above factors with less influence.



Physical Characteristics: The physical characteristics of a site determine if there is land available to support the migration of tidal habitats, and the probability that colonizers will be able to access and utilize the migration space. These factors focus on the size, shape, volume, and configuration of the migration space. For all the physical characteristics, we assumed that both a large range and a more dynamic response increased resilience because variation and flexibility increase the options for adaptation. For example, a large migration space that encompasses a range of tidal classes offers more possibilities for sustaining diversity than a small migration space with one tidal class. The condition of the physical factors is also important and is addressed separately in an upcoming section focused on the processes that enable or facilitate the migration of the tidal complex to the new space.

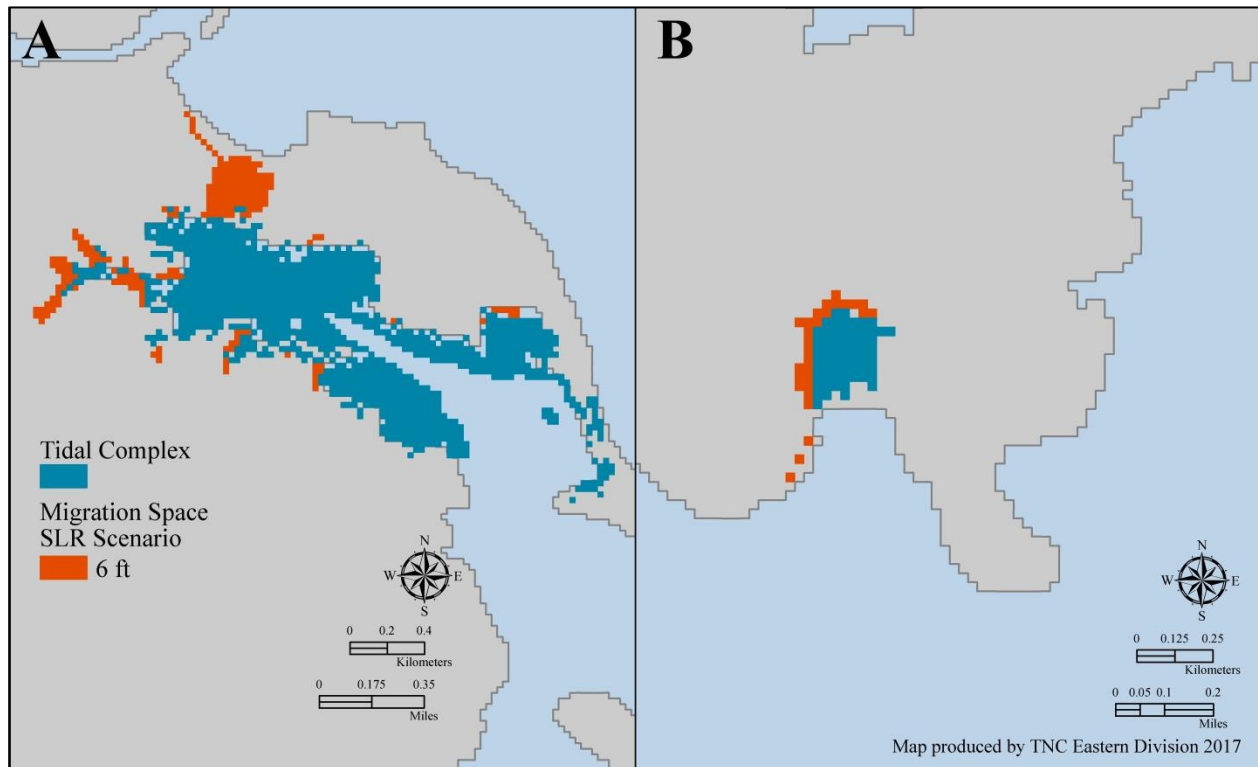
The physical attributes described below are arranged in order of influence. For each, we first describe how the attribute contributes to the site's resilience and then we explain the data sources and method through which we mapped the attribute. The attributes were ordered with respect to their direct importance to site resilience, and then weighted on a numeric scale from 1 to 5 to reflect their influence, with 5 indicating the greatest influence. Among the steering committee, there was unanimous agreement on the order of importance and high agreement on the numeric weights. The numeric weights were used as a multiplier when combining factors to give more weight to factors with more influence: 5 (very high), 4 (high), 3 (moderate), 2 (low) and 1 (very low). The numeric weight is listed in parentheses after each attribute.

Physical Characteristics of the Migration Space

SIZE OF MIGRATION SPACE (WEIGHT = 5): The size of future tidal complexes is a function of the size of the available migration space. A large migration space is an essential condition for a large tidal complex in the future, although we don't know how closely the space and the future size will correlate. In fact, most of the other physical and condition attributes we describe are aimed at identifying the sites where the migration space is most likely to fully transition to new tidal habitat. Large areas of tidal habitat are more resilient because they sustain demographic and ecological processes that inherently require space within which to function, and support robust populations of keystone species such as saltmarsh grasses. Large marshes store more carbon, provide more storm buffer and are less susceptible to degradation from stochastic events, and they are also more likely to host rare species such as Saltmarsh Sparrow. Tidal complexes with small migration spaces are vulnerable if inundation levels reach the expected 2 to 4 feet, because existing tidal marshes will be stressed for oxygen and will likely degrade or disappear.

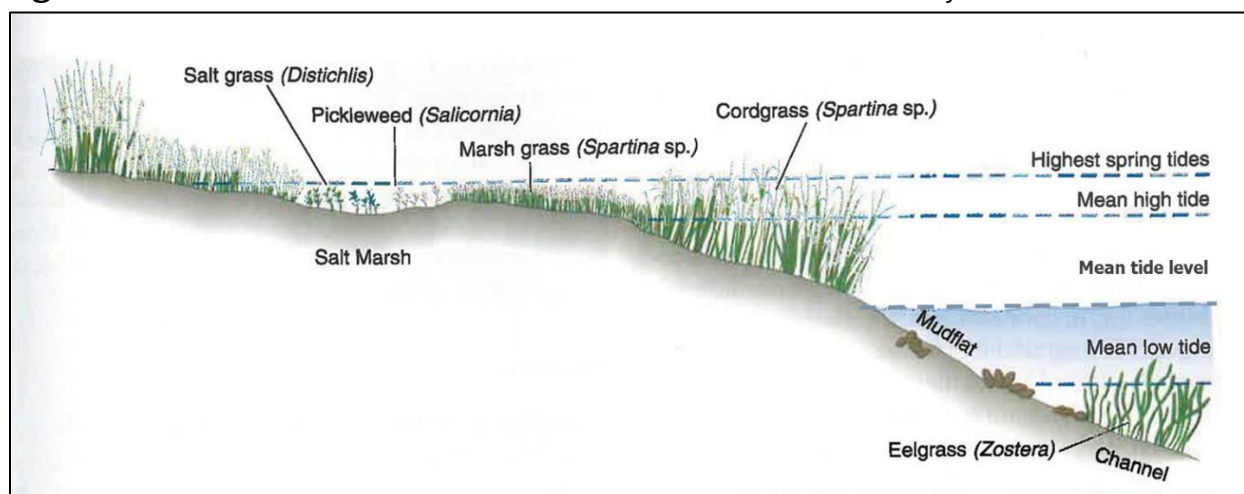
Our methods for mapping migration space and assigning it to each tidal complex were described in the previous section. A single tidal complex may have many non-contiguous regions of associated migration space and our estimate of size is based on the sum of all migration space that is adjacent to a tidal complex (Figure 5.2). For each SLR scenario, our estimate of migration space size is based on the total amount of space predicted to be there, which is the total of previous scenarios minus the amount converted to open water.

Figure 5.2. Tidal complex and migration space association. Panel A) shows a complex in Maine that has 15 distinct migration space units whose summed area served as the complex's total migration space. Panel B shows a tidal complex in Maine with only one migration space unit.



TIDAL HEIGHT CLASSES VARIETY AND EVENNESS (WEIGHT = 3): The types and proportion of estuarine habitats expected to occur in the migration space are partially a function of the type and proportion of tidal classes the space encompasses. The NOAA SLR Viewer relates tide levels to various ecological thresholds and the upper boundaries of various habitat: open water is bounded by mean low water (MLW), unconsolidated shore is bounded by mean tide level (MTL), salt marsh is bounded by mean high water (MHW), and brackish marsh is bounded by mean high water in spring (MHWS, Figure 5.3). Although there is disagreement among scientists as to how perfectly these tidal thresholds match observable habitat transitions, there was agreement that having many evenly distributed tidal classes within the migration space offers the potential for a larger variety of habitats in the future.

Figure 5.3. Tidal classes and habitats. Credit: Clemson University



Tidal classes were generated using the NOAA SLR data. In fact, we had previously aggregated the four classes to calculate the total migration space. For each migration space unit, we counted the total number of classes, and the area of each. We then calculated Simpson's evenness index as a measure of the diversity and evenness of tidal classes using the following formula:

Calculate Simpson's diversity index as:

$$D = (1 / \sum p_i^2) \text{ where } p_i \text{ is the proportional representation of each habitat.}$$

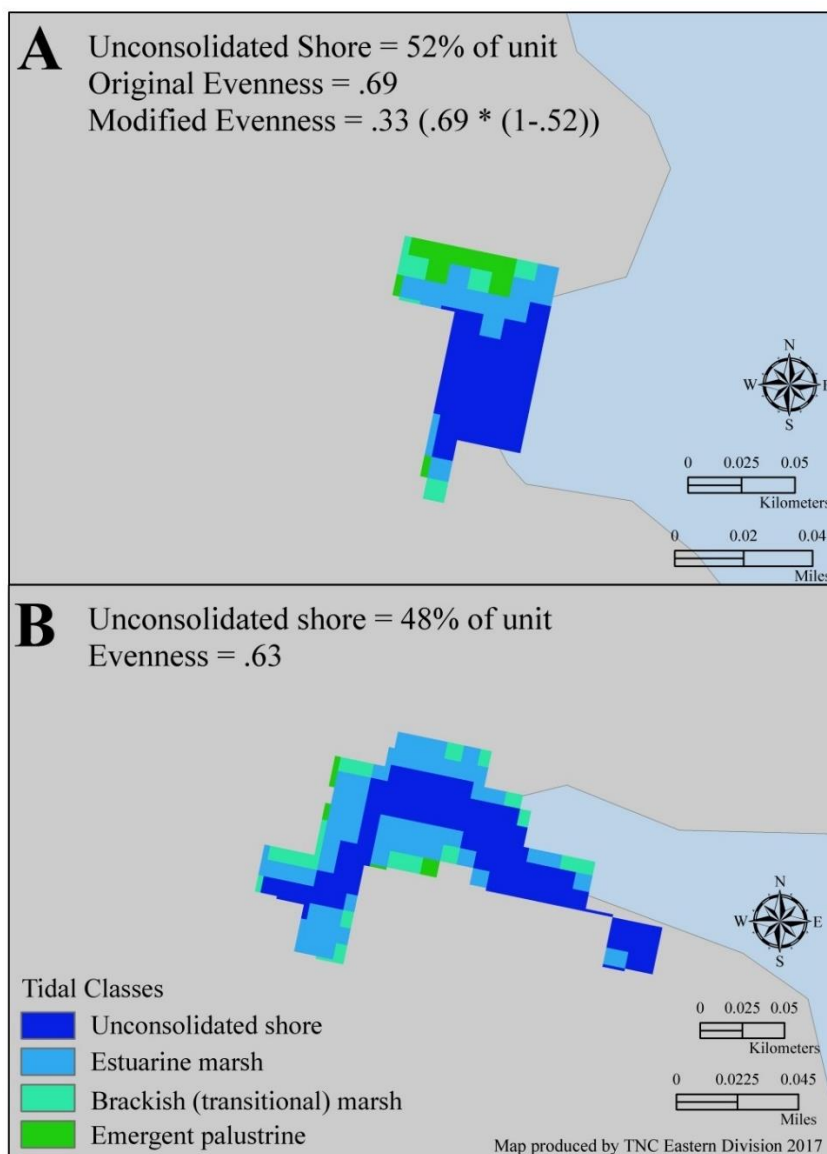
Calculate Simpson's Evenness as:

$$E = D / D_{\max} \text{ where } D_{\max} \text{ is the maximum possible number of habitats}$$

Steering committee participants felt it was important to give more weight to the MHW (salt marsh) and MHWS (brackish marsh) tidal classes, as the MTL (unconsolidated shore) subtidal class could easily shift to permanently submerged. At the same time, the sand and mud flats mapped as unconsolidated shore provide a distinct type of habitat that enhances the diversity of a site. To balance these competing demands, we calculated the proportion of unconsolidated shore in each migration space unit. If the

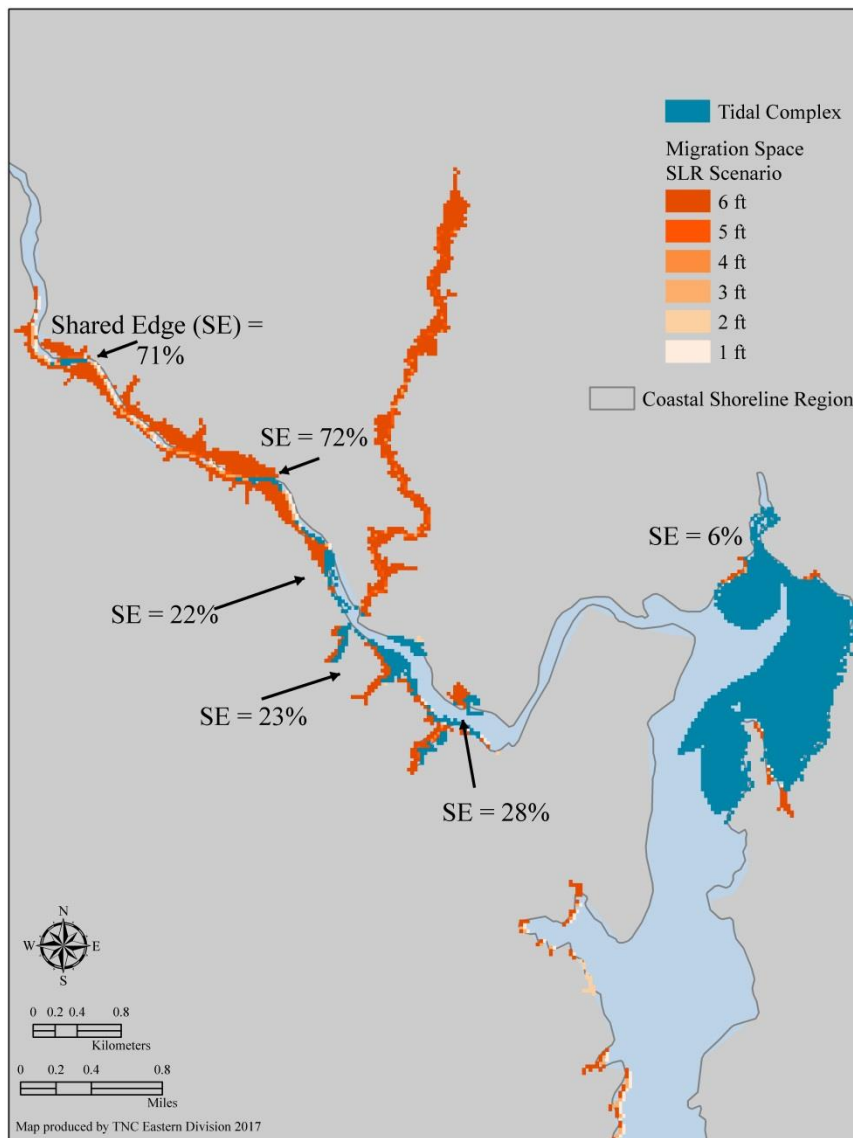
proportion of unconsolidated shore was greater than half (0.50), we penalized the evenness value by the non-unconsolidated shore proportion. For example, if a site had an evenness score of 0.69 because it had a somewhat equitable distribution of all four tidal classes, but 52% of the unit was unconsolidated shore, the final evenness score was calculated as $0.69 * (1 - 0.52) = 0.33$ (Figure 5.4 A). This allowed us to discount the tidal variability of migration space units that were predominantly unconsolidated shore and unlikely to provide much marsh habitat as SLR increases, yet also value this unique habitat when it was one piece of a complex habitat mosaic (Figure 5.4 B).

Figure 5.4. Tidal class diversity and evenness. A) More than 50% of the migration space unit was unconsolidated shore so the evenness score was modified as described in the methods. B) The migration space had less than 50% unconsolidated shore and the evenness score remained the same.



SHARED EDGE (WEIGHT = 3): The migration of existing tidal habitats into the adjacent lowlands is facilitated by having migration space directly adjacent to the existing habitats. Having a high proportion of shared edge between the existing complex and the migration space helps ensure that all regions of the tidal complex and all types of habitats have direct access to the migration space. It was not uncommon to have a relatively large patch of migration space touch only a small part of the existing complex, especially if the migration space was associated with a small river inlet. In these cases, migration could be hampered as not all the existing complex has easy access to the migration space (Figure 5.5).

Figure 5.5. Shared edge between migration space and tidal complex. Examples of different spatial relationships between tidal complexes and their migration space and the resulting differences in percent shared edge values.



To map the shared edge, each migration space was linked to their respective tidal complex units with a unique ID. This linkage enabled us to calculate the percent of the tidal complex perimeter that was immediately adjacent to migration space. To calculate shared edge, we spatially intersected the migration space units with the tidal complex units and set polyline as the output in a GIS. We calculated the length of the polyline output from the intersection analysis (the shared edge). Lastly, we divided the total shared length by the total length of each tidal complex and calculated the percent of the tidal complex edge that was shared with migration space. While the tidal complexes did not change with SLR scenario in our analysis, the migration space configuration did change with each sea level rise scenario. Accordingly, the shared edge was only calculated for the first SLR scenario and served as the baseline connection for the other SLR scenarios.

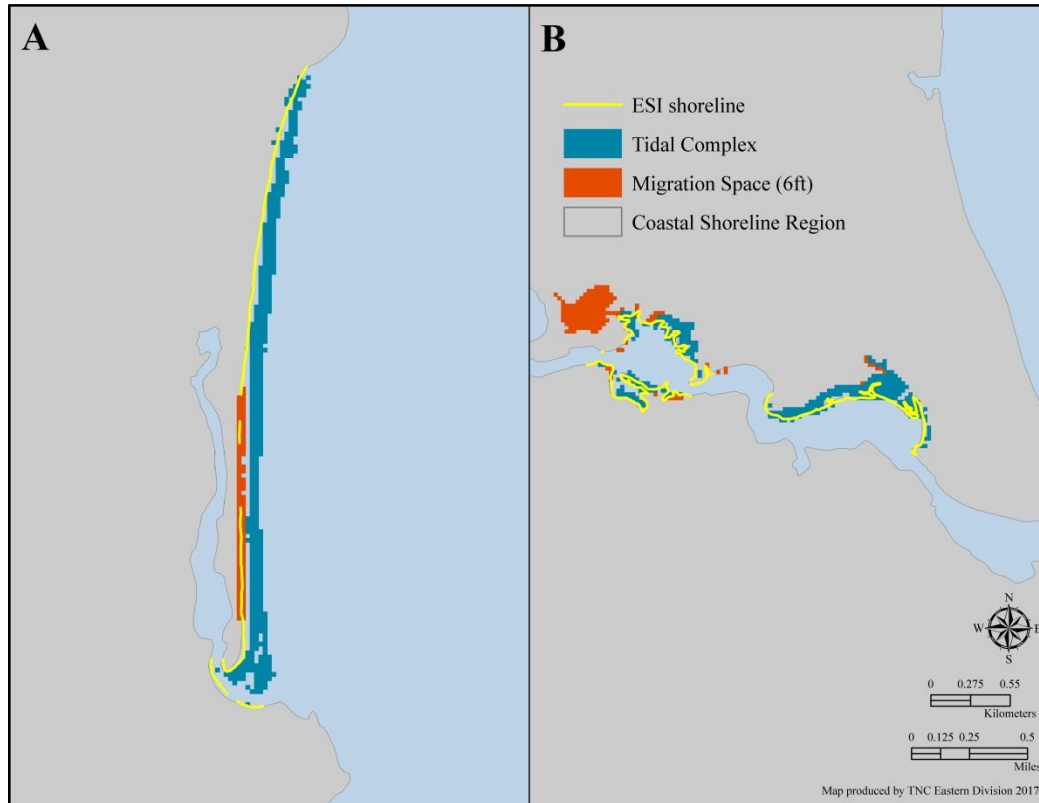
Physical Characteristics of the Existing Tidal Complex

SHORELINE COMPLEXITY (WEIGHT = 2): An intricate shoreline with lots of inlets and variable physical characteristics provides diverse habitat options and harbors greater ecological diversity than a simple shoreline, and creates resilience by dividing and distributing inundation levels. Although we do not know exactly what the future shoreline will be, we assumed that sites where the current geomorphology creates a complex shoreline will continue to have a complex shoreline in the future.

To calculate the complexity of a tidal complex's shoreline, we first linked a shoreline dataset to the tidal complex units as we did not want to use the artificial pixel-based complex edge (Figure 5.6). We selected NOAA's Environmental Sensitivity Index (ESI, Peterson et al. 2002) dataset to use as the shoreline for the tidal complexes. The ESI provides a continuous shoreline derived from overflights, aerial photography and remotely sensed data with systematic ground-truthing through visits to individual shorelines. The dataset classifies the shoreline into several categories that include natural shoreline types (e.g., exposed rocky shores, fine-to-medium grained beaches) and anthropogenic shoreline types (e.g., exposed, solid man-made structures, exposed riprap, sheltered, solid man-made structures, sheltered riprap). The first step in linking the tidal complexes to the ESI was to use a 30-m Euclidean allocation in ArcGIS to assign the tidal complex ID to any pixels within 90 meters of the respective tidal complex. We chose 90 m after experimenting with different distance thresholds between the ESI shoreline and the 30-m raster tidal complexes. After removing all manmade shoreline features from the ESI, we converted the Euclidean allocation grid to a polygon and ran an identity analysis in ArcGIS between the allocation polygon and the ESI shoreline. We then selected all ESI shorelines that intersected a tidal complex allocation polygon. Lastly, we used the ET GeoWizards Polyline Characteristics (11.2 extension, <http://www.ian-ko.com/>) to calculate sinuosity and fractal dimension values. ET GeoWizards calculates sinuosity as the ratio of the length of the polyline to

the length of the line connecting the start and end points of the polyline, and the values range from 1 (straight line) to infinity (closed polyline = 0). For locations where the sinuosity of a tidal complex was 0, indicating a closed polyline ($n=172$) we used the fractal dimension to measure polyline complexity using the Box Counting method (Bourke 1993).

Figure 5.6. Tidal complex shoreline complexity. A) Tidal complex with low shoreline complexity. B) Tidal complexes with more complex shorelines.



SIZE OF EXISTING TIDAL COMPLEX (WEIGHT = 2): The size of the existing tidal complex is likely to influence its ability to migrate because large complexes provide large sources of biotic material such as propagules and rhizomes. We gave this metric a low weight for influence, however, because most tidal complexes are already decreasing in size due to inundation and are not stable over the next century (Ganju et al. 2017). Researchers have found that aboveground and belowground biomass of *Spartina sp.* decreases exponentially with increased flood duration and higher salinities, and that even subtle increases in sea level may lead to substantial reductions in productivity and organic accretion (Sneddon et al. 2015).

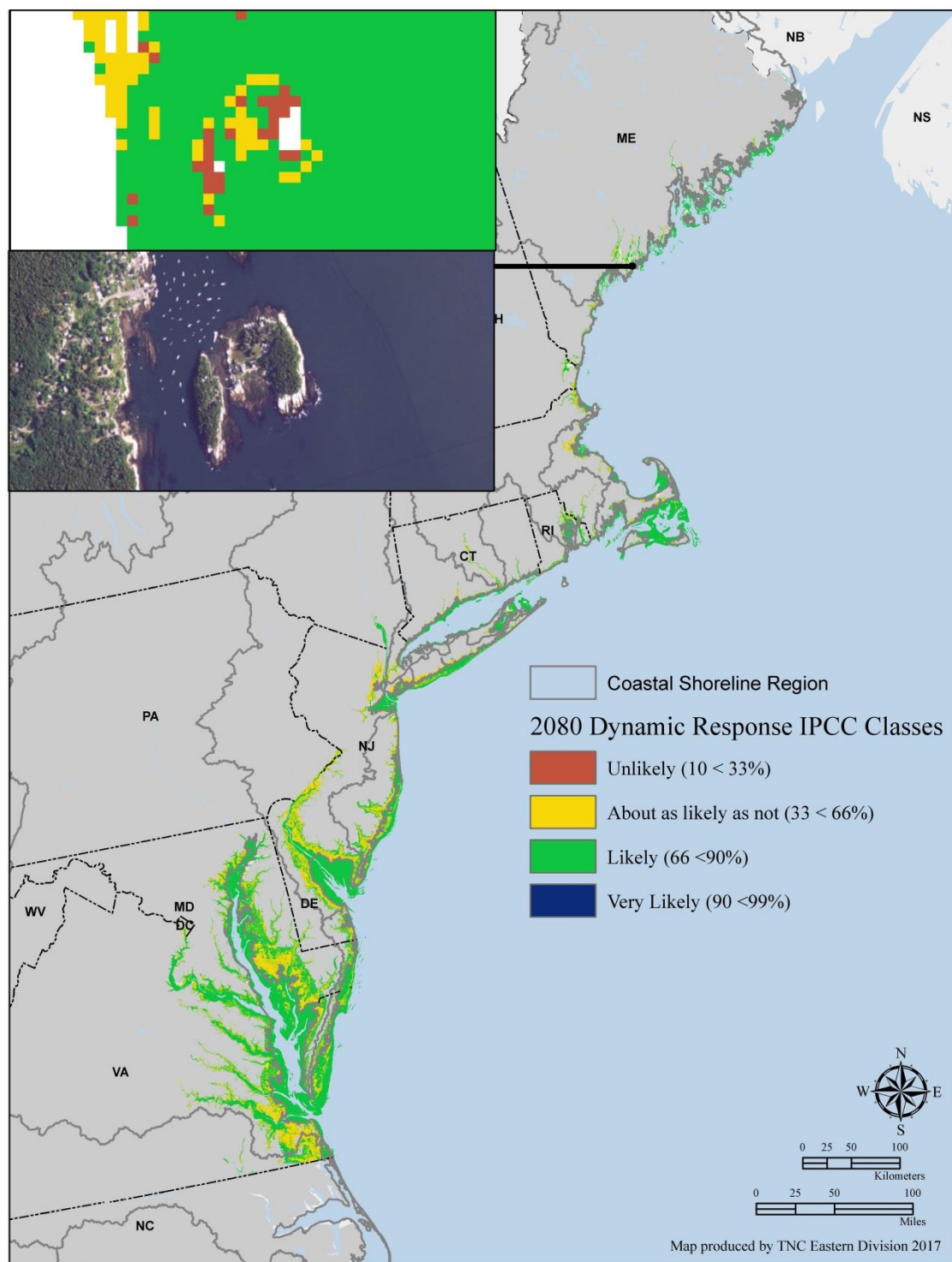
Our final physical metric, STATIC COASTAL RESPONSE (WEIGHT = 5), was applied differently than the previous metrics in that the results were extracted from an independently completed study by USGS (Lentz et al. 2016) that identified the shoreline of 148 sites in this study area as very unlikely to respond dynamically. We accepted the results of the study and penalized the 148 sites in proportion to the amount of static shoreline each contained. The net effect was that 37 sites received a “below average” score for this metric, 27 received “slightly below average,” and 84 received an “average” score, with most of these sites hemmed in by landforms or by development (Figure 5.7). To ensure that the other 10,588 sites were not impacted by the absence of this metric value, the estimated resilience score for tidal complexes affected by this metric was calculated separately.

The USGS dynamic response model was based on a probabilistic model that evaluates the likelihood that a site will statically inundate (flood) or dynamically respond (adapt) to SLR (Lentz et al. 2016). The model utilized information on sea level rise projections, vertical land movement rates, elevation data, land cover data, and literature on the response of six different land cover classes to estimate whether the response of the tidal complex will be dynamic or static. Per the lead author’s recommendation, we classified the 2080 dynamic response results into Intergovernmental Panel on Climate Change (IPCC) probability classes (Table 5.1, Mastrandrea et al. 2010). We spatially linked the results to the individual sites in this study area and found that 99% were rated “about as likely as not” to have a dynamic response (Figure 5.7). We also found a strong visual correspondence between sites ranked “likely or very likely” to have a dynamic response and sites with high erosion and accretion rates, but we could not confirm that the dynamic nature of these sites made them more resilient.

Table 5.1 IPCC probability classes (Mastrandrea et al. 2010) used to classify the 2080 Dynamic Response model probabilities (Lentz et al. 2016).

IPCC Term	Likelihood of the Outcome	Probability of a Dynamic Response in 2080
Virtually certain	99-100% probability	≥ 99 [No pixels]
Very likely	90-100% probability	$90 < 99\%$
Likely	66-100% probability	$66 < 90\%$
About as likely as not	33-66% probability	$33 < 66\%$
Unlikely	0-33% probability	$10 < 33\%$
Very unlikely	0-10% probability	$1-10\%$ [No pixels]
Exceptionally unlikely	0-1% probability	1 [No pixels]

Figure 5.7. 2080 Dynamic response model (Lentz et al. 2016). Model results were translated to IPCC probability categories, which show that most subtidal offshore areas (green) fell into “likely,” while 99% of the intertidal land-based sites we assessed in this study fell into “about as likely as not” (yellow) to dynamically respond. The inset shows an area that was “unlikely to respond dynamically” due to the landforms.



Current Condition: The condition factors describe characteristics that increase the probability of a tidal complex moving into the migration space. While the physical factors focused on the size and geometry of the migration space, the condition factors focus on the processes that enable the migration or formation of new tidal complex. Migration of a tidal complex can be obstructed by barriers, degraded substrate, an inadequate sediment supply, or poor water quality that hampers normal vegetation growth. The condition metrics are designed to help determine if the migration space is usable, and whether the expected ecological processes are functioning. In our model, a migration space with few barriers, low nitrogen inputs, an adequate supply of sediment, and regular freshwater flushing has the enabling conditions needed to facilitate migration.

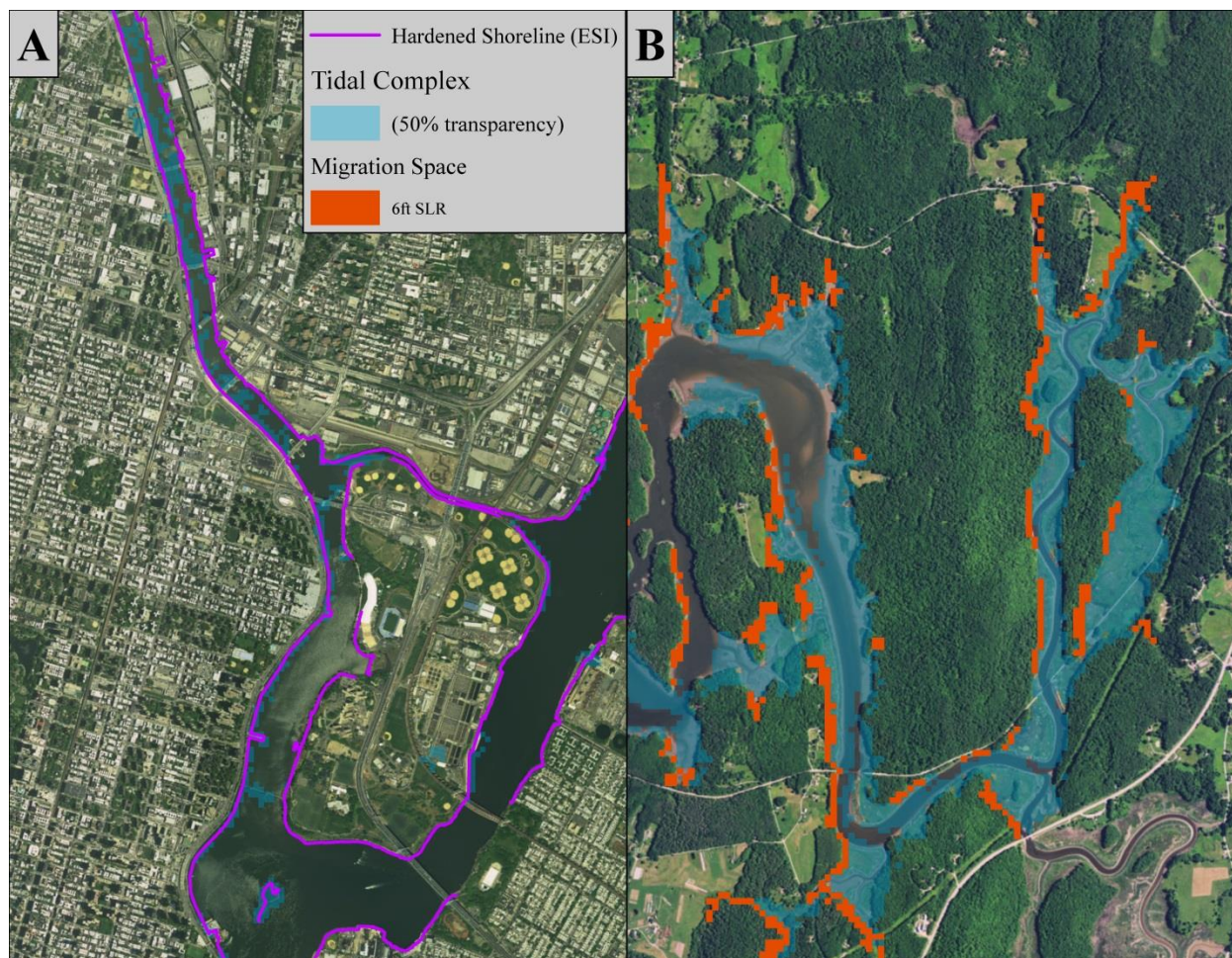
The condition attributes described below are arranged in order of influence. For each, we first describe how the attribute contributes to the site's resilience and then we explain the data sources and method through which we mapped the attribute. The condition attributes were ordered with respect to their direct importance to site resilience, and then weighted on a numeric scale from 1 (low influence) to 5 (high influence). Among the steering committee, there was unanimous agreement on the order of importance and high agreement on the numeric weights. The numeric weights were used as a multiplier when combining factors to give more weight to factors with more influence: 5 (very high), 4 (high), 3 (moderate), 2 (low) and 1 (very low). The numeric weight is listed in parentheses after each attribute.

Current Condition Characteristics of the Existing Tidal Complex

HARDENED SHORELINE (WEIGHT = 5): Tidal complexes with a large portion of their shoreline hardened by roads, revetments, docks, parking lots or other anthropogenic barriers will be less adaptable because those areas are no longer available as habitat and migration of the marsh will be prevented by the barriers.

We calculated the percent hardened shoreline for each site, by using the same approach as described for the shoreline complexity physical attribute to spatially link the NOAA ESI shoreline to the tidal complex units. First, we extracted the manmade shoreline from the ESI and spatially linked it to the tidal complexes. We then spatially linked the full ESI shoreline to each complex. Lastly, we divided the total manmade shoreline length by the full length of the shoreline to calculate the percent of shoreline that was manmade for each tidal complex (Figure 5.8).

Figure 5.8. Tidal complex hardened shoreline. A) Tidal complexes in an urbanized area that have a very high proportion of hardened shoreline. B) Tidal complex with no hardened shoreline.



Current Condition Characteristics of the Migration Space

WATER QUALITY / NITROGEN INPUTS (WEIGHT = 5): Excessive nutrient inputs are the single largest pollution problem impacting US coastal waters (Howarth et al. 2000), and eutrophication results in systems with lower dissolved oxygen, less ability to adapt, and consequently lower resilience. Nitrogen has emerged as a focal nutrient in salt marshes because nitrogen eutrophication can reduce organic matter accumulation by increasing rates of decomposition and hindering sediment accretion, limiting increases in marsh elevation (Olcott 2011). Nutrient loading also leads to weakened root systems and reduced geomorphic stability (Deegan et al 2012).

To estimate and map the nitrogen loading for each tidal complex and migration space we updated the USGS SPARROW 2002 Total Nitrogen model (Moore et al. 2011) using the current 2011 National Land Cover Dataset (NLCD, Homer et al. 2015). To accomplish this, we cross-walked the stream reach dataset (NHDPlus v1, USEPA & USGS 2006) from the 2002 model to the newer 2012 version stream reach dataset (NHDPlus v2, USEPA & USGS 2012). Next, we assembled a variety of hydrologic, geophysical, and land use (2001 NLCD) variables (e.g., % agriculture, % impervious surface, mean base flow, mean contact time, soil texture class, etc.) for the NHDPlus v2 local and cumulative drainage catchments for each stream reach in the project area. We created five total nitrogen yield classes from the Northeastern USGS SPARROW 2002 model (Table 5.2). We assessed the relationship between the spatially explicit catchment variables and the total N yield classes using the 2001 land cover data for which the SPARROW 2002 model was based upon. Specifically, we used the random forest (RF) algorithm in R (Liaw and Wiener 2002) to develop a predictive model between nitrogen class and the predictor variables.

We found a strong relationship between many of the variables and the nitrogen class response variable that allowed us to accurately estimate the 2001 nitrogen class for each stream reach (RF error rate of 15.8%). We used this relationship to estimate the current total nitrogen class, using the newer NLCD 2011 land use data in place of the 2001 NLCD-based variables (Figure 5.9). As multiple streams can flow into a single migration space, we used the NHDPlus v2 cumulative drainage-area of each flowline to calculate a weighted average nitrogen class for each migration space. That is, the total cumulative drainage area of all the streams entering a migration space was calculated, and then the contribution of each flowline to this total was used as each flowline's weight for the predicted nitrogen class average (Figure 5.10). This approach assumes that streams with larger drainage areas will have more influence on the migration space.

Table 5.2. Water quality model classes. Nitrogen yield (kg/km²/yr.) values and their corresponding class used in the water quality model for the migration space units.

Nitrogen Class	Total Nitrogen Yield (Kg/km²/yr.)
1 (Low, good water quality)	< 210
2	210 – 300
3	300 – 470
4	470 – 830
5 (High, poor water quality)	> 830

Figure 5.9. Water quality model results for the project area. The 2011 estimated nitrogen yield is shown for stream reaches in the project area. The reach results were translated to each migration space unit using a cumulative drainage-area weighted average.

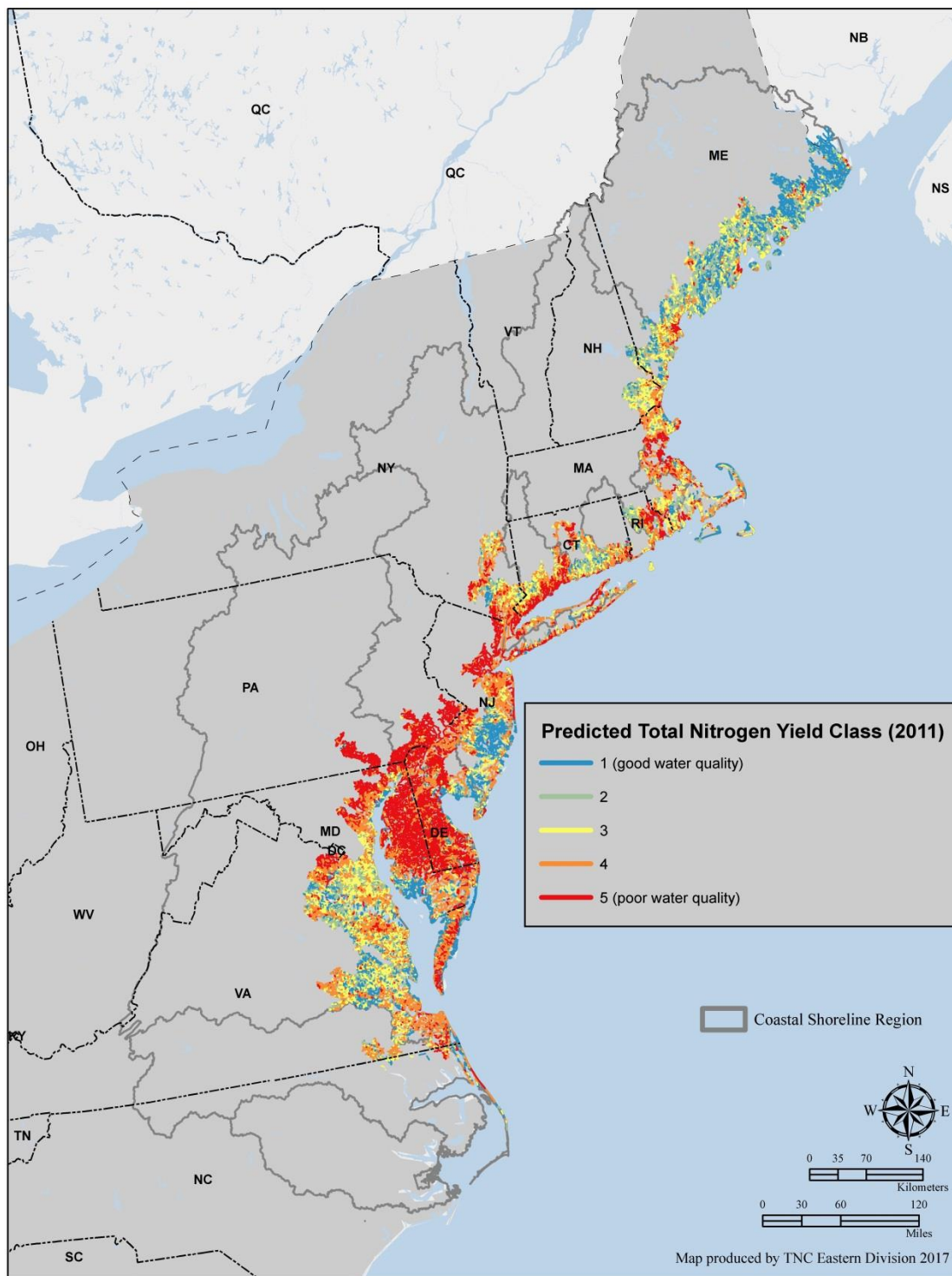
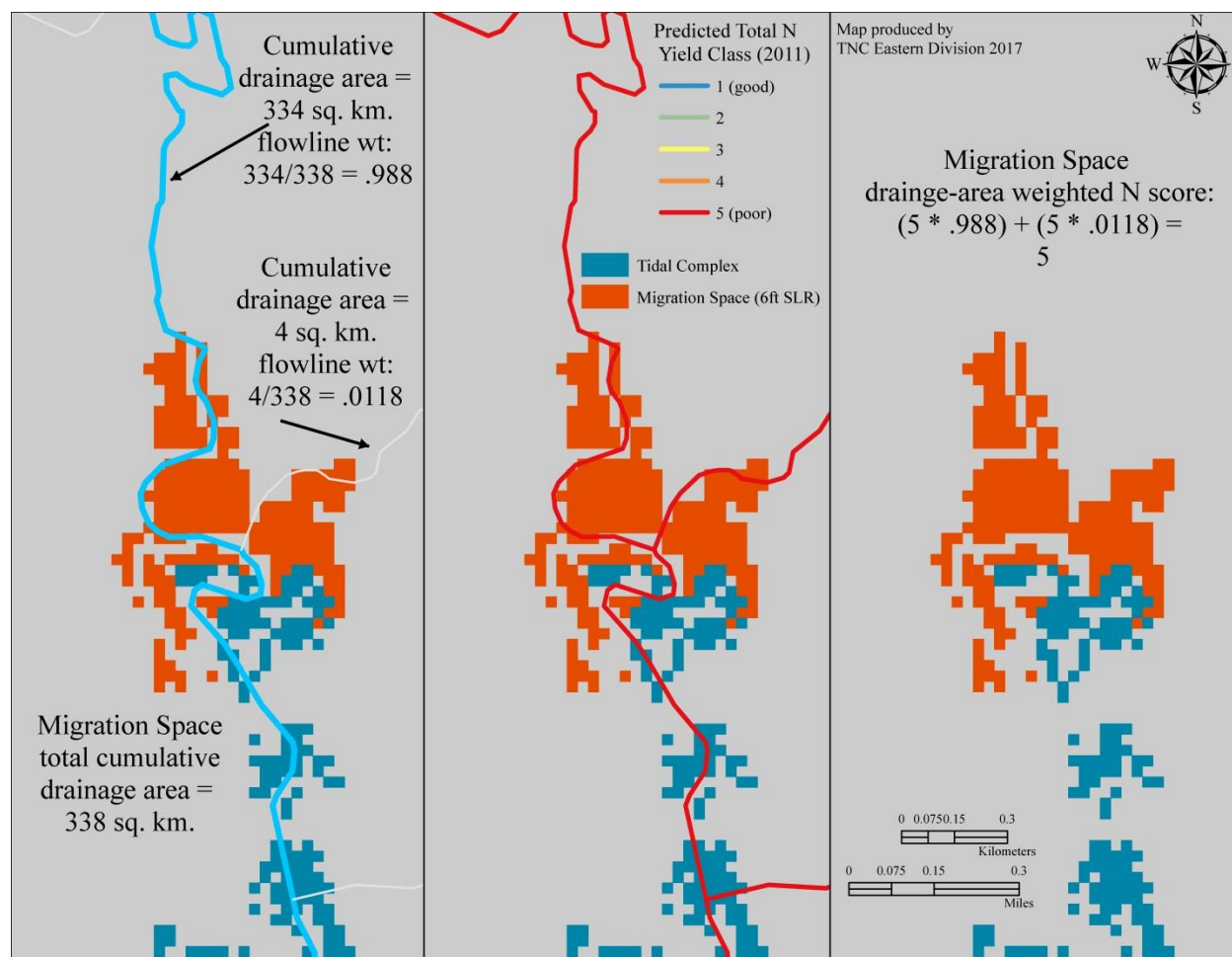


Figure 5.10. Drainage-area weighted average approach. Illustration of the approach that uses the cumulative drainage-area of flowlines or catchments to translate hydrologically-based condition attributes to the migration space unit.



FRESHWATER FLOW (WEIGHT = 4, RIVER-DOMINATED CSRS ONLY): Freshwater inflow is necessary for healthy and productive coastal estuaries and strongly influences the role and abundance of plant composition in tidal wetlands. In drier coastal zones, relatively small changes in rainfall could produce comparatively large landscape-scale changes in the abundance of foundation plant species that would affect some ecosystem goods and services. Whereas a drier future would result in a decrease in the coverage of foundation plant species, a wetter future would result in an increase in foundation plant species coverage (Osland et al. 2014). Freshwater supply must compete with upstream demands from farms, cities, and industry, consequently many coastal sites receive less freshwater than would be expected under natural conditions with the delivery of freshwater altered in timing and quantity. We assumed that sites with natural or less altered flows would be more resilient to environmental and climatic changes because the flow sustains the expected transitions and migration of current tidal complexes into the migration space. The variable was applied only to the two river-dominated shoreline regions where freshwater inputs are a significant part of the tidal system.

Studies have shown a strong relationship between mean annual flow and cumulative drainage area, with drainage area explaining over 90% of observed annual streamflow (Vogel et al. 1999). We used this relationship to determine if the mean annual flow of streams in the project area was greater than, equal to, or less than expected based on drainage area. We used a linear regression to predict cumulative mean annual flow for each NHDPlus v2 flowline using divergence-routed cumulative drainage area. For the dependent flow variable, we used the NHDPlus Enhanced Unit Runoff Method (EROM) gage-adjusted mean annual flow estimate. This dataset is considered the best NHDPlus v2 flow estimate to use in models and analysis (McKay et al. 2012), and is not based on drainage area. The divergence-routed cumulative drainage area was assembled from the NHDPlus v2 value added attributes (VAA) dataset (USEPA & USGS 2012). Both the dependent and independent variables were compiled for flowlines in the two river-dominated coastal shoreline regions (i.e., Chesapeake and Piedmont River and the Northeast River). We log-transformed both variables and stratified by coastal shoreline region for the regression. The resulting relationship was significant ($p \leq 2.2e-16$) and had an adjusted R^2 of 0.9915 (Figure 5.11).

We calculated standardized residuals from the regression and assigned streams to flow alteration classes based on how much their predicted flow deviated from their expected flow (e.g., 1 SD above mean indicates the mean annual flow is one standard deviation higher than expected based on cumulative drainage area, Figure 5.12). To understand what it means to be above the mean for expected flow, we examined the results in conjunction with other datasets (i.e., impervious surface, land use, dams, etc.) and with USGS trends in water use by sector. We found that most systems were altered by some degree of development (i.e. “average” = slightly altered mean annual

flow), while those catchments with above-average expected mean annual flow occur in very intact and natural landscapes. In contrast, systems with below-average expected mean annual flow were in agricultural settings, leading us to conclude that water for agriculture was a key driver of declines in expected mean annual flow. This agrees with a USGS 2010 study (Maupin et al. 2014) that found irrigation accounted for the largest water withdrawals in the US, outside of thermoelectric power, which returns water to the system. Finally, to translate the flow alteration results to the migration space of each unit, we used the same drainage-area weighted average approach as described above for the water quality attribute.

Figure 5.11. Mean annual flow and cumulative drainage area. Plot shows the strong relationship between mean annual flow and divergence-routed cumulative drainage area for flowlines in the two river-dominated CSRs.

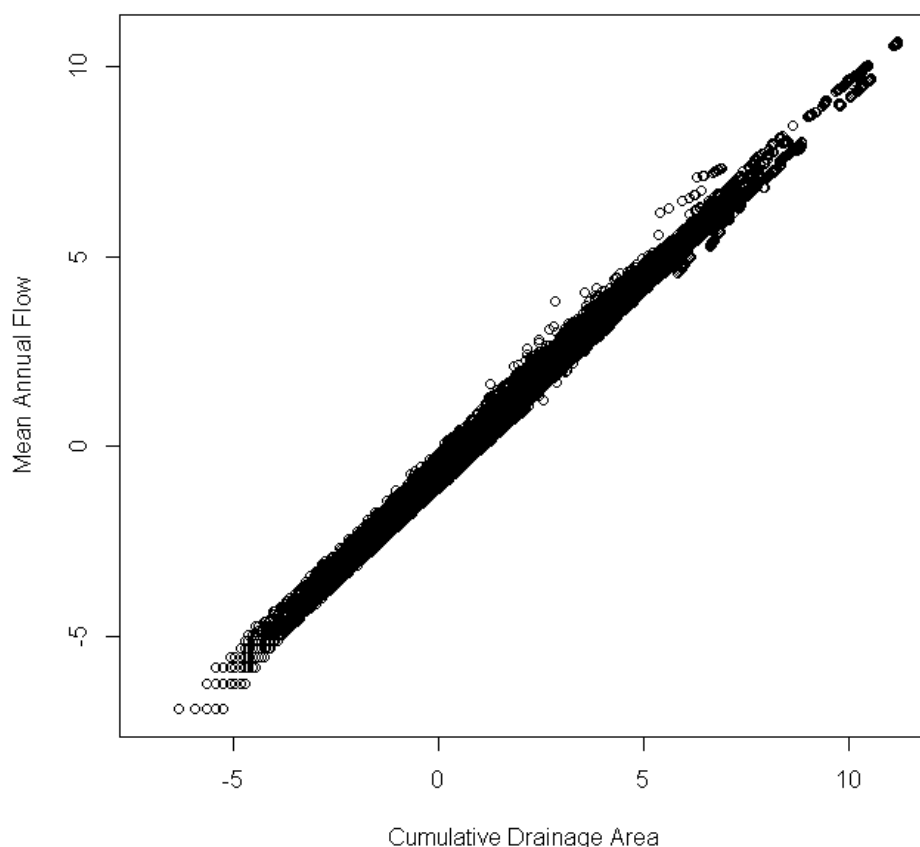
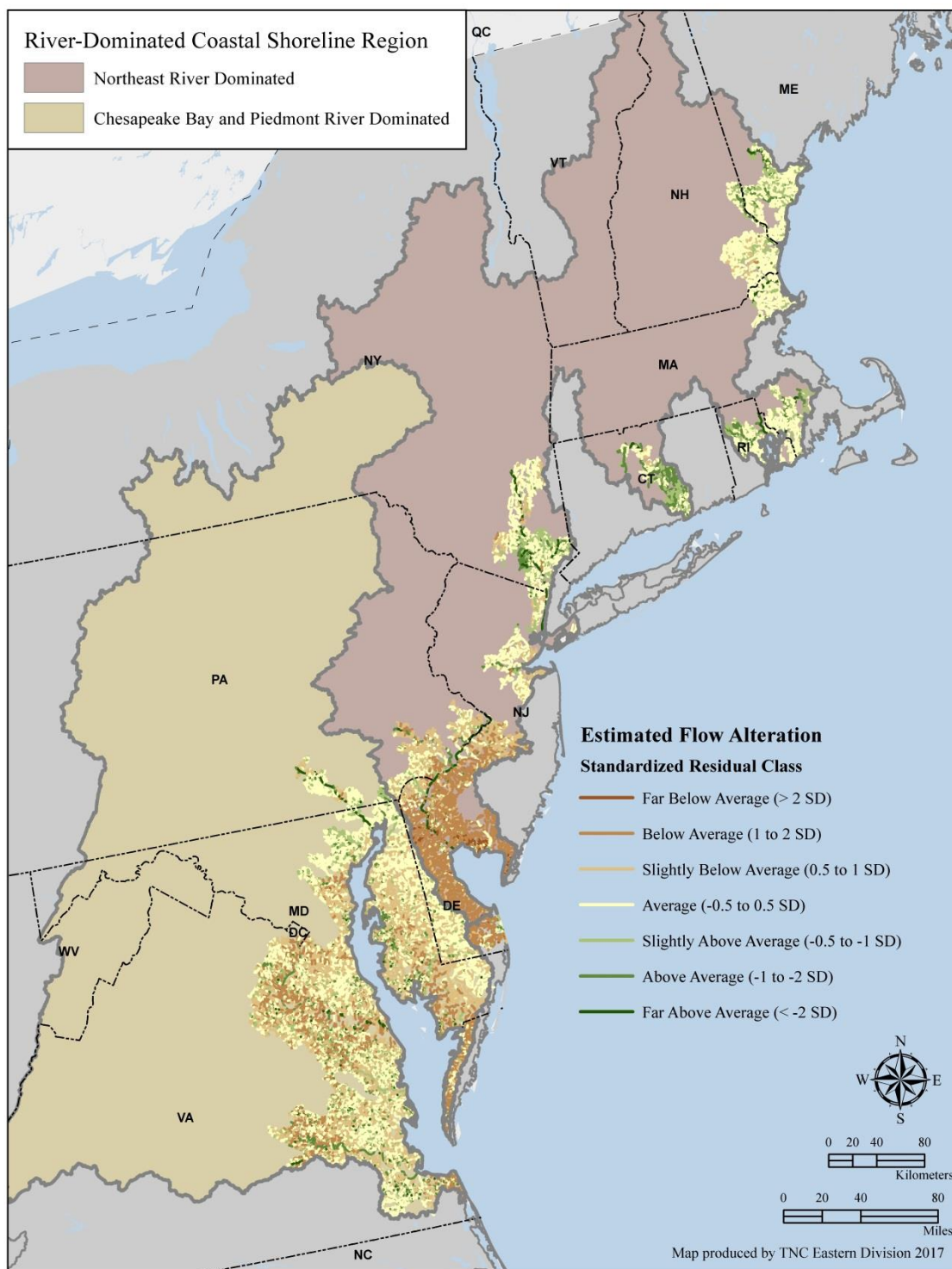


Figure 5.12. Estimated flow alteration for the project area. Estimated flow alteration is shown for stream reaches in the project area with flowlines in yellow indicating locations where mean annual flow is as expected given the drainage area. The reach results were translated to each migration space unit using a cumulative drainage-area weighted average



SEDIMENT INPUT (WEIGHT = 3): Watershed-derived sediment is a key source of tidal wetland accretion. However, because marshes build vertically, lateral erosion can lead to rapid marsh loss. In fact, declines in sediment delivery due to agriculture and dams have played a major role in tidal wetland declines (Weston 2014). A sediment surplus may result in either vertical growth and/or lateral expansion, while a sediment deficit may result in drowning and/or lateral contraction. Many sites in the Northeast are exhibiting a sediment deficit, with half of them having projected lifespans of less than 350 years at current rates of sea-level rise and sediment availability (Ganju et al. 2017).

Absolute sediment inputs differ greatly among marshes. To quantify and map estimated sediment inputs, we developed two separate models: one for large catchments over 1000 km², and one for smaller catchments. For large catchments, we adopted the approach of Weston (2014) who found that 80% of the variation in the flow-weighted average suspended sediment concentrations (FWA-SSC) among large watersheds could be predicted using a simple linear equation with three variables: watershed area, percent agricultural land use, and erodibility (k-factor). For each NHDPlus v2 catchment with a cumulative drainage area greater than 1000 km², we compiled cumulative drainage area from the NHDPlus v2 VAA dataset; calculated percent agriculture using the NLCD 2011; and calculated the average k-factor using SSURGO (gSSURGO 2014). We applied Weston's equation to get an estimate of sediment for each large river system, and converted the estimated FWA-SSC results to rank-based z-scores so the values would be on the same scale as the estimated sediment results for the smaller catchments. Weston's equation was:

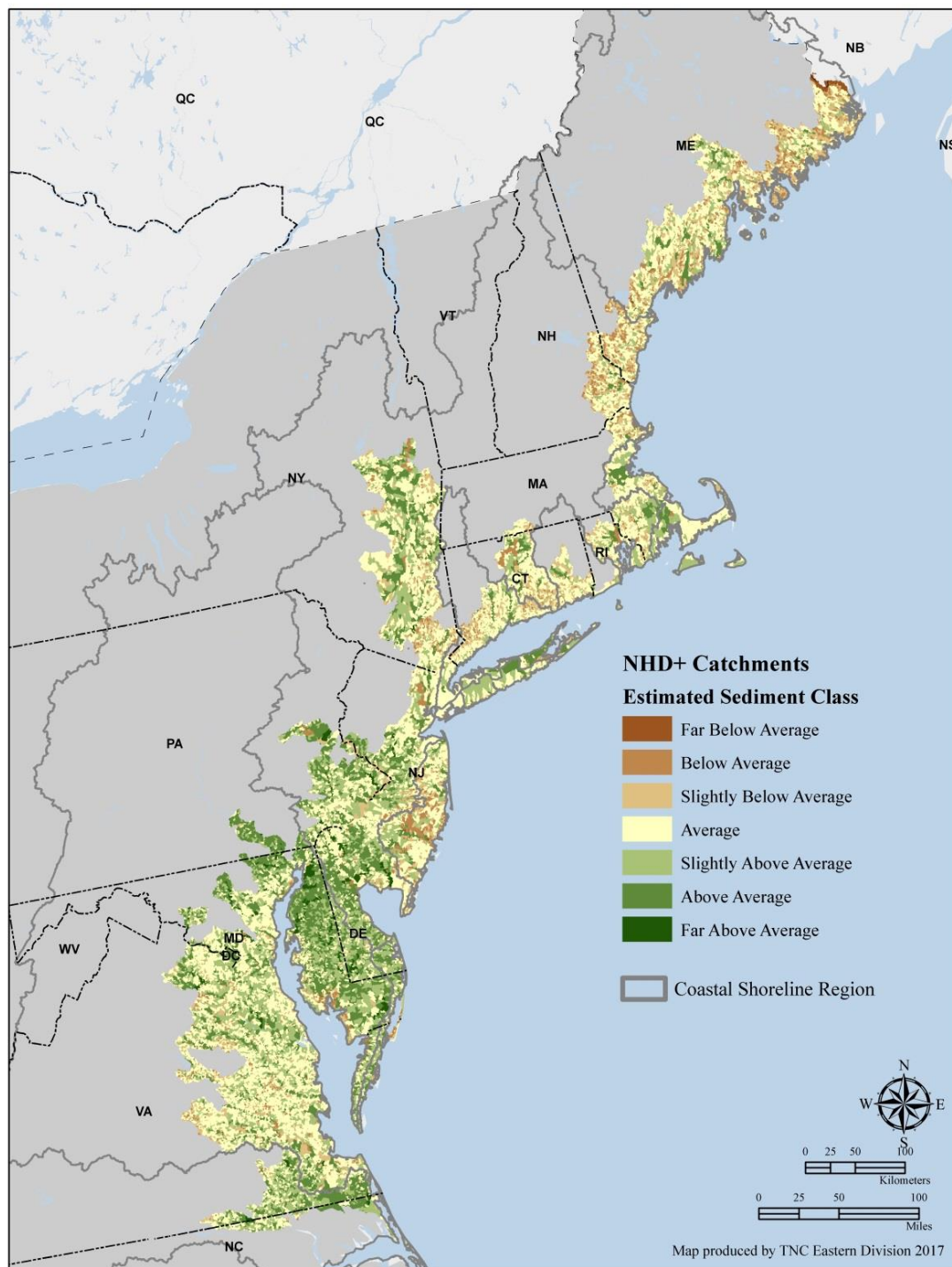
$$FWA-SSC = 64.8 (area) + 0.71(percent\ agriculture) + 87.2(erodibility) - 23.5$$

Weston (2014) found the FWA-SSC linear equation above did not perform well on smaller catchments (≤ 1000 km² cumulative drainage area). For these we used the Natural Capital's InVEST (Sharp et al. 2016) sediment delivery ratio model. This model maps overland sediment generation and delivery to the stream based on seven inputs: (1) a hydrologically modified digital elevation model (from NHDPlus v2), (2) Land Use (from augmented NLCD 2011), (3) Erodibility (k-factor from SSURGO), (4) Rainfall erosivity raster (Renard et al. 1997), (5) Watershed summary unit (NHDPlus v2 catchment), the Universal Soil Loss Equation cover factor (6) and practice factor (7) for each land use class. The output of this model is sediment export in tons per pixel and tons per watershed. Full details on the model can be found at:

<http://data.naturalcapitalproject.org/nightly-build/invest-users-guide/html/sdr.html>.

As we did for the large catchments, we converted the estimated sediment per catchment (tons) to rank-based z-scores. The results for both the large and small catchments were merged into a single dataset (Figure 5.13). Finally, the results were translated to the migration space units using a drainage-area weighted average, as previously described for the water quality metric.

Figure 5.13. Estimated sediment inputs for the project area. The estimated sediment contribution class is shown for NHDPlus catchments in the project area with catchments in yellow indicating locations where sediment inputs are “average,” relative to the project area. The catchment results were translated to each migration space unit using a cumulative drainage-area weighted average.



INTEGRATION OF PHYSICAL AND CONDITION CHARACTERISTICS: The final score for the tidal complex and its migration space was calculated for each site using a weighted sum of the two categories: physical options and current condition as shown below:

Physical Options

Size of Migration Space (5)
Tidal Height Classes (3)
Shared Edge (3)
Shoreline Complexity (2)
Size of Complex (2)
*Static Response (5)**

Weighted Sum = Physical ScoreCurrent Condition

% Hardened Shoreline (5)
Water Quality/Nitrogen (5)
Freshwater Flow (4)
Sediment Inputs (3)

Weighted Sum = Condition Score

*the coastal response model was only applied to 148 sites

Buffer Area

This section focuses on the characteristics of the buffer area surrounding the tidal complex and migration space, and specifically on characteristics that sustain the migrating tidal complex and provide options for species to move and interact with other natural systems. Identification of the buffer area is recognition that the coastal sites occur within a larger landscape, and the quality and condition of each site's surrounding area can affect its long-term resilience. Tidal complexes interact with their inland surroundings through species movement, nutrient and water flow, wind movement and atmospheric cooling. These processes depend on both the physical structure of the buffer area (e.g., size, landforms, and soils) and the condition of the buffer area (e.g., natural cover, connectivity among wetlands). As part of the resilience estimates, physical and condition characteristics of the buffer were given different numeric weights depending on their expected influence on resilience (Box and Figure 5.14).

Buffer Area: Summary of Attributes and Data Sources

Physical Characteristics

Size of the Buffer Area (Weight = 5): A large buffer area provides space for species populations to breed, disperse and migrate, and to accommodate flood and wind disturbances. Data source: augmented version of NLCD 2011 (Homer et al 2015) published in Anderson et al. (2016).

Landform Diversity (Weight = 4): A diversity of available landforms in lands immediately adjacent to the tidal complex and migration space provides more options for species adaptation as they create more habitats and microclimates. Data source: TNC Eastern US Landform Model (Anderson et al. 2016),

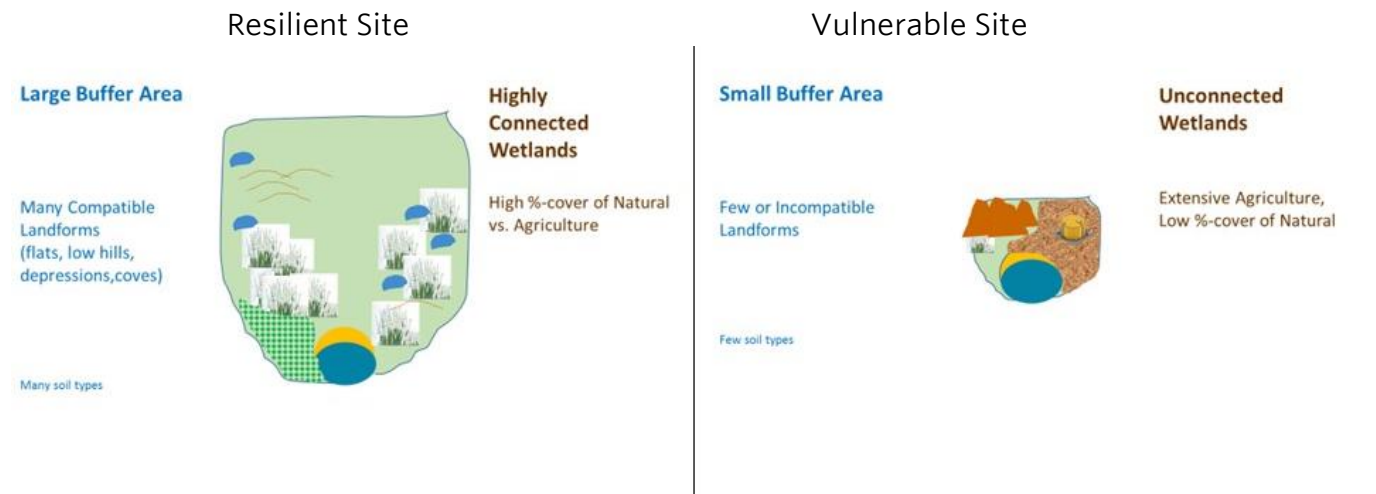
Soil Diversity (Weight = 2): A diversity of soil types in lands adjacent to the sites creates more options for sustaining species diversity as they offer a wider variety of habitats (loam, peat, sand, etc.) Data source: gSSURGO (2014) simplified into 12 major types and published in Anderson et al. (2016).

Condition Characteristics

Wetland Connectedness (Weight = 5): Dense and connected wetlands in the buffer area create a permeable landscape that allows for interactions among freshwater, brackish, and saltmarsh species. TNC landform model (Anderson et al. 2016), UMASS Resistant Kernel Model (Compton et al. 2007).

Percent Natural Cover (Weight = 5): Natural areas in the immediately adjacent buffer area allow the system to interact with other marshes, swamps, forests, and grasslands. Areas currently in agriculture were included in the buffer because they are permeable to movement and will likely revert to marsh, but because they are intensively managed, often treated with chemicals, and regularly replanted, they do not provide the range of options for native species that natural cover does. Data source: augmented version of NLCD 2011 (Homer et al 2015) published in Anderson et al. (2016).

Figure 5.14. Buffer area characteristics that increase resilience. Characteristics of a buffer area expected to improve coastal resilience are shown on the left, and are contrasted with a buffer area that is unlikely to improve resilience on the right. Physical factors are listed in blue and condition factors in brown. Factors with a strong influence are listed in bold and above factors with less influence. The tidal complex is shown as a blue circle at the base.



Physical Options: Resilience characteristics are those that increase the probability that the changing and migrating tidal complex will be nested in a larger landscape that sustains ecological processes. The buffer area's physical characteristics include its size, landforms, and soils, and for each of these we assumed that a larger amount or a higher diversity of features increased resilience by increasing the available habitats, microclimates and options for adaptation. For example, a large buffer area with a range of compatible landforms and soils can sustain a wider diversity of species.

SIZE OF THE BUFFER AREA (WEIGHT = 5): A buffer area provides space for species populations to breed, disperse and migrate, and to accommodate flood and wind disturbances. As the sea level rises, the ecological interactions between the coastal zone and the adjacent terrestrial and freshwater systems will become more critical and thus resilience increases with the size of the surrounding and intact buffer area.

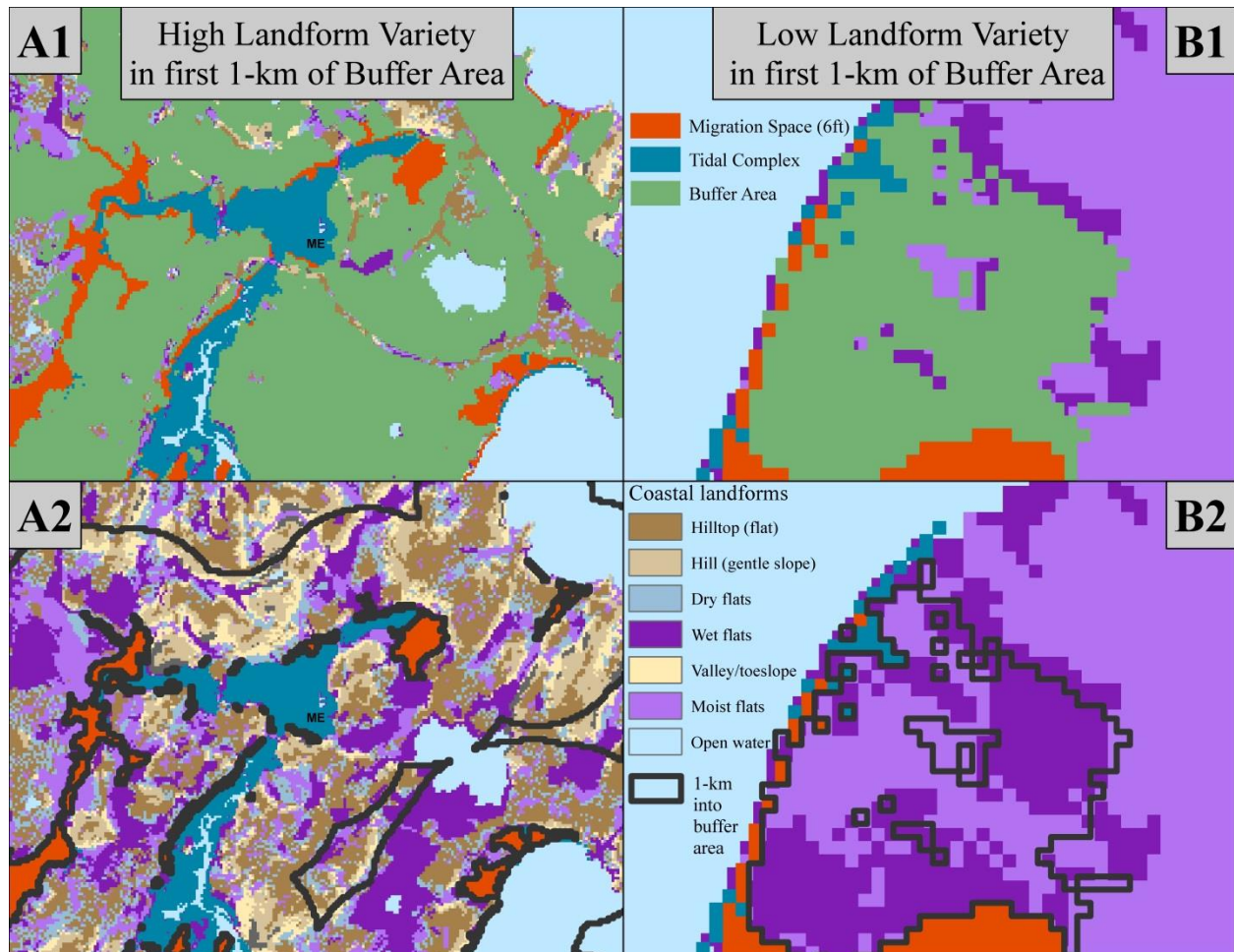
As described in the previous chapter, a one-to-many spatial join was used to link each buffer area polygon with each migration space unit and/or tidal complex unit that it intersected. With the buffer area units linked to the migration space and tidal complex units, the cumulative size of all intersecting buffer areas was calculated for each tidal complex.

LANDFORM DIVERSITY (WEIGHT = 4): A diversity of landforms in land immediately adjacent to the tidal complex and migration space (first 1-km of the buffer area) provides more options for species adaptation in response to SLR because a variety of landforms equates to a variety of habitats and microclimates. For example, depressions, flats, slope bottoms, and hummocks all create complexity and microtopography in the landscape and redistribute moisture and temperature. Landforms compatible with tidal habitats are arguably the most important to the coastal wetlands as they could support species that utilize both fresh and salt water.

We developed a spatially comprehensive map of 17 landform types at a 30-m scale for the entire Eastern US and then extracted 7 types that are compatible with coastal wetlands for this analysis (Anderson et al. 2016). Details on the creation of the landform map can be found in Anderson et al. (2016), and the original map can be viewed at <http://maps.tnc.org/resilientland/>

To measure landform diversity, we tabulated the variety of landforms within a 100-acre circle around each pixel based on 7 landform types compatible with tidal habitats: dry flat, moist flat, wet flat, valley/toeslope, gentle slope, hilltop flat, and open water. Then, we calculated the mean landform variety score in the first 1-km of each buffer area for both migration space and tidal complex units (Figure 5.15). We restricted the analysis to the first 1-km of buffer area for each migration space to ensure we focused on the region most likely to interact with the coastal wetlands. To perform this, we calculated a 1-km Euclidean distance from each migration space for each SLR scenario, and then recoded all distances greater than 0 as 1. We then spatially combined the re-classed Euclidean distance output with the buffer grid for each SLR scenario, and used a Lookup operation in ArcGIS to set the value of the combination grid to the unique ID of each buffer area. We repeated this same process for the tidal complexes.

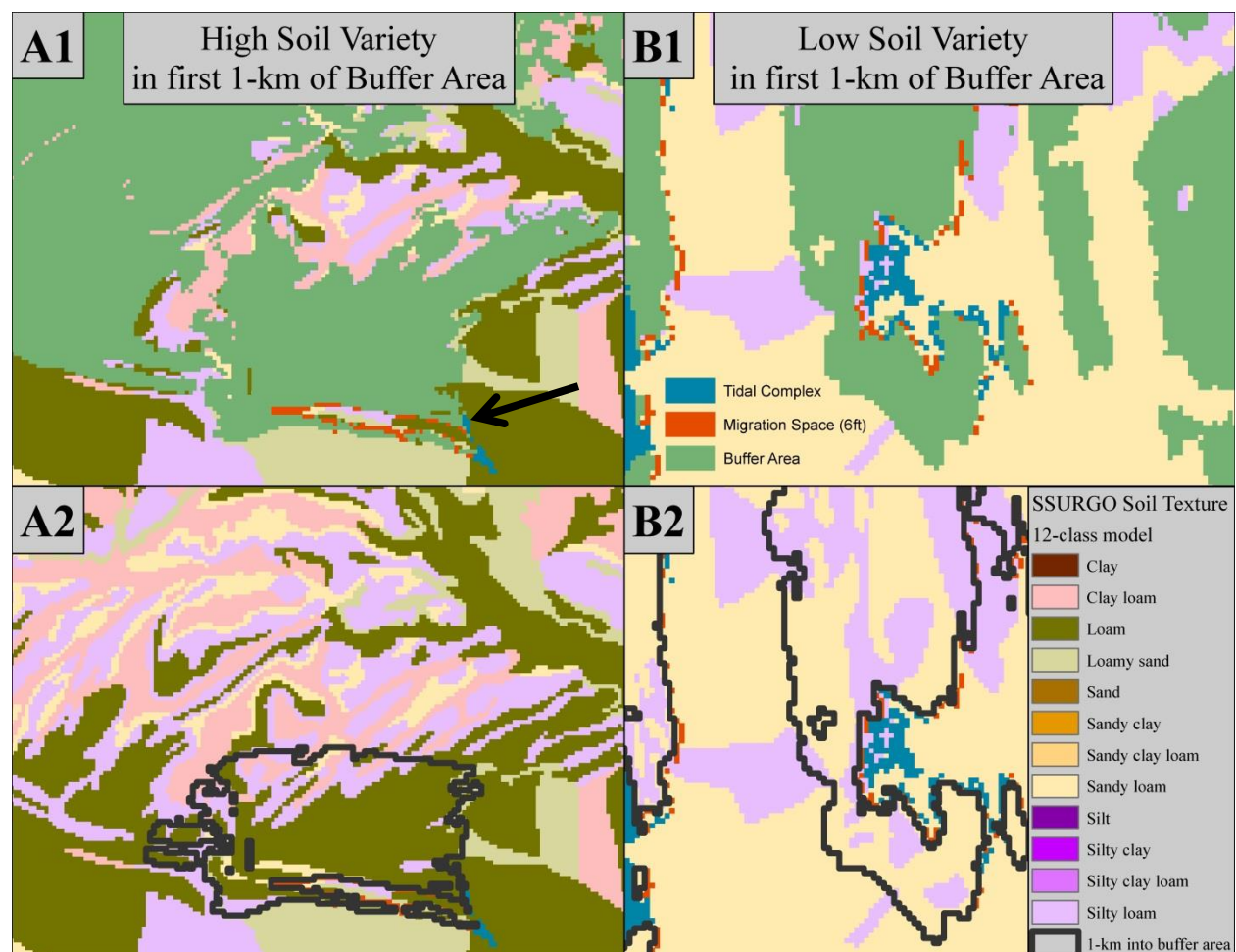
Figure 5.15. Landform variety in first 1-km of buffer area. A1 and A2 show a tidal complex and migration space with high landform variety in the first 1-km of their buffer areas. B1 and B2 show a tidal complex and migration space with low landform variety in the first 1-km of their buffer area.



SOIL DIVERSITY (WEIGHT = 2): A diversity of soil types in lands adjacent to the sites creates more options for sustaining species diversity under SLR. For example, migration space that is adjacent to fertile loams, sandy beach and organic peat will offer a wider variety of habitats than a single soil type could offer.

We measured soil diversity using a spatially comprehensive map of 12 soil texture groups previously assembled from the SSURGO county-level soil texture classes (Anderson et al. 2016, gSSURGO 2014). We calculated soil texture variety within a 100-acre circle around each pixel, and then calculated the mean 100-acre soil texture variety in the first 1 km of each buffer area using the 1-km boundary areas identified for the landform variety metric (Figure 5.16).

Figure 5.16. Soil variety in first 1-km of buffer area. A1 and A2 show a tidal complex and migration space with high soil variety in the first 1-km of their buffer area. An arrow shows the focal complex and migration space. B1 and B2 show a tidal complex with low soil variety in the first 1-km of their buffer area.



Current Condition: The condition of the buffer area was measured by the connectedness of its wetlands and the amount of natural cover. Our assumption was that an intact natural buffer with highly connected wetlands offers more options for adaptation than an agricultural buffer with a few isolated wetlands.

WETLAND CONNECTEDNESS (WEIGHT = 5): This metric measured the density and connectivity among wetlands in the buffer area. A permeable wetland landscape allows for extensive interactions among species that require some degree of freshwater inundation or tolerate a mixture of fresh and salt water. There is strong agreement among scientists that the more connected the landscape is, the more it can facilitate expected range shifts and community reorganization (Heller and Zavalata 2009).

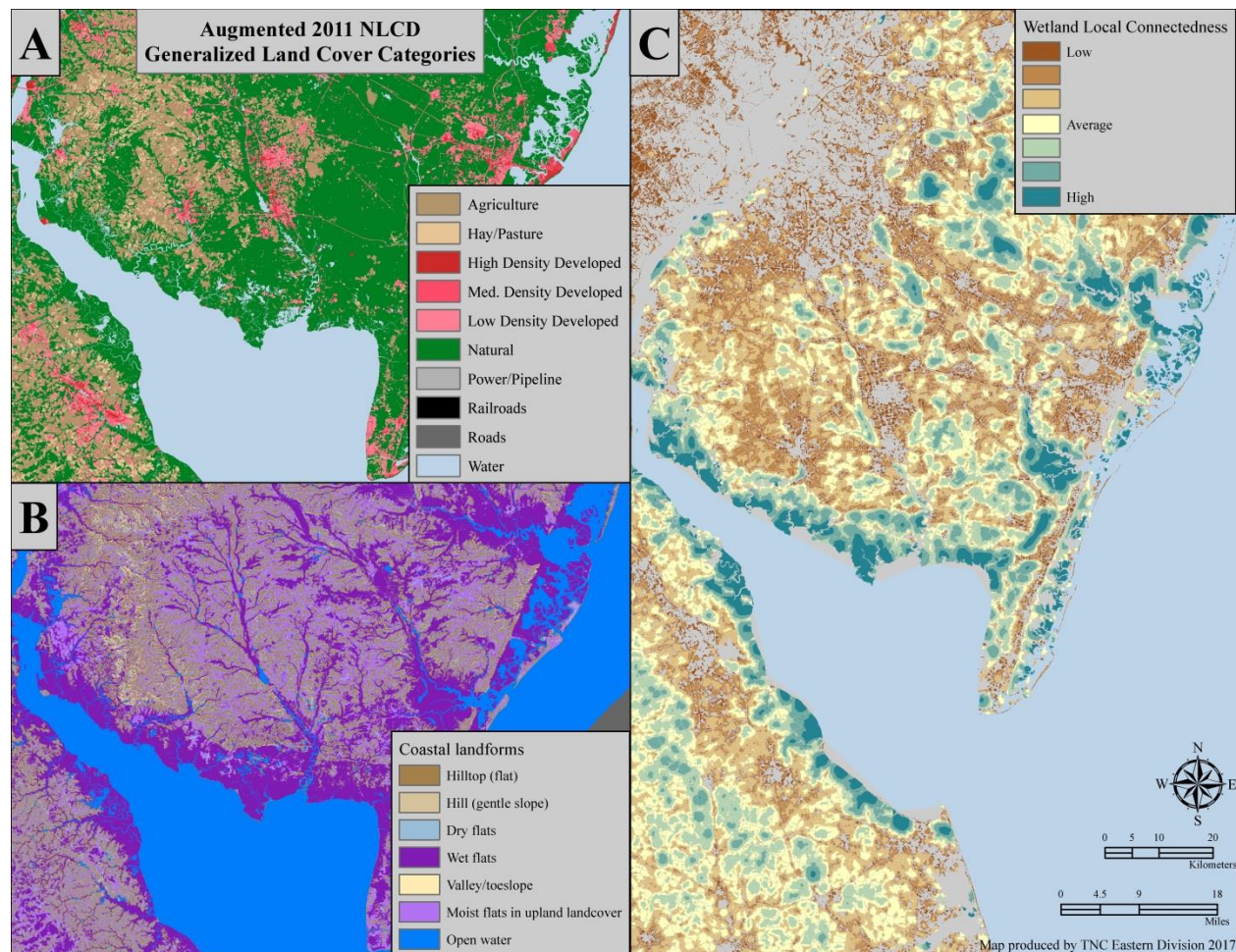
We used resistant kernel analysis to map wetland local connectedness. This analysis was developed by Brad Compton using software developed by the UMASS CAPS program (Compton et al. 2007). Connectedness refers to the connectivity of a focal cell to its ecological neighborhood when it is viewed as a source. The results can reveal the extent that ecological flows outward from the focal cell are impeded or facilitated by the surrounding landscape. To calculate connectedness, each cell of a resistance grid is coded with a resistance weight based on land cover, road class, or landform. The theoretical spread of a species or process outward from a focal cell is a function of the resistance values of the neighboring cells and their distance from a focal cell out to a maximum distance of three kilometers (the recommended distance determined by the software developer).

To identify and map connected wetlands within the buffer area, we used a resistance grid based on landforms. Landforms compatible with coastal wetlands (open water, wet flat, moist flat, dry flat, valley and toeslope, gentle slope, hilltop flat) were given low resistance weights, while developed land and incompatible landforms (sideslope, steep slope, summit, ridge) were assigned high resistance weights (Table 5.3, Figure 5.17). We increased the grid cell size from 30 m to 90 m to run the local connectedness analysis on the resistance surface which allowed us to run the analysis with a reasonable processing time because the CAPS software program is computationally intensive. We averaged the resistance weight values (Table 5.3) of the 30 m cells to the 90 m cells, resulting in a grid of 90-m cells for the project area where each cell was scored with a local connectivity value from 0 (least connected) to 100 (most connected). Lastly, we calculated the average local connectedness score for each buffer unit under each SLR scenario.

Table 5.3. Resistance weights used in the local connectedness model. Small weights indicate landforms that are compatible with coastal wetlands.

Landform	Resistance
Steep slope (cool/warm aspect)	10
Cliff	10
Summit/ridgetop	5.5
Slope crest	7.5
Hilltop (flat)	3.5
Hill (gentle slope)	3.5
Sideslope (cool/warm)	5.5
Dry flats	1.5
Wet flats	1
Valley/toeslope	2
Moist flats	1.25
Flat at the bottom of a steep slope	1
Cove/footslope (cool/warm aspect)	3.5
Open water	1.5
Development	20

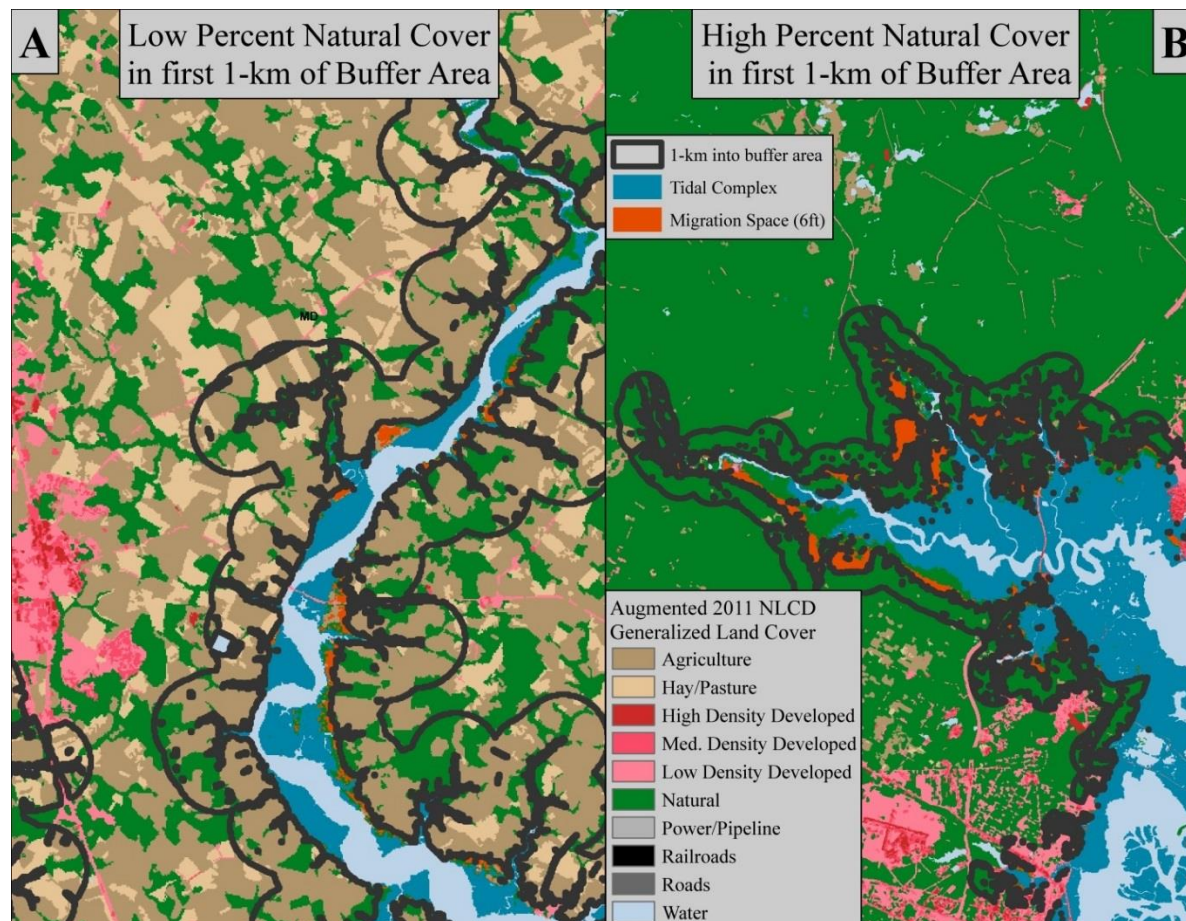
Figure 5.17. Local connectedness components. A) Developed categories in the augmented NLCD 2011 land cover received the highest resistance weight in the local connectedness model. B) Coastal landforms received the lowest resistance weights. C) Local connectedness results for the location.



PERCENT NATURAL COVER (WEIGHT = 5): This metric measured the naturalness of the land cover within the first 1 km of the buffer area. Natural areas immediately adjacent to the migration space and tidal complex allow the coastal systems to interact with freshwater marshes and swamps, coastal forests, and native grasslands, supporting species like marsh hawks and mink that use a mosaic of habitats to meet their resource needs. Areas that are currently in agriculture were included in the buffer because they are permeable to movement by many species and, once inundated, they will likely revert to marsh. However, because agriculture is often intensively managed, treated with chemicals, and regularly replanted, these areas do not provide the range of options for native species that natural cover does.

To measure percent natural cover, we tabulated the area of the natural land cover using the 2011 augmented NLCD generalized land cover dataset (Anderson et al. 2016) for the first 1-km of each buffer area adjacent to the migration space or tidal complex. The 1-km boundaries were delineated for the landform variety metric as previously described (Figure 5.18).

Figure 5.18. Natural land cover in the first 1-km of the buffer area. A) Buffer areas with high proportions of agricultural land use immediately adjacent to tidal complex and migration space units. B) Tidal complex and migration space units with very natural buffer areas.



Integration of Physical and Condition Characteristics

The final score for the buffer area was calculated for each site as a weighted sum of the two categories: physical options and current condition as shown below:

Physical Options

- Size of Buffer Areas (5)
- Variety of Landforms (4)
- Variety of Soil Classes (2)

Weighted Sum = Physical Score

Current Condition

- Wetland Connectedness (5)
- Percent Natural Cover (5)

Weighted Sum = Condition Score

Integration

The final resilience score was calculated for each site as the weighted sum of the tidal complex and migration space score (80%) and the buffer area score (20%). In turn, the final score for each the migration space or buffer area was itself calculated from the weighted sum of the physical and condition scores:

<u>Tidal Complex / Migration Space (80%)</u>	<u>Buffer Area (20%)</u>
Physical Options	Physical Options
Size of Migration Space (5)	Size of Buffer Areas (5)
<i>Static Response</i> (5)	Variety of Landforms (4)
Tidal Height Classes (3)	Variety of Soil Classes (2)
Shared Edge (3)	Current Condition
Shoreline Complexity (2)	Wetland Connectedness (5)
Size of Complex (2)	Percent Natural Cover (5)
Current Condition	
% Hardened Shoreline (5)	
Water Quality/Nitrogen (5)	
Freshwater Flow (4)	
Sediment Inputs (3)	
<hr/>	
= Complex/Migration Space Score	= Buffer Area Score

Site Resilience Score = $0.80 \times \text{Complex/Migration Space Score} + 0.20 \times \text{Buffer Area Score}$

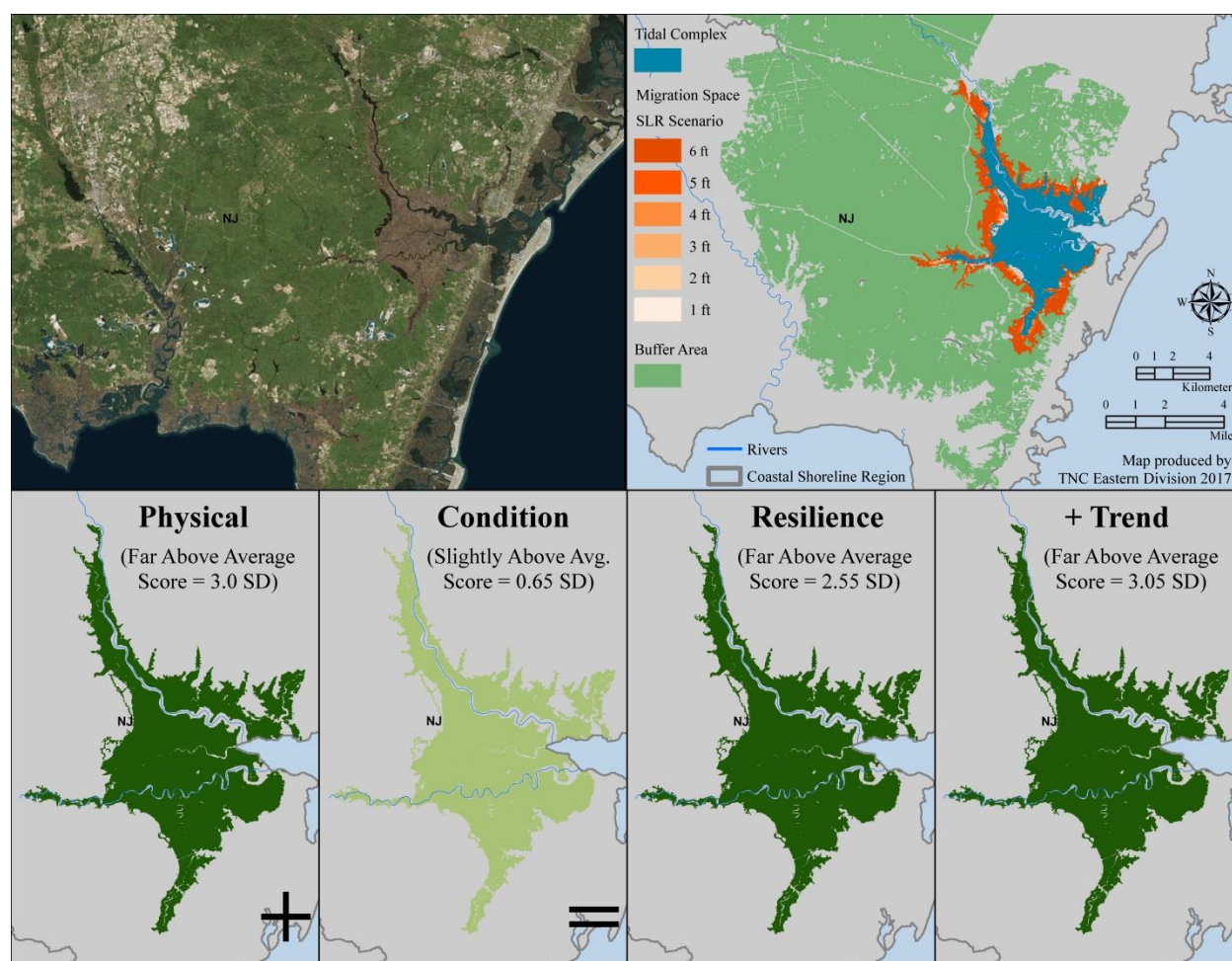
The final scores were converted to standard normal units (z-scores) relative to the site's coastal shoreline region (river dominated, lagoon, etc.). To create the final scores, we calculated the mean and variance of site resilience scores within each coastal shoreline region (z-scores have a mean of 0 and standard deviation of 1). Use of this scheme assumed that the scores followed a normal distribution with a mean and standard deviation that accurately summarized the data. Rank based z-scores were used where the distribution of raw scores did not approximate a normal distribution or could not be transformed into a normal distribution. We grouped the scores into the following categories, which are used throughout the results section and serve as the legend for the various maps:

- Far below average (<-2 standard deviations) - Most Vulnerable
- Below average (-1 to -2 standard deviations) - More Vulnerable
- Slightly below average (-0.5 to -1 standard deviations) - Somewhat Vulnerable
- Average (-0.5 to 0.5 standard deviations) - Average
- Slightly above average (0.5 to 1 standard deviations) - Somewhat Resilient
- Above average (1- 2 standard deviations) - More Resilient
- Far above average (>2 standard deviations) - Most Resilient

Following this scheme ensured that the results were seamless across the Northeast and Mid-Atlantic coast, and allows comparisons with our terrestrial resilience analysis.

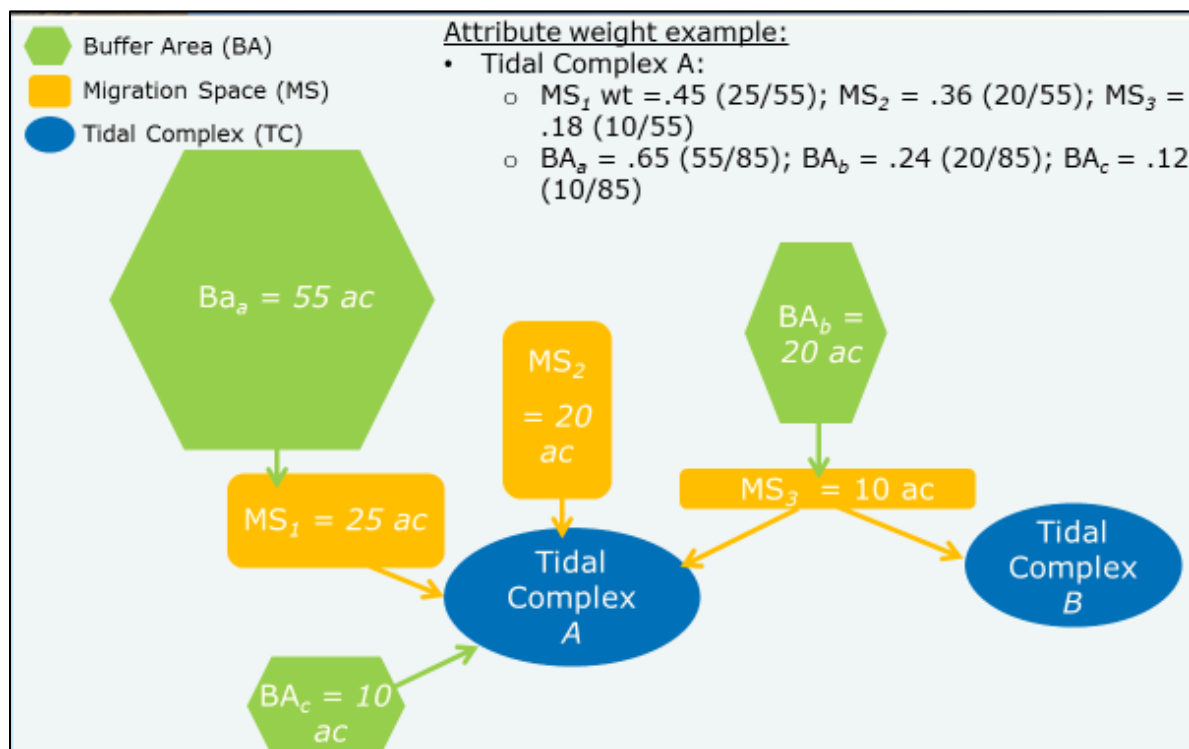
The results we present focus on both the 6-foot scenario, and the 6-foot scenario with trend, as these provide the most comprehensive estimate of a site's resilience over the next century. However, we calculated scores for each of the six SLR scenarios, and these results are available to download (Figure 5.19).

Figure 5.19. Calculating estimated resilience. This image shows the process used to estimate the resilience score for a tidal complex in Tuckahoe, NJ.



Spatial Integration: We have described the analysis process as if each tidal complex had its own migration space and buffer area. In reality, different tidal complexes often share the same migration space and buffer area, and one tidal complex can potentially have several migration spaces. To address this, we used a spatial model that assigned the influence of each component in proportion to the spatial extent of each component for the focal tidal complex. For example, if a tidal complex had two migration space units, one covering 75% of the total migration space area and the second covering 25% of the area, the attributes of the first would be weighted by 0.75 and the characteristics of the second would be weighted by 0.25 when combined into a final score for the site (Figure 5.20).

Figure 5.20. Approach to calculate physical and condition attribute values for the tidal complex unit.



ADDITIONAL CHARACTERISTICS TO INFORM MANAGEMENT STRATEGIES

Securement

As migration space represents potential future habitat for important and productive coastal systems, we examined how much of this critical land is already in permanent protection. We used information from TNC's Eastern Conservation Science team's 2013 dataset of Secured Land. Specifically, we extracted all parcels that were permanently protected from development (GAP status 1, 2, or 3, Crist et al. 1998). We overlaid the selected secured lands with the migration space polygons and calculated the percent of each unit for each SLR scenario. We also examined the percent securement by each estimated resilience class for each SLR scenario.

Migration Space Development

Due to inconsistencies in the spatial resolution of various datasets used in this analysis (i.e., 10-m elevation and 30-m land cover products), and how roads are inaccurately mapped in base land cover grids such as the NLCD and C-CAP products, there are cases where some development occurs within the migration space mapped at the 30-m scale. We used the development categories in our augmented NLCD 2011 land cover grid to calculate how much of each migration space for each SLR scenario was developed.

Migration Space Future Development

Development is perhaps the greatest and most permanent threat to natural systems. In the US between 1982 and 2001, more than 34 million acres of open space were lost to development, about 6000 acres per day or 4 acres a minute. In addition to habitat destruction, high-density development of natural habitats can transform a landscape by changing local hydrology, increasing recreation pressure, and introducing invasive species either by design or by accident (e.g., introduced by vehicles). Moreover, urbanization and fragmentation are inextricably linked since the dispersal and movement of forest plants and animals are disrupted by development and roads. We used future development predictions to examine the risk of development by 2100 in migration space units. We extracted pixels that were modeled to be developed in 2100 in the 30-m Land Transformation Model (LTM) Version 3, developed by the Human-Environment Modeling and Analysis Laboratory at Purdue (Tayyebi et al. 2013), and that were not currently in permanent protection. We then calculated the percent of each migration space that was expected to be developed by 2100. This information can be used by natural resource managers to understand the potential for development in important migration space areas.

RESULTS

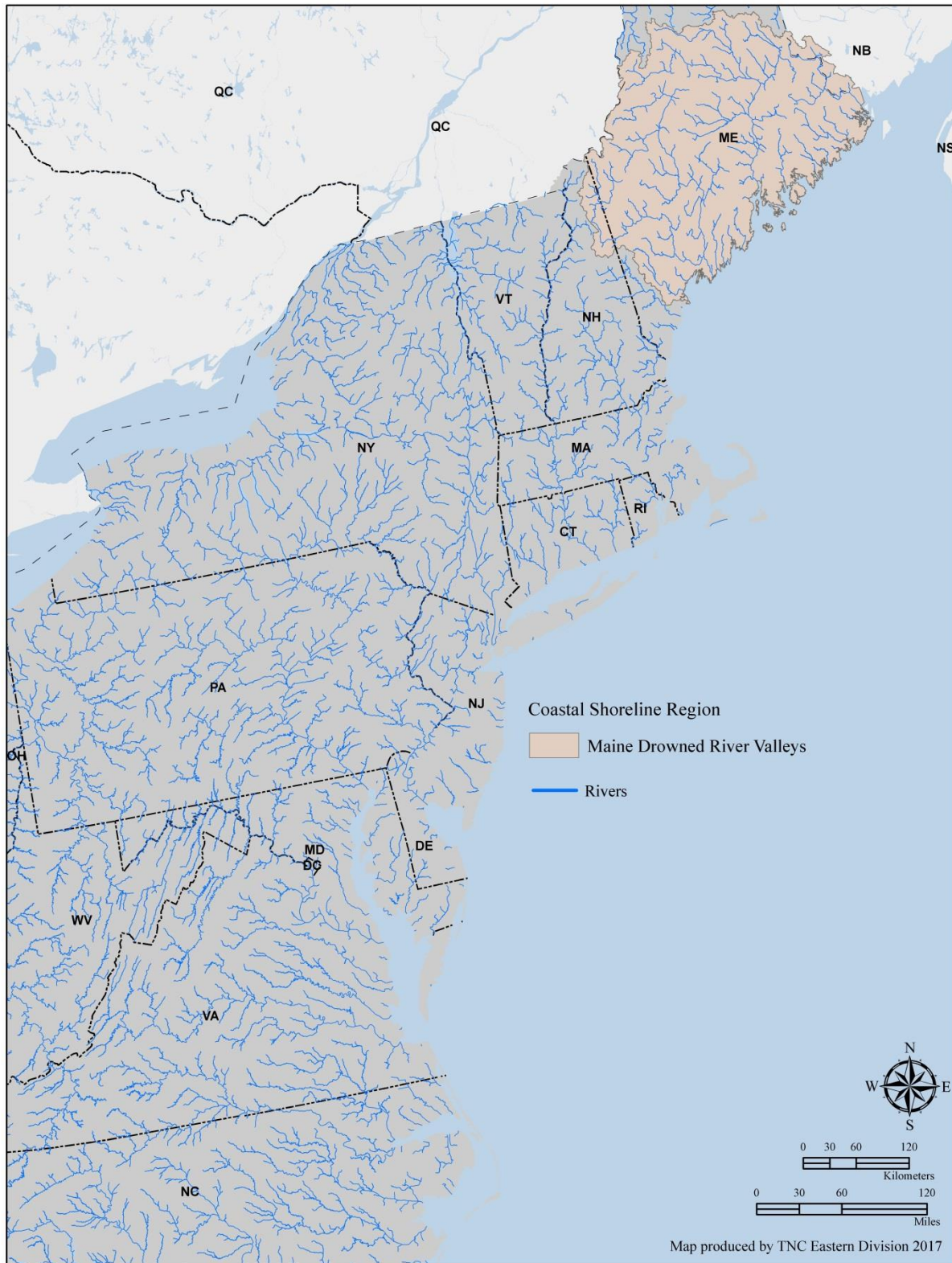
This section presents the results of the 6-foot SLR scenario for each coastal shoreline region. Although we calculated all the physical, condition, and final resilience scores for each tidal complex unit under each sea level rise scenario, we chose to show the 6-foot scenario as it identifies the sites that were robust to the most extreme events. Many sites had ample migration space until the 3-foot SLR scenario, when the space began to decrease or disappear with further inundation. In the results presented here, these sites were scored as more vulnerable than sites that continue to have migration space even at 6 feet of inundation.

Six feet of SLR is well within the realm of possibility in the next century. New techniques to better incorporate Antarctic ice sheet dynamics in global sea level modeling have led researchers to conclude that oceans could rise more than six feet by 2100 under current emissions rates, essentially doubling previous projections (DeConto & Pollard 2016). Furthermore, recent studies suggest that the US Atlantic coast is particularly vulnerable to sea level rise due to enhanced warming and slowing of the Atlantic Ocean circulation (Krasting et al. 2016, Saba et al. 2016, Sallenger et al. 2012), as well as high subsidence rates relative to global rates (Karegar et al. 2016). Regardless of the exact increase in Atlantic Ocean levels by 2100, seas will continue to rise beyond 2100 and it is critical that conservation and restoration actions be undertaken now to prepare for this future reality. Thus, the following sections highlight the results for the 6-foot scenario for each CSR.

This section summarizes the results across all shoreline units starting with the North and moving South. It is organized so that readers can focus on the regions that interest them, and the sections can stand alone as individual documents:

- Maine Drowned Rivers and Valley
- Northeast River Dominated
- Southern New England Embayment
- Mid Atlantic Lagoon
- Chesapeake Bay and Piedmont River Dominated
- Full Region

Maine Drowned River Valleys CSR: Results



The Maine Drowned River Valleys CSR had the smallest number of tidal complex units in the project area with a total of 650. The average size of the tidal complexes was 63 acres with a median size of 8 acres. The largest unit in this CSR was 4344 acres (Figures 7.1-7.2).

Figure 7.1. Distribution of tidal complex size (acres) by ten size classes in the Maine Drowned River Valleys CSR.

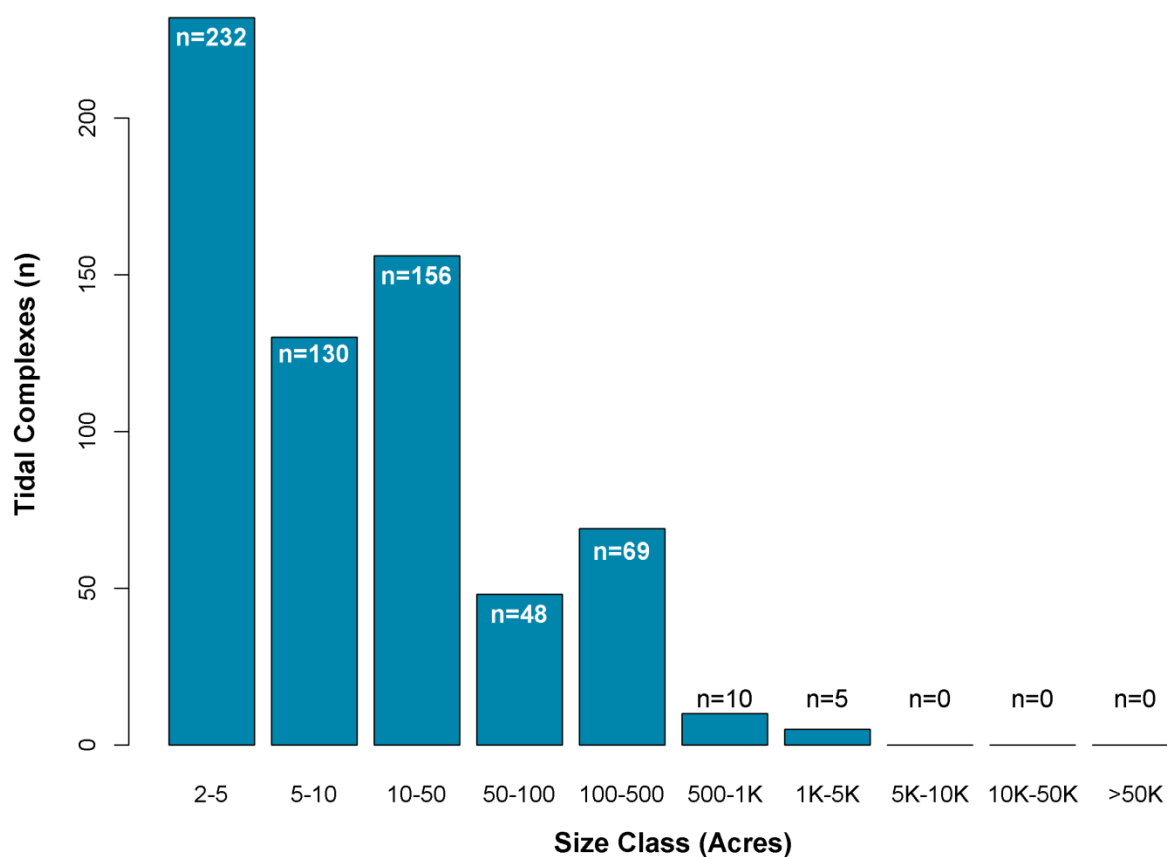
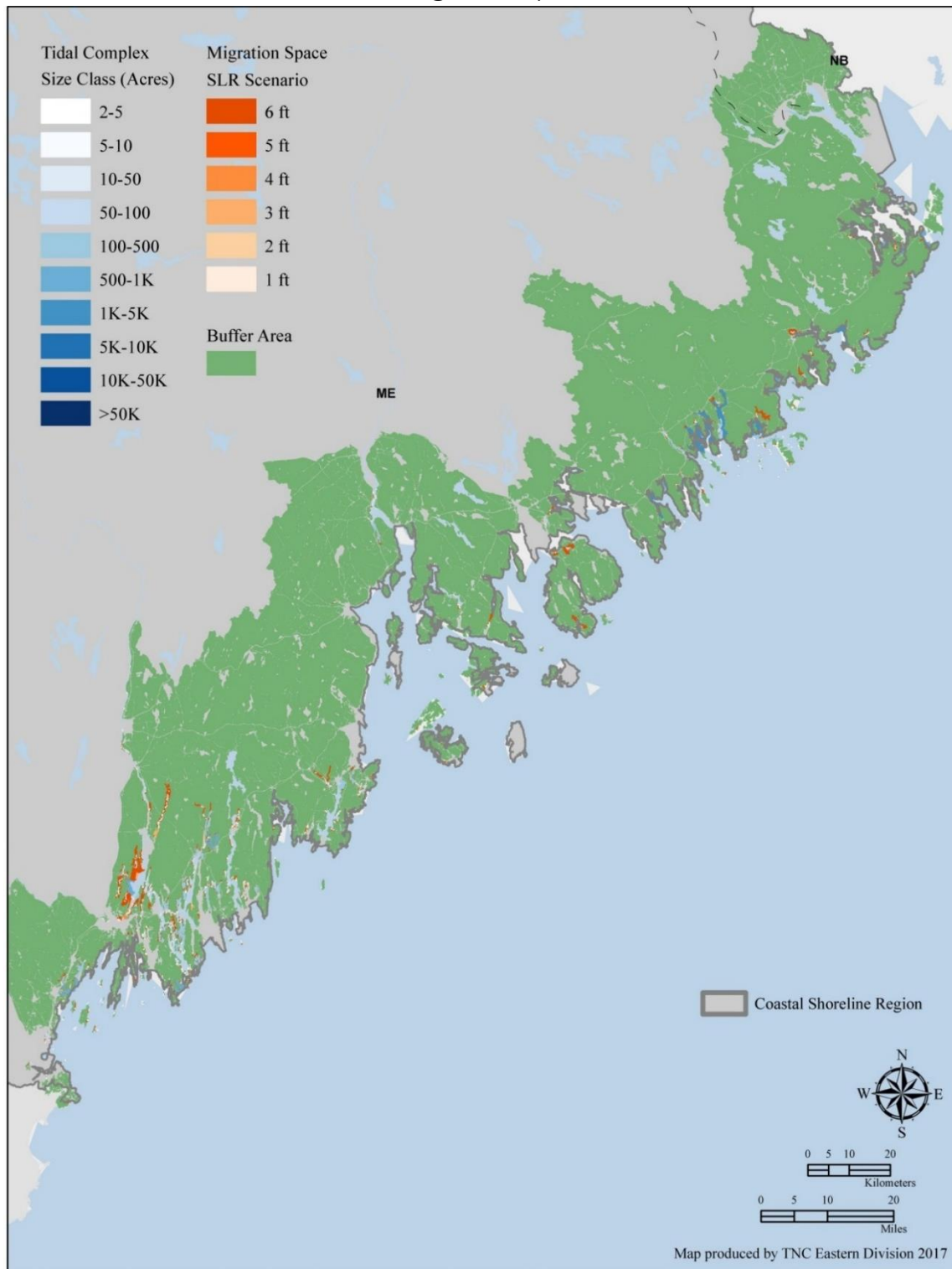
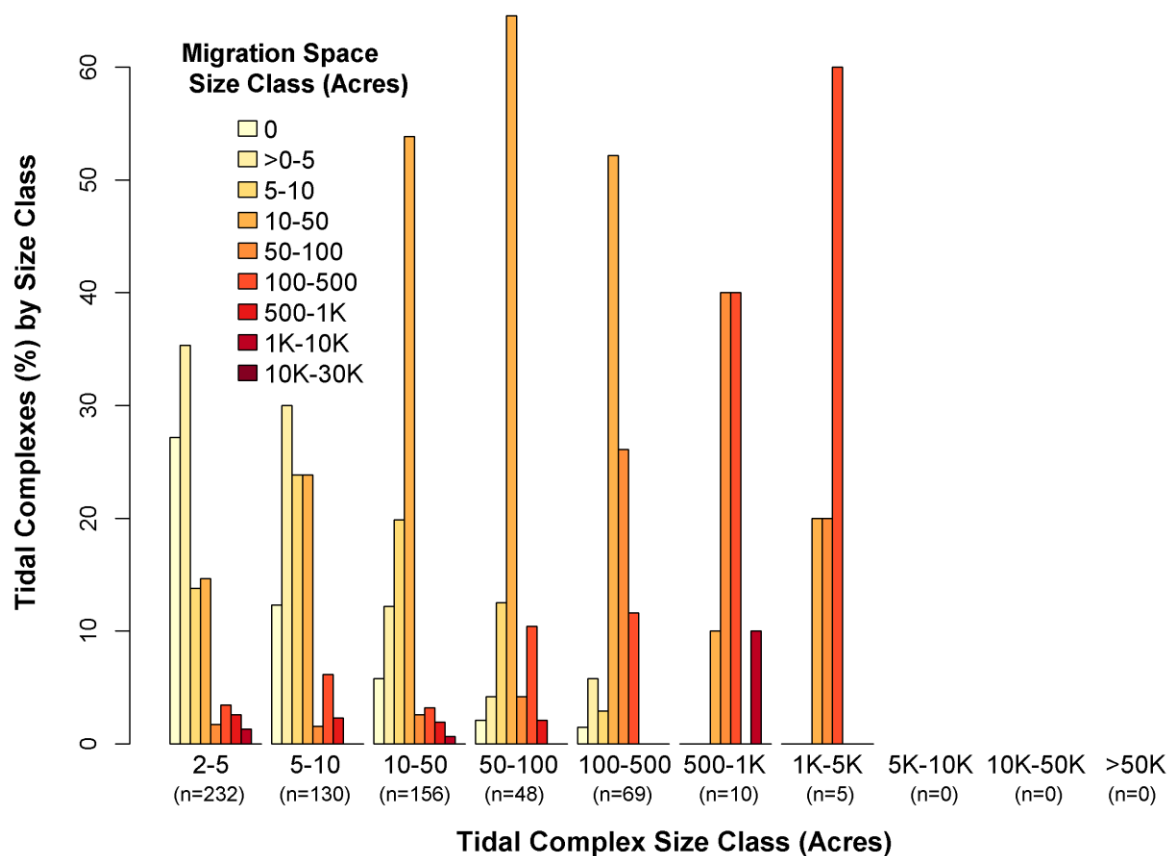


Figure 7.2. Tidal complex, migration space, and buffer area units in the Maine Drowned River Valleys CSR. The color of the tidal complex units reflects their size class (n=10), while the color of the migration space indicates the SLR scenario (n=6).



Of the 650 tidal complexes, 560 (86%) had migration space at a sea level rise of 6 feet (Figure 7.3), the highest percentage of all the CSRs. The average migration space size was 57 acres with a median size of 9 and a maximum size of 2696 acres. As Figure 7.3 shows, small tidal complexes had a wide variety of migration space sizes but most of the small tidal complexes had small migration space areas (size class >0 to 5). However, the largest tidal complexes in this CSR (≥ 500 acres) all had large migration space areas, reflecting the larger geophysical setting within which these tidal complexes occur.

Figure 7.3. Migration space class distribution by tidal complex size class for the 6-foot sea level rise scenario. The y-axis is the percent of tidal complexes within a size class that had migration space of a particular size. Small migration space size classes are shown in light yellow shades that transition to darker oranges as the migration space size class increases.

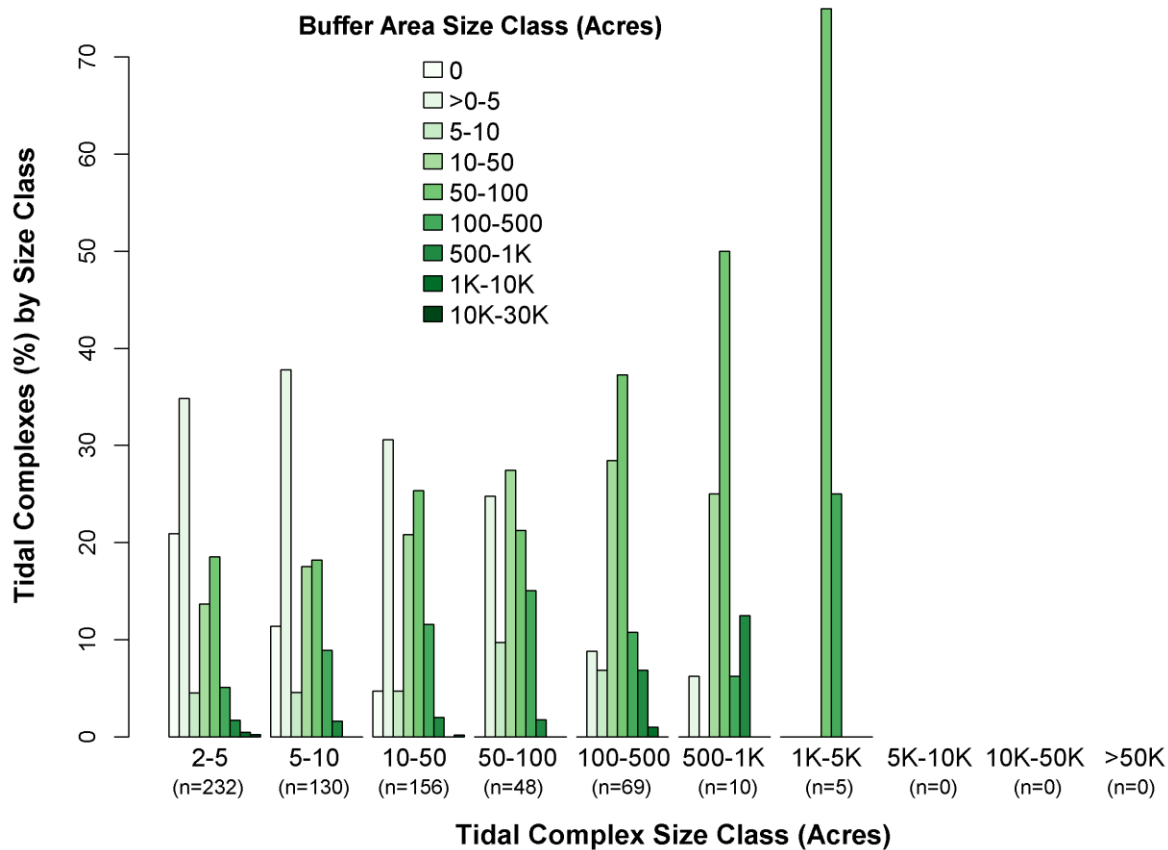


A Spearman's rank-order correlation found the tidal complex size and migration space size were strongly and positively correlated, and this relationship was statistically significant ($r_s = .52$, $p < 2.2e-10$). This strong correlation, compared to that found in the other CSRs, is likely due to the physical structure of the coastline in this region. Maine's coast is rocky and rugged with coves and cliffs that can constrain tidal marsh and its

migration space. The presence of a larger tidal complex in this region is probably indicative of a flatter and less constrained portion of the coastline where there is also likely to be a larger area available for migration.

Most of the tidal complexes, 636 (98%) had buffer area at a sea level rise of 6 feet (Figure 7.4), the highest percentage of all the CSRs. The mean buffer size was 231,100 acres with the largest buffer area encompassing over 1M acres, the largest across all the regions. The large and intact buffer areas reflect Maine's undeveloped landscape relative to the other states in the project area. All tidal complexes of 1000 acres or greater had large buffer areas whereas tidal complexes less than 1000 acres had a mix of buffer area sizes (Figure 7.4). There was a moderately positive and significant relationship between tidal complex size and buffer area size ($r_s = .37$, $p\text{-value} < 2.2e-16$).

Figure 7.4. Buffer area class distribution by tidal complex size class for the 6-foot sea level rise scenario. The y-axis is the percent of tidal complexes within a size class that had buffer area of a particular size. Small buffer area size classes are shown in light green shades that change to darker greens as the buffer area size class increases.



Physical and Condition Scores

The estimated resilience score for a tidal complex consists of the condition and physical components, each weighted equally. Figure 7.5 shows the geographic distribution of physical scores within the CSR for a sea level rise of 6 feet. As both Figure 7.5 and Table 7.1 show, most scores fall in the “average” class, with the next largest category being the “far below average” category. This contrasts with all the other CSRs, except for the Chesapeake Bay, where the highest proportion of scores occur in the “far below average” category for both the physical and condition components. The lowest scoring tidal complexes are predominantly those with no migration space and a less geophysically diverse buffer area. The spatial pattern of the condition scores is shown in Figure 7.6 with the numeric distribution highlighted in Table 7.1. This region had the lowest proportion of tidal complexes in the “far below average” category for both the physical (16%) and condition (6%) characteristics.

Figure 7.5. Estimated physical score for the Maine Drowned River Valleys CSR. Tidal complex units in green score “above average” and had physical characteristics hypothesized to increase resilience including a large migration area with a diversity of tidal classes that are evenly distributed, a complex shoreline, and a geophysically diverse buffer area. Tidal complexes in yellow had “average” physical characteristics relative to all the units in the CSR. Tidal complexes in brown are “below average” and are estimated to respond poorly to sea level rise.

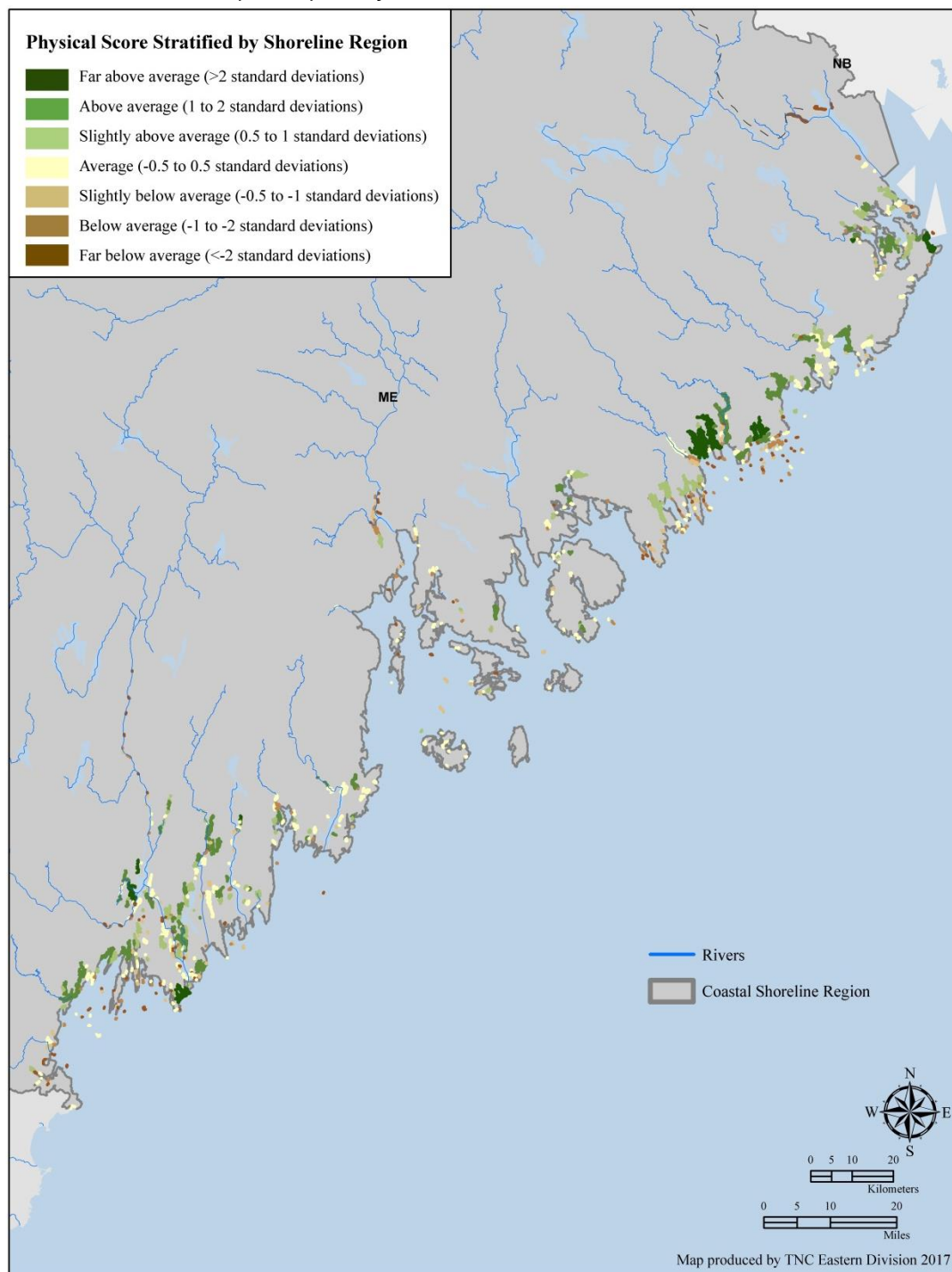


Figure 7.6. Estimated condition score for the Maine Drowned River Valleys CSR.

Tidal complex units in green score “above average” and are estimated to be in good condition based on a low percentage of hardened shoreline; good water quality and quantity, and high sediment contributions in the migration space; and a natural buffer area with highly connected wetlands. Tidal complexes in yellow are “average.” Tidal complexes in brown are “below average” and are estimated to be in poor condition.

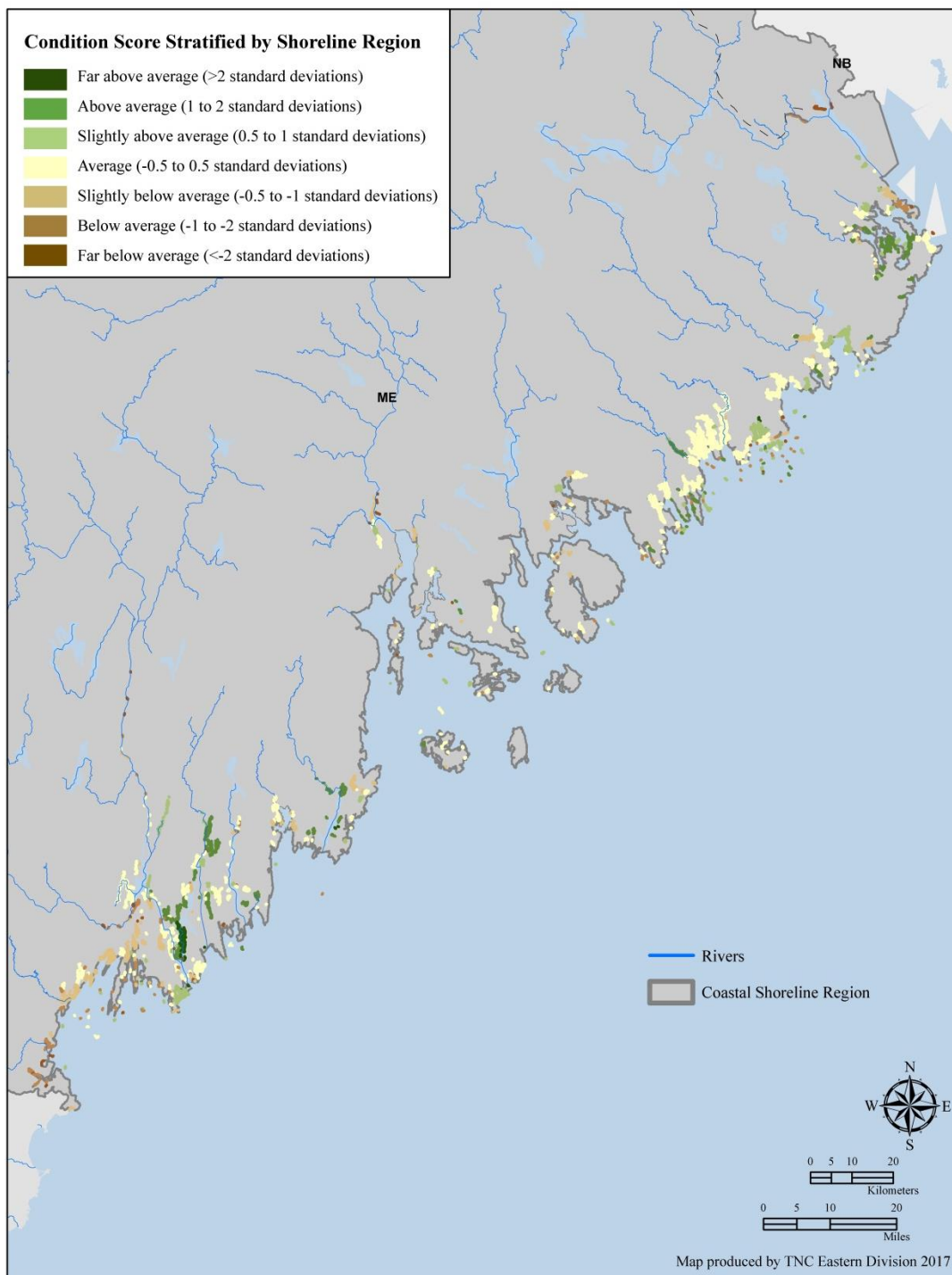


Table 7.1. Frequency of physical and condition scores in the Maine Drowned River Valleys CSR for the 6-foot sea level rise scenario.

Z-Score Class	Tidal Complex (n)	
	Physical	Condition
Far Below Average	106	38
Below Average	75	85
Slightly Below Average	84	94
Average	213	240
Slightly Above Average	84	94
Above Average	75	84
Far Above Average	13	15

There was no significant relationship between the condition and physical scores ($r = .033$, $p = .4271$, Figure 7.7). Most tidal complexes with a high physical score did not have a high condition score as evidenced in Figures 7.7- 7.8 and Table 7.2, but the high scoring physical sites do not tend to have very poor condition scores. There are only three tidal complexes that had “far above average” for both physical and condition characteristics (Table 7.2). These three sites were all located along the Indian River, north of Crowley Island in northern Maine. “Average” was the lowest condition class that a “far above average” physical site had in this CSR, but an “above average” physical site can have a “slightly below average” condition value (Table 7.2).

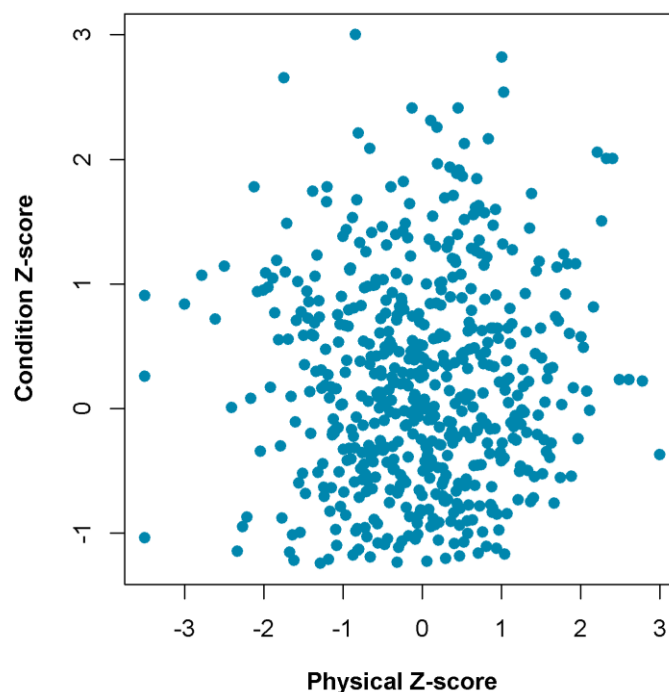
Figure 7.7. Relationship between the tidal complex units' physical and condition z-scores for the 6-foot sea level rise scenario, after removing complexes with no migration space.

Figure 7.8. Distribution of the physical scores for each condition class at a sea level rise of 6 feet. The distribution of the physical scores is shown for each condition score class using our standard z-score color palette.

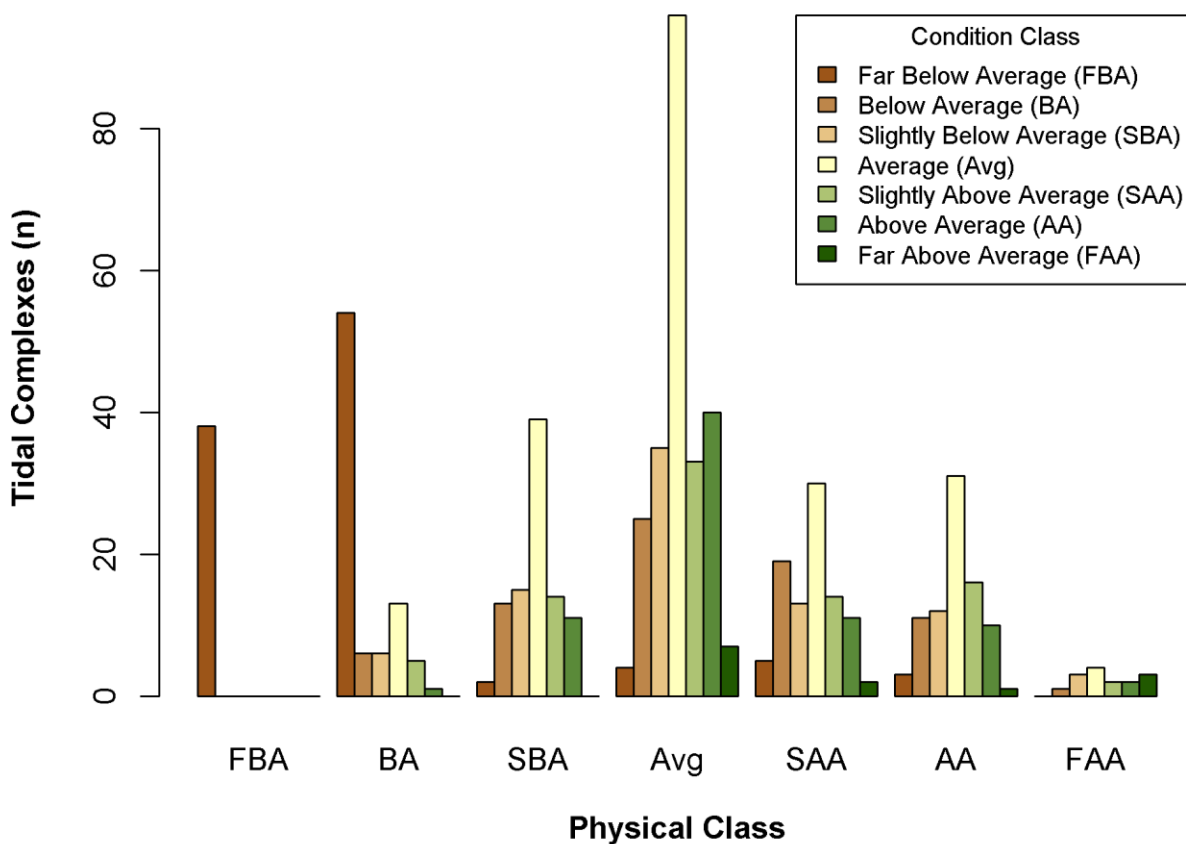
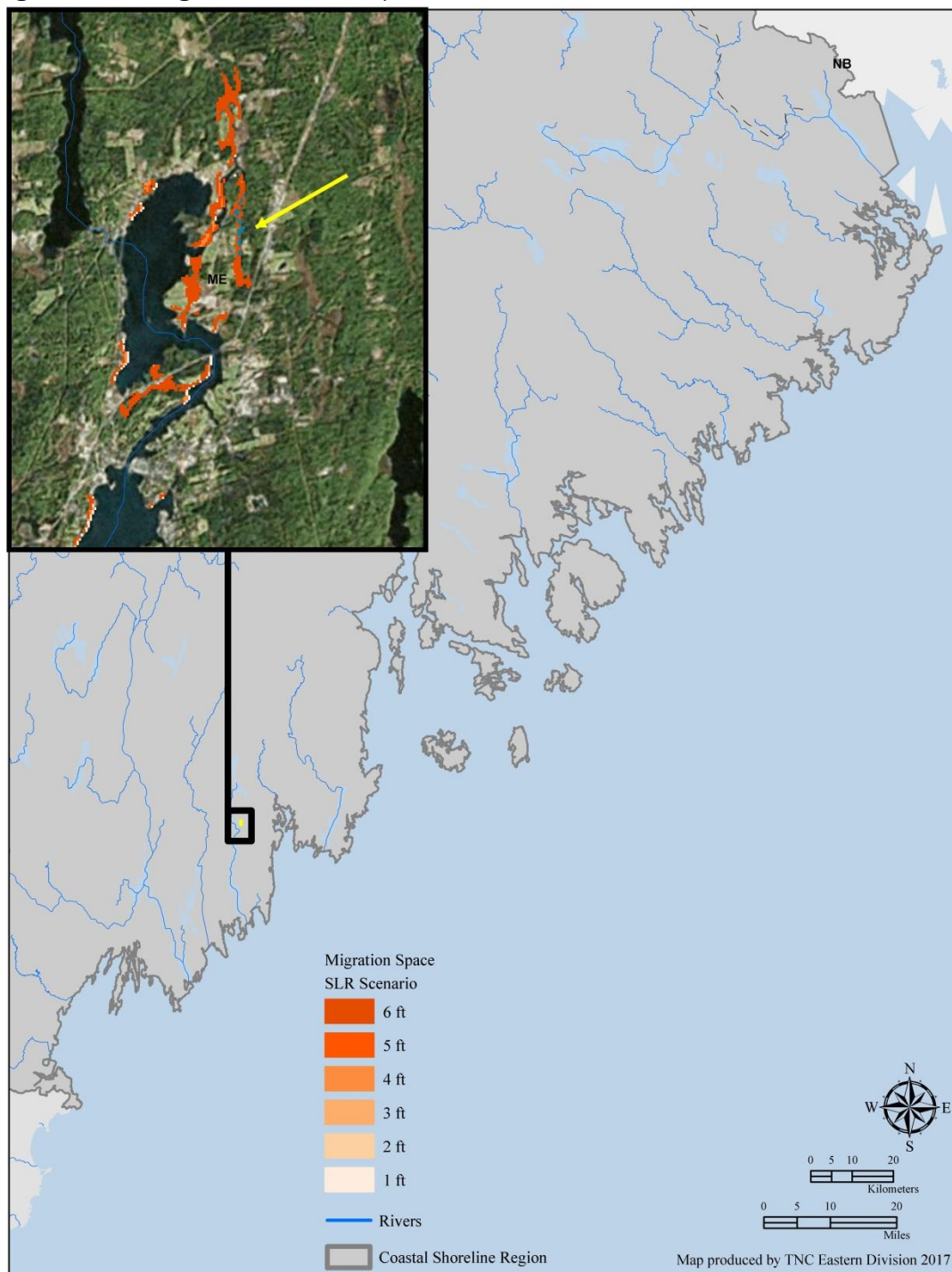


Table 7.2. The number of tidal complex units in each physical and condition score category. A two-by-two frequency table shows the count of tidal complexes occurring in each physical and condition class combination. Physical classes are by row and condition classes are by column. Boxes shaded in gray indicate tidal complexes with the same physical and condition score class. For example, only 1 tidal complex scored “far above average” for both physical and condition characteristics.

Physical Class	Condition Class						
	Far Below Average	Below Average	Slightly Below Average	Average	Slightly Above Average	Above Average	Far Above Average
Far Below Average	38	54	2	4	5	3	0
Below Average	0	6	13	25	19	11	1
Slightly Below Average	0	6	15	35	13	12	3
Average	0	13	39	96	30	31	4
Slightly Above Average	0	5	14	33	14	16	2
Above Average	0	1	11	40	11	10	2
Far Above Average	0	0	0	7	2	1	3

As shown in Figure 7.9, there was only one site that had a low condition score (i.e., “below average”) and a high physical score (i.e., “above average”). This particular site, located near Salt Bay and the Damariscotta River, would likely be a good candidate for restoration as there was a moderate amount of migration space available (26 acres) at the 6-ft SLR scenario for this CSR, and the migration space was modeled to have a high diversity and evenness of tidal classes as well as a large shared edge with the current tidal complex. While the physical template was suitable for marsh migration, condition issues could hinder migration. In particular, this site had high estimated nitrogen loads relative to other sites in the CSR, and sits within a developed landscape that had minimal agricultural areas and thus low sediment inputs.

Figure 7.9. Tidal complex (n=1) with high physical score but in poor condition. This site, near the Damariscotta River and Salt Bay, was estimated to be in relatively poor condition due to nitrogen loadings, low sediment inputs, and a non-natural portion of the buffer area immediately adjacent to the complex and migration space. However, this site had physical characteristics hypothesized to increase resilience to sea level rise, including a moderately sized migration space with a diversity of tidal classes and a large shared edge with the complex.



Estimated Resilience Score

The physical and condition scores were equally weighted and combined to calculate an estimated resilience score for each tidal complex. High scoring sites were those with a large migration space, intact buffer area, and whose condition was not expected to exacerbate the impacts of sea level rise and climate change, with all these characteristics relative to other sites in the CSR. The role of some of the physical factors was evident in Figure 7.10 where high scoring tidal complexes shown in dark green have a large migration space (shown in orange shades), and very vulnerable complexes shown in dark brown have no migration space. The resilience values are in z-scores which follow a normal distribution except for the “far below average” category because tidal complexes with no migration space were manually assigned a -3.5 SD score for all migration space attributes. The relationship between the physical and condition scores and the role of that relationship in the estimated resilience score can be seen in Figure 7.11. As Figure 7.11 shows, for the most part, a site could not have average physical conditions and receive a “far above average” resilience score (there was an extremely small proportion of “average” physical scores in the “far above average” class). There were no “far above average” physical or condition scores in the “average” resilience class and only a small proportion of “above average” sites. In contrast to the condition score patterns, it was unusual for a site to have higher-than-average physical conditions and have a lower- than-average resilience score.

The ten tidal complexes with the highest estimated resilience score are shown in Figure 7.12. The average tidal complex size of this group was 215 acres with an average migration space size at a 6-foot sea level rise of 232 acres (min = 26, max = 491, SD = 188 acres) and a large average buffer area (>500K acres). Vulnerable sites (i.e., those having below average estimated resilience) are shown in Figure 7.13. These tidal complexes are locations with little to no migration space and whose poor condition relative to all other sites in the CSR, is expected to exacerbate the impacts of sea level rise and climate change. The results of a Pearson correlation analysis show the role of tidal complex size, migration space size, and buffer area size in the condition, physical, and resilience score (Table 7.4). As expected, given the weight of the size attributes in the physical component score, size was significantly and positively correlated with the physical score, particularly for the migration space and tidal complex size. The condition score was not significantly correlated with the migration space or tidal complex size and had only a slight positive relationship with buffer area size.

Figure 7.10. Estimated resilience score. This map shows the estimated resilience score for the Maine Drowned River Valleys CSR for the 6-foot sea level rise scenario. The map shows areas that are above (green) or below (brown) the mean. Areas in green score “above average” and are estimated to be more resilient based on their physical and condition characteristics. Areas in yellow are “average.” Areas in brown are “below average” and are estimated to be vulnerable to sea level rise and climate change.

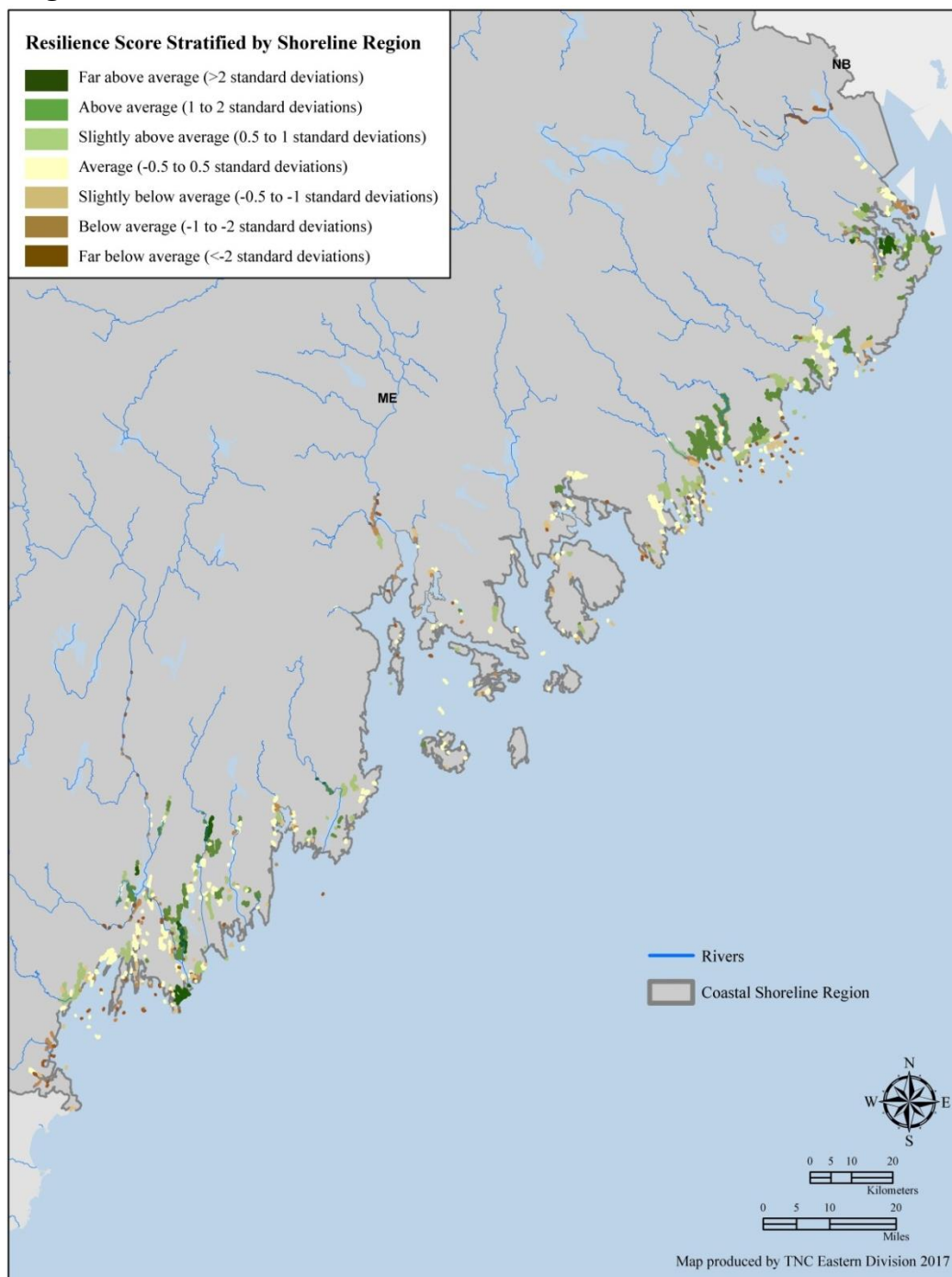


Figure 7.11. Relationship between condition and physical components for each estimated resilience class at a sea level rise of 6 feet. The physical and condition bars are split vertically based on the proportion of each score for each resilience class.

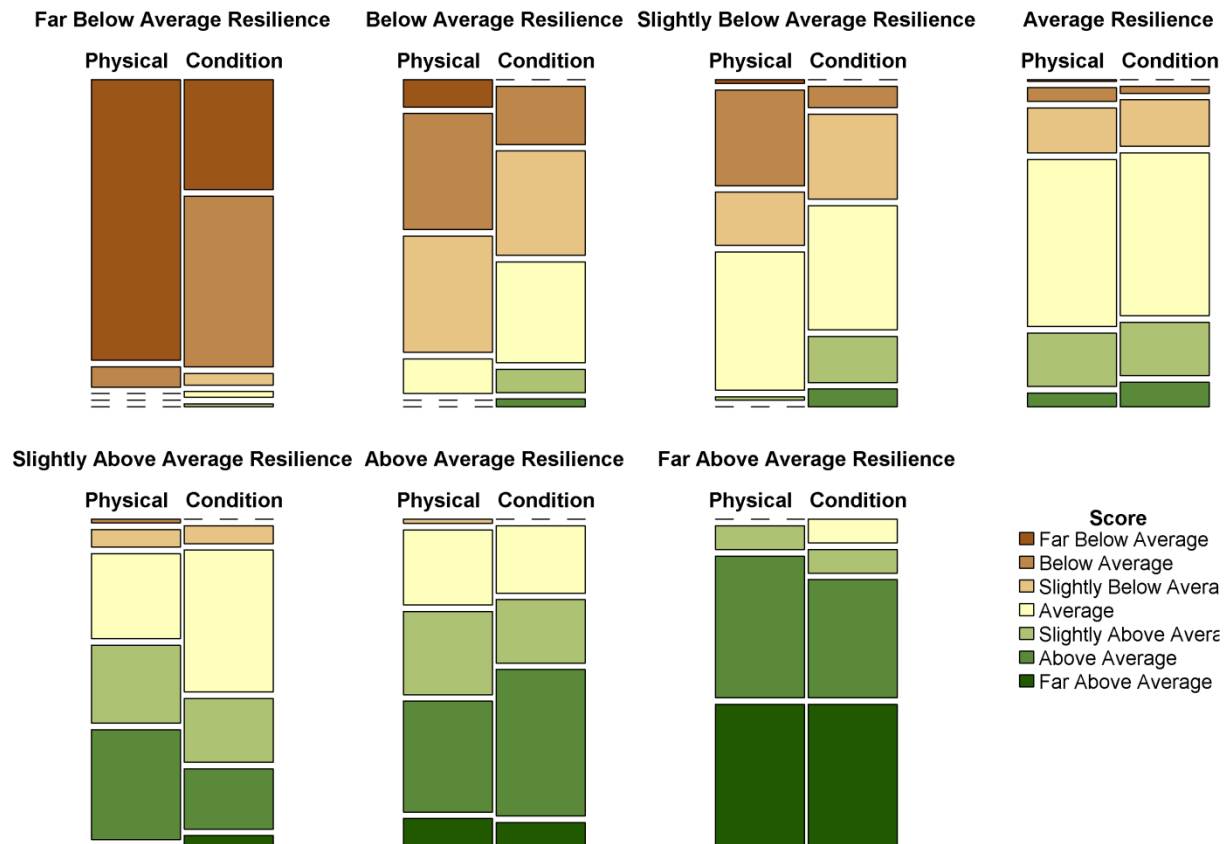


Table 7.3. Distribution of estimated resilience scores in the Maine Drowned River Valleys CSR for the 6-foot sea level rise scenario.

Z-Score Class	Estimated Resilience	Estimated Resilience with Migration Space Trend
Far Below Average	104	105
Below Average	76	68
Slightly Below Average	83	81
Average	215	192
Slightly Above Average	83	80
Above Average	76	101
Far Above Average	13	23

Figure 7.12. The top ten highest scoring tidal complexes in the Maine CSR. The ten tidal complexes with the highest estimated resilience score in the CSR are highlighted in yellow. Three of the top ten occur along the Indian River in northern Maine and are highlighted in the inset. While the complexes themselves are “average” in size, they all have high shoreline complexity and a large migration space with good water quality and better than average sediment inputs. In addition, they have a buffer area of over 1M acres with the portion immediately adjacent to the complex and the migration space largely in natural cover with diverse soil and landform types as well as better than average wetland connectivity.

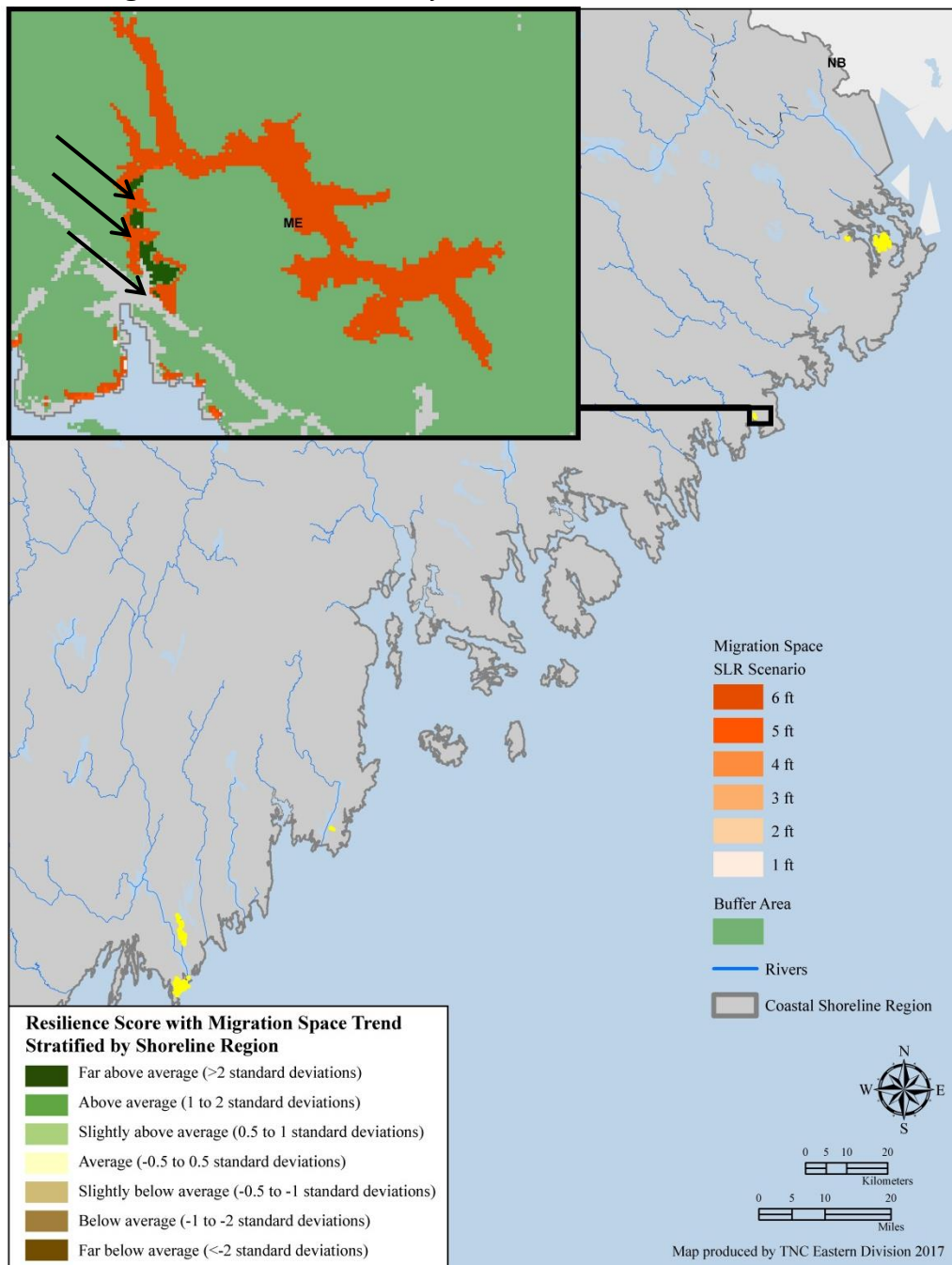


Figure 7.13. Vulnerable tidal complexes. Sites that scored below the mean are considered vulnerable. Sea level rise is expected to worsen the degradation of vulnerable sites, but these sites may still provide valuable ecosystem services (i.e., buffering storm effects, wildlife habitat, etc.).

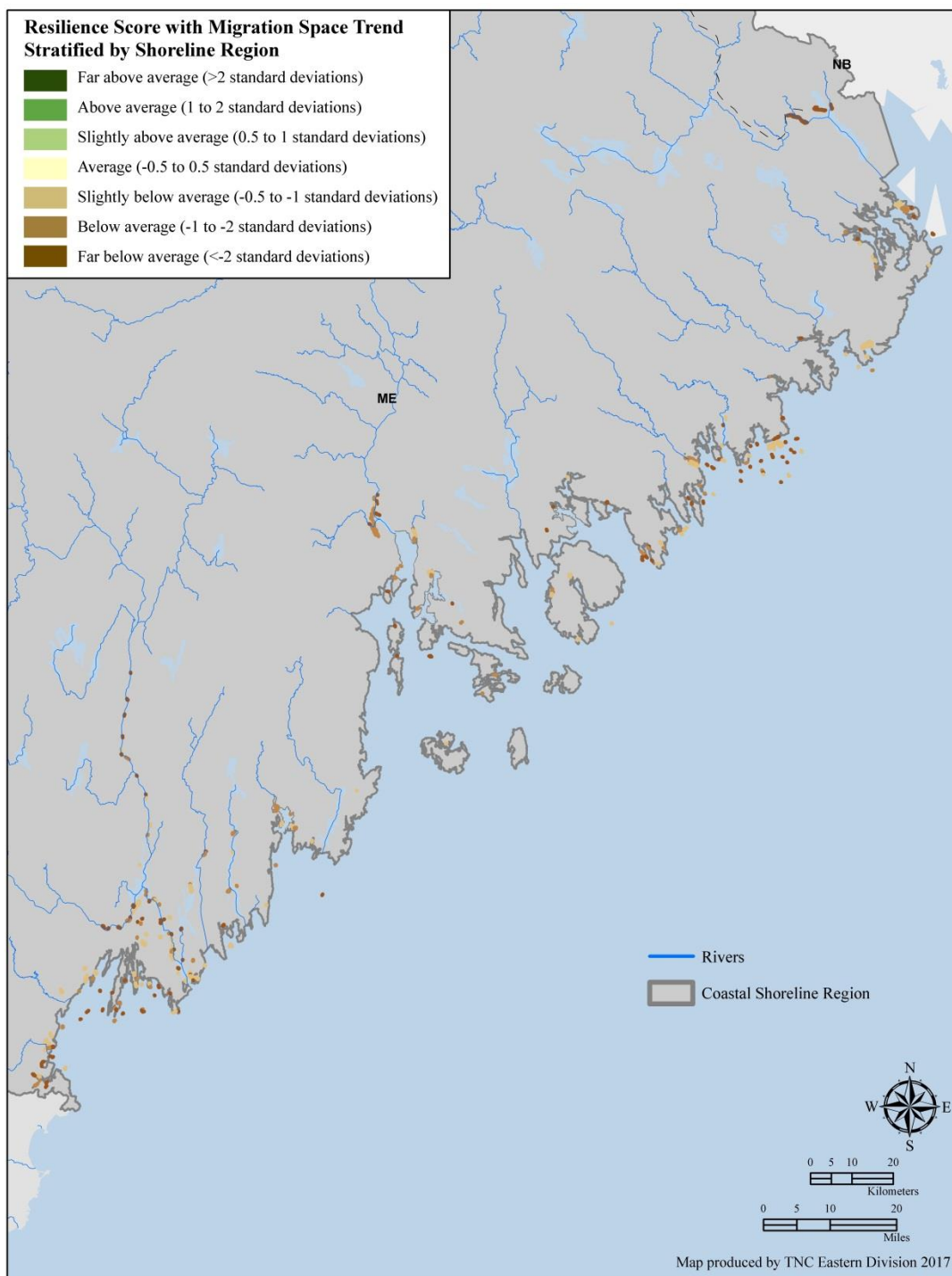


Table 7.4. Relationship between resilience components and analysis unit size.

Pearson correlation coefficients between the condition, physical, and estimated resilience scores and the size (acres) of the tidal complex, migration space, and buffer area, after removing complexes with no migration space. A star indicates a significant ($p \leq .05$) relationship.

	Tidal Complex Size	Migration Space Size	Buffer Area Size
Physical Z-score	.46*	.84*	.57*
Condition Z-score	-.003	-.024	.09*
Resilience Z-score	.35*	.63	.49*

Trends in Migration Space Size

Unlike the other coastal regions, the mean size across all migration spaces increased from the 1 to 6-foot sea level rise (except for a small decrease at 4 feet; Table 7.5). Linear regressions identified 316 tidal complex units with a statistically significant ($p \leq .05$) relationship between the latter three sea level rise scenarios (3 – 6 feet) and migration space size. Of those tidal complex units with a significant relationship, some had decreasing migration space, but the majority experienced an increase in migration space (Table 7.5). The mean increase in size was approximately 7 acres while the average decrease was 3 acres (Table 7.6). Tidal complexes with a significant migration space trend were assigned to one of three trend categories: increase, decrease, no change, and we adjusted their score to reflect the trend. The 180 tidal complexes whose migration space showed an increasing trend were awarded an additional 0.50 SD points to their estimated resilience score. The 34 tidal complexes that experienced a decline in migration space size from the 3 to the 6-foot SLR scenario had their estimated resilience scores reduced by 0.50 SD. The resilience score of the 102 tidal complexes with no significant change in migration space size was not impacted by the trend analysis. The map in Figure 7.14 shows the spatial distribution of the resilience scores with the trend analysis incorporated. Of the top ten highest scoring sites shown in Figure 7.12, 8 (80%) of the tidal complexes received a boost to their score from a positive migration space size trend. The other two tidal complexes had stable migration space sizes and thus had no change to their resilience score. The use of 0.50 SD to adjust the resilience score meant that no tidal complex's score could change by more than one resilience class (Table 7.7). After incorporating migration space trend, the resilience class did not change for 518 (80%) of the tidal complexes, while only 50 (3%) of sites went to the next lower class and 112 (17%) complexes moved up a class (Figure 7.15, Table 7.7). The percentage of sites whose score decreased due to a negative migration space trend was the lowest of the five coastal regions.

Table 7.5. Summary statistics for migration space size by sea level rise scenario.

SLR Scenario (feet)	Migration Space (Acres)				
	1 st Quartile	Median	Mean	3 rd Quartile	Max
1	2.057	7.561	42.35	19.07	2380
2	1.557	6.227	45.31	16.9	2523
3	1.557	6.672	49.22	18.9	2733
4	1.557	6.227	47.76	19.24	2520
5	1.334	6.227	49.51	19.96	2565
6	2.446	9.229	56.62	26.46	2696

Table 7.6 Summary of regression coefficients for tidal complex units (n=316) with a significant ($p \leq .05$) relationship between sea level rise scenario (≥ 3 feet) and migration space size.

Migration Space Size (acres) Change					
Trend direction	Count	Minimum	Median	Mean	Max
Decrease	34	-12.42	-1.52	-3.15	-0.09
Increase	180	0.05	2.53	6.64	87.60
No change	102	0	0	0	0

Figure 7.14. Estimated resilience score with migration space trend. This map shows the estimated resilience score after incorporating the trend in migration space size for the Maine Drowned River Valleys CSR at the 6-foot sea level rise scenario. Tidal complex units whose migration space showed a significant increase ($p \leq .05$) from the three to 6-foot SLR received an additional 0.50 standard deviation units to their score, while the score of units with a significant decrease in migration space was reduced by 0.50 SD units.

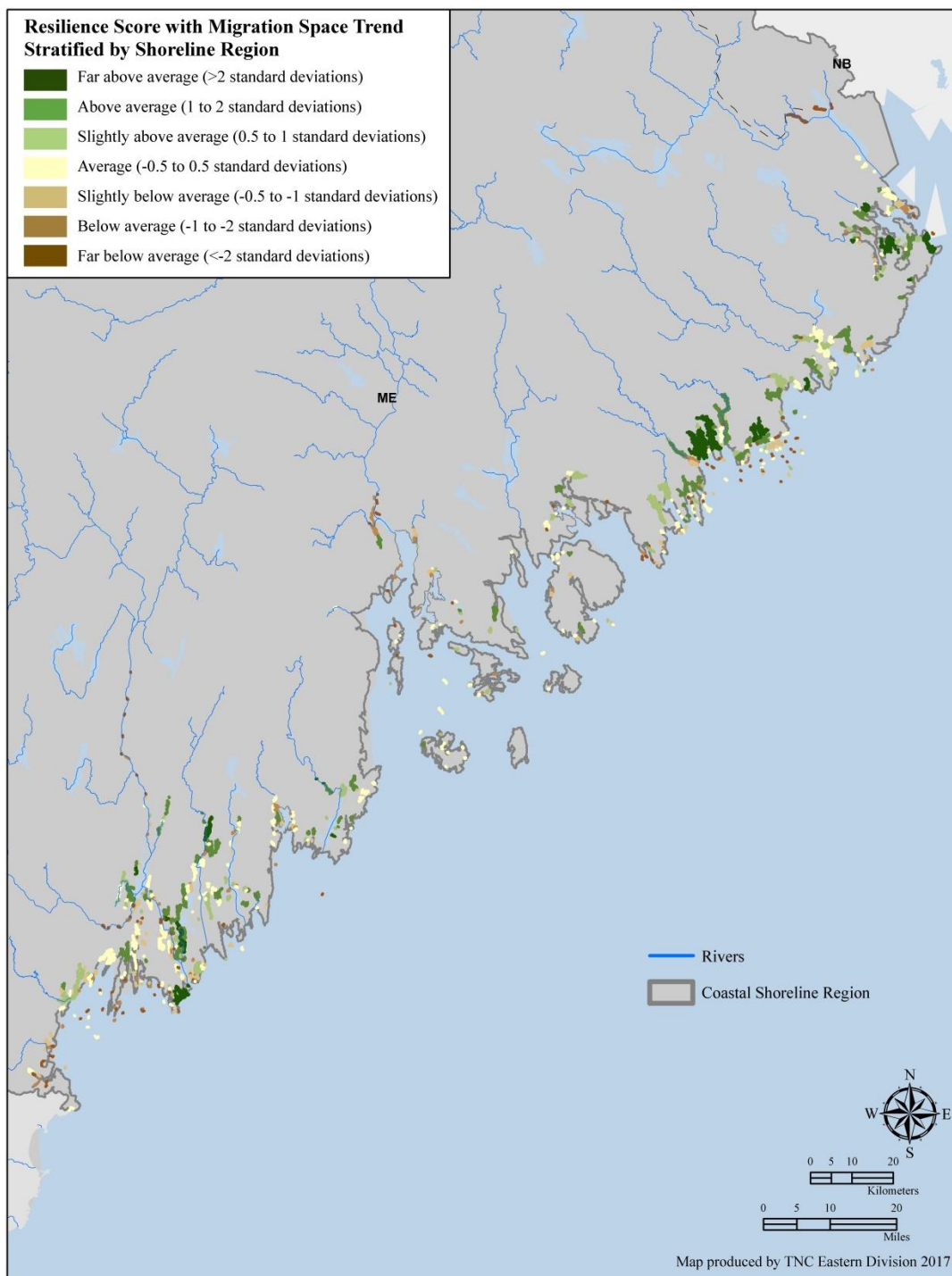
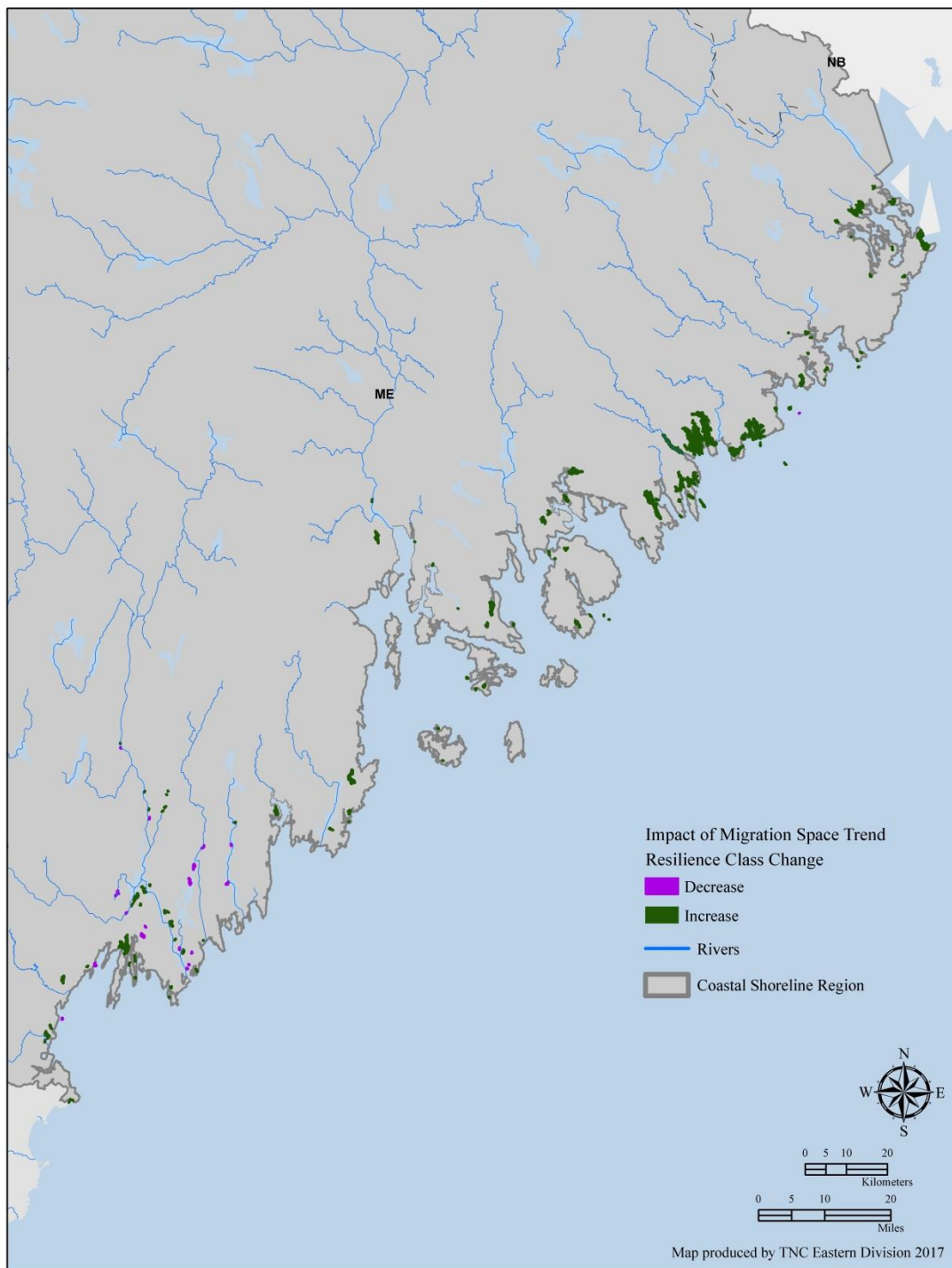


Table 7.7. The change in resilience class after incorporating the trend in migration space size. Tidal complex units whose migration space showed a significant increase ($p \leq .05$) from the 3 to 6-foot sea level rise received an additional 0.50 standard deviation units to their score, while the score of units with a significant decrease in migration space size was reduced by 0.50 SD units. The purple boxes indicate the number of tidal complex units that moved to the next lower resilience class, and the green boxes highlight the number of units whose class improved when the migration space trend was considered.

Resilience Class	Resilience class with Trend						
	Far Below Average	Below Average	Slightly Below Average	Average	Slightly Above Average	Above Average	Far Above Average
Far Below Average	104	0	0	0	0	0	0
Below Average	1	63	12	0	0	0	0
Slightly Below Average	0	5	61	17	0	0	0
Average	0	0	8	172	35	0	0
Slightly Above Average	0	0	0	3	42	38	0
Above Average	0	0	0	0	3	63	10
Far Above Average	0	0	0	0	0	0	13

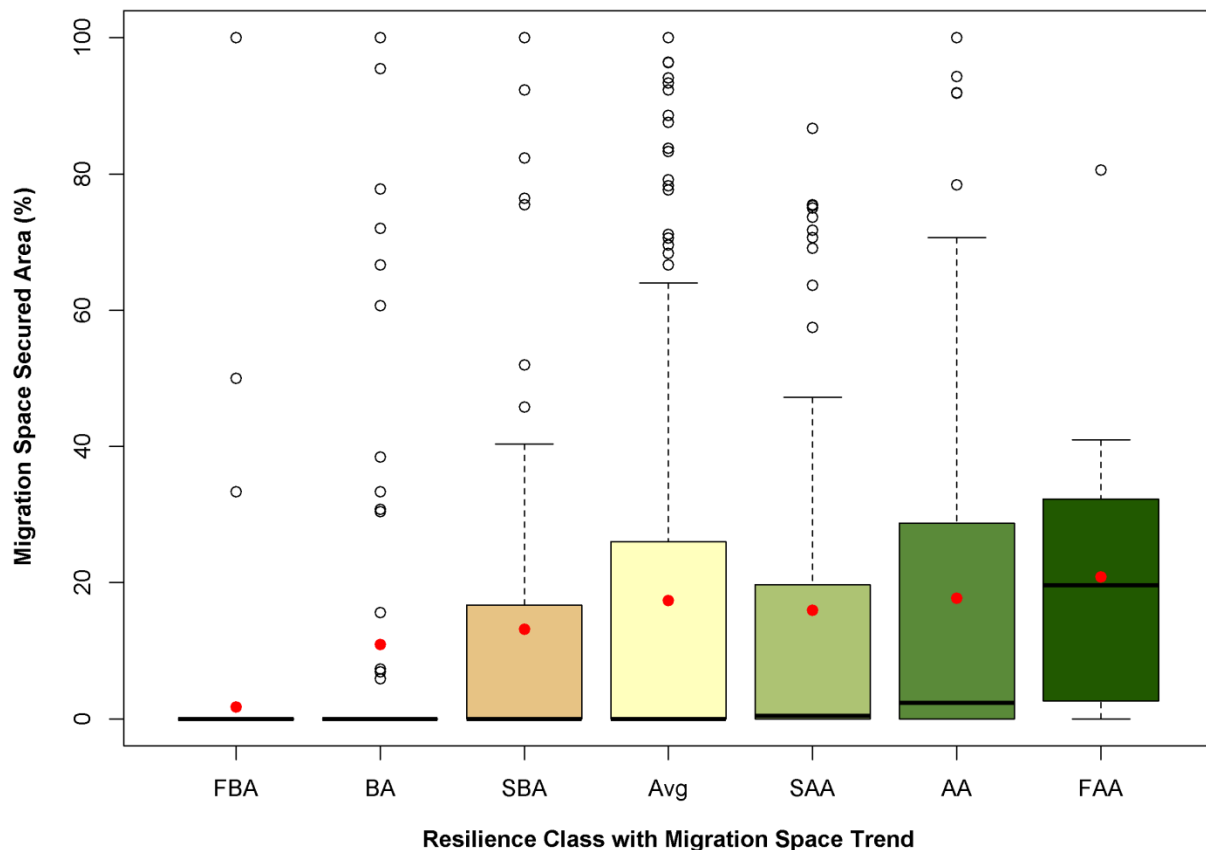
Figure 7.15. Estimated resilience class changes after incorporating migration space trend. This map shows the tidal complexes whose estimated resilience class either increased (n=117) or decreased (n=52) after incorporating the trend in migration space size for the Maine Drowned River Valleys CSR at the 6-foot sea level rise scenario.



Migration Space Securement

The amount of a tidal complex's total migration space that was already protected (GAP status 1-3) varied substantially by resilience z-score category (Figure 7.16). Tidal complexes estimated to be the most resilient ("far above average") had the greatest percentage of their migration space in securement (mean=21%). Meanwhile the "far below average" complexes had the lowest average percent protected with approximately 2% (Figure 7.16). The worst scoring units had very little if any migration space, hence the low percentage of migration space secured.

Figure 7.16. Amount (%) of migration space in permanent protection by estimated resilience class. The boxplot shows the distribution of migration space securement (%) by resilience class. The mean percent secured is denoted by a red circle. The resilience classes are shown using our standard z-score color palette and abbreviations.



Migration Space Development and Future Development

Due to inconsistencies in spatial resolution of various datasets used in this analysis (i.e., 10-m elevation and 30-m land cover products), and how roads are inaccurately mapped in base land cover grids such as the NLCD and C-CAP products, there are cases where some development occurs within the migration space mapped at the 30-m scale. Given the relatively undeveloped Maine landscape, none of the resilience classes have more than 8% of their migration space in development with the “slightly below average” class having the highest at 8% (Figure 7.17). There are tidal complexes that have 80-100% development for the average and lower resilience classes, and this typically occurs for very small migration space areas where a single pixel of development leads to a high percentage. While the risk of future development was very low across all the resilience classes (Table 7.8), the information is available for each tidal complex and could be useful for practitioners in considering appropriate strategies for a specific site.

Figure 7.17. Amount (%) of migration space comprised of developed land, by estimated resilience class. The boxplot shows the distribution of migration space development (%) by resilience class with the mean denoted by a red circle. The resilience classes are shown using our standard z-score color palette and abbreviations.

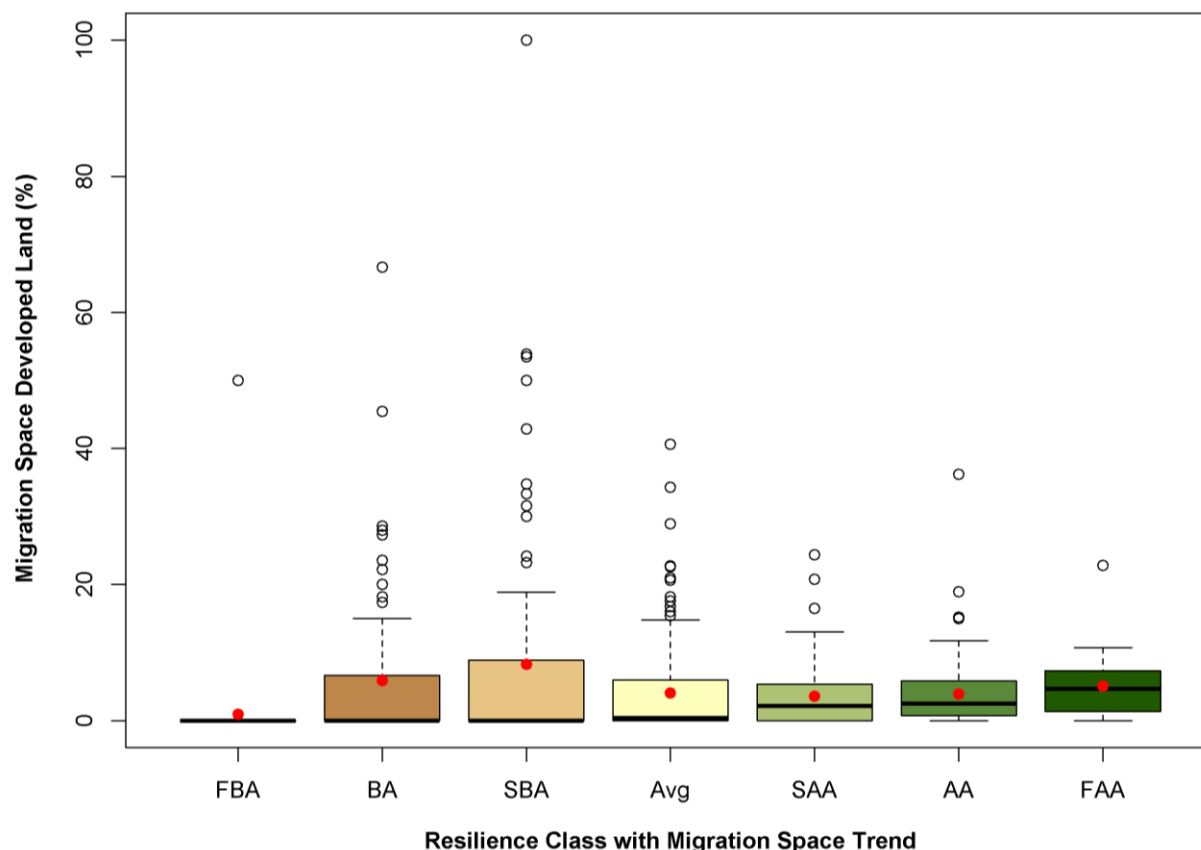
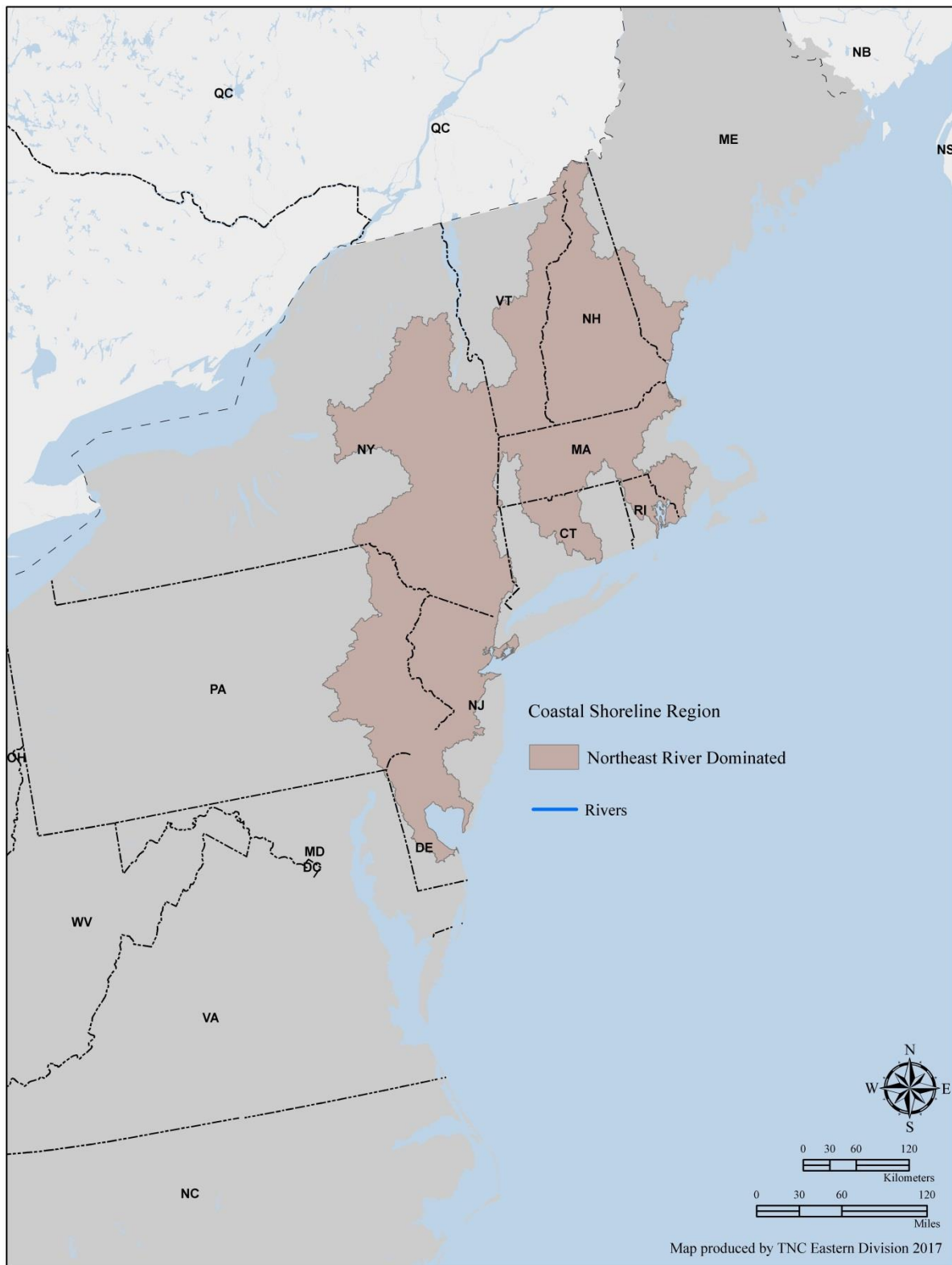


Table 7.8. Amount (%) of migration space estimated to be developed in 2100, by estimated resilience class. Summary statistics for migration space future development (%) are shown by resilience class.

Resilience Class with Migration Trend	Migration Space Future Development (%)					
	Min	1 st Quartile	Median	Mean	3 rd Quartile	Max
Far Below Average	0	0	0	0	0	0
Below Average	0	0	0	0	0	0
Slightly Below Average	0	0	0	0	0	0
Average	0	0	0	0.034	0	3.33
Slightly Above Average	0	0	0	0	0	0
Above Average	0	0	0	0.001	0	0.15
Far Above Average	0	0	0	0	0	0

Northeast River-Dominated CSR: Results



The **Northeast River-Dominated CSR** had a total of 1566 tidal complex units, with an average size of 136 acres and a median size of 6 acres. The largest tidal complex was 40,620 acres (Figures 7.18-7.19).

Figure 7.18. Distribution of tidal complex size (acres) by ten size classes in the Northeast River-Dominated CSR.

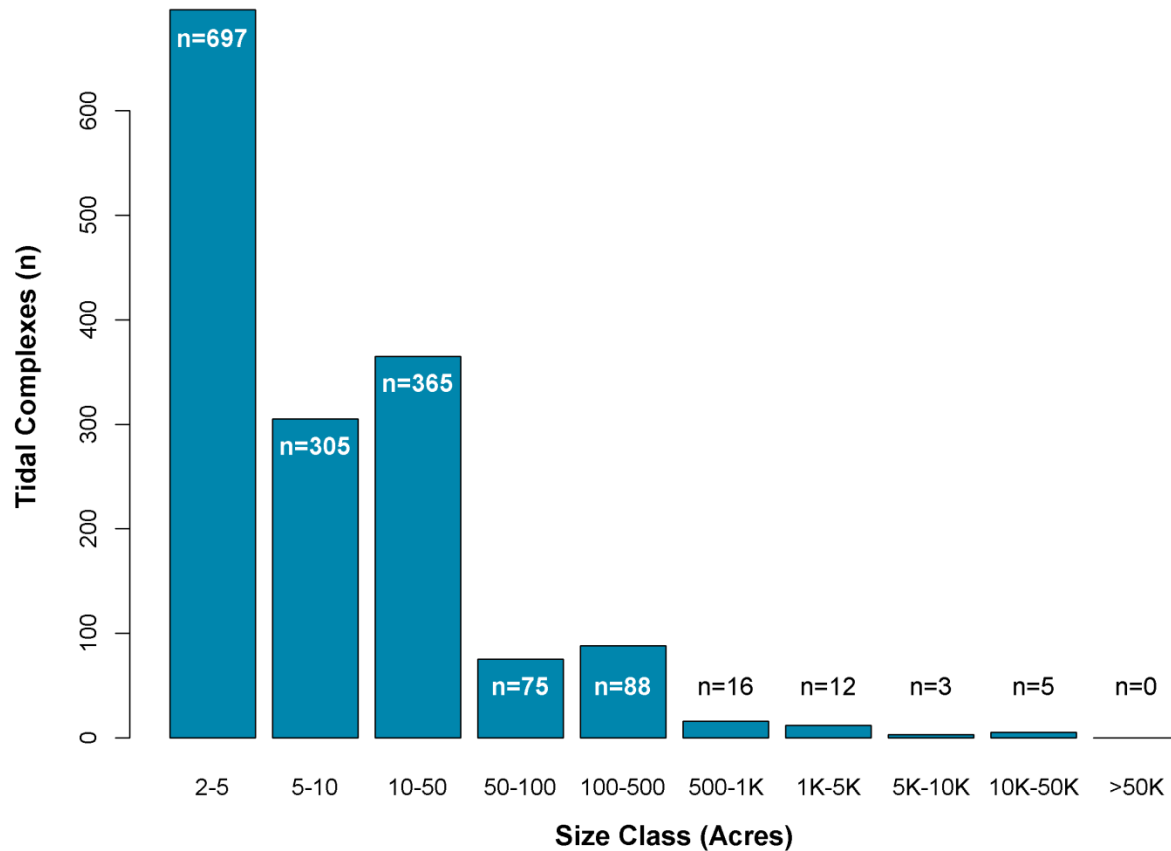
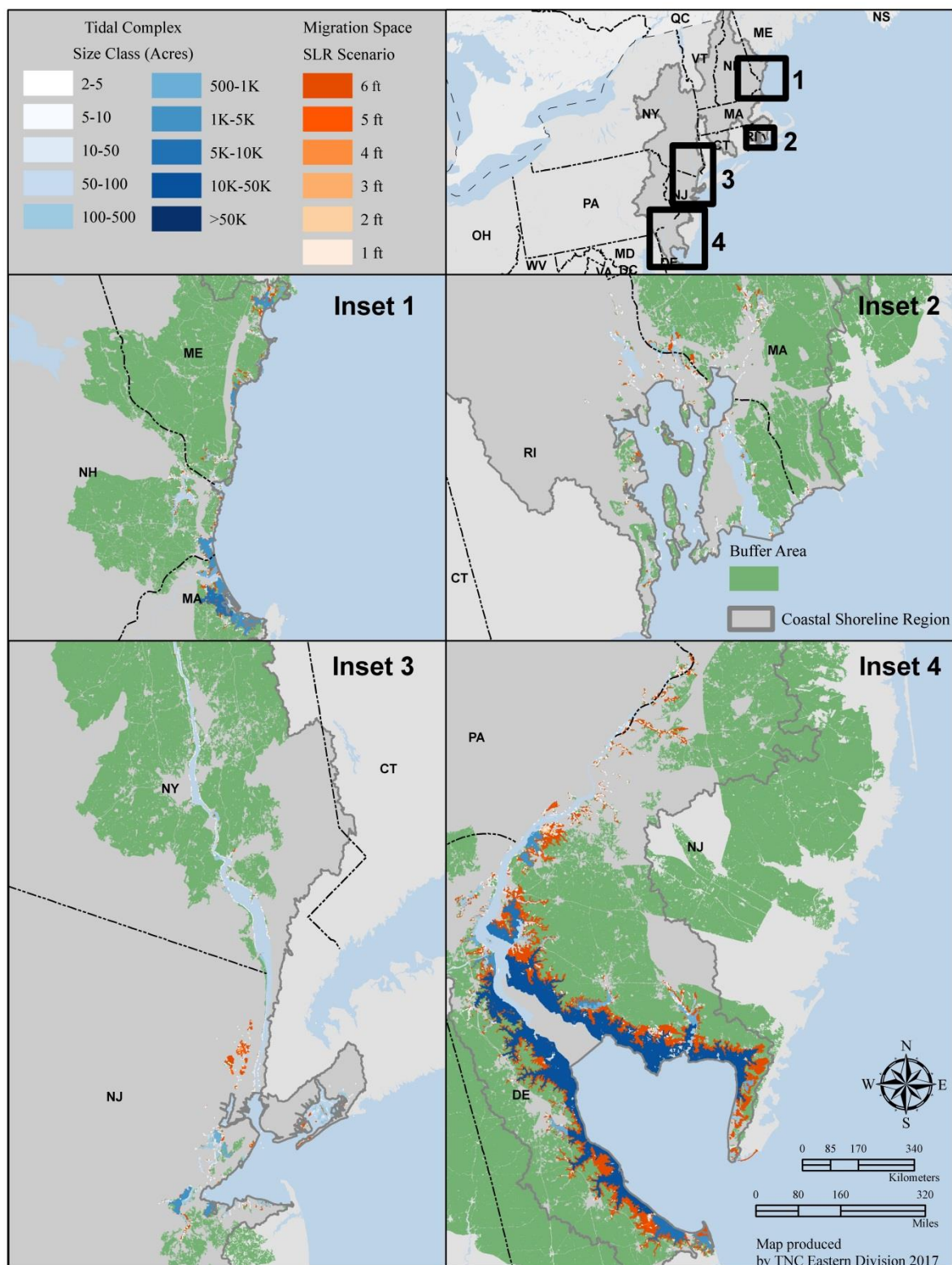
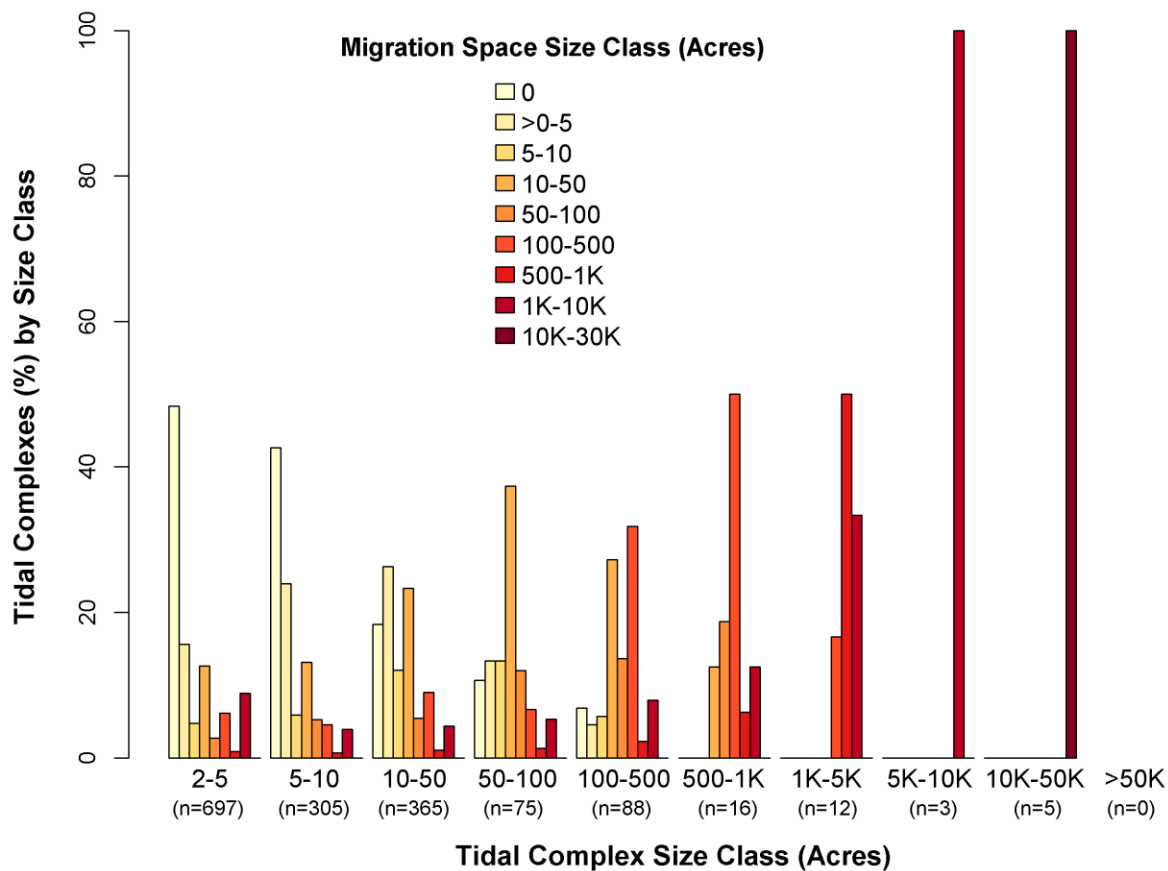


Figure 7.19. Tidal complex, migration space, and buffer area units in the Northeast River-Dominated CSR. The color of the tidal complex units reflects their size class (n=10), while the color of the migration space indicates the SLR scenario (n=6).



At a sea level rise of 6 feet, 1018 or 65% of the tidal complexes had migration space (Figure 7.20). The average migration space size was 329 acres with a median size of 3 and a maximum size of 17,430 acres. As Figure 7.20 shows, small tidal complexes in this CSR can have little to no migration space or very large migration space areas at a sea level rise of 6ft. However, the largest tidal complexes in this CSR (≥ 1000 acres) all have expansive migration space areas, reflecting the larger geophysical setting within which these tidal complexes occur.

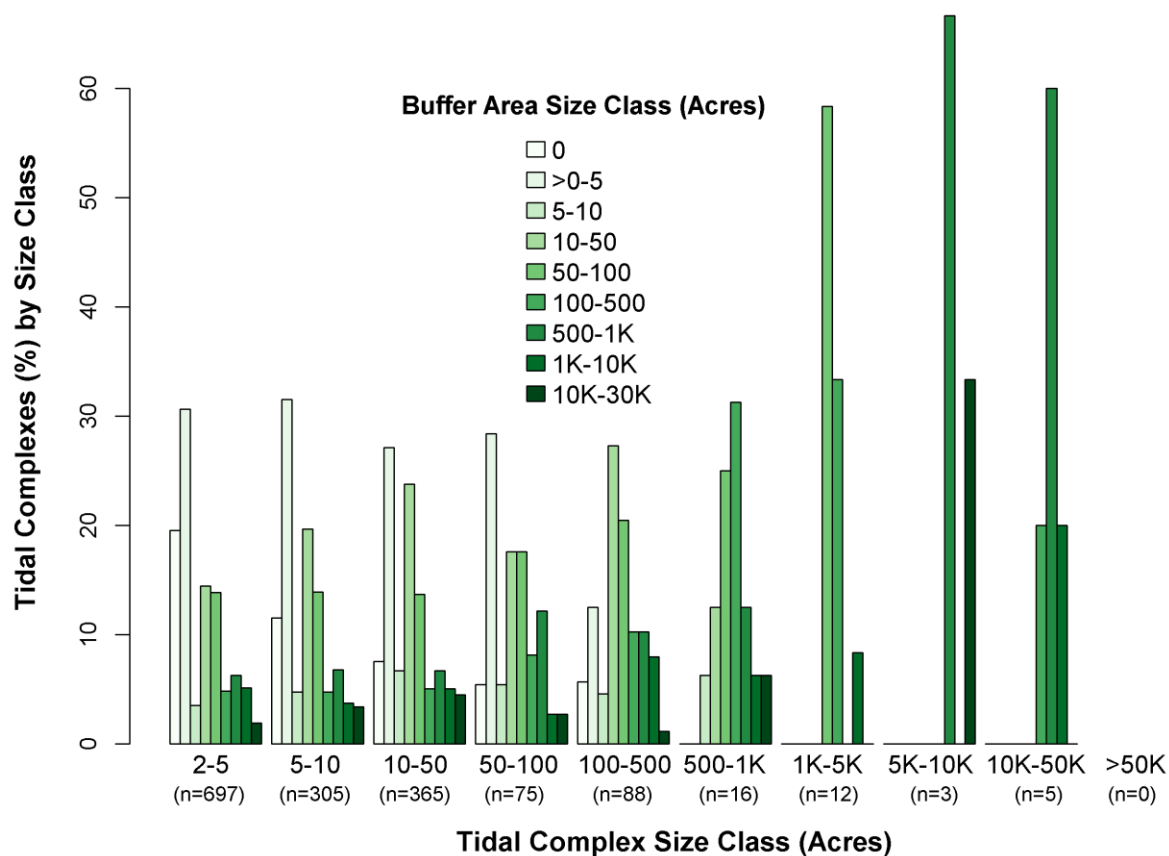
Figure 7.20. Migration space class distribution by tidal complex size class for the 6-foot sea level rise scenario. The y-axis is the percent of tidal complexes within a size class that have migration space of a particular size. Small migration space size classes are shown in light yellow shades that transition to darker oranges as the migration space size class increases.



A Spearman's rank-order correlation found the tidal complex size and migration space size were somewhat positively correlated and this relationship was statistically significant ($r_s = .30$, $p < 2.2e-16$).

Almost all the tidal complexes, 1362 or 87%, had buffer area at a sea level rise of 6 feet (Figure 7.21). The mean buffer size was 43,670 acres with the largest buffer area encompassing 948,000 acres. Similar to the relationship between tidal complex size and migration space size, all tidal complexes of 1000 acres or greater have large buffer areas whereas tidal complexes less than 1000 acres have a mix of buffer area sizes (Figure 7.21). This was quite different than the tidal complex and buffer area pattern in the other river-dominated CSR, the Chesapeake Bay and Piedmont River region. There was a small positive relationship between tidal complex size and buffer area size ($r_s = .11$, $p = 5.002e-3$).

Figure 7.21. Buffer area class distribution by tidal complex size class for the 6-foot sea level rise scenario. The y-axis is the percent of tidal complexes within a size class that have buffer area of a particular size. Small buffer area size classes are shown in light green shades that change to darker greens as the buffer area size class increases.



Physical and Condition Scores

The estimated resilience score for a tidal complex consists of the condition and physical components, each weighted equally. Figure 7.22 shows the geographic distribution of physical scores within the CSR for a sea level rise of 6 feet. As Table 7.9 shows, most scores fall in the “average” class, with the next largest category being the “far below average” category. The lowest scoring tidal complexes are predominantly those with no migration space and a less geophysically diverse buffer area. The spatial pattern of the condition scores is shown in Figure 7.23 with the numeric distribution highlighted in Table 7.9. As Table 7.9 shows, a higher proportion of tidal complexes scored “far below average” in physical versus condition characteristics.

Figure 7.22. Estimated physical score for the Northeast River-Dominated CSR. Tidal complex units in green score “above average” and have physical characteristics hypothesized to increase resilience including a large migration area with a diversity of tidal classes that are evenly distributed, a complex shoreline, and a geophysically diverse buffer area. Tidal complexes in yellow have “average” physical characteristics relative to all the units in the CSR. Tidal complexes in brown are “below average” and are estimated to respond poorly to sea level rise.

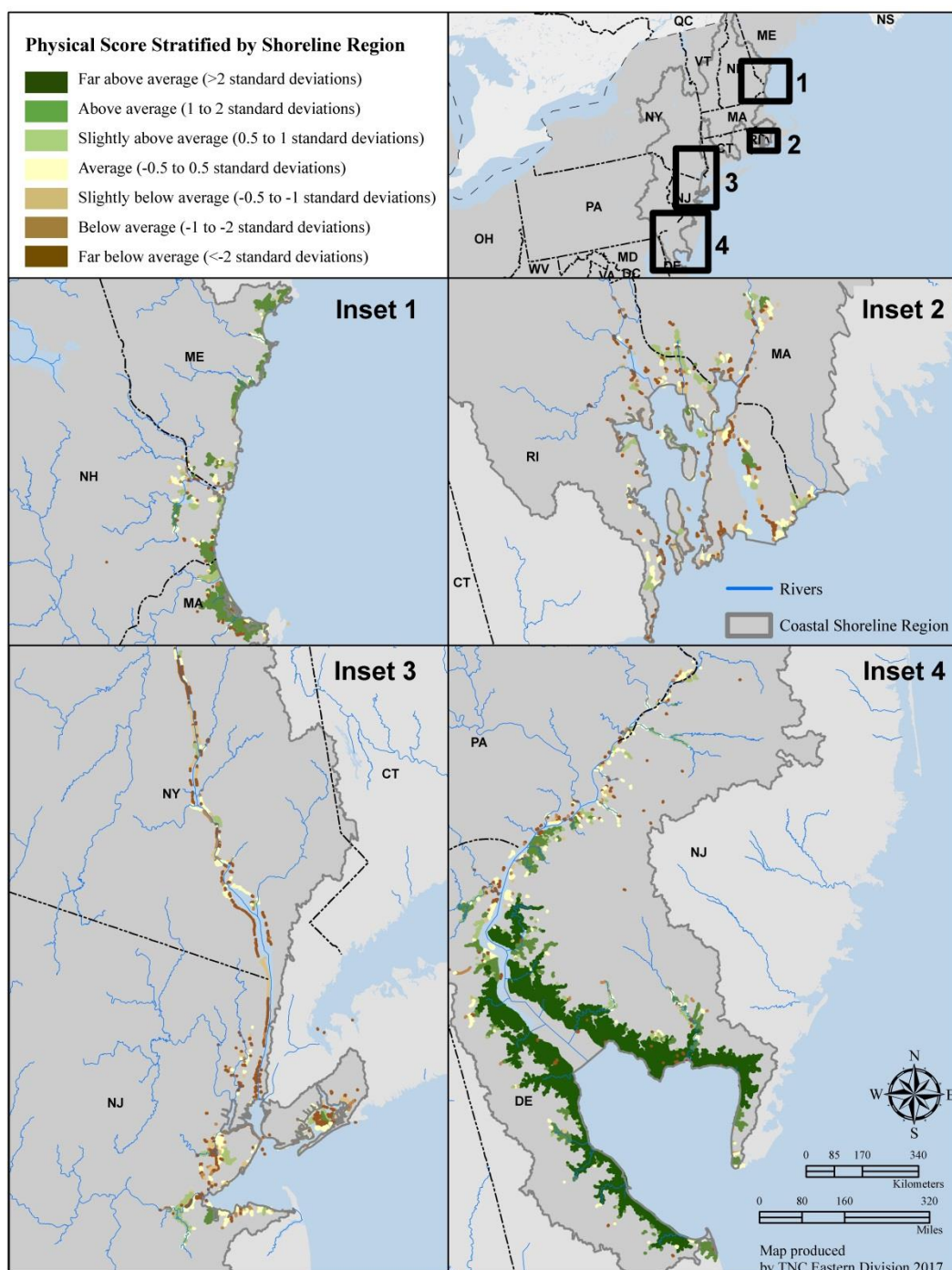


Figure 7.23. Estimated condition score for the Northeast River-Dominated CSR. Tidal complex units in green score “above average” and are estimated to be in good condition based on a low percentage of hardened shoreline; good water quality and quantity, and high sediment contributions in the migration space; and a natural buffer area with highly connected wetlands. Tidal complexes in yellow are “average.” Tidal complexes in brown are “below average” and are estimated to be in poor condition.

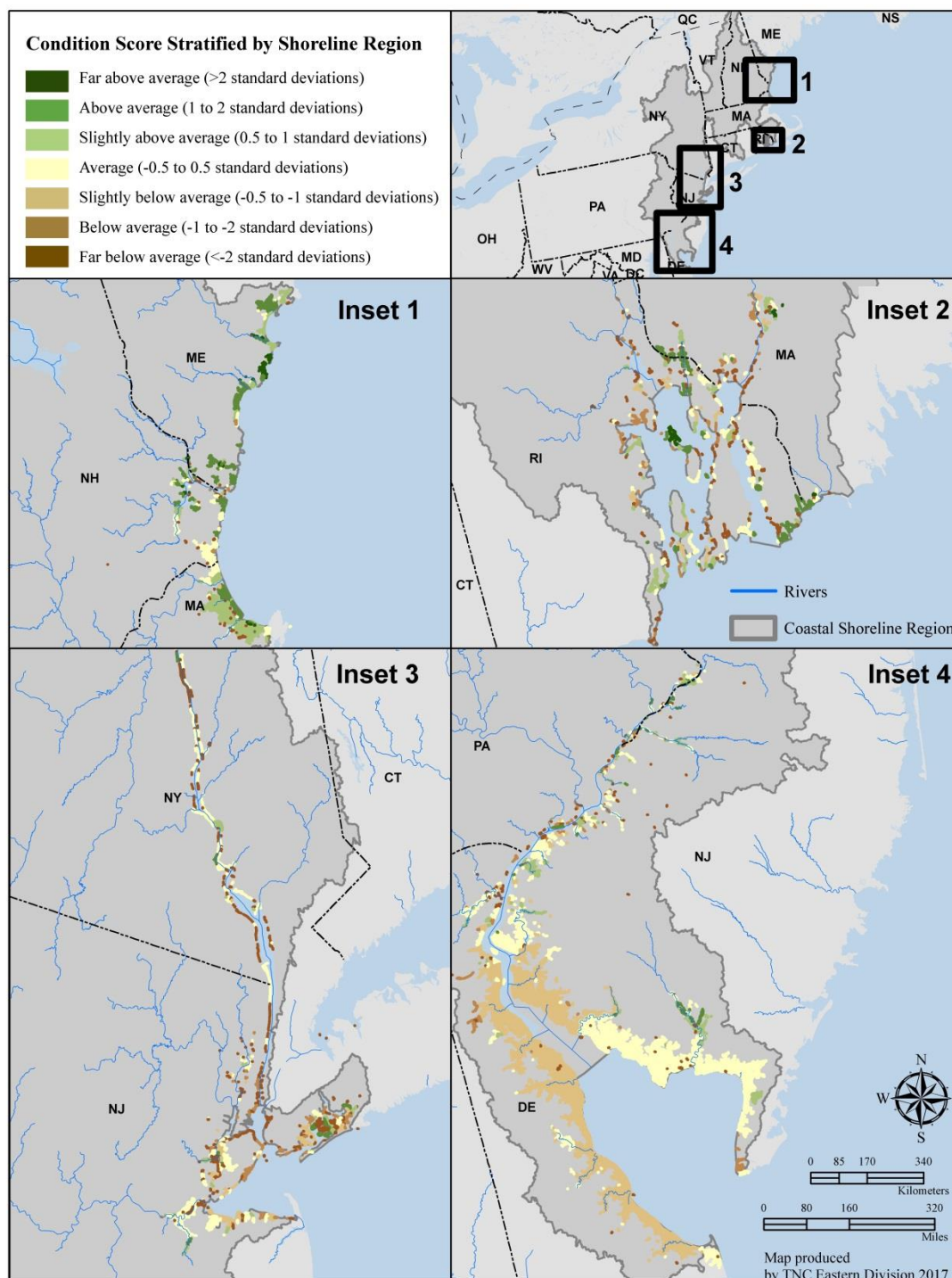


Table 7.9. Frequency of physical and condition scores in the Northeast River-Dominated CSR for the 6-foot sea level rise scenario.

Z-Score Class	Tidal Complex (n)	
	Physical	Condition
Far Below Average	571	519
Below Average	139	151
Slightly Below Average	152	160
Average	390	407
Slightly Above Average	152	160
Above Average	139	145
Far Above Average	23	24

The relationship between the condition and physical scores was slightly positively correlated (Pearson's $r = .10$, $p = 8.41e-4$, Figure 7.24). A tidal complex with a high physical score does not necessarily have a high condition score as evidenced in Figures 7.24-7.25 and Table 7.10. For example, there are 7 tidal complexes that have an "above average" physical score but a "below average" condition score (Figure 7.26). There are no tidal complexes that have "below average" physical characteristics and "far above average" condition, but there are 10 tidal complexes that have "below average" physical scores and "above average" condition scores (Table 7.10). As many of the condition characteristics were calculated for the migration space component of a unit, if there was no migration space, a tidal complex was likely to score "far below average" for both physical and condition characteristics, hence the large dark brown bar for the "far below average" physical class in Figure 7.25.

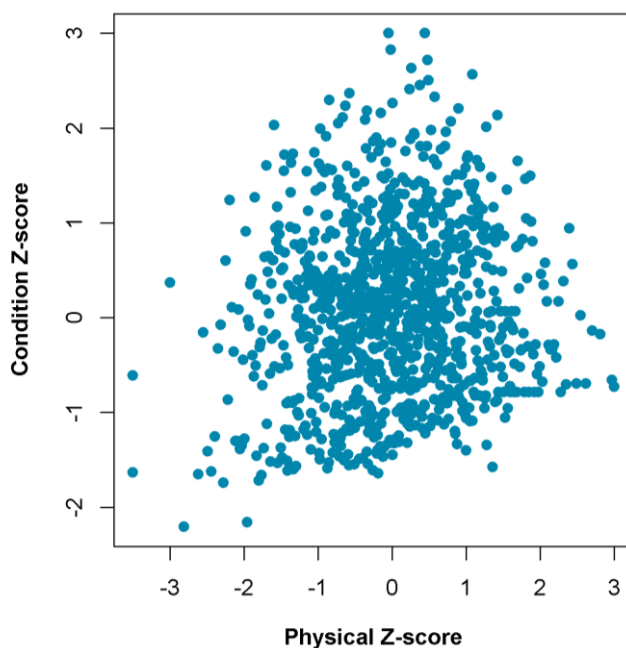
Figure 7.24. Relationship between the tidal complex units' physical and condition z-scores for the 6-foot sea level rise scenario, after removing units with no migration space.

Figure 7.25. Distribution of the physical scores for each condition class at a sea level rise of 6 feet. The distribution of the physical scores is shown for each condition score class using our standard z-score color palette.

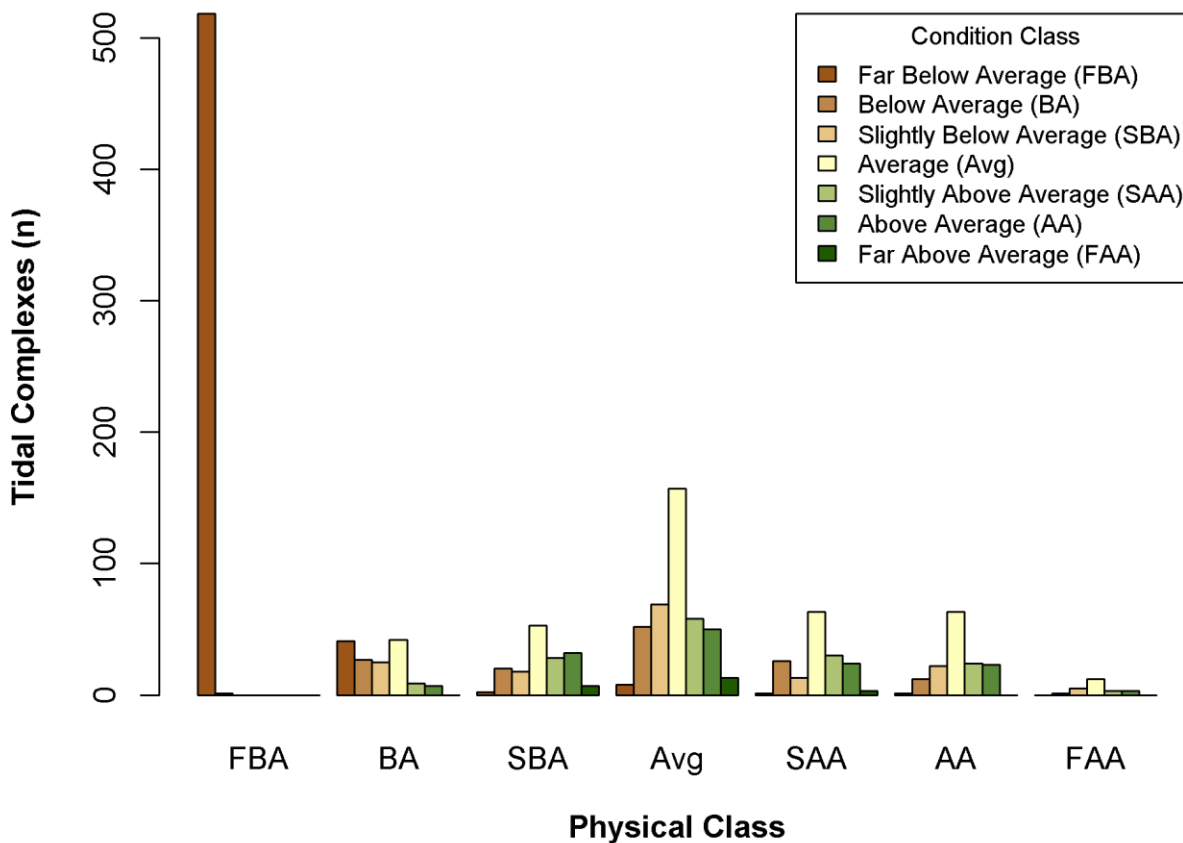


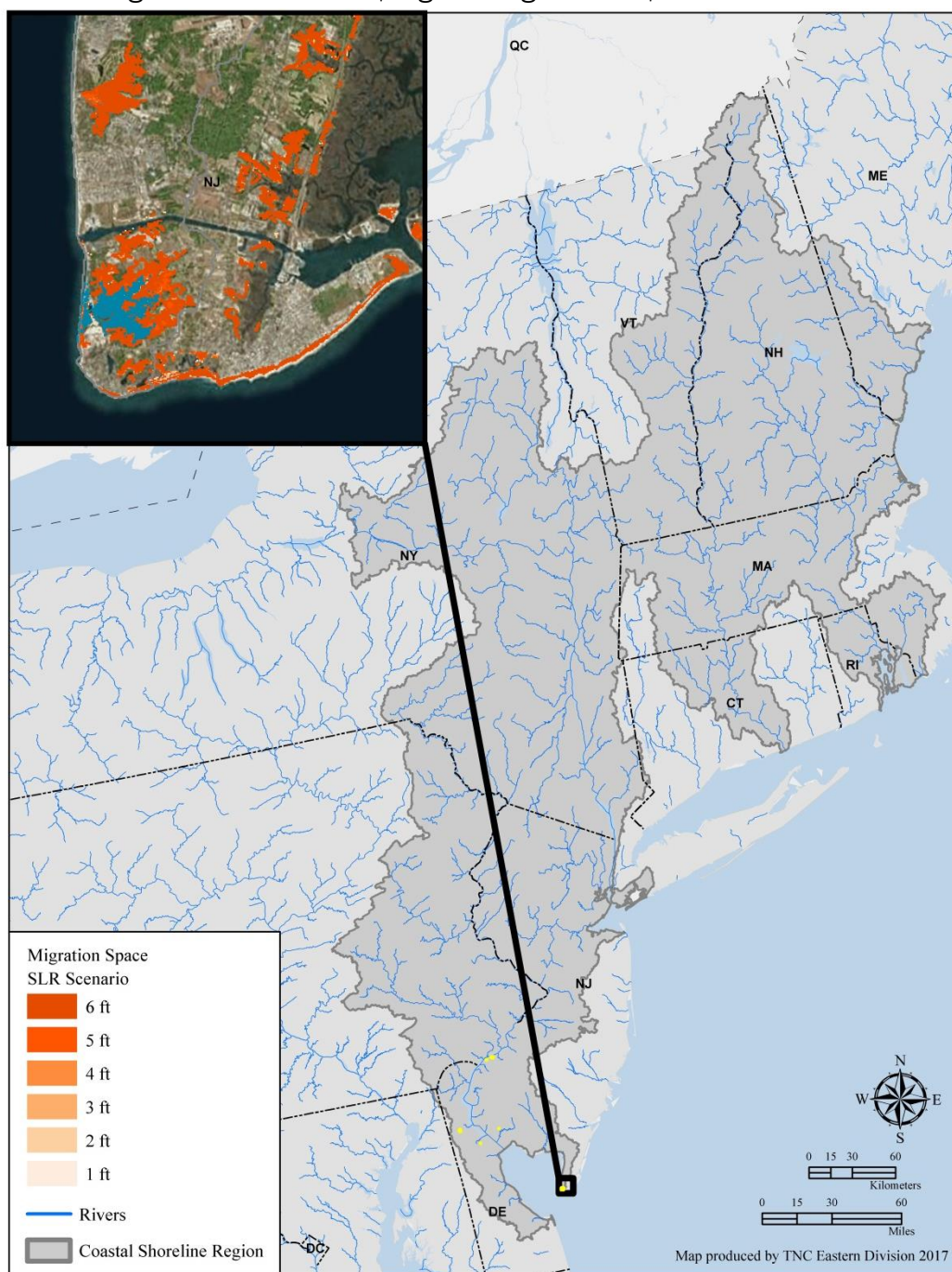
Table 7.10. The number of tidal complex units in each physical and condition score category. A two-by-two frequency table shows the count of tidal complexes occurring in each physical and condition class combination. Physical classes are by row and condition classes are by column. Boxes shaded in gray indicate tidal complexes with the same physical and condition score class. For example, 23 tidal complexes scored above average for both physical and condition characteristics.

Physical Class	Condition Class						
	Far Below Average	Below Average	Slightly Below Average	Average	Slightly Above Average	Above Average	Far Above Average
Far Below Average	518	41	2	8	1	1	0
Below Average	1	27	20	52	26	12	1
Slightly Below Average	0	25	18	69	13	22	5
Average	0	42	53	157	63	63	12
Slightly Above Average	0	9	28	58	30	24	3
Above Average	0	7	32	50	24	23	3
Far Above Average	0	0	7	13	3	0	0

There were 7 sites that had a low condition score (i.e., “below average”) and a high physical score (i.e., “above average”). The location of these sites is highlighted in yellow in Figure 7.26. These are potential areas for restoration as the physical template is suitable for marsh migration, but issues related to the condition of the migration space (e.g., poor water quality, hardened shoreline) would have to be addressed. The focal tidal complex in Figure 7.26 was along Higbee Beach in Cape May, NJ and had a high physical score due to its size (289 acres), a relatively complex shoreline, extensive migration space (441 acres), an “above average” shared edge with the tidal complex, and a buffer area with diverse soil classes. However, this site was immediately adjacent to agriculture, and the larger landscape within which it occurs was highly developed, resulting in several poor condition characteristics including the presence of hardened shoreline, severe flow alteration, and a buffer area with a high proportion of agricultural land.

Figure 7.26. Tidal complexes (n=7) with high physical scores but in poor condition.

These sites are estimated to be in poor condition (poor water quality, hardened shoreline, non-natural buffer area, etc.), but have physical characteristics hypothesized to increase resilience to sea level (large tidal complex, complex shoreline, migration space with diversity of tidal classes, etc.). The site in the inset map was along Higbee Beach in Cape May, NJ. The site had a large tidal complex (blue) surrounded by a large migration space, but occurs in a very developed landscape, contributing to flow alteration, high nitrogen loads, and some hardened shoreline.



Estimated Resilience Score

The physical and condition scores were equally weighted and combined to calculate an estimated resilience score for each tidal complex. High scoring sites were those with a large migration space, intact buffer area, and whose condition was not expected to exacerbate the impacts of sea level rise and climate change, with all these characteristics relative to other sites in the CSR. The role of some of the physical factors was evident in Figure 7.27 where high scoring tidal complexes shown in dark green have a large migration space (shown in orange shades), and very vulnerable complexes shown in dark brown have no migration space. The resilience values are in z-scores which follow a normal distribution except for the “far below average” category because tidal complexes with no migration space were manually assigned a -3.5 SD score for all migration space attributes. The relationship between the physical and condition scores and the role of that relationship in the estimated resilience score can be seen in Figure 7.28. The proportions of each class for the physical and condition components are fairly similar across all the resilience classes except for the “slightly below average” and “far above average” resilience categories. Most of the “far above average” condition scores occur in the “far above average” resilience class while the “far above average” physical scores are distributed across the “far above average” and “above average” resilience classes with a small amount in the “slightly above average”. In contrast to the Chesapeake, a larger proportion of “average” physical scores are in the “far above average” resilience class.

The ten tidal complexes with the highest estimated resilience score are shown in Figure 7.29. The average tidal complex size of this group was 366 acres with an average migration space size at a 6-foot sea level rise of 377 acres (min = 33, max = 1780, SD = 492 acres) and a large average buffer area (110,701 acres). While the average size of the top ten complexes was almost double that of the other river-dominated CSR, their migration space was significantly smaller than that of the Chesapeake, reflecting geophysical and land use differences between the two regions. Vulnerable sites, those having “below average” estimated resilience, are shown in Figure 7.30. These tidal complexes are locations with little to no migration space and whose poor condition, again relative to all other sites in the CSR, is expected to exacerbate the impacts of sea level rise and climate change. The results of a Pearson correlation analysis show the role of tidal complex size, migration space size, and buffer area size in the condition, physical, and resilience score (Table 7.12). As expected, given the weight of these attributes in the physical component score, size was significantly and positively correlated with the physical score, particularly for the migration space size. The condition score was also significantly and somewhat correlated with the tidal complex and buffer area size, which was likely the result of land use and geophysical patterns in the larger landscape whereby smaller migration spaces occur in areas with greater elevation and slope and/or in more developed locations.

Figure 7.27. Estimated resilience score. This map shows the estimated resilience score for the Northeast River-Dominated CSR for the 6-foot sea level rise scenario. The map shows areas that are above (green) or below (brown) the mean. Areas in green score “above average” and are estimated to be more resilient based on their physical and condition characteristics. Areas in yellow are “average.” Areas in brown are “below average” and are estimated to be vulnerable to sea level rise and climate change.

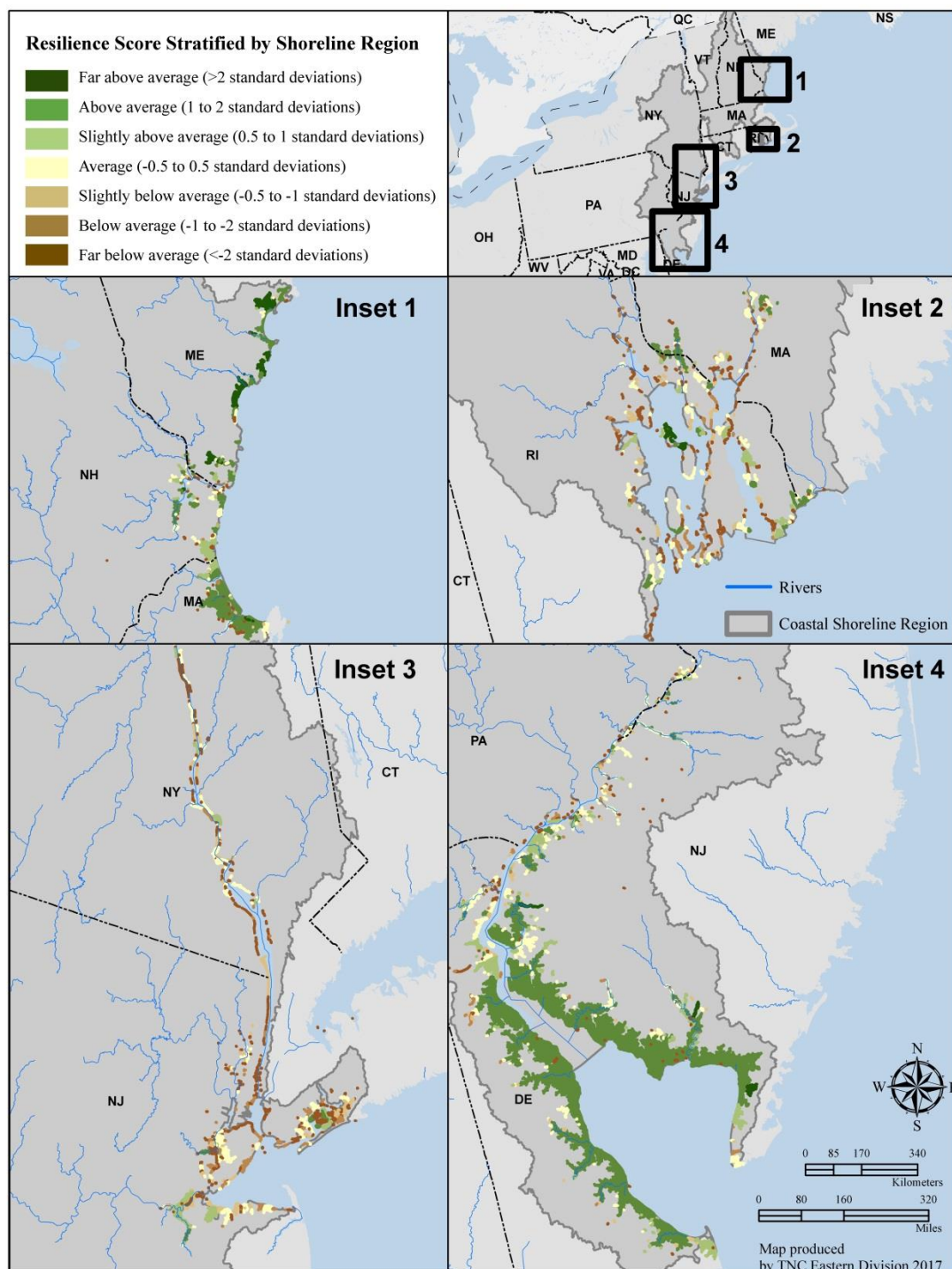


Figure 7.28. Relationship between condition and physical components for each estimated resilience class at a sea level rise of 6 feet. The physical and condition bars are split vertically based on the proportion of each score for each resilience class.

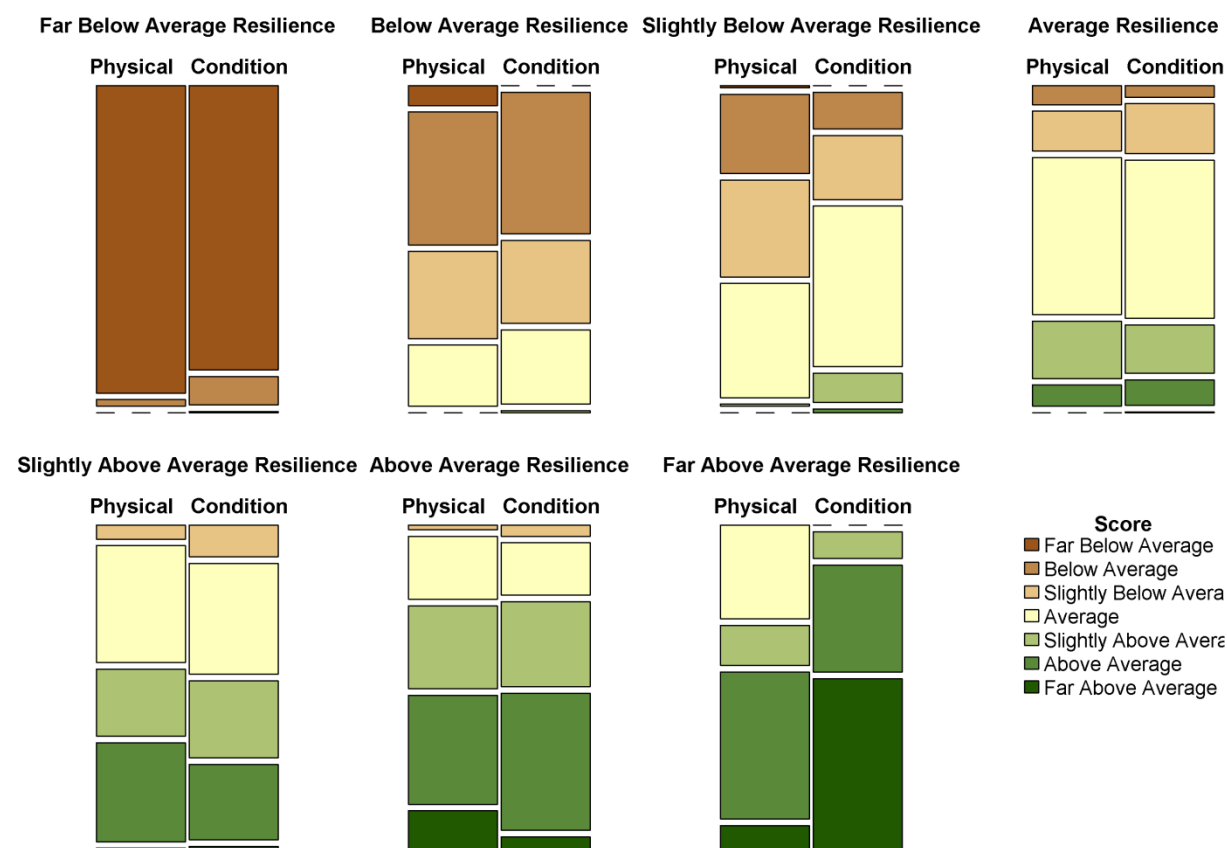


Table 7.11. Distribution of estimated resilience scores in the Northeast River-Dominated CSR for the 6-foot sea level rise scenario.

Z-Score Class	Estimated Resilience	Estimated Resilience with Migration Space Trend
Far Below Average	573	574
Below Average	138	132
Slightly Below Average	152	135
Average	390	329
Slightly Above Average	152	171
Above Average	138	174
Far Above Average	23	51

Figure 7.29. The top ten highest scoring tidal complexes in the Northeast River-Dominated CSR. The ten tidal complexes with the highest estimated resilience score are highlighted in yellow. The focal tidal complex along the York River in southern Maine was “above average” in size (464 acres), had a complex shoreline, a “slightly above average” migration space (245 acres), a very large buffer area (483K acres), no hardened shoreline, good water quality, and “average” sediment contributions.

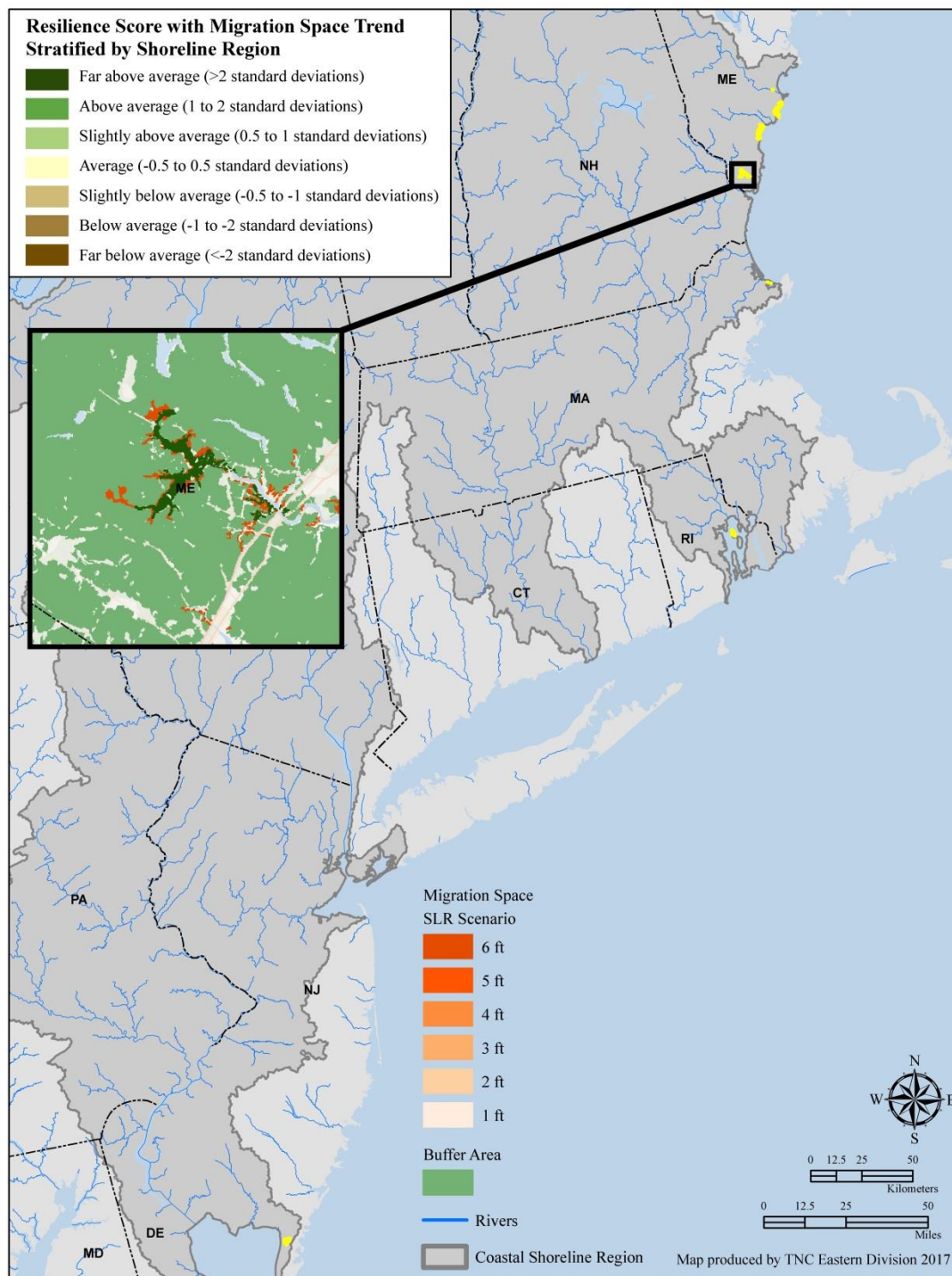


Figure 7.30. Vulnerable tidal complexes. Sites that scored below the mean are considered vulnerable. Sea level rise is expected to worsen the degradation of vulnerable sites, but these sites may still provide valuable ecosystem services (i.e., buffering storm effects, wildlife habitat, etc.).

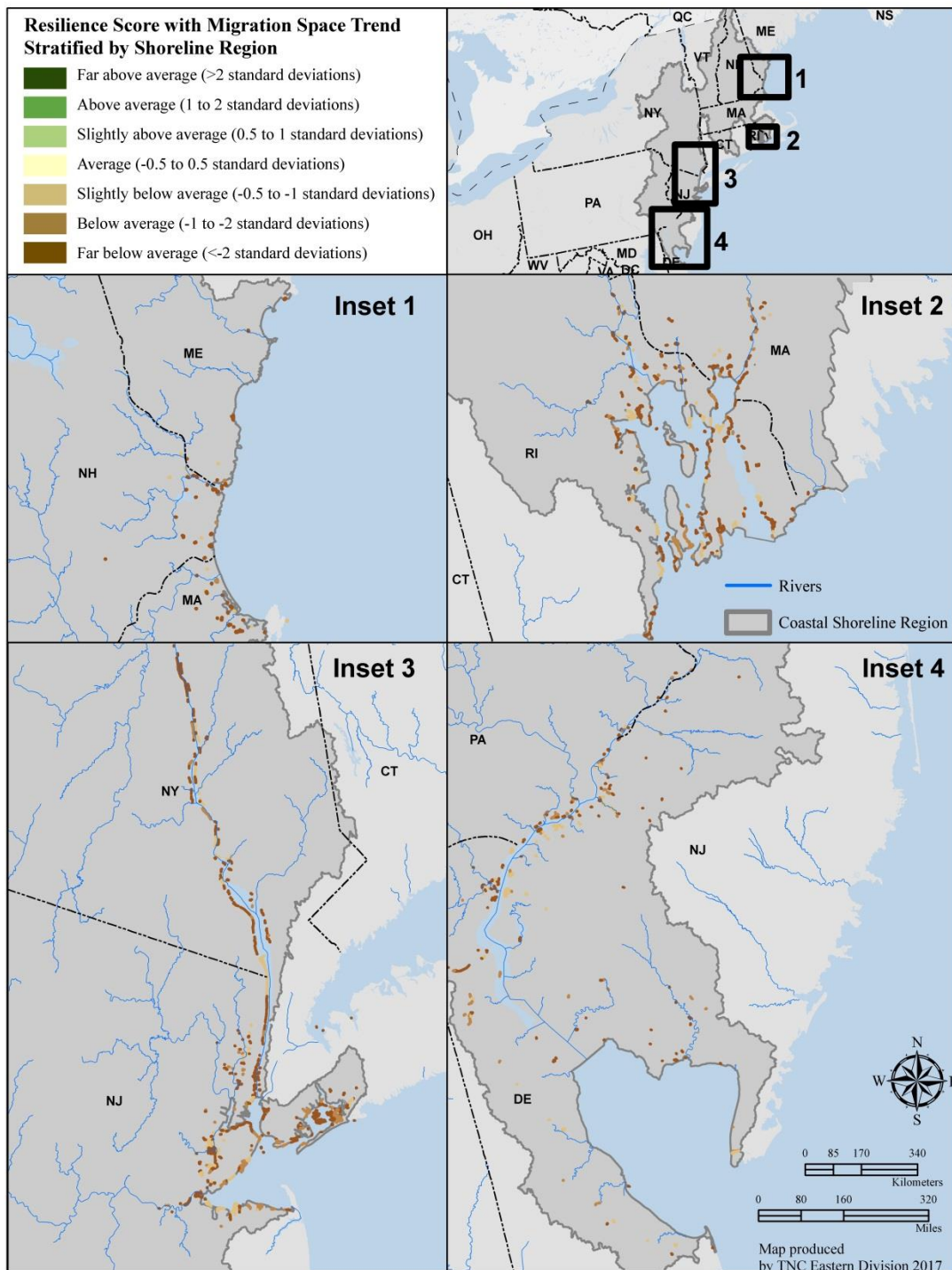


Table 7.12. Relationship between resilience components and analysis unit size.

Pearson correlation coefficients between the condition, physical, and estimated resilience scores and the size (acres) of the tidal complex, migration space, and buffer area, after removing tidal complexes with no migration space. A star indicates a significant ($p \leq .05$) relationship.

	Tidal Complex Size	Migration Space Size	Buffer Area Size
Physical Z-score	.30*	.765	.574*
Condition Z-score	.11*	-0.055	.260*
Resilience Z-score	.285*	.502*	.561*

Trends in Migration Space Size

Similar to the Chesapeake Bay CSR, the mean migration space size of tidal complex units in the Northeast River-Dominated region increased from a 1 to 3-foot sea level rise but then showed a decline from 3 to 6 feet (Table 7.13). Linear regressions identified 1186 tidal complex units with a statistically significant ($p \leq .05$) relationship between the latter three sea level rise scenarios (3 – 6 feet) and migration space size. Of those tidal complex units with a significant relationship, some had decreasing migration space but the majority experienced an increase in migration space (Table 7.14). The mean increase in size was 68 acres while the average decrease was similar at 62 acres (Table 7.14). Tidal complexes with a significant migration space trend were assigned to one of three trend categories: increase, decrease, no change, and we adjusted their score to reflect the trend. The 472 tidal complexes whose migration space showed an increasing trend were awarded an additional 0.50 SD points to their estimated resilience score. The 150 tidal complexes that experienced a decline in migration space size from the 3 to the 6-foot SLR scenario had their estimated resilience scores reduced by 0.50 SD. The resilience score of the 564 tidal complexes with no significant change in migration space size was not impacted by the trend analysis. The map in Figure 7.31 shows the spatial distribution of the resilience scores with the trend analysis incorporated. Of the top ten highest scoring sites shown in Figure 7.29, all ten received a boost to their score from a positive migration space size trend. The use of 0.50 SD to adjust the resilience score meant that no tidal complex's score could change by more than one resilience class (Table 7.15). After incorporating migration space trend, 26% (403) of the tidal complexes changed resilience classes with 101 or 6% of sites going to the next lower class and 302 or 19% moving up a class (Figure 7.32, Table 7.15).

Table 7.13. Summary statistics for migration space size by sea level rise scenario.

SLR Scenario (feet)	Migration Space (Acres)				
	1 st Quartile	Median	Mean	3 rd Quartile	Max
1	0	1.779	238.5	25.02	10,760
2	0	2.002	260.7	27.35	13,350
3	0	2.224	295.3	32.3	16,230
4	0	2.446	322	36.31	18,620
5	0	2.669	332.5	38.25	18,340
6	0	3.114	329	38.97	17,430

Table 7.14. Summary of regression coefficients for tidal complex units (n=1186) with a significant ($p \leq .05$) relationship between sea level rise scenario (≥ 3 feet) and migration space size.

Migration Space Size (acres) Change					
Trend direction	Count	Minimum	Median	Mean	Max
Decrease	150	-457.80	-3.542	-62.57	-0.083
Increase	472	0.051	4.642	68.45	1896
No change	564	0	0	0	0

Figure 7.31. Estimated resilience score with migration space trend. This map shows the estimated resilience score after incorporating the trend in migration space size for the Northeast River-Dominated CSR at the 6-foot sea level rise scenario. Tidal complex units whose migration space showed a significant increase ($p \leq .05$) from the three to 6-foot SLR received an additional 0.50 standard deviation units to their score, while the score of units with a significant decrease in migration space was reduced by 0.50 SD units.

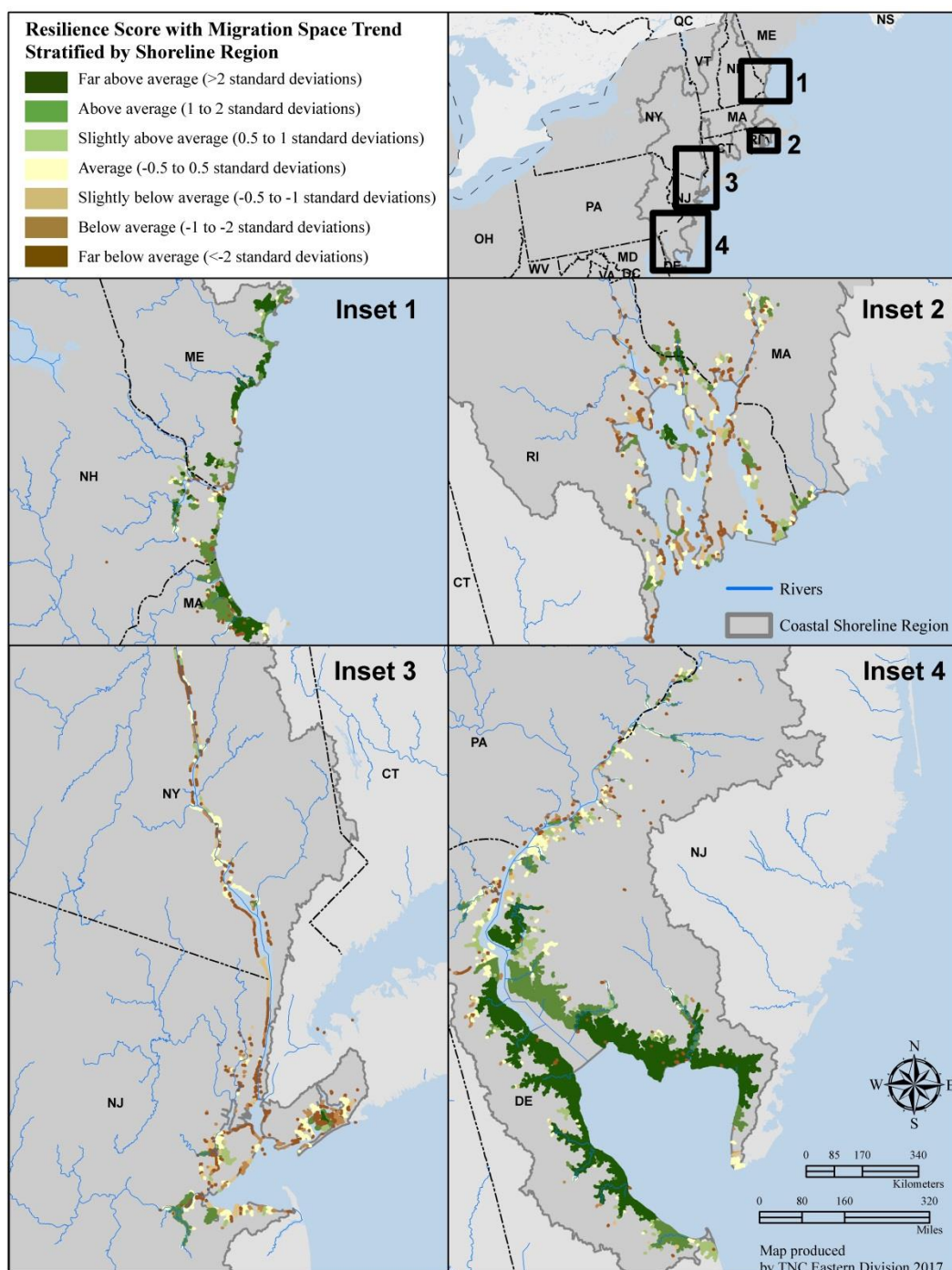
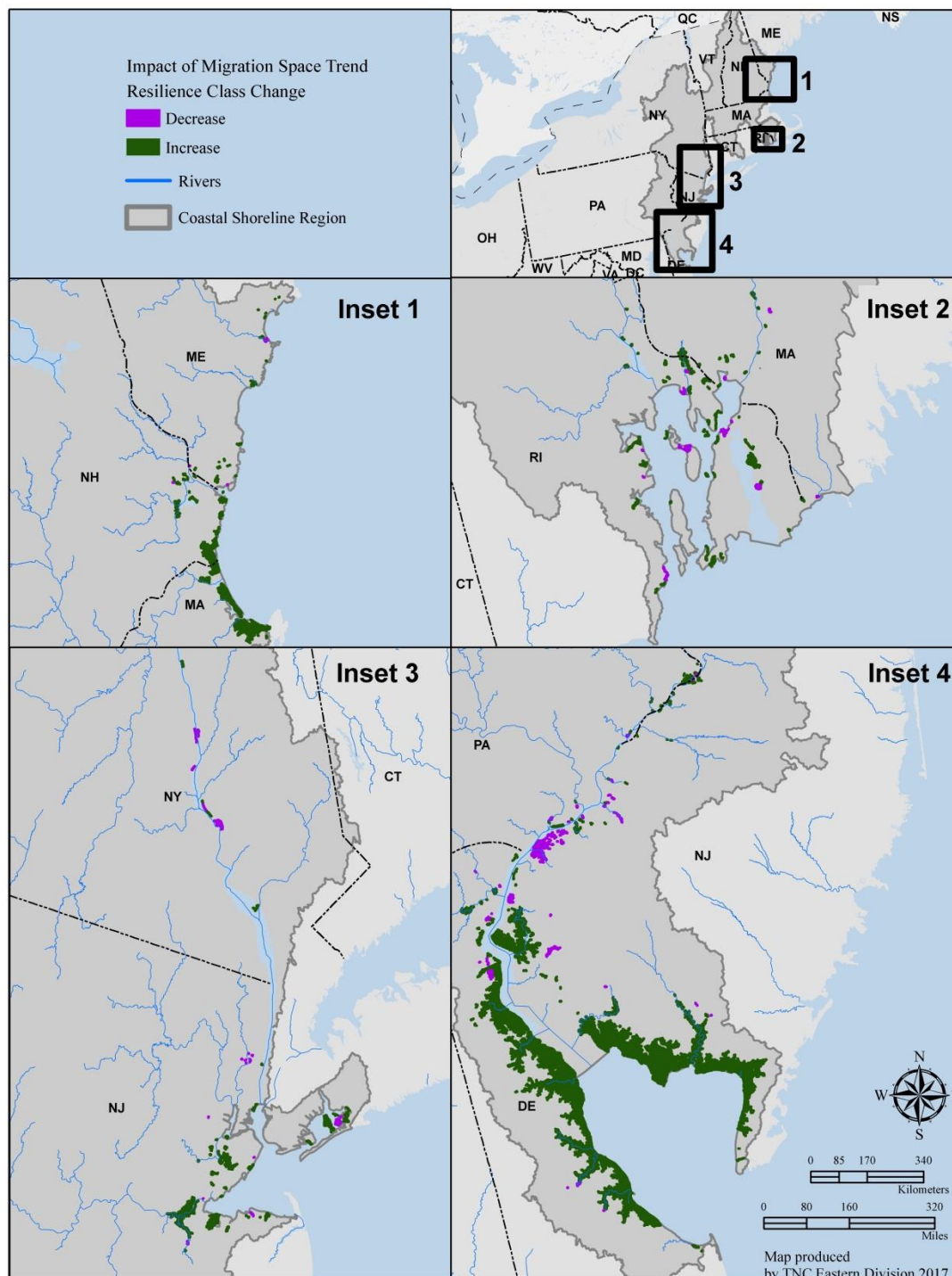


Table 7.15. The change in resilience class after incorporating the trend in migration space size. Tidal complex units whose migration space showed a significant increase ($p \leq .05$) from the three to 6-foot sea level rise received an additional 0.50 standard deviation units to their score, while the score of units with a significant decrease in migration space size was reduced by 0.50 SD units. The purple boxes indicate the number of tidal complex units that moved to the next lower resilience class, and the green boxes highlight the number of units whose class improved when the migration space trend was considered.

Resilience Class	Resilience class with Trend						
	Far Below Average	Below Average	Slightly Below Average	Average	Slightly Above Average	Above Average	Far Above Average
Far Below Average	569	4	0	0	0	0	0
Below Average	5	100	33	0	0	0	0
Slightly Below Average	0	28	69	55	0	0	0
Average	0	0	33	257	100	0	0
Slightly Above Average	0	0	0	17	56	79	0
Above Average	0	0	0	0	15	92	31
Far Above Average	0	0	0	0	0	3	20

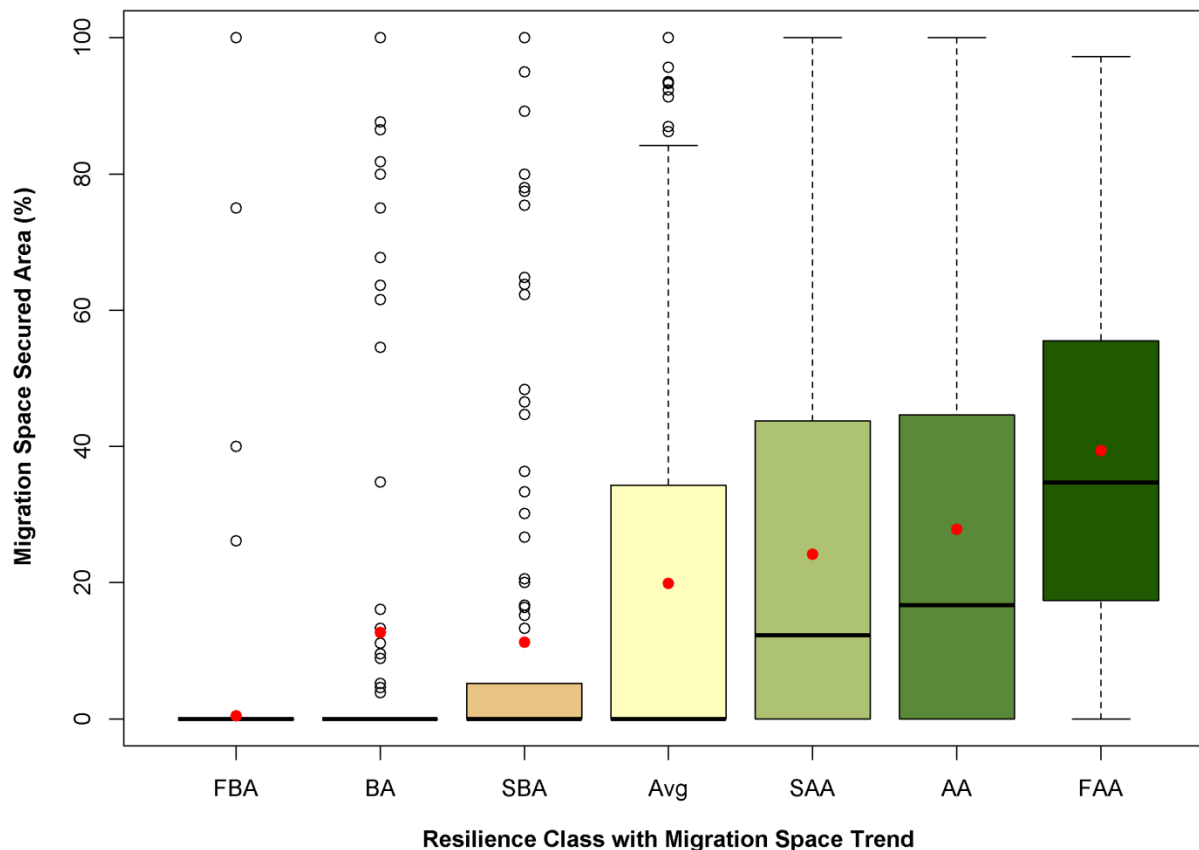
Figure 7.32. Estimated resilience class changes after incorporating migration space trend. This map shows the tidal complexes whose estimated resilience class either increased (n=472) or decreased (n=150) after incorporating the trend in migration space size for the Northeast River-Dominated CSR at the 6-foot sea level rise scenario.



Migration Space Securement

The amount of a tidal complex's total migration space that was already protected (GAP status 1-3) varied substantially by resilience z-score category (Figure 7.33). Tidal complex units that had the highest estimated resilience also had the highest mean percentage of their migration space permanently protected (39%), and the worst scoring tidal complex units had the lowest average percent protected with less than half a percent (Figure 7.33), which was due largely to the fact that the worst scoring units had very little if any migration space.

Figure 7.33. Amount (%) of migration space in permanent protection by estimated resilience class. The boxplot shows the distribution of migration space securement (%) by resilience class. The mean percent secured is denoted by a red circle. The resilience classes are shown using our standard z-score color palette and abbreviations.



Migration Space Development and Future Development

Due to inconsistencies in spatial resolution of various datasets used in this analysis (i.e., 10-m elevation and 30-m land cover products), and how roads are inaccurately mapped in base land cover grids such as the NLCD and C-CAP products, there are cases where some development occurs within the migration space mapped at the 30-m scale. The two highest scoring resilience classes had the lowest mean amount of development (<10%). The below and “slightly below average” classes had the highest average development percentage, reflecting the more developed landscapes and poorer conditions in which these tidal complexes likely occur (Figure 7.34). There are tidal complexes that have 80-100% development for several of the resilience classes, and this typically occurs for very small migration space areas where a single pixel of development leads to a high percentage. The risk of future development in the migration space by 2100 was similar across resilience classes, but the below average sites do have the highest likelihood of future development with almost 6% (Table 7.16). This information is intended to help natural resource managers when they are considering restoration or protection strategies for a specific location.

Figure 7.34. Amount (%) of migration space comprised of developed land, by estimated resilience class. The boxplot shows the distribution of migration space development (%) by resilience class with the mean denoted by a red circle. The resilience classes are shown using our standard z-score color palette and abbreviations.

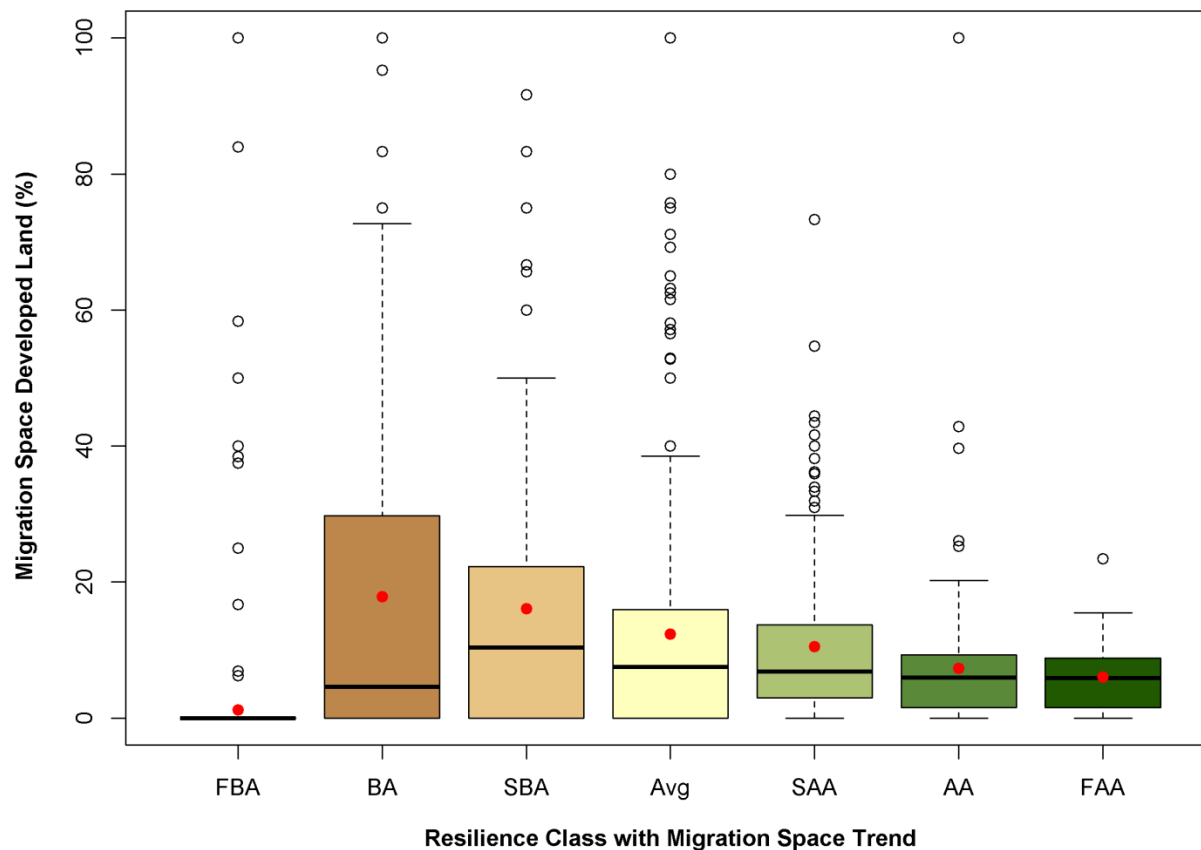
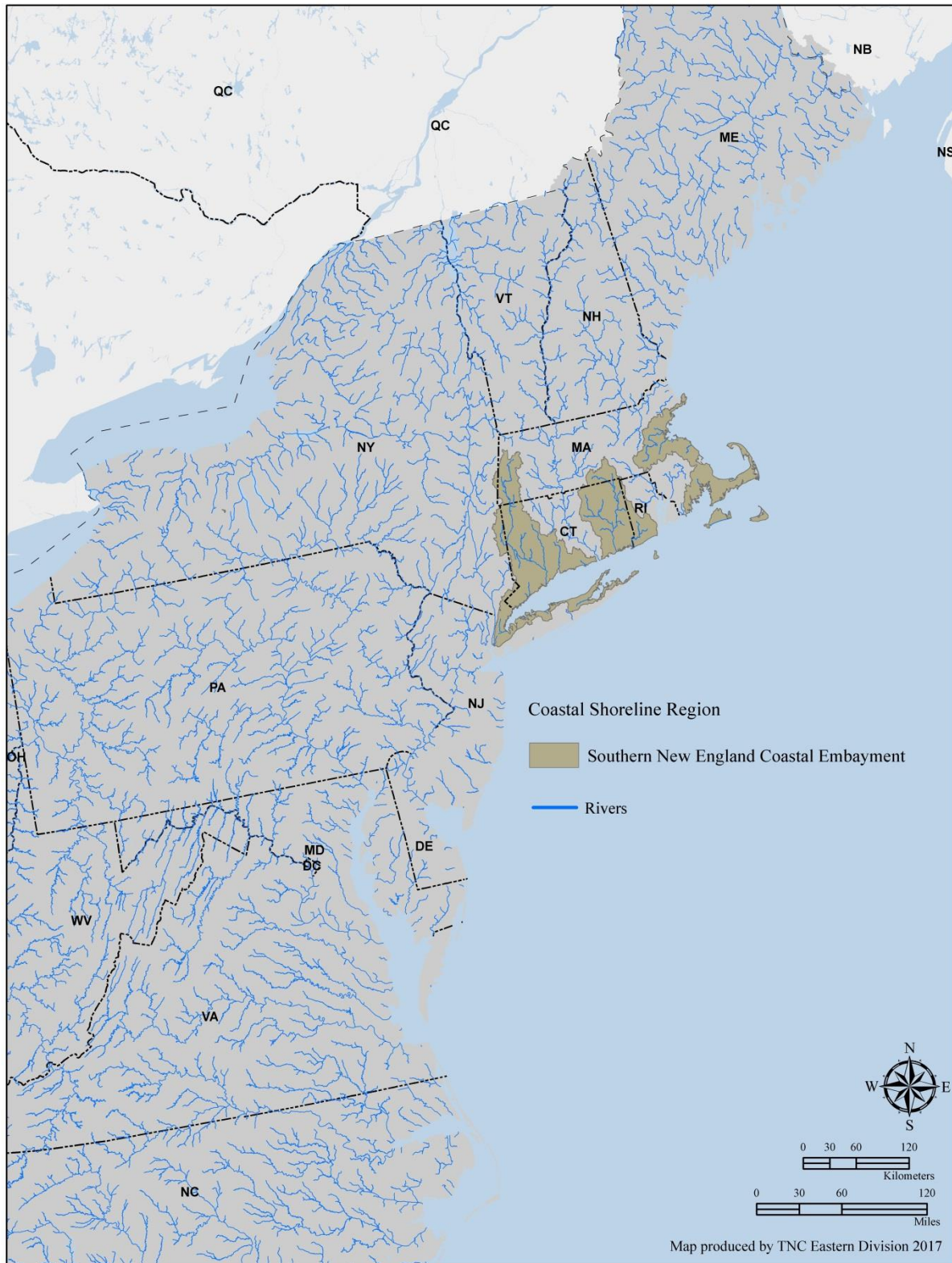


Table 7.16. Amount (%) of migration space estimated to be developed in 2100, by estimated resilience class. Summary statistics for migration space future development (%) are shown by resilience class.

Resilience Class with Migration Trend	Migration Space Future Development (%)					
	Min	1 st Quartile	Median	Mean	3 rd Quartile	Max
Far Below Average	0	0	0	0.539	0	100
Below Average	0	0	0	5.698	0	100
Slightly Below Average	0	0	0	3.247	0	100
Average	0	0	0	2.554	0	100
Slightly Above Average	0	0	0	1.321	0	92.86
Above Average	0	0	0	1.212	0	70.83
Far Above Average	0	0	0	0.1208	0.01	2.61

Southern New England Coastal Embayment CSR: Results



In the **Southern New England Coastal Embayment CSR**, there was a total of 2110 tidal complex units, with an average size of 30 acres and a median size of 6 acres (Figures 7.35-7.36). The largest unit in this CSR was 3540 acres. Both the average and largest tidal complex values were the lowest of the five coastal regions.

Figure 7.35. Distribution of tidal complex size (acres) by ten size classes in the Southern New England Coastal Embayment CSR.

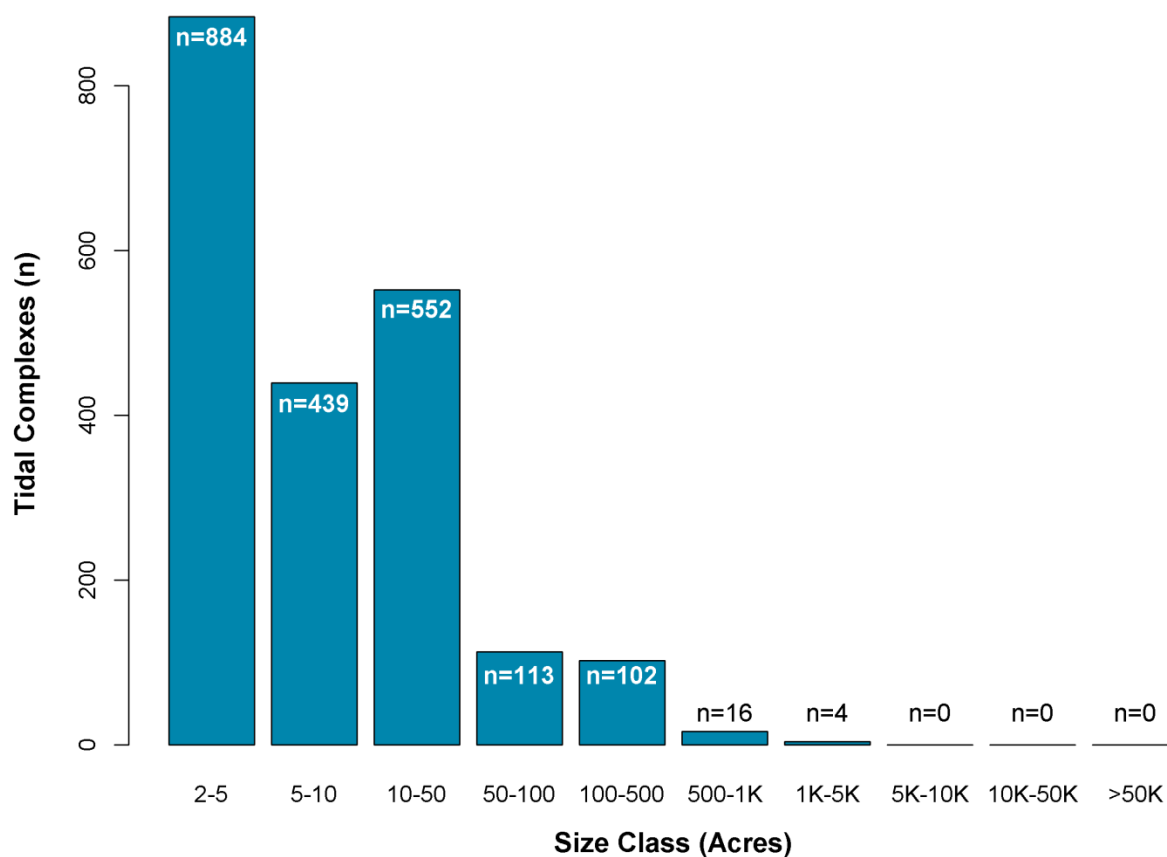
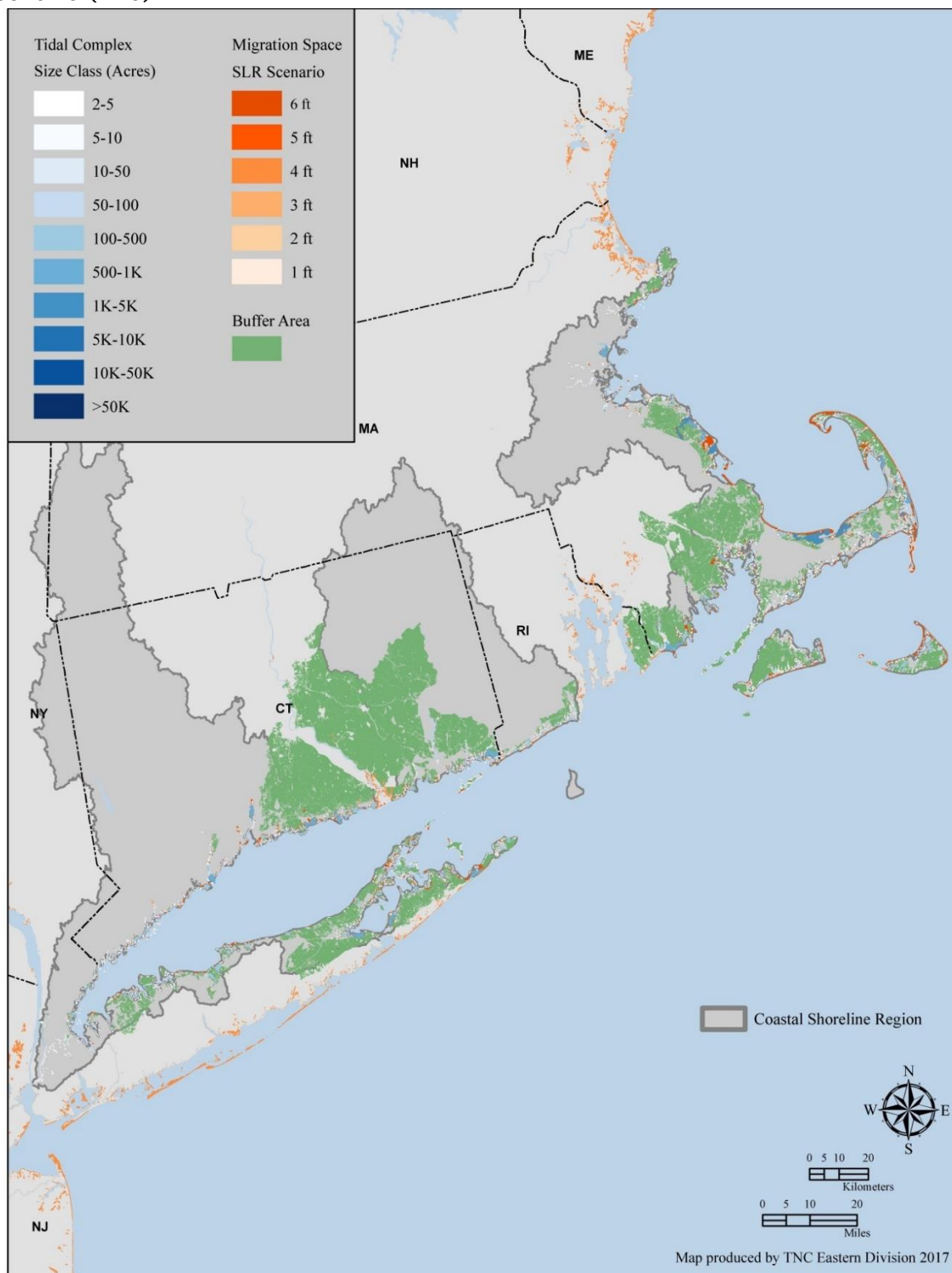
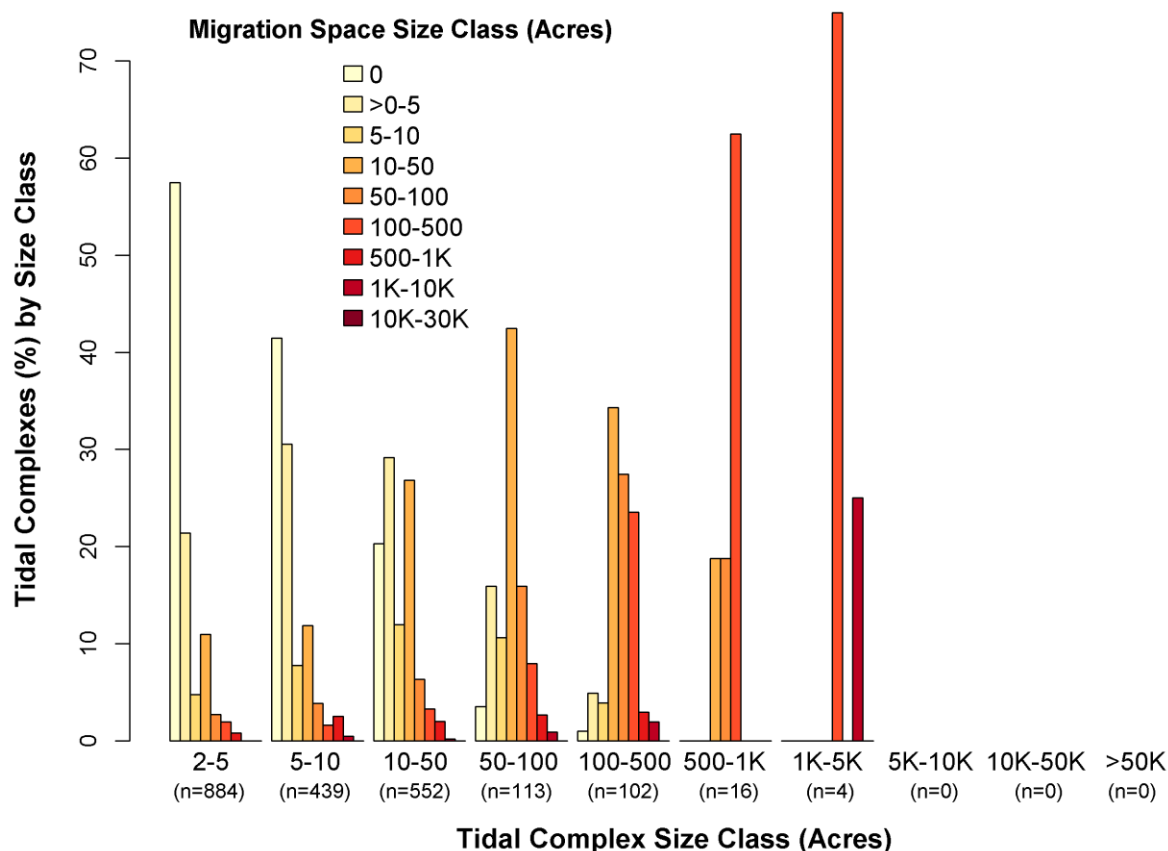


Figure 7.36. Tidal complex, migration space, and buffer area units in the Southern New England Coastal Embayment CSR. The color of the tidal complex units reflects their size class (n=10), while the color of the migration space indicates the SLR scenario (n=6).



Of the 2110 tidal complexes, 1303 or 62%, had migration space at a sea level rise of 6 feet (Figure 7.37), the second lowest percentage behind the Lagoon region. The average migration space size was 35 acres with a median size of 1 and a maximum size of 1458 acres, again the smallest of the five CSRs. As Figure 7.37 shows, the majority of small tidal complexes less than 50 acres in size have no migration space. The 20 largest complexes all have fairly large migration spaces.

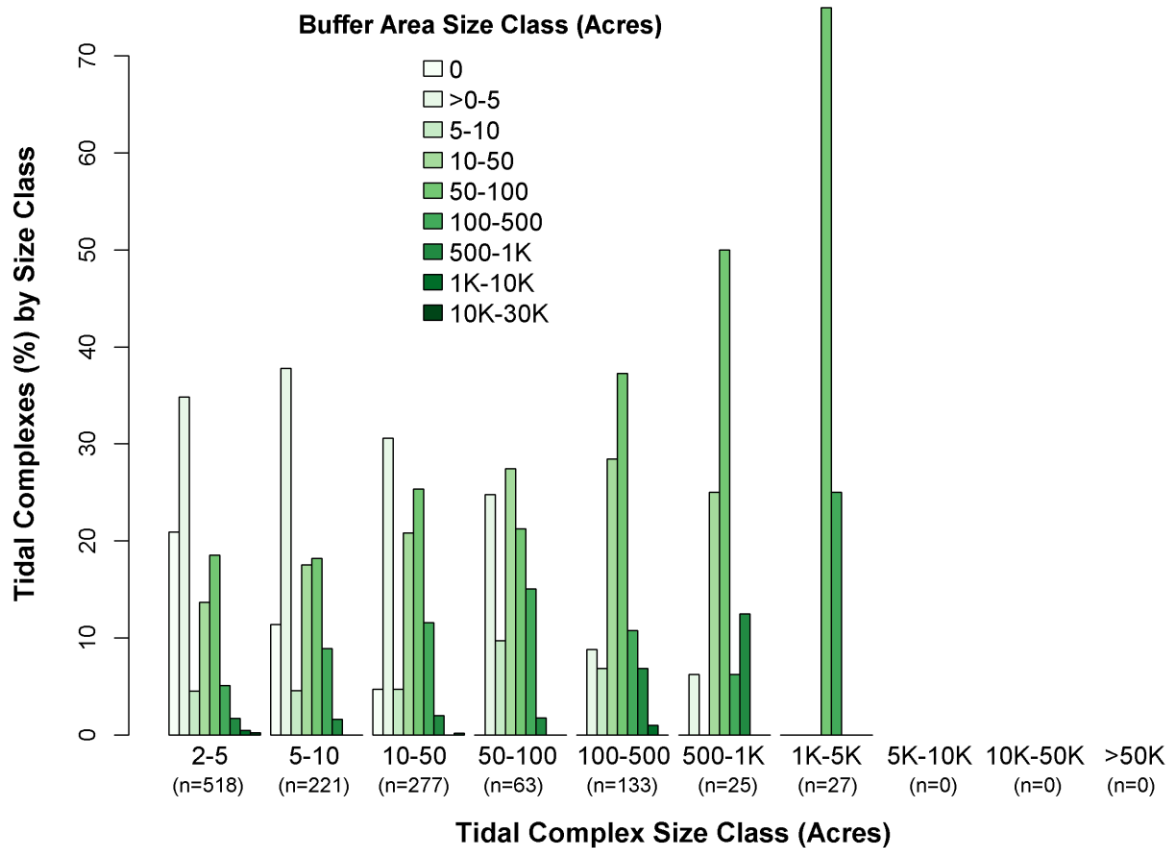
Figure 7.37. Migration space class distribution by tidal complex size class for the 6-foot sea level rise scenario. The y-axis is the percent of tidal complexes within a size class that have migration space of a particular size. Small migration space size classes are shown in light yellow shades that transition to darker oranges as the migration space size class increases.



A Spearman's rank-order correlation found the tidal complex size and migration space size were moderately positively correlated and this relationship was statistically significant ($r_s = .47$, $p < 2.2e-10$).

Most of the tidal complexes, 1849 or 88%, had buffer area at a sea level rise of 6 feet (Figure 7.38). The mean buffer size was 5262 acres with the largest buffer area encompassing 357,100 acres, the smallest buffer statistics of the five coastal regions. In contrast to the pattern between tidal complex size and migration space size, the majority of small tidal complexes have some buffer area whereas some larger tidal complexes do not have any buffer area (Figure 3.38). There was a somewhat positive relationship between tidal complex size and buffer area size that was significant ($r_s = .28$, $p\text{-value} < 2.2e-10$).

Figure 7.38. Buffer area class distribution by tidal complex size class for the 6-foot sea level rise scenario. The y-axis is the percent of tidal complexes within a size class that have buffer area of a particular size. Small buffer area size classes are shown in light green shades that change to darker greens as the buffer area size class increases.



Physical and Condition Scores

The estimated resilience score for a tidal complex consists of the condition and physical components, each weighted equally. Figure 7.39 shows the geographic distribution of physical scores within the CSR for a sea level rise of 6 feet. As Figure 7.39 and Table 7.17 show, most scores fall in the “far below average” class, with the next largest category being “average.” The lowest scoring tidal complexes are predominantly those with no migration space and a less geophysically diverse buffer area. The spatial pattern of the condition scores is shown in Figure 7.40 with the numeric distribution highlighted in Table 7.17.

Figure 7.39. Estimated physical score for the Southern New England Coastal Embayment CSR. Tidal complex units in green score “above average” and have physical characteristics hypothesized to increase resilience including a large migration area with a diversity of tidal classes that are evenly distributed, a complex shoreline, and a geophysically diverse buffer area. Tidal complexes in yellow have “average” physical characteristics relative to all the units in the CSR. Tidal complexes in brown are “below average” and are estimated to respond poorly to sea level rise.

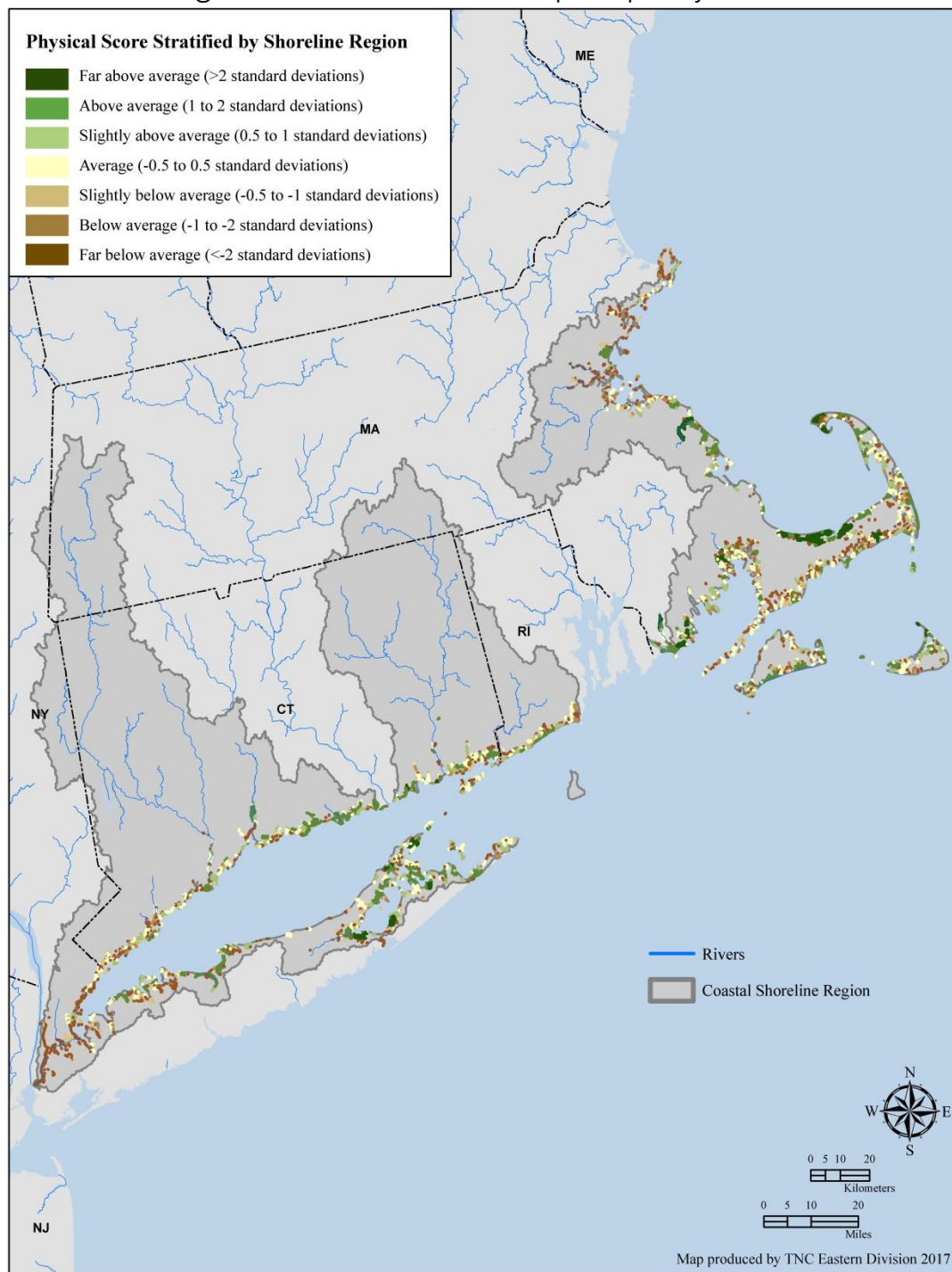


Figure 7.40. Estimated condition score for the Southern New England Coastal Embayment CSR. Tidal complex units in green score “above average” and are estimated to be in good condition based on a low percentage of hardened shoreline; good water quality and quantity, and high sediment contributions in the migration space; and a natural buffer area with highly connected wetlands. Tidal complexes in yellow are “average.” Tidal complexes in brown are “below average” and are estimated to be in poor condition.

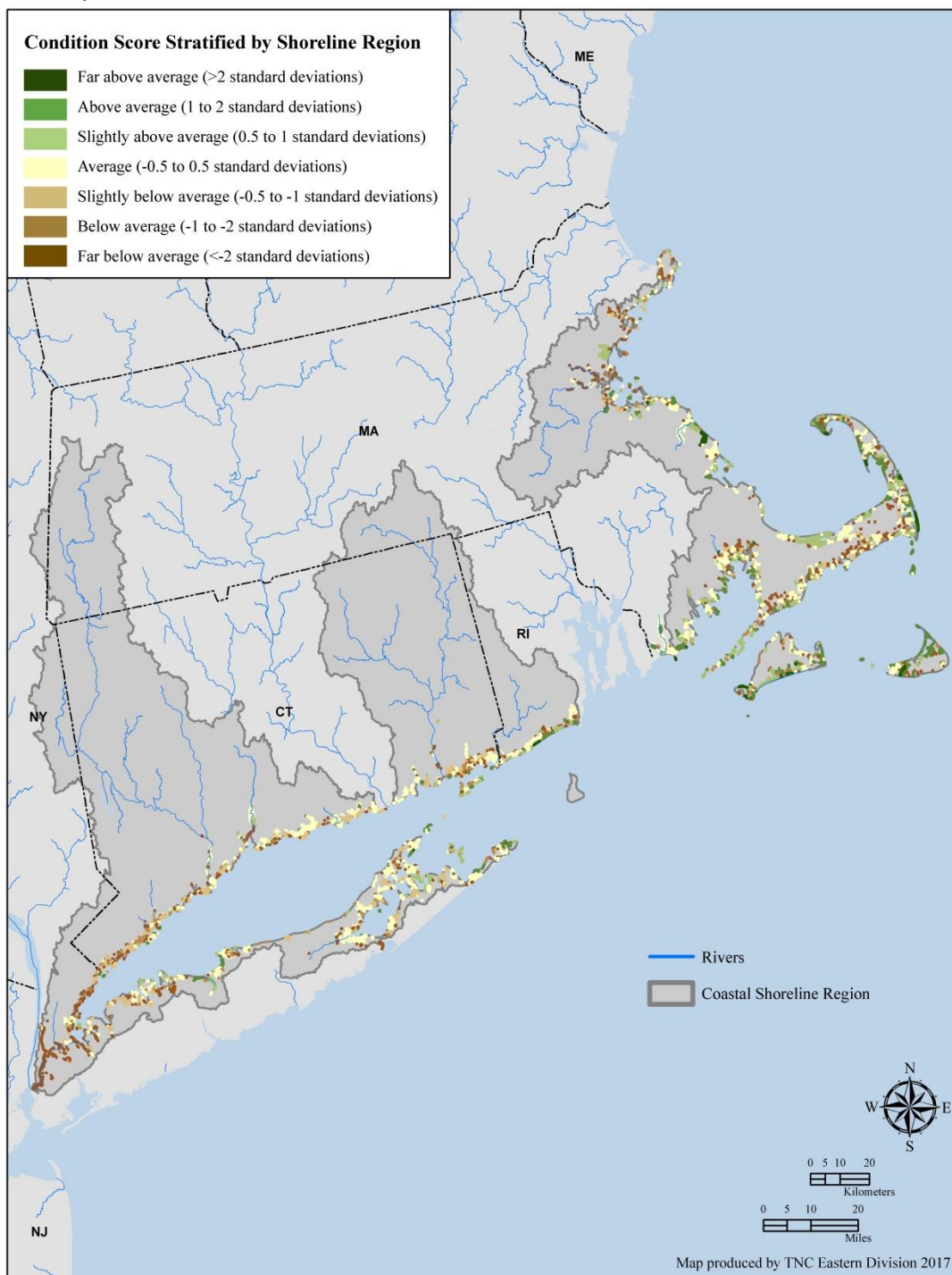


Table 7.17. Frequency of physical and condition scores in the Southern New England Coastal Embayment CSR for the 6-foot sea level rise scenario.

Z-Score Class	Tidal Complex (n)	
	Physical	Condition
Far Below Average	839	646
Below Average	176	204
Slightly Below Average	195	224
Average	499	574
Slightly Above Average	195	224
Above Average	176	203
Far Above Average	30	35

The relationship between the condition and physical scores was somewhat positively correlated (Pearson's $r = .25$, $p = 2.2e-10$, Figure 7.41). A tidal complex with a high physical score does not necessarily have a high condition score as evidenced in Figures 7.41-7.42 and Table 7.18. However, there were more sites that had better than average physical scores and better than average condition scores versus a combination of poor physical and poor condition scores. Much of the coastal zone of this CSR was highly urbanized, often limiting the area available for a marsh to migrate and contributing to poor conditions. Thus, a site that occurs in a less developed location would be likely to score relatively high for both physical and condition characteristics. Nonetheless, it was probably easier to have a better condition score than physical because a less urbanized area would automatically have better condition characteristics relative to most of the other sites while the physical setting could still limit the migration space, despite having compatible land use and management.

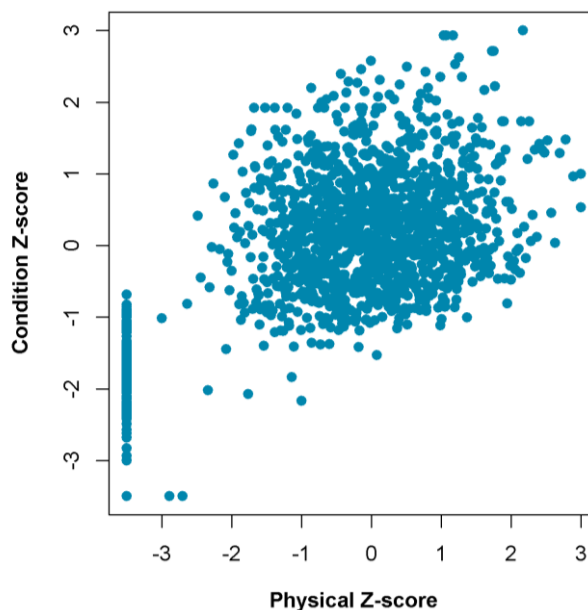
Figure 7.41. Relationship between the tidal complex units' physical and condition z-scores for the 6-foot sea level rise scenario, after removing complexes with no migration space.

Figure 7.42. Distribution of the physical scores for each condition class at a sea level rise of 6 feet. The distribution of the physical scores is shown for each condition score class using our standard z-score color palette.

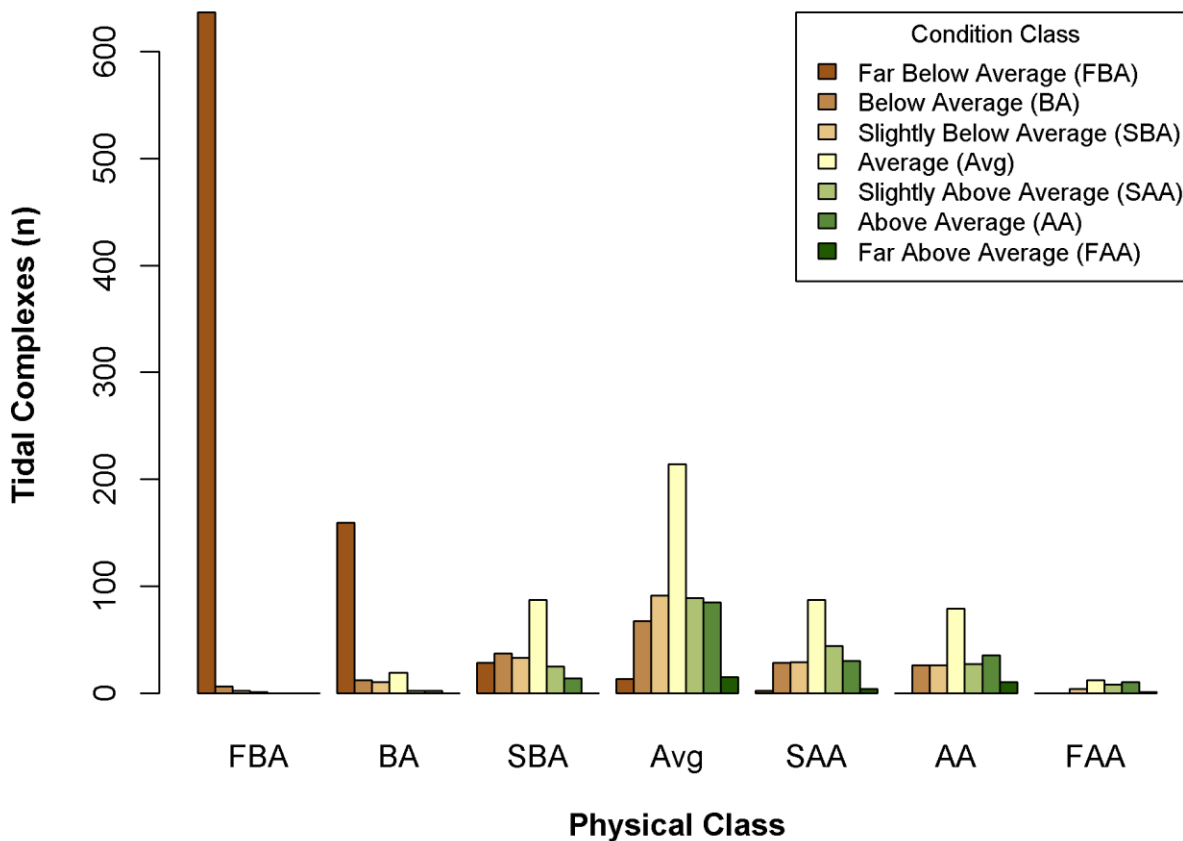


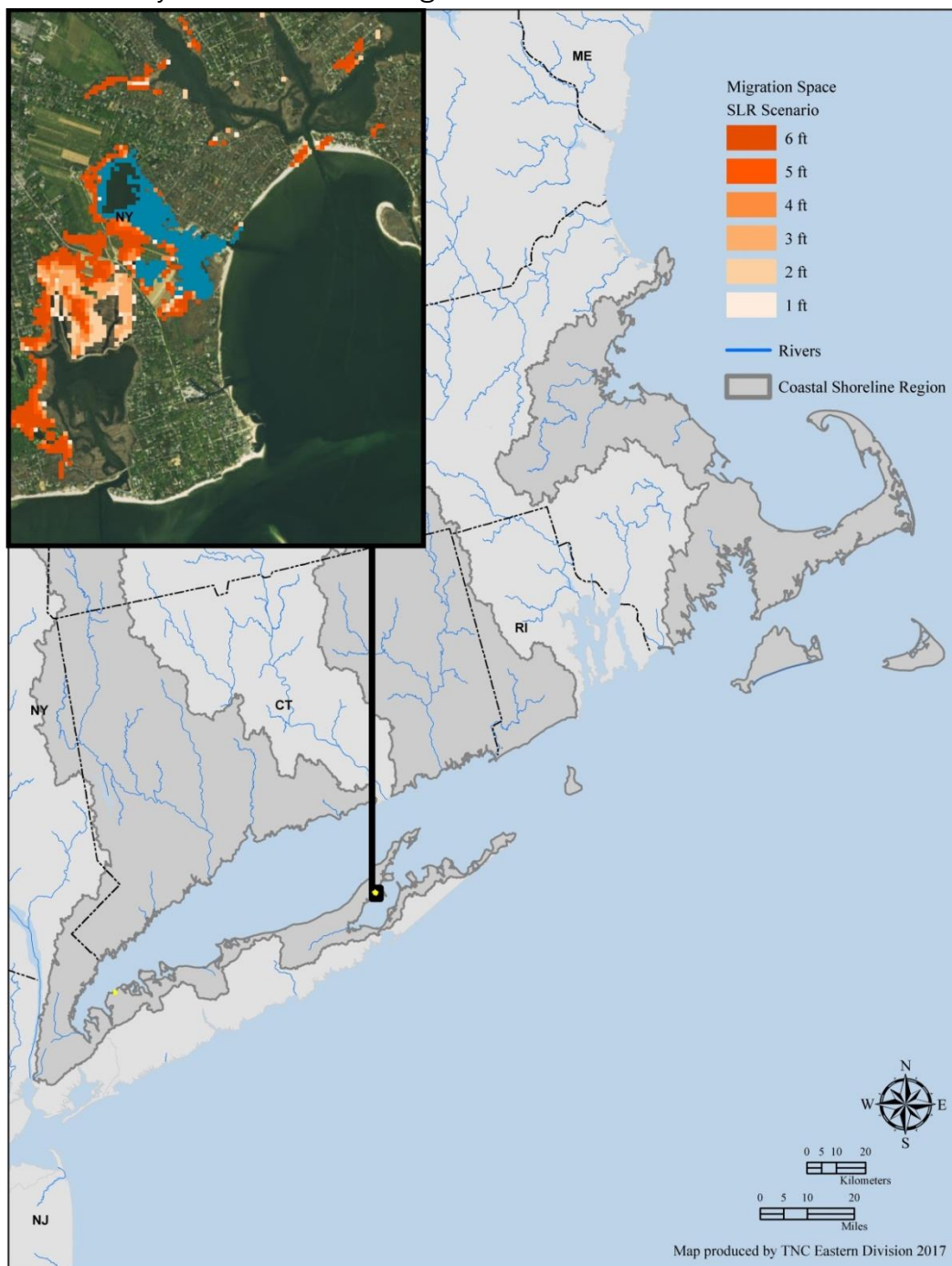
Table 7.18. The number of tidal complex units in each physical and condition score category. A two-by-two frequency table shows the count of tidal complexes occurring in each physical and condition class combination. Physical classes are by row and condition classes are by column. Boxes shaded in gray indicate tidal complexes with the same physical and condition score class. For example, only 1 tidal complex scored “far above average” for both physical and condition characteristics.

Physical Class	Condition Class						
	Far Below Average	Below Average	Slightly Below Average	Average	Slightly Above Average	Above Average	Far Above Average
Far Below Average	637	159	28	13	2	0	0
Below Average	6	12	37	67	28	26	0
Slightly Below Average	2	10	33	91	29	26	4
Average	1	19	87	214	87	79	12
Slightly Above Average	0	2	25	89	44	27	8
Above Average	0	2	14	85	30	35	10
Far Above Average	0	0	0	15	4	10	1

There were only two sites that had a low condition score (i.e., “below average”) and a high physical score (i.e., “above average”). The location of these sites is highlighted in yellow in Figure 7.43. These are potential areas for restoration as the physical template was suitable for marsh migration, but issues related to the condition of the migration space (e.g., poor water quality, hardened shoreline) would have to be addressed. The focal tidal complex in Figure 7.43 was located along Wickham Creek and drains into Little Peconic Bay in NY. This site had a high physical score due to the following factors: large size (64 acres), complex shoreline, moderately-sized migration space (47 acres), and a buffer area with a high diversity of soil types. However, this site had poor condition characteristics including high estimated nitrogen loadings, low sediment inputs, and a buffer area that was predominantly in agriculture. As the map shows, the site’s migration space was immediately surrounded by some patches of agricultural land, but the larger landscape was urban, resulting in poor water quality and low sediment inputs.

Figure 7.43. Tidal complexes (n=2) with high physical scores but in poor condition.

These two sites are estimated to be in poor condition (poor water quality, hardened shoreline, non-natural buffer area, etc.) but have physical characteristics hypothesized to increase resilience to sea level (large tidal complex, complex shoreline, migration space with diversity of tidal classes, etc.). The site shown in the inset is located along Wickham Creek and Little Peconic Bay in NY. The site's tidal complex had moderate migration space on one side, but the migration space and the complex were surrounded by a combination of agricultural and urban land cover.



Estimated Resilience Score

The physical and condition scores were equally weighted and combined to calculate an estimated resilience score for each tidal complex. High scoring sites were those with a large migration space, intact buffer area, and whose condition was not expected to exacerbate the impacts of sea level rise and climate change, with all these characteristics relative to other sites in the CSR. The role of some of the physical factors was evident in Figure 7.44 where high scoring tidal complexes shown in dark green have a large migration space (shown in orange shades), and very vulnerable complexes shown in dark brown have no migration space. The resilience values are in z-scores which follow a normal distribution except for the “far below average” category because tidal complexes with no migration space were manually assigned a -3.5 SD score for all migration space attributes. The relationship between the physical and condition scores and the role of that relationship in the estimated resilience score can be seen in Figure 7.45. A site had to have better than average physical and condition scores in order to receive a “far above average” score (Figure 7.45). As noted earlier, it was likely harder to have a high physical score versus a high condition score in this CSR, which was supported by the mosaic plot in Figure 7.45 and the class summary in Table 7.19.

The ten tidal complexes with the highest estimated resilience score are shown in Figure 7.46. The average tidal complex size of this group was 201 acres with an average migration space size at a 6-foot sea level rise of 428 acres (min = 50, max = 1458, SD = 431 acres), and a large average buffer area (11,545 acres). Vulnerable sites, those having “below average” estimated resilience, are shown in Figure 7.47. These tidal complexes are locations with little to no migration space and whose poor condition, again relative to all other sites in the CSR, is expected to exacerbate the impacts of sea level rise and climate change. The results of a Pearson correlation analysis show the role of tidal complex size, migration space size, and buffer area size in the condition, physical, and resilience scores (Table 7.20). Given the weight of the size attributes in the physical component score, it was not surprising that size was significantly and positively correlated with the physical score, particularly for the migration space size. The condition score was also significantly and mildly positively correlated with the migration space size, and moderately positively correlated with the buffer area size.

Figure 7.44. Estimated resilience score. This map shows the estimated resilience score for the Southern New England Coastal Embayment CSR for the 6-foot sea level rise scenario. The map shows areas that are above (green) or below (brown) the mean. Areas in green score “above average” and are estimated to be more resilient based on their physical and condition characteristics. Areas in yellow are “average.” Areas in brown are “below average” and are estimated to be vulnerable to sea level rise and climate change.

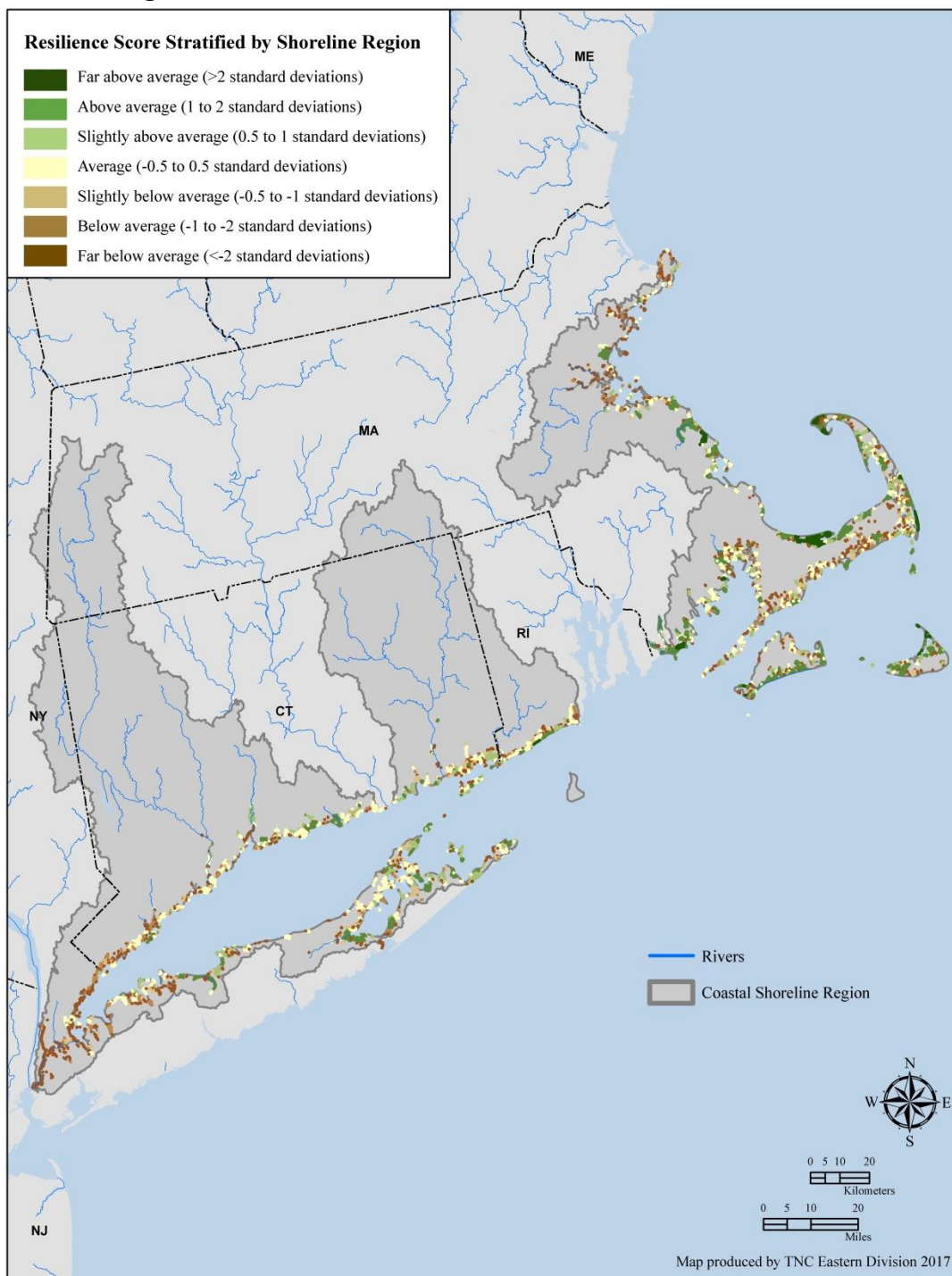


Figure 7.45. Relationship between condition and physical components for each estimated resilience class at a sea level rise of 6 feet. The physical and condition bars are split vertically based on the proportion of each score for each resilience class.

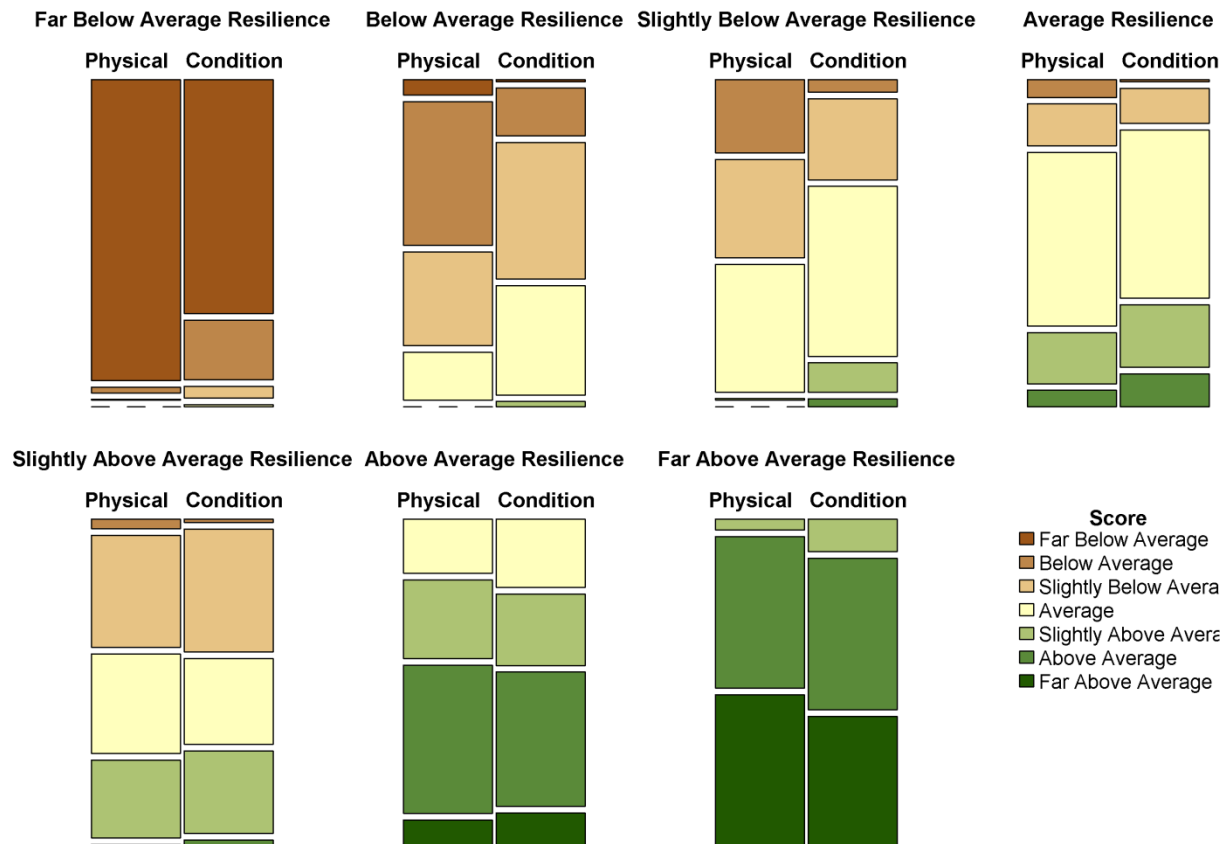


Table 7.19. Distribution of estimated resilience scores in the Southern New England Coastal Embayment CSR for the 6-foot sea level rise scenario.

Z-Score Class	Estimated Resilience	Estimated Resilience with Migration Space Trend
Far Below Average	848	852
Below Average	176	170
Slightly Below Average	193	176
Average	495	441
Slightly Above Average	193	187
Above Average	176	233
Far Above Average	29	51

Figure 7.46. The top ten highest scoring tidal complexes in the Southern New England Coastal Embayment CSR. The ten tidal complexes with the highest estimated resilience score are highlighted in yellow. Relative to other sites in this CSR, the focal tidal complex along Aucoot Creek and flowing into Aucoot Cove in southern MA was large (117 acres), had a complex shoreline, a moderately sized migration space (50 acres) with good tidal class evenness and variety, “above average” water quality, no hardened shoreline, and a buffer area with good wetland connectivity.

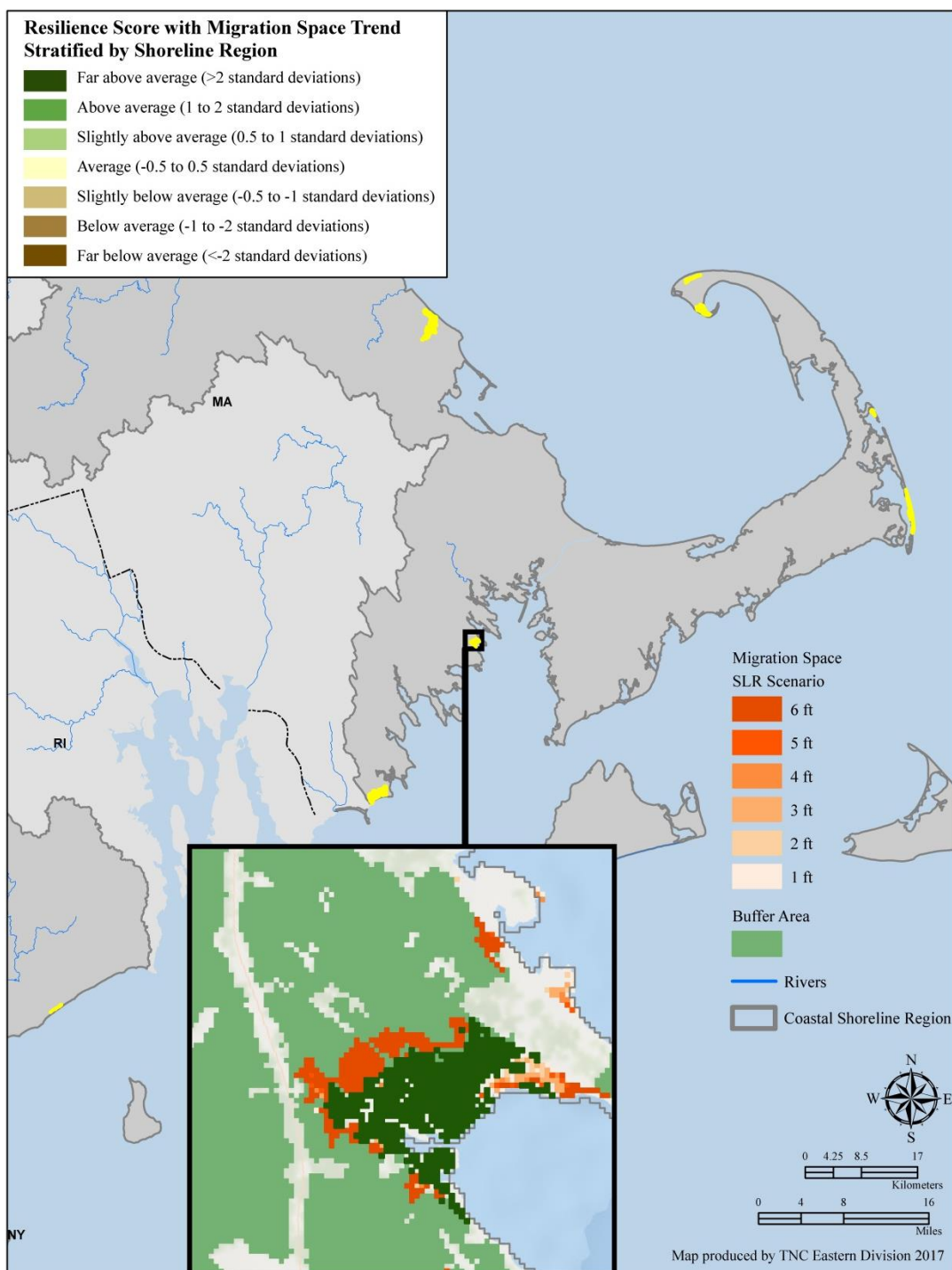


Figure 7.47. Vulnerable tidal complexes. Sites that scored below the mean are considered vulnerable. Sea level rise is expected to worsen the degradation of vulnerable sites, but these sites may still provide valuable ecosystem services (i.e., buffering storm effects, wildlife habitat, etc.).

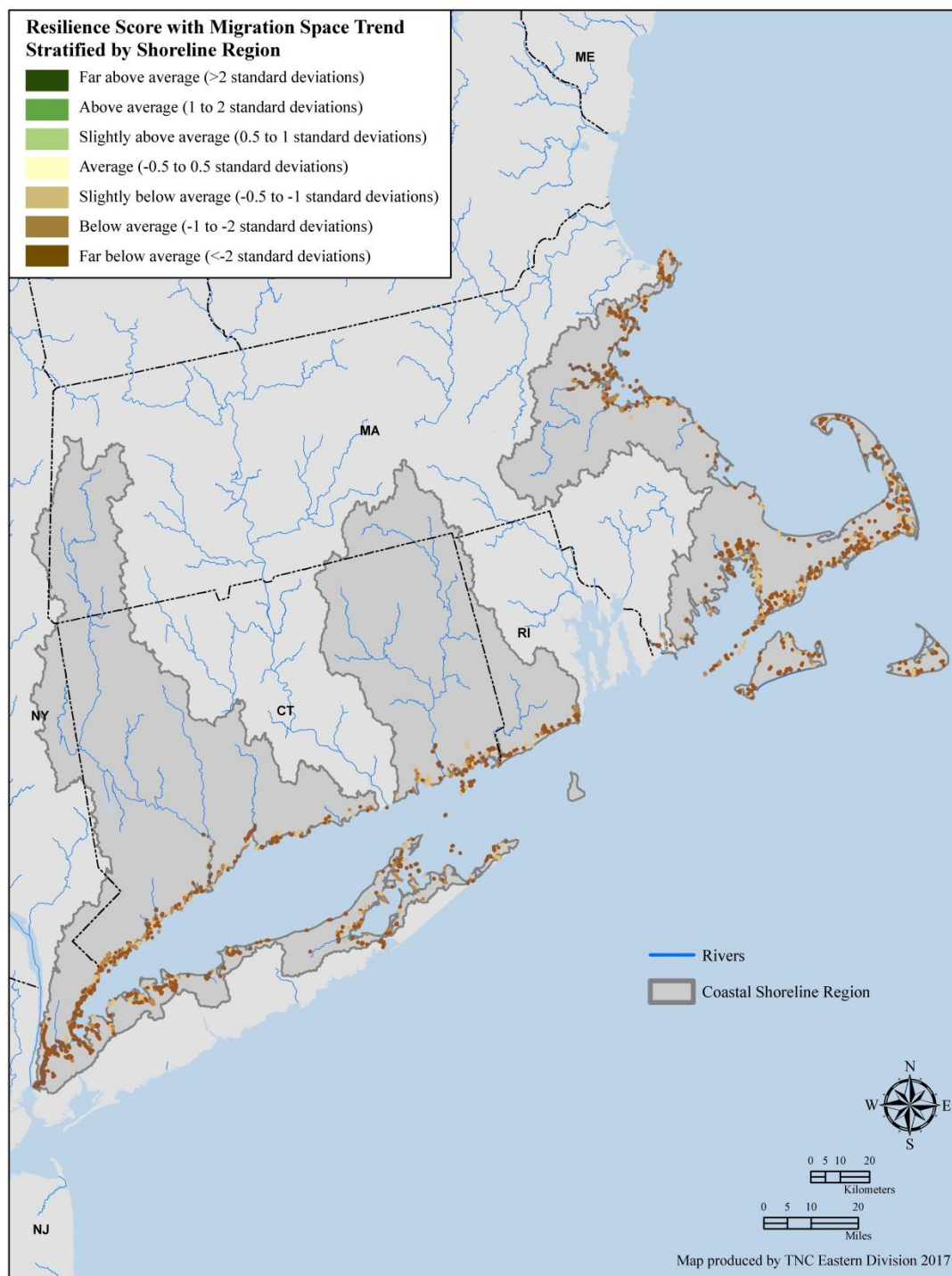


Table 7.20. Relationship between resilience components and analysis unit size.

Pearson correlation coefficients between the condition, physical, and estimated resilience scores and the size (acres) of the tidal complex, migration space, and buffer area, after removing complexes with no migration space. A star indicates a significant ($p \leq .05$) relationship.

	Tidal Complex Size	Migration Space Size	Buffer Area Size
Physical Z-score	.50*	.80*	.52*
Condition Z-score	.04	.22*	.40*
Resilience Z-score	.36*	.67*	.58*

Trends in Migration Space Size

For tidal complex units in the Southern New England Coastal Embayment setting, the mean size across all migration spaces increased from a 1 to 3-foot sea level rise but then showed a decline from 3 to 5 feet and a small increase at 6 feet (Table 7.21). Linear regressions identified 1470 tidal complex units with a statistically significant ($p \leq .05$) relationship between the latter three sea level rise scenarios (3 – 6 feet) and migration space size. Of those tidal complex units with a significant relationship, some had decreasing migration space but the majority experienced an increase in migration space (Table 7.22). The mean increase in size was 6 acres while the average decrease was 9 acres (Table 7.22). Tidal complexes with a significant migration space trend were assigned to one of three trend categories: increase, decrease, no change, and we adjusted their score to reflect the trend. The 466 tidal complexes whose migration space showed an increasing trend were awarded an additional 0.50 SD points to their estimated resilience score. The 178 tidal complexes that experienced a decline in migration space size from the 3 to the 6-foot SLR scenario had their estimated resilience scores reduced by 0.50 SD. The resilience score of the 826 tidal complexes with no significant change in migration space size was not impacted by the trend analysis. The map in Figure 7.48 shows the spatial distribution of the resilience scores with the trend analysis incorporated. Of the top ten highest scoring sites shown in Figure 7.46, only four received a boost to their score from a positive migration space size trend, and one was penalized for a shrinking migration space with increased sea level rise. The remaining five sites had stable migration space sizes and thus had no change to their resilience score. The use of 0.50 SD to adjust the resilience score meant that no tidal complex's score could change by more than one resilience class (Table 7.23). After incorporating migration space trend, the resilience class did not change for 1707 or 81% of the tidal complexes, while 106 or 5% of sites went to the next lower class and 14% or 297 complexes moved up a class (Figure 7.49, Table 7.23).

Table 7.21. Summary statistics for migration space size by sea level rise scenario.

SLR Scenario (feet)	Migration Space (Acres)				
	1 st Quartile	Median	Mean	3 rd Quartile	Max
1	0	1.112	29.76	9.118	1677
2	0	1.334	33.05	10.23	1738
3	0	1.334	35.89	12.45	1690
4	0	1.112	34.75	13.79	1387
5	0	1.112	34.68	13.79	1312
6	0	1.334	35.49	15.35	1458

Table 7.22 Summary of regression coefficients for tidal complex units (n=1470) with a significant ($p \leq .05$) relationship between sea level rise scenario (≥ 3 feet) and migration space size.

Migration Space Size (acres) Change					
Trend direction	Count	Minimum	Median	Mean	Max
Decrease	178	-125.30	-0.921	-9.053	-0.057
Increase	466	0.051	2.516	6.034	74.27
No change	826	0	0	0	0

Figure 7.48. Estimated resilience score with migration space trend. This map shows the estimated resilience score after incorporating the trend in migration space size for the Southern New England Coastal Embayment CSR at the 6-foot sea level rise scenario. Tidal complex units whose migration space showed a significant increase ($p \leq .05$) from the three to 6-foot SLR received an additional 0.50 standard deviation units to their score, while the score of units with a significant decrease in migration space was reduced by 0.50 SD units.

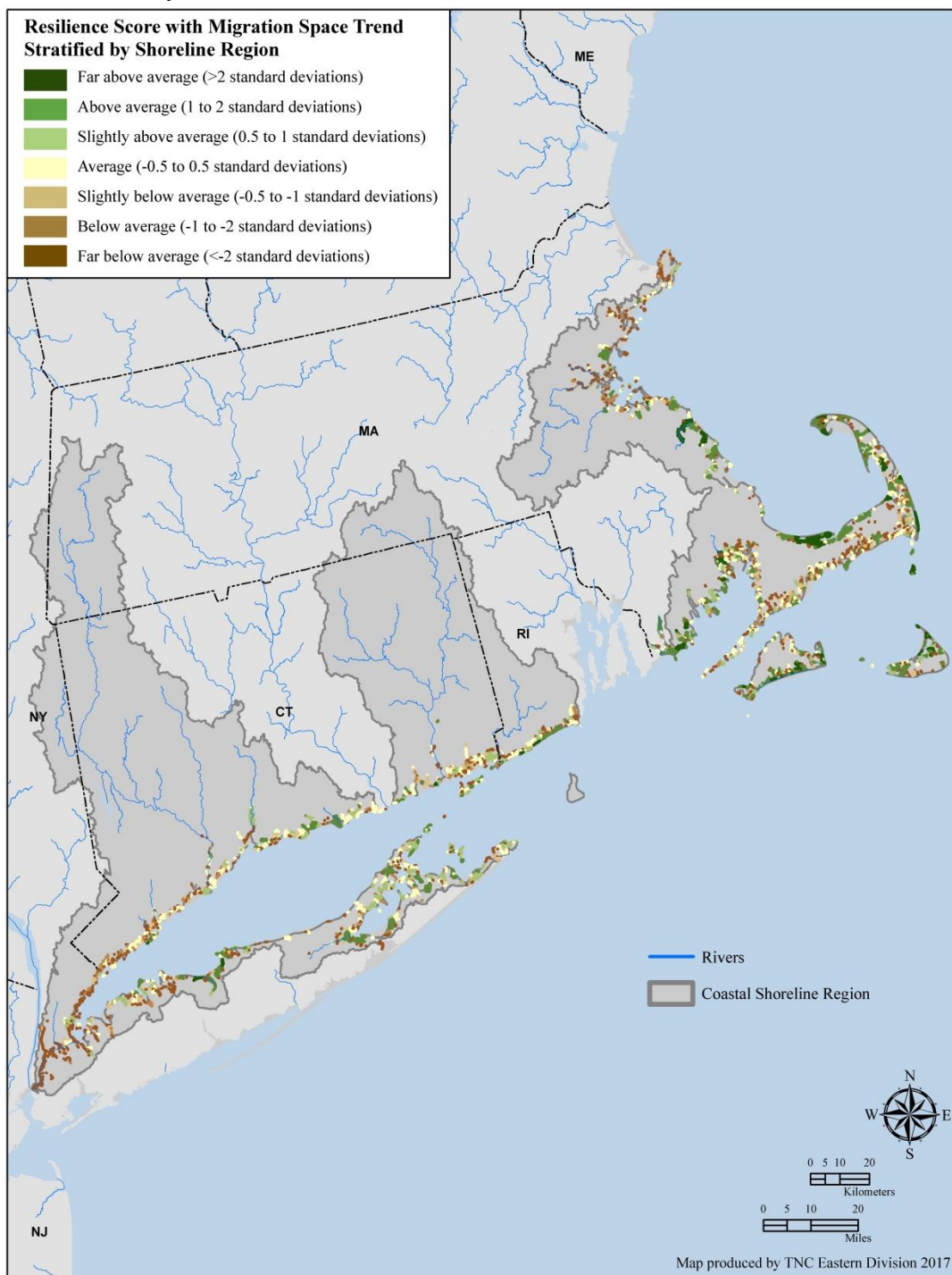
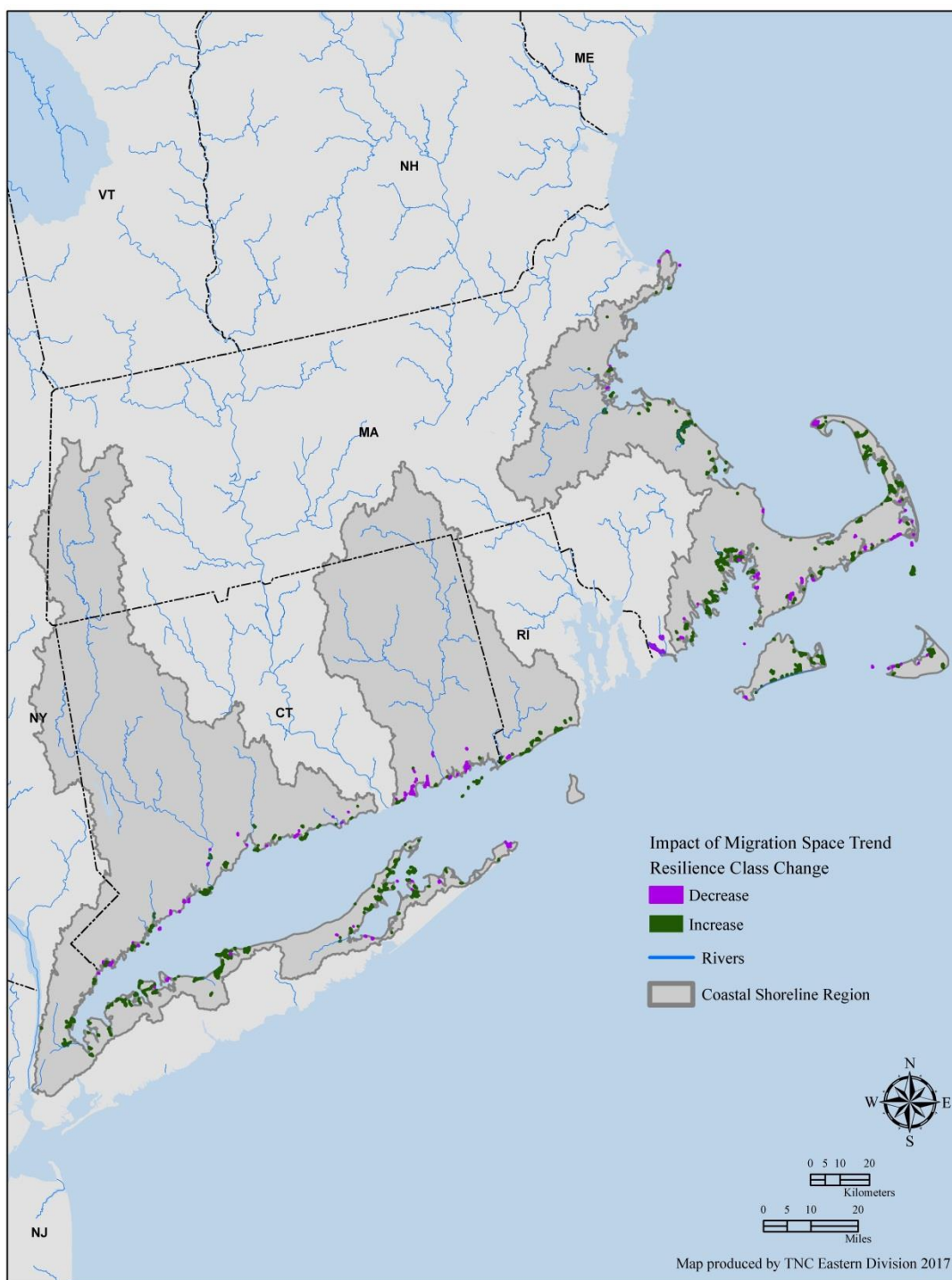


Table 7.23. The change in resilience class after incorporating the trend in migration space size. Tidal complex units whose migration space showed a significant increase ($p \leq .05$) from the three to 6-foot sea level rise received an additional 0.50 standard deviation units to their score, while the score of units with a significant decrease in migration space size was reduced by 0.50 SD units. The purple boxes indicate the number of tidal complex units that moved to the next lower resilience class, and the green boxes highlight the number of units whose class improved when the migration space trend was considered.

Resilience Class	Resilience class with Trend						
	Far Below Average	Below Average	Slightly Below Average	Average	Slightly Above Average	Above Average	Far Above Average
Far Below Average	845	3	0	0	0	0	0
Below Average	7	135	34	0	0	0	0
Slightly Below Average	0	32	112	49	0	0	0
Average	0	0	30	370	95	0	0
Slightly Above Average	0	0	0	22	84	87	0
Above Average	0	0	0	0	8	139	29
Far Above Average	0	0	0	0	0	7	22

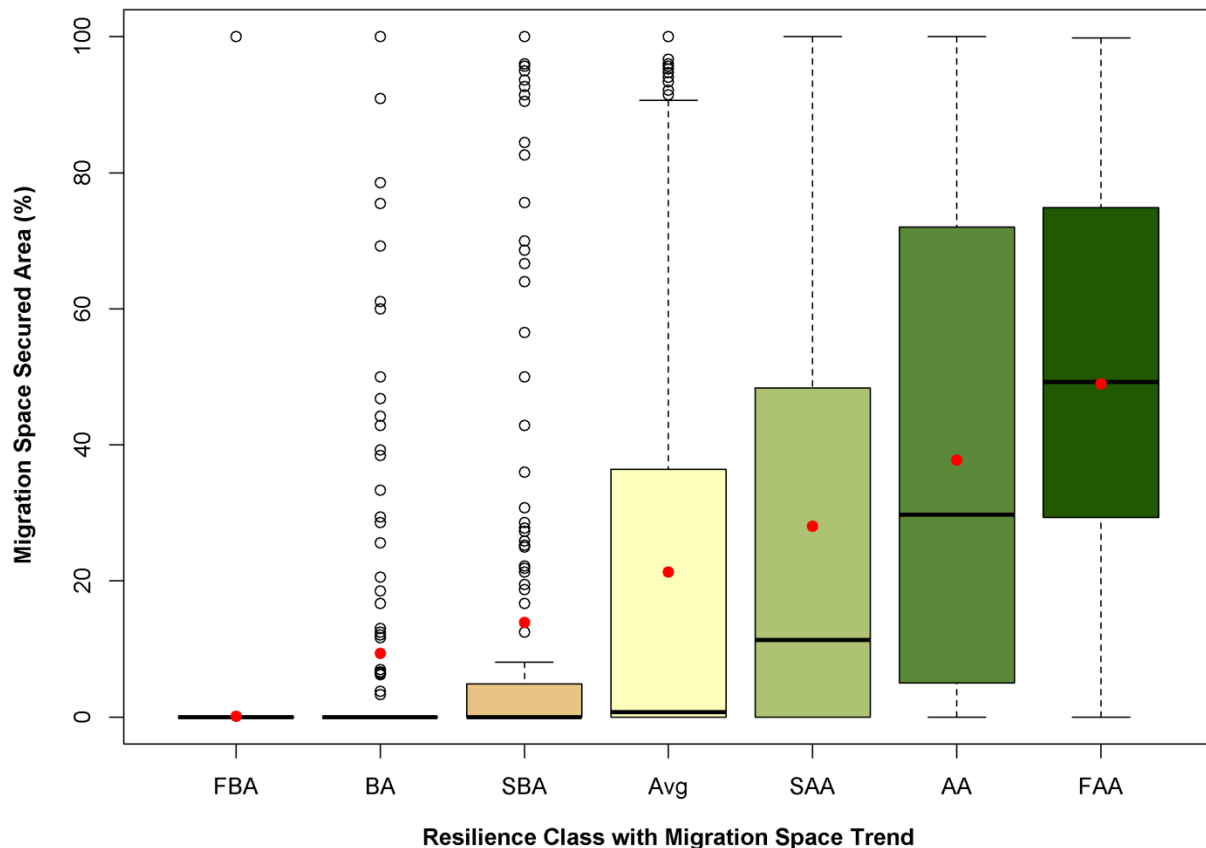
Figure 7.49. Estimated resilience class changes after incorporating migration space trend. This map shows the tidal complexes whose estimated resilience class either increased (n=297) or decreased (n=106) after incorporating the trend in migration space size for the Southern New England Coastal Embayment CSR at the 6-foot sea level rise scenario.



Migration Space Securement

The amount of a tidal complex's total migration space that was already protected (GAP status 1-3) varied substantially by resilience z-score category (Figure 7.50). Sites estimated to be highly resilient had the highest rate of securement of the five coastal regions. Specifically, tidal complex units with "far above average" scores had, on average, 49% of their migration space permanently protected, followed by the "above average" category with 38% secured. The worst scoring tidal complex units had the lowest average percent protected with less than half a percent (Figure 7.50), due largely to the absence of migration space for these units.

Figure 7.50. Amount (%) of migration space in permanent protection by estimated resilience class. The boxplot shows the distribution of migration space securement (%) by resilience class. The mean percent secured is denoted by a red circle. The resilience classes are shown using our standard z-score color palette and abbreviations.



Migration Space Development and Future Development

Due to inconsistencies in spatial resolution of various datasets used in this analysis (i.e., 10-m elevation and 30-m land cover products), and how roads are inaccurately mapped in base land cover grids such as the NLCD and C-CAP products, there are cases where some development occurs within the migration space mapped at the 30-m scale. While the percent of developed land in the migration space varied for each resilience class, there was a consistent trend where development increased with decreasing resilience score until reaching the “far below average” class (Figure 7.51), which had very little migration space. The “below average” class had the highest amount of development with a mean of 27% followed by the “slightly below average” class with a mean of 25% development. There are tidal complexes that have 80-100% development for the “average” and lower resilience classes, and this typically occurs for very small migration space areas where a single pixel of development leads to a high percentage. Regardless of resilience score, this CSR had the highest risk of future development in the migration space (Table 7.24), suggesting that sites in this particular setting occur in close proximity to current population centers that are expected to grow outward.

Figure 7.51. Amount (%) of migration space comprised of developed land, by estimated resilience class. The boxplot shows the distribution of migration space development (%) by resilience class with the mean denoted by a red circle. The resilience classes are shown using our standard z-score color palette and abbreviations.

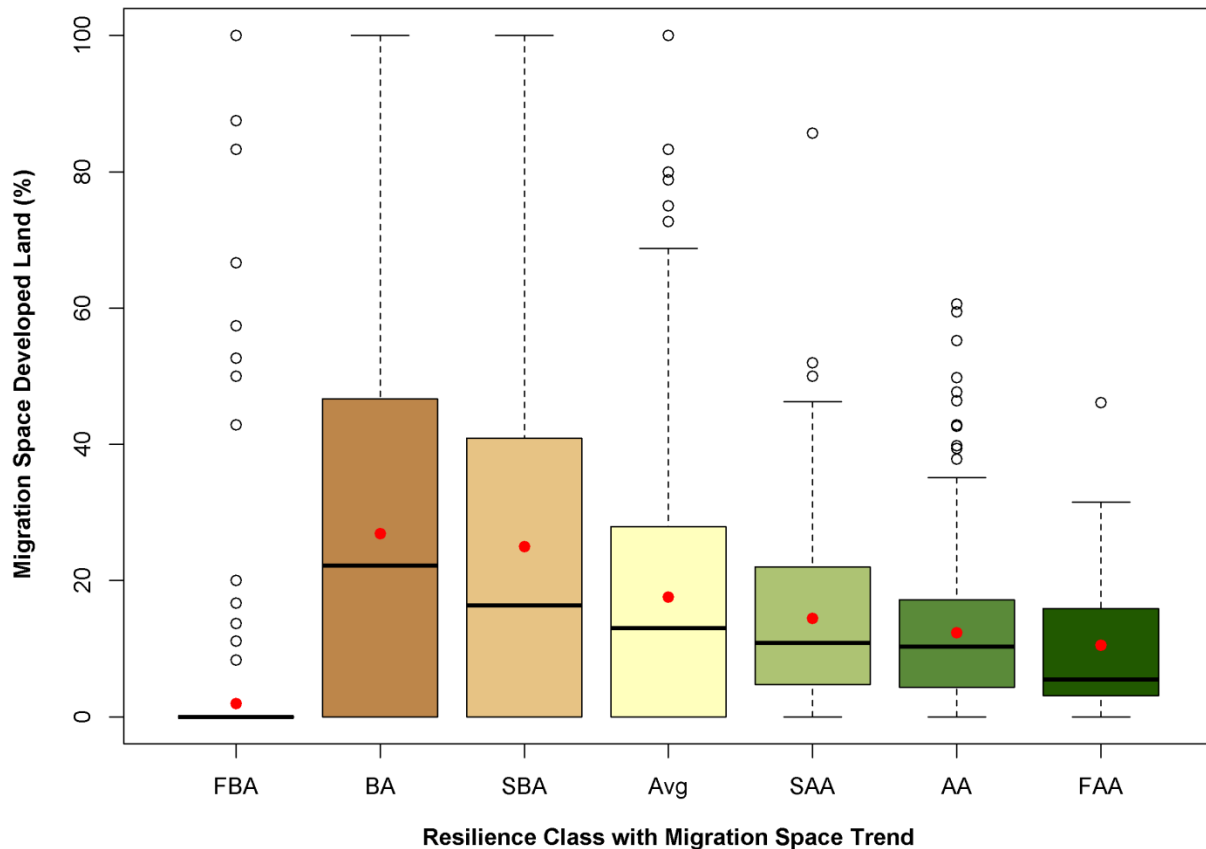
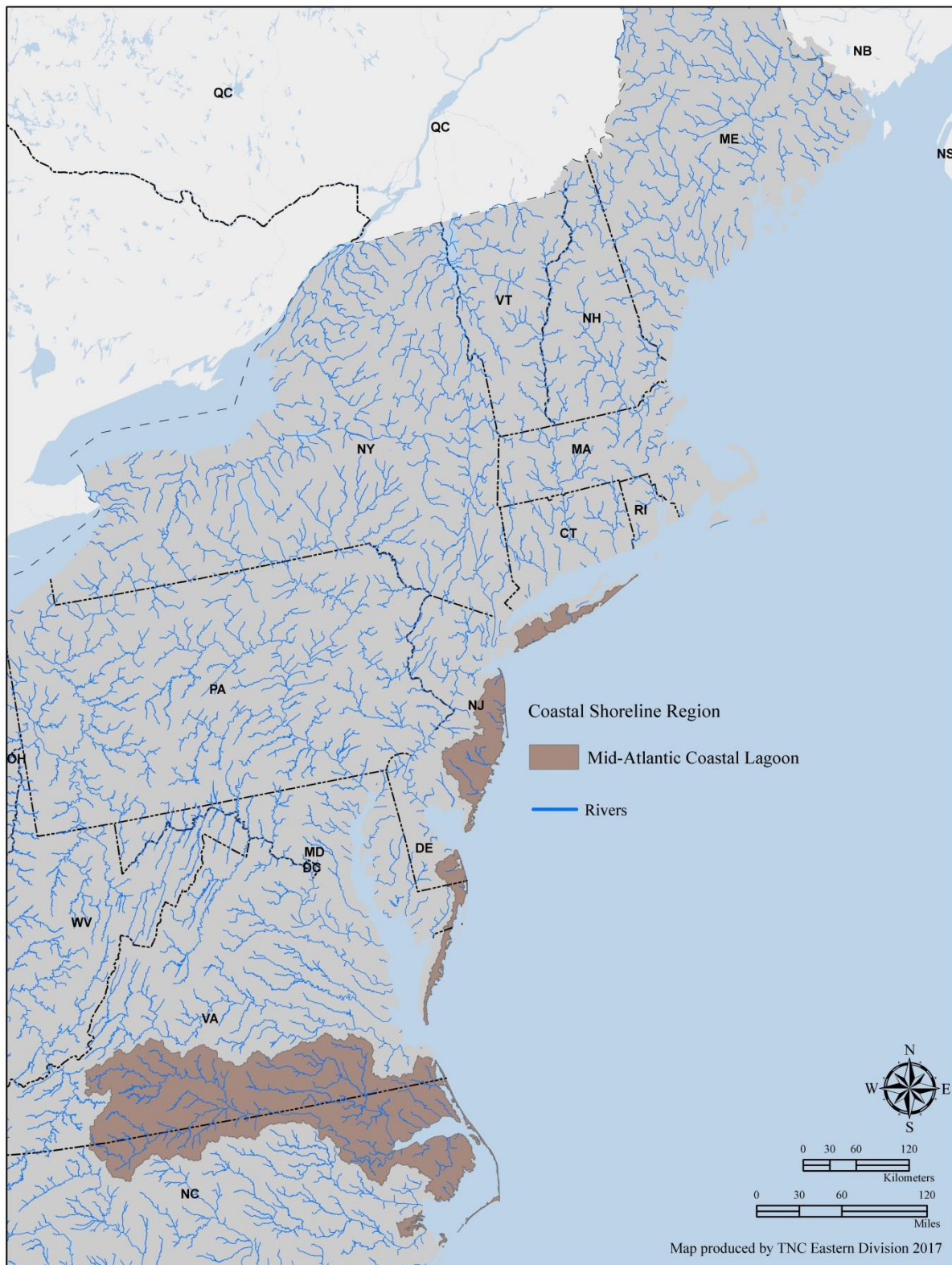


Table 7.24. Amount (%) of migration space estimated to be developed in 2100, by estimated resilience class. Summary statistics for migration space future development (%) are shown by resilience class.

Resilience Class with Migration Trend	Migration Space Future Development (%)					
	Min	1 st Quartile	Median	Mean	3 rd Quartile	Max
Far Below Average	0	0	0	1.053	0	100
Below Average	0	0	0	9.392	0	100
Slightly Below Average	0	0	0	8.433	0	100
Average	0	0	0	7.891	3.58	100
Slightly Above Average	0	0	0	5.704	3.615	82.96
Above Average	0	0	0	4.246	2.69	93.61
Far Above Average	0	0	0	3.028	2.02	50

Mid-Atlantic Coastal Lagoon CSR: Results



In the **Mid-Atlantic Coastal Lagoon CSR**, there was a total of 1275 tidal complex units, with an average size of 225.60 acres, the largest average size of all the CSRs. The median size was 7.12 acres with the largest unit occupying 39,040 acres (Figures 7.52-7.53).

Figure 7.52. Distribution of tidal complex size (acres) by ten size classes in the Mid-Atlantic Coastal Lagoon CSR.

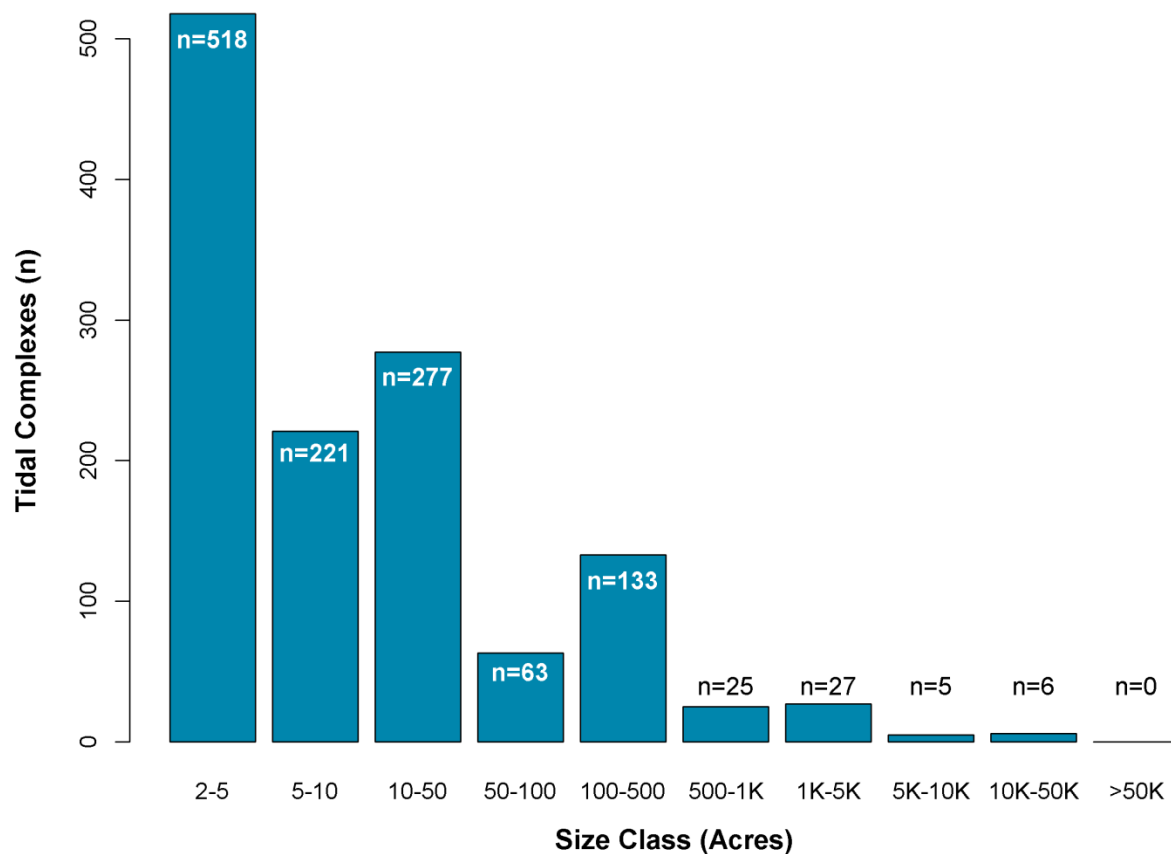
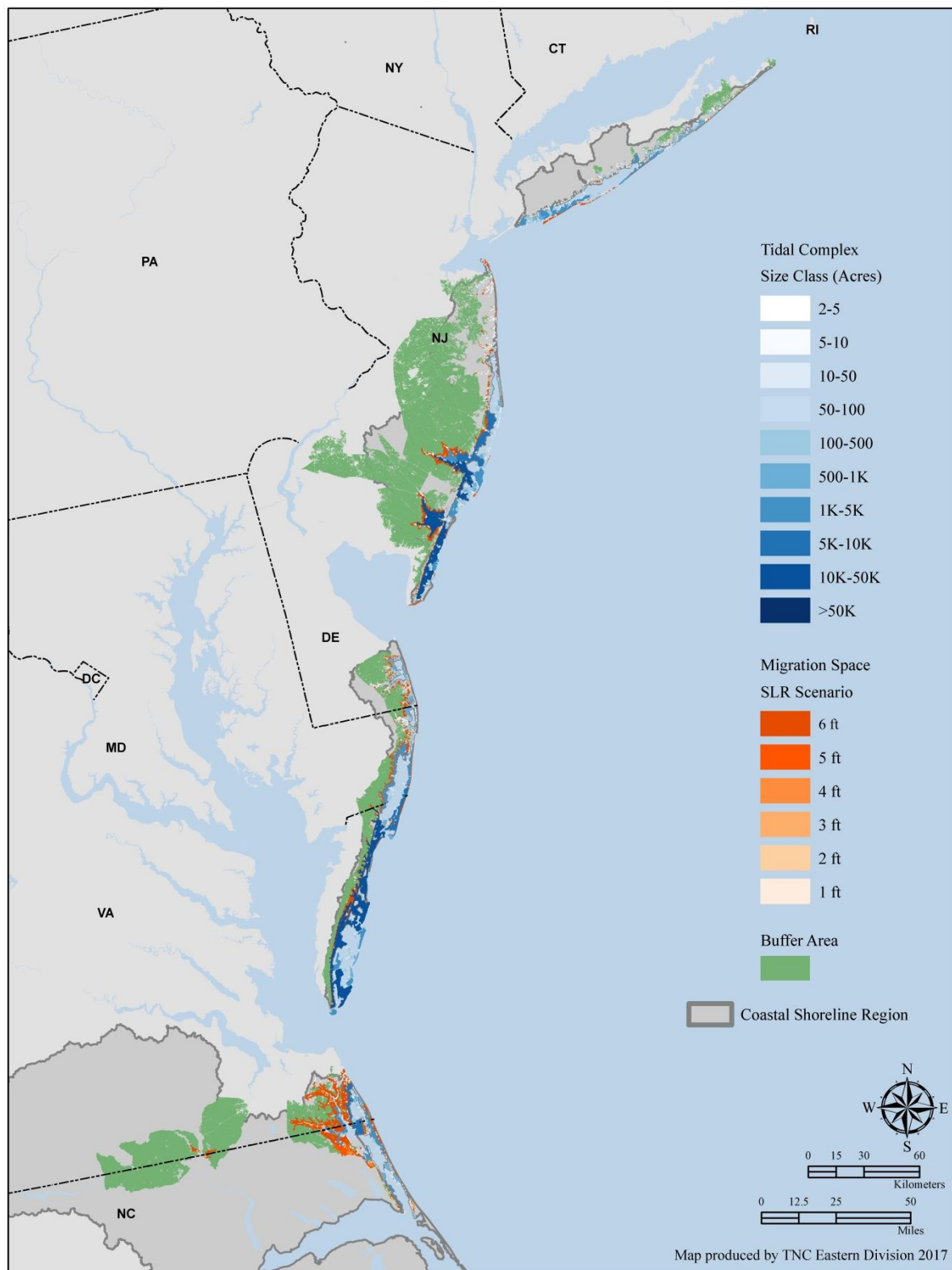
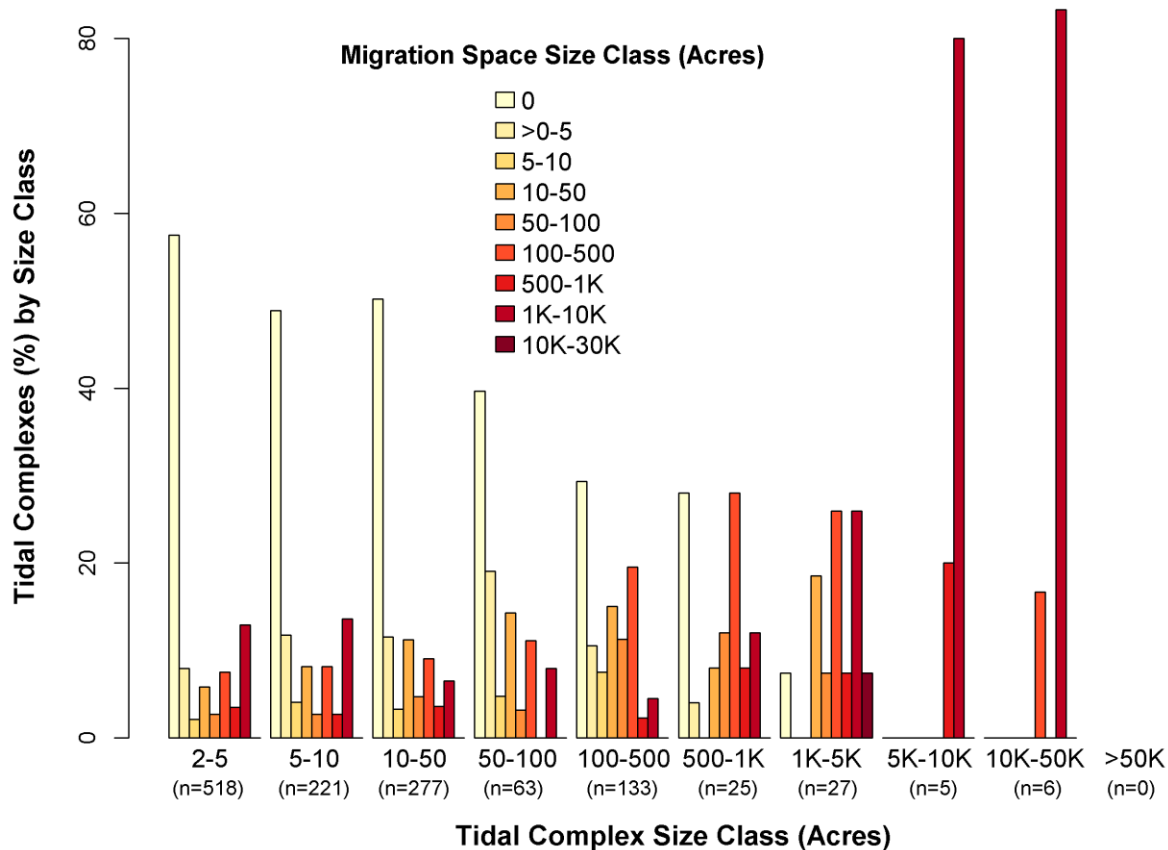


Figure 7.53. Tidal complex, migration space, and buffer area units in the Mid-Atlantic Coastal Lagoon CSR. The color of the tidal complex units reflects their size class (n=10), while the color of the migration space indicates the SLR scenario (n=6).



This CSR had the lowest percentage of tidal complexes with migration space at a sea level rise of 6 feet. Of the 1275 tidal complexes, 657 or 52%, had migration space at a sea level rise of 6 feet (Figure 7.54). The average migration space size was 538.8 acres with a median size of 0.445 and a maximum size of 18,100 acres. As Figure 7.54 shows, the majority of tidal complexes in the small size classes have no migration space. However, the largest tidal complexes in this CSR (≥ 5000 acres) all have expansive migration space areas, reflecting the larger geophysical setting within which these tidal complexes occur.

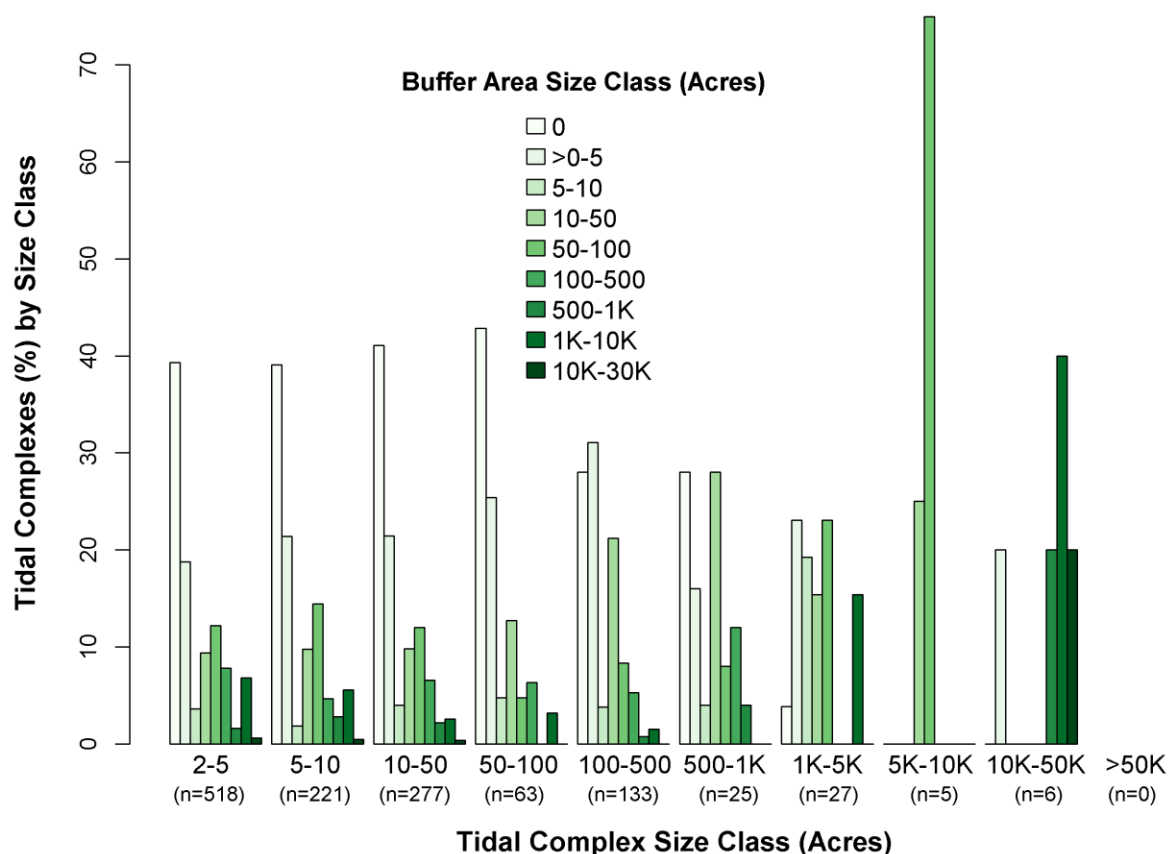
Figure 7.54. Migration space class distribution by tidal complex size class for the 6-foot sea level rise scenario. The y-axis is the percent of tidal complexes within a size class that have migration space of a particular size. Small migration space size classes are shown in light yellow shades that transition to darker oranges as the migration space size class increases.



A Spearman's rank-order correlation found the tidal complex size and migration space size were minimally positively correlated and this relationship was statistically significant ($r_s = .17$, $p < 1.227e-9$).

A little more than half the tidal complexes, 809 or 63%, had buffer area at a sea level rise of 6 feet (Figure 7.55), the lowest percentage of the five regions. The mean buffer size was 26,370 acres with the largest buffer area encompassing 656,200 acres. Similar to the relationship pattern between tidal complex size and migration space size, all tidal complexes of 1000 acres or greater have large buffer areas whereas tidal complexes less than 1000 acres have a mix of buffer area sizes with the majority not having any buffer areas (Figure 7.55). This was quite different than the tidal complex and buffer area pattern in the Chesapeake Bay CSR where the majority of small tidal complexes had large buffer areas. Unlike in the other CSRs, there was no statistically significant relationship between tidal complex size and buffer area size.

Figure 7.55. Buffer area class distribution by tidal complex size class for the 6-foot sea level rise scenario. The y-axis is the percent of tidal complexes within a size class that have buffer area of a particular size. Small buffer area size classes are shown in light green shades that change to darker greens as the buffer area size class increases.



Physical and Condition Scores

The estimated resilience score for a tidal complex consists of the condition and physical components, each weighted equally. Figure 7.56 shows the geographic distribution of physical scores within the CSR for a sea level rise of 6 feet. As both Figure 7.56 and Table 7.25 show, the highest proportion of scores falls in the “far below average” class, with the next largest category being “average.” The lowest scoring tidal complexes are predominantly those with no migration space and a less geophysically diverse buffer area. The spatial pattern of the condition scores is shown in Figure 7.57 with the numeric distribution highlighted in Table 7.25. Likely the result of almost half of the tidal complexes not having any migration space, there were more complexes in the low physical classes than in the low condition classes. Of all the coastal regions, the Lagoon region had the highest percentage of physical (50%) and condition scores (47%) in the “far below average” class.

Figure 7.56. Estimated physical score for the Mid-Atlantic Coastal Lagoon CSR. Tidal complex units in green score “above average” and have physical characteristics hypothesized to increase resilience including a large migration area with a diversity of tidal classes that are evenly distributed, a complex shoreline, and a geophysically diverse buffer area. Tidal complexes in yellow have “average” physical characteristics relative to all the units in the CSR. Tidal complexes in brown are “below average” and are estimated to respond poorly to sea level rise.

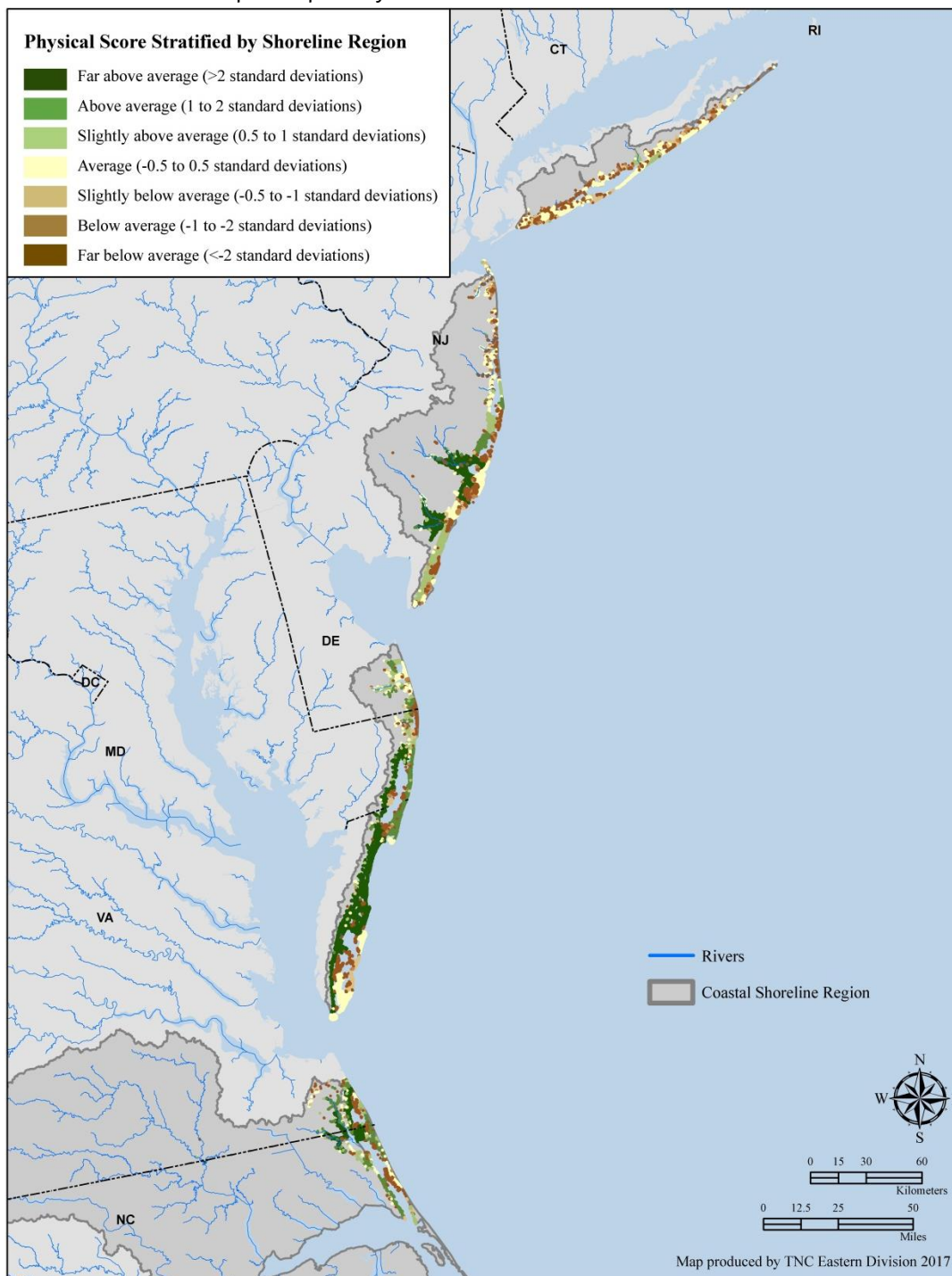


Figure 7.57. Estimated condition score for the Mid-Atlantic Coastal Lagoon CSR.

Tidal complex units in green score “above average” and are estimated to be in good condition based on a low percentage of hardened shoreline; good water quality and quantity, and high sediment contributions in the migration space; and a natural buffer area with highly connected wetlands. Tidal complexes in yellow are “average.” Tidal complexes in brown are “below average” and are estimated to be in poor condition.

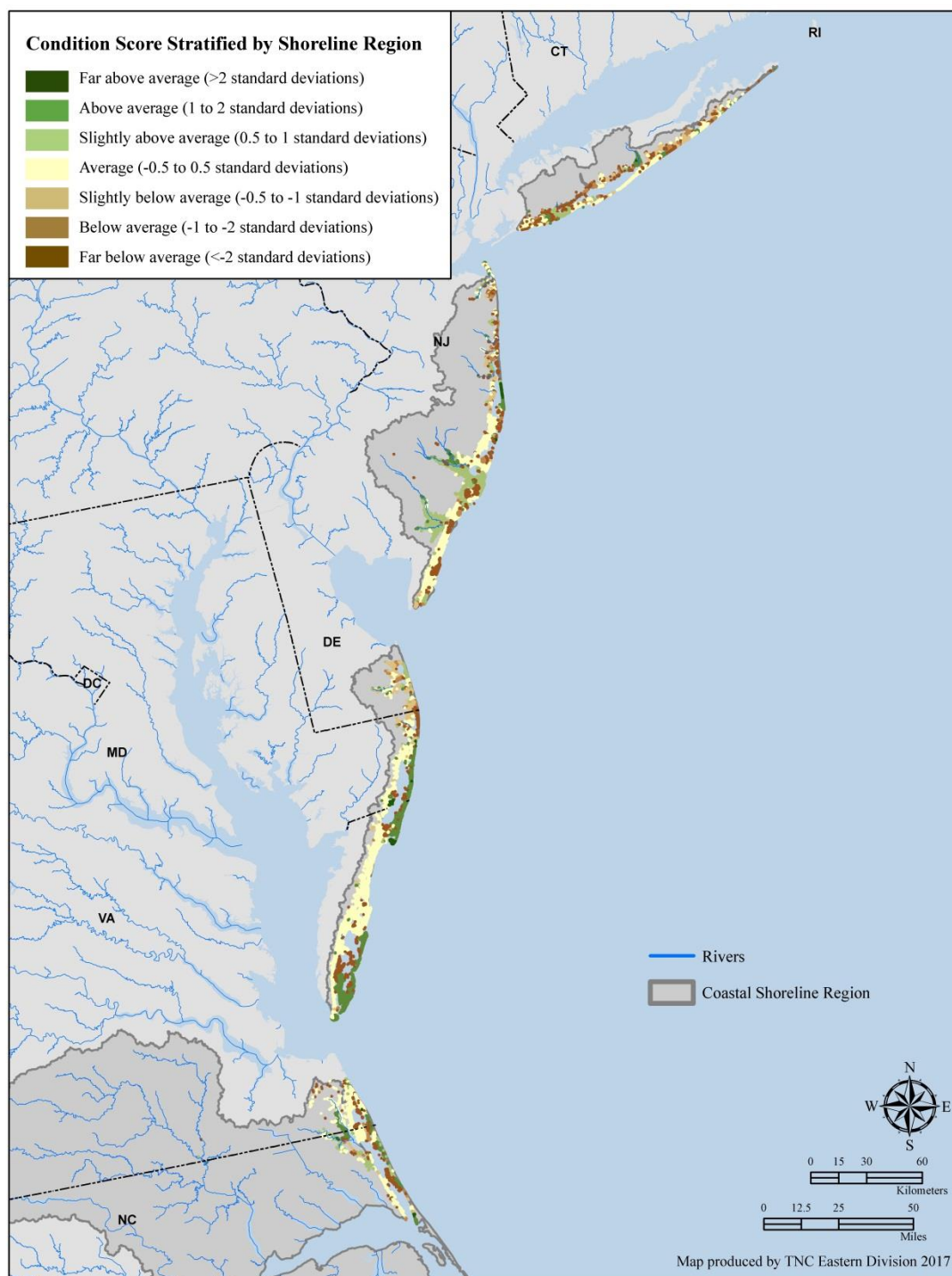


Table 7.25. Frequency of physical and condition scores in the Mid-Atlantic Coastal Lagoon CSR for the 6-foot sea level rise scenario.

Z-Score Class	Tidal Complex (n)	
	Physical	Condition
Far Below Average	639	598
Below Average	88	94
Slightly Below Average	98	104
Average	249	265
Slightly Above Average	98	104
Above Average	88	94
Far Above Average	15	16

The relationship between the condition and physical scores was moderately and positively correlated (Pearson's $r = .33$, $p = 2.2e-16$, Figure 7.58). In this CSR, a tidal complex with a high physical score does not typically have a high condition score as evidenced in Figures 7.58-7.59 and Table 7.26. There was only one complex that scores "far above average" for both physical and condition. The biggest proportion of high condition scores are found in the "average" and "slightly above average" physical classes.

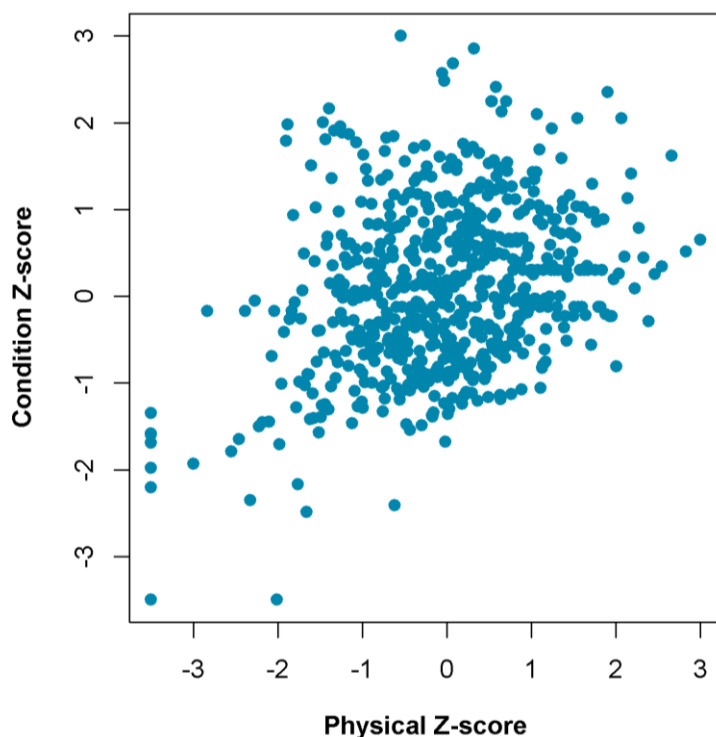
Figure 7.58. Relationship between the tidal complex units' physical and condition z-scores for the 6-foot sea level rise scenario, after removing unit with no migration space.

Figure 7.59. Distribution of the physical scores for each condition class at a sea level rise of 6 feet. The distribution of the physical scores is shown for each condition score class using our standard z-score color palette.

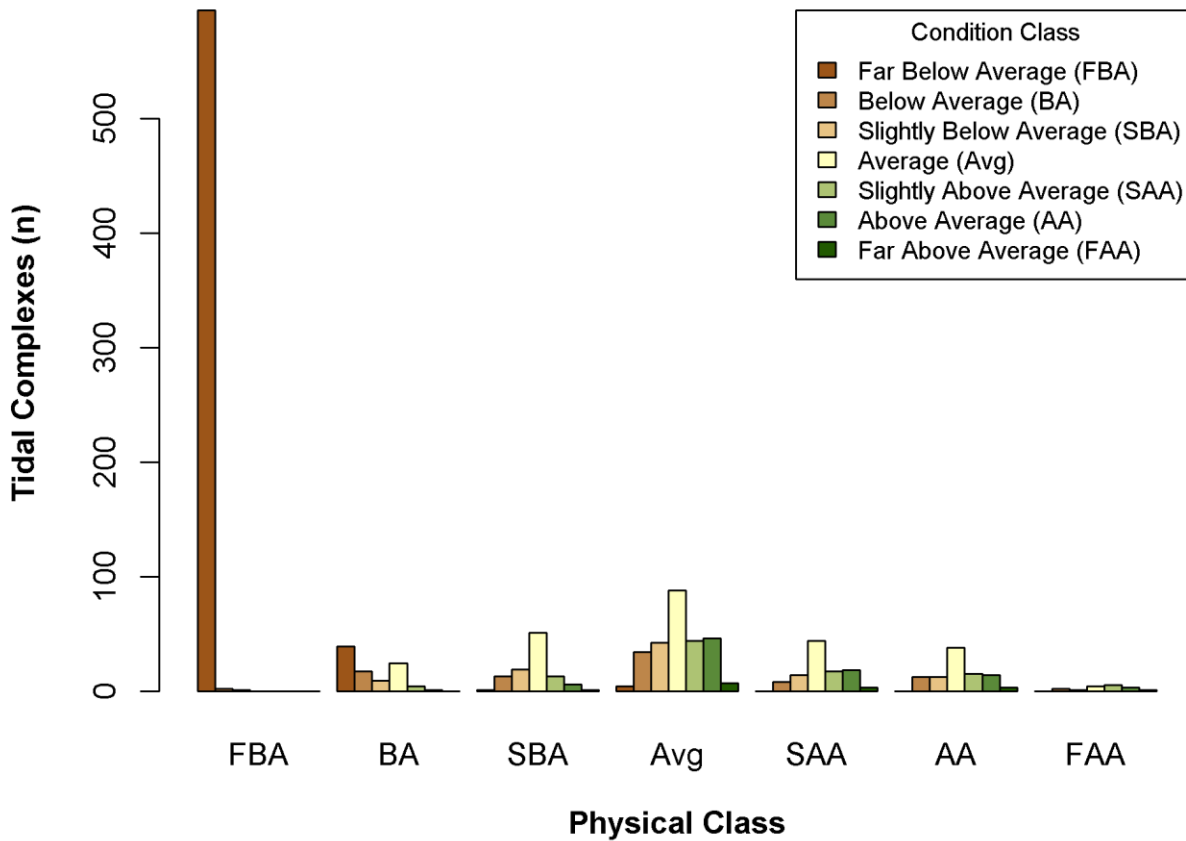
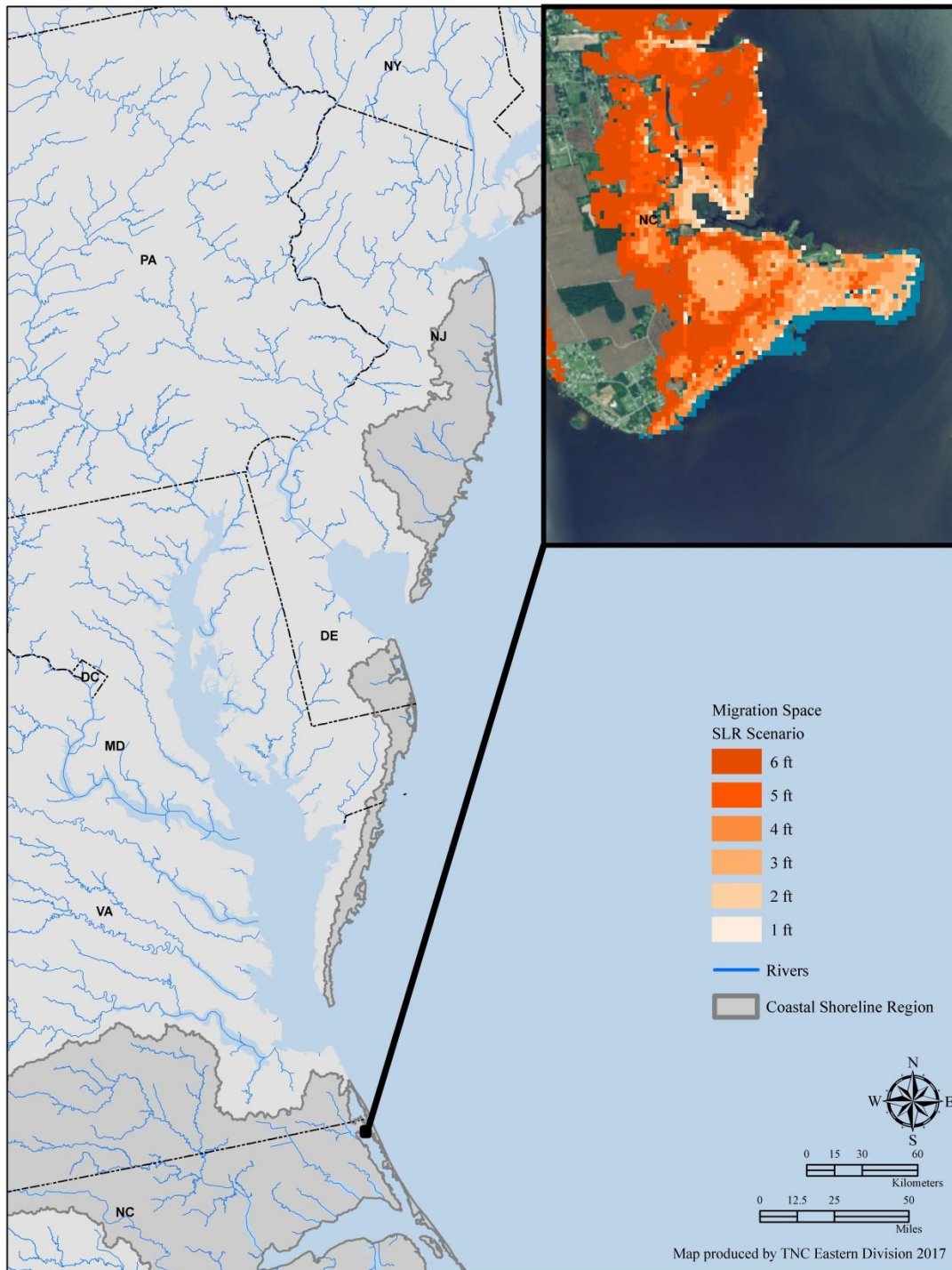


Table 7.26. The number of tidal complex units in each physical and condition score category. A two-by-two frequency table shows the count of tidal complexes occurring in each physical and condition class combination. Physical classes are by row and condition classes are by column. Boxes shaded in gray indicate tidal complexes with the same physical and condition score class. For example, only 1 tidal complex scored “far above average” for both physical and condition characteristics.

Physical Class	Condition Class						
	Far Below Average	Below Average	Slightly Below Average	Average	Slightly Above Average	Above Average	Far Above Average
Far Below Average	595	39	1	4	0	0	0
Below Average	2	17	13	34	8	12	2
Slightly Below Average	1	9	19	42	14	12	1
Average	0	24	51	88	44	38	4
Slightly Above Average	0	4	13	44	17	15	5
Above Average	0	1	6	46	18	14	3
Far Above Average	0	0	1	7	3	3	1

As shown in Figure 7.60, there was only one site that had a low condition score (i.e., “below average”) and a high physical score (i.e., “above average”). This particular site, located at Bay Point, NC along the Currituck Sound, would likely be a good candidate for restoration as there was a large amount of migration space available (774 acres) at the 6-ft SLR scenario, and the migration space is modeled to have a high diversity and evenness of tidal classes as well as a large shared edge with the current tidal complex. While the physical template was suitable for marsh migration, condition issues could hamper marsh migration. Notably, the site had high estimated nitrogen loads relative to other sites in the CSR, had almost 30% hardened shoreline, and occurs within an agricultural setting so the buffer area had a low proportion of natural land.

Figure 7.60. Tidal complex with high physical score but in poor condition. This site, located at Bay Point, NC along the Currituck Sound, was estimated to be in poor condition (poor water quality, hardened shoreline, non-natural buffer area), but had physical characteristics hypothesized to increase resilience to sea level rise (relatively large tidal complex mostly surrounded by migration space that was expected to have a high diversity and evenness of tidal classes).



Estimated Resilience Score

The physical and condition scores were equally weighted and combined to calculate an estimated resilience score for each tidal complex. High scoring sites were those with a large migration space, intact buffer area, and whose condition was not expected to exacerbate the impacts of sea level rise and climate change, with all these characteristics relative to other sites in the CSR. The role of some of the physical factors was evident in Figure 7.61 where high scoring tidal complexes shown in dark green have a large migration space (shown in orange shades), and very vulnerable complexes shown in dark brown have no migration space. The resilience values are in z-scores which follow a normal distribution except for the “far below average” category because tidal complexes with no migration space were manually assigned a -3.5 SD score for all migration space attributes. The relationship between the physical and condition scores and the role of that relationship in the estimated resilience score can be seen in Figure 7.62. While the patterns in the proportion of each class for the physical and condition components are relatively similar, there are some interesting patterns. For example, for the “far above average” resilience class, the physical component had a higher proportion of the two highest classes compared to the condition score distribution, indicating it was hard to score very high for both condition and physical characteristics. A “far above average” resilience score was largely comprised of “far above average” and “above average” condition and physical scores but could also occur from other combinations such as “average” physical and “far above average” condition as well as “slightly above average” condition and “far above average” physical.

The ten tidal complexes with the highest estimated resilience score are shown in Figure 7.63. The average tidal complex size of this group was 8596 acres with an average migration space size at a 6-foot sea level rise of 7950 acres (min = 92, max = 18,100, SD = 4917 acres) and a large average buffer area (206,366 acres). Vulnerable sites, those having below average estimated resilience, are shown in Figure 7.64. These tidal complexes were locations with little to no migration space and whose poor condition, again relative to all other sites in the CSR, was expected to exacerbate the impacts of sea level rise and climate change. The results of a Pearson correlation analysis show the role of tidal complex size, migration space size, and buffer area size in the condition, physical, and resilience score (Table 7.28). As expected, given the weight of these attributes in the physical component score, size was significantly and positively correlated with the physical score, particularly for the migration space and buffer area size. The condition score was also significantly, albeit only mildly positively, correlated with the migration space size. As tidal complex units with no migration space were removed from the correlation analysis to better understand the relationship among the variables, this relationship probably results from land use and geophysical patterns in the larger landscape where smaller migration spaces are likely in areas with greater elevation and slope and/or with more development.

Figure 7.61. Estimated resilience score. This map shows the estimated resilience score for the Mid-Atlantic Coastal Lagoon CSR for the 6-foot sea level rise scenario. The map shows areas that are above (green) or below (brown) the mean. Areas in green score “above average” and are estimated to be more resilient based on their physical and condition characteristics. Areas in yellow are “average.” Areas in brown are “below average” and are estimated to be vulnerable to sea level rise and climate change.



Figure 7.62. Relationship between condition and physical components for each estimated resilience class at a sea level rise of 6 feet. The physical and condition bars are split vertically based on the proportion of each score for each resilience class.

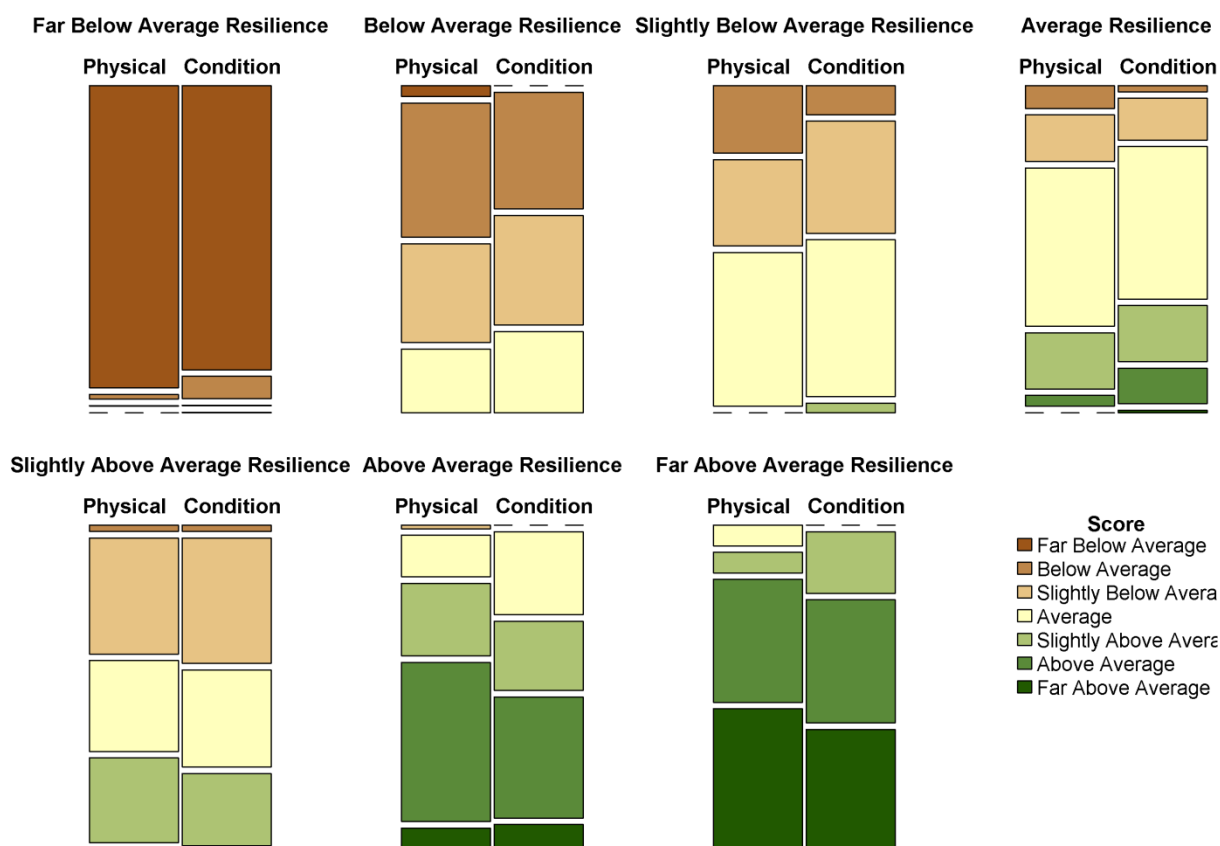


Table 7.27. Distribution of estimated resilience scores in the Mid-Atlantic Coastal Lagoon CSR for the 6-foot sea level rise scenario.

Z-Score Class	Estimated Resilience	Estimated Resilience with Migration Space Trend
Far Below Average	647	648
Below Average	87	82
Slightly Below Average	96	84
Average	247	240
Slightly Above Average	96	100
Above Average	87	102
Far Above Average	15	19

Figure 7.63. The top ten highest scoring tidal complexes in the Mid-Atlantic Coastal Lagoon CSR. The ten tidal complexes with the highest estimated resilience score in the CSR are highlighted in yellow. For this region, the focal tidal complex at Swan Bay State wildlife management area, NJ was very large (4202 acres), had a large migration space (3242 acres) that surrounded a large portion of the tidal complex (i.e., high shared edge), had “above average” water quality, “average” sediment, and a large buffer area with good wetland connectivity.

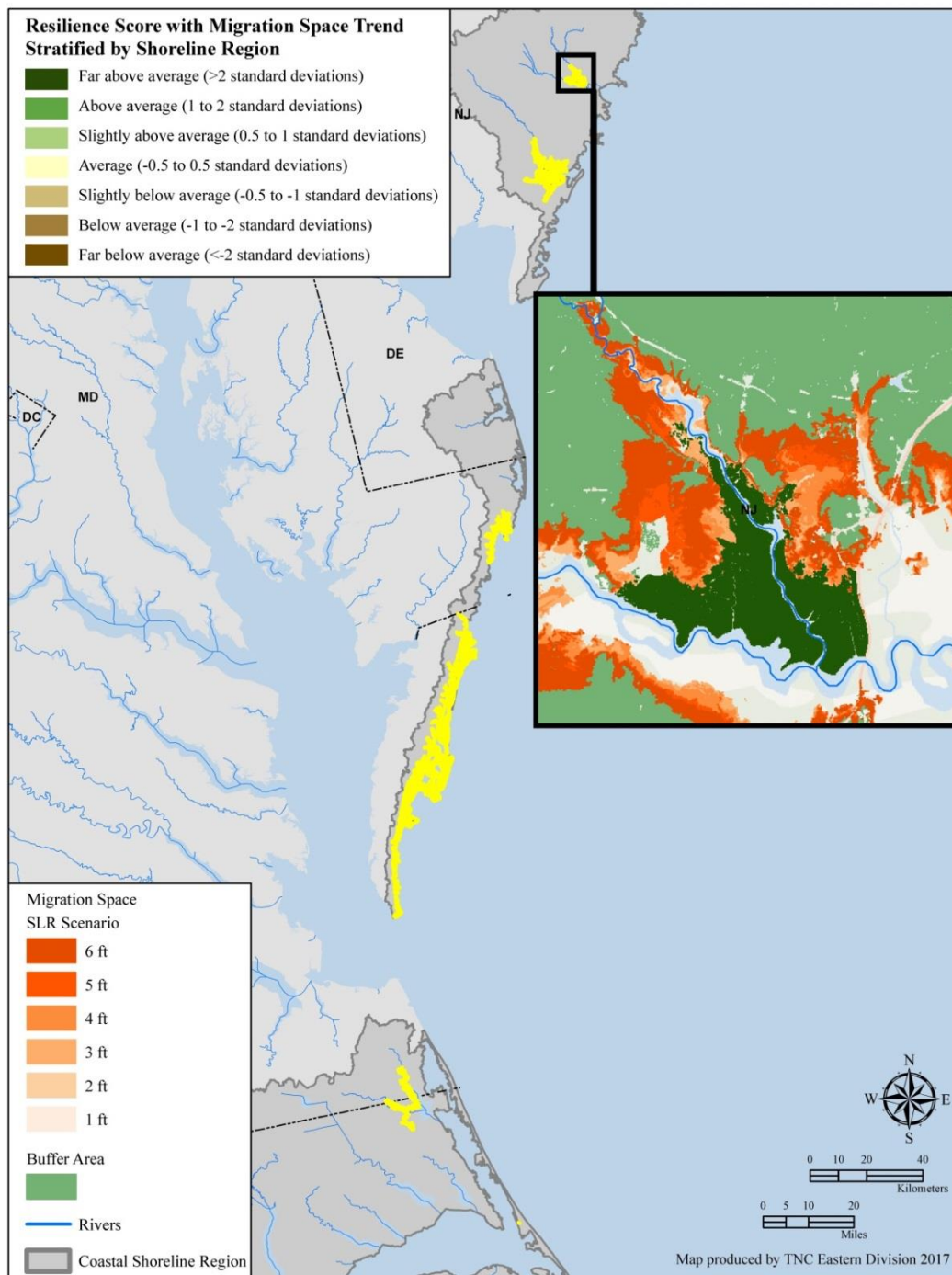


Figure 7.64. Vulnerable tidal complexes. Sites that scored below the mean are considered vulnerable. Sea level rise is expected to worsen the degradation of vulnerable sites, but these sites may still provide valuable ecosystem services (i.e., buffering storm effects, wildlife habitat, etc.).

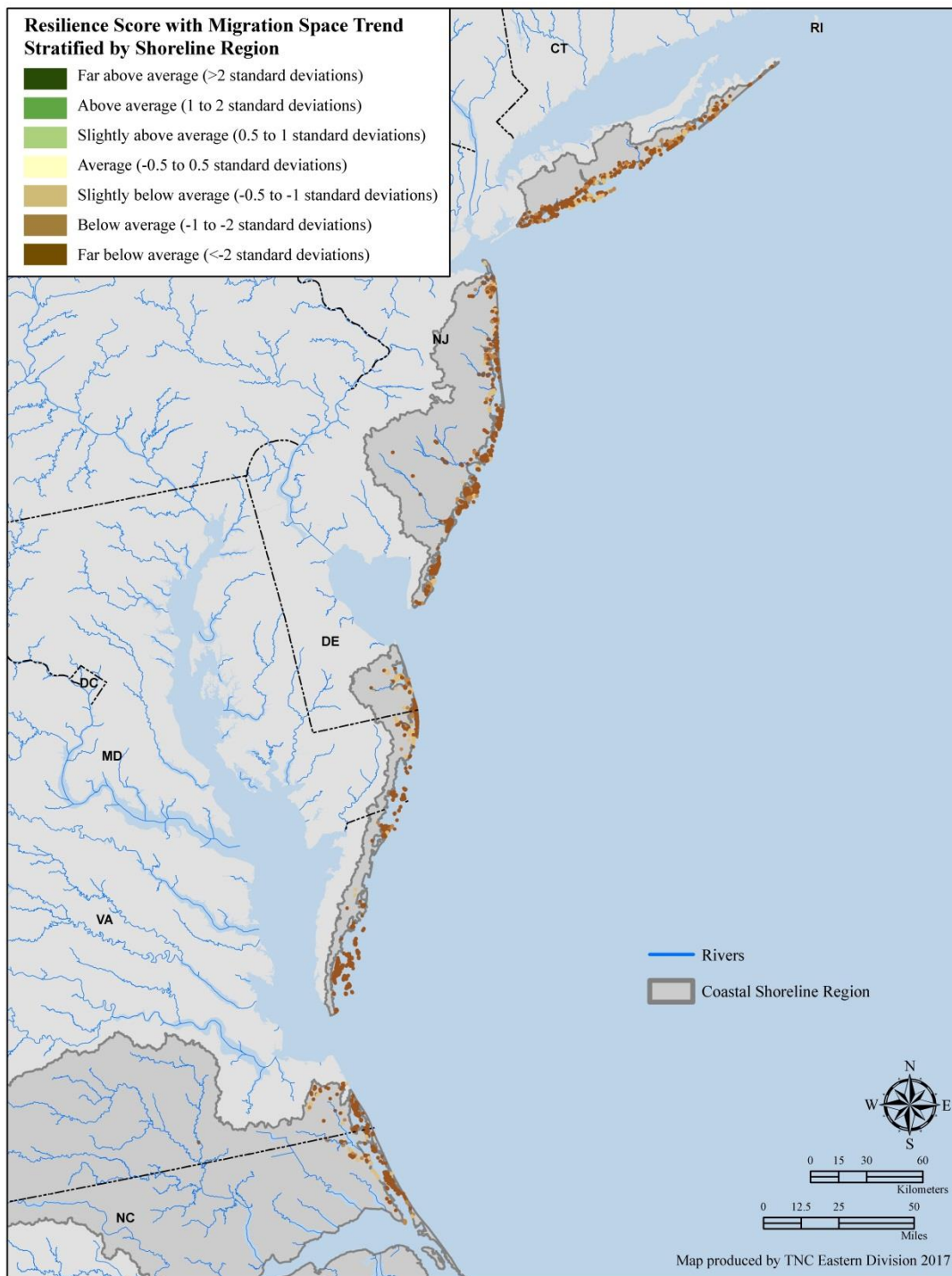


Table 7.28. Relationship between resilience components and analysis unit size.

Pearson correlation coefficients between the condition, physical, and estimated resilience scores and the size (acres) of the tidal complex, migration space, and buffer area, after removing tidal complexes with no migration space. A star indicates a significant ($p \leq .05$) relationship.

	Tidal Complex Size	Migration Space Size	Buffer Area Size
Physical Z-score	.20*	.74*	.71*
Condition Z-score	.01	.23*	.36*
Resilience Z-score	.14*	.62*	.67*

Trends in Migration Space Size

For tidal complex units in the Mid-Atlantic Coastal Lagoon setting, the mean size across all migration spaces increased from the 1 to 3-foot sea level rise but then showed a decline from 3 to 6 feet (Table 7.29). Linear regressions identified 899 tidal complex units with a statistically significant ($p \leq .05$) relationship between the latter three sea level rise scenarios (3 – 6 feet) and migration space size. Of those tidal complex units with a significant relationship, some had decreasing migration space but the majority experienced an increase in migration space (Table 7.30). The mean increase in size was 78 acres while the average decrease was 110 (Table 7.30). Tidal complexes with a significant migration space trend were assigned to one of three trend categories: increase, decrease, no change, and we adjusted their score to reflect the trend. The 191 tidal complexes whose migration space showed an increasing trend were awarded an additional 0.50 SD points to their estimated resilience score. The 98 tidal complexes that experienced a decline in migration space size from the 3 to the 6-foot SLR scenario had their estimated resilience scores reduced by 0.50 SD. The resilience score of the 610 tidal complexes with no significant change in migration space size was not impacted by the trend analysis. The map in Figure 7.66 shows the spatial distribution of the resilience scores with the trend analysis incorporated. Of the top ten highest scoring sites shown in Figure 7.63, only four received a boost to their score from a positive migration space size trend and one was penalized for a decreasing migration space trend. The remaining five had stable migration space sizes and thus had no change to their resilience score. The use of 0.50 SD to adjust the resilience score meant that no tidal complex's score could change by more than one resilience class (Table 7.31). After incorporating migration space trend, the resilience class changed for 169 or 13% of the tidal complexes with 52 or 4% of sites going to the next lower class and 9% or 117 complexes moving up a class (Figure 7.67, Table 7.31). Compared to the other CSRs, the Lagoon region had the lowest percentage of tidal complexes with an increasing migration space trend.

Table 7.29. Summary statistics for migration space size by sea level rise scenario.

SLR Scenario (feet)	Migration Space (Acres)				
	1 st Quartile	Median	Mean	3 rd Quartile	Max
1	0	0.2224	403.1	33.36	16000
2	0	0.6672	563.1	65.61	20130
3	0	0.6672	623.4	91.63	19460
4	0	0.6672	575.4	101.4	15020
5	0	0.6672	560.7	108	15720
6	0	0.4448	538.8	99.86	18100

Table 7.30. Summary of regression coefficients for tidal complex units (n=899) with a significant ($p \leq .05$) relationship between sea level rise scenario (≥ 3 feet) and migration space size.

Migration Space Size (acres) Change					
Trend direction	Count	Min	Median	Mean	Max
Decrease	98	-999.40	-10.58	-109.60	-0.083
Increase	191	0.083	11.20	77.98	1885
No change	610	0	0	0	0

Figure 7.65. Estimated resilience score with migration space trend. This map shows the estimated resilience score after incorporating the trend in migration space size for the Mid-Atlantic Coastal Lagoon CSR at the 6-foot sea level rise scenario. Tidal complex units whose migration space showed a significant increase ($p \leq .05$) from the three to 6-foot SLR received an additional 0.50 standard deviation units to their score, while the score of units with a significant decrease in migration space was reduced by 0.50 SD units.

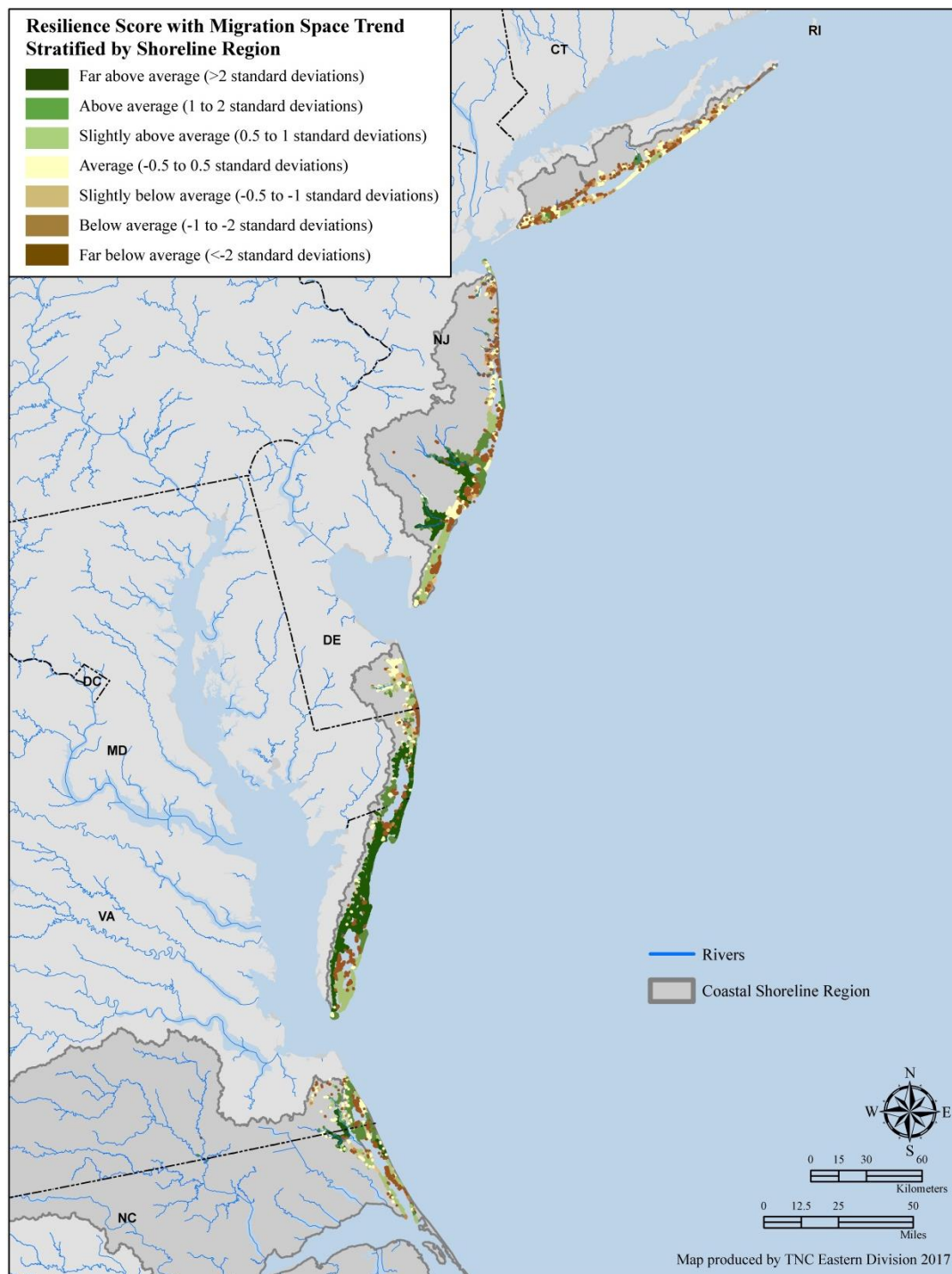
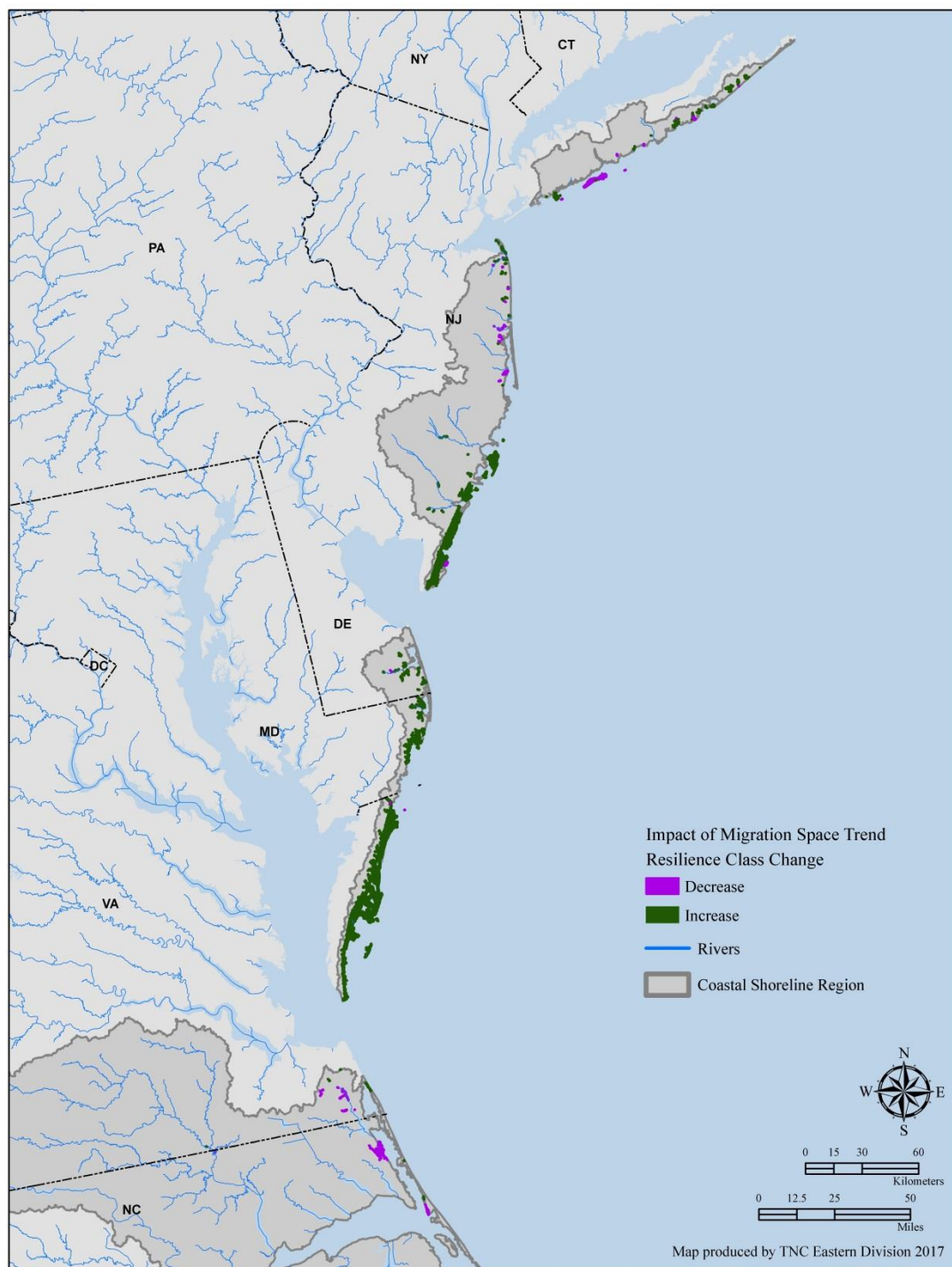


Table 7.31. The change in resilience class after incorporating the trend in migration space size. Tidal complex units whose migration space showed a significant increase ($p \leq .05$) from the three to 6-foot sea level rise received an additional 0.50 standard deviation units to their score, while the score of units with a significant decrease in migration space size was reduced by 0.50 SD units. The purple boxes indicate the number of tidal complex units that moved to the next lower resilience class, and the green boxes highlight the number of units whose class improved when the migration space trend was considered.

Resilience Class	Resilience class with Trend						
	Far Below Average	Below Average	Slightly Below Average	Average	Slightly Above Average	Above Average	Far Above Average
Far Below Average	643	4	0	0	0	0	0
Below Average	5	66	16	0	0	0	0
Slightly Below Average	0	12	52	32	0	0	0
Average	0	0	16	198	33	0	0
Slightly Above Average	0	0	0	10	60	26	0
Above Average	0	0	0	0	7	74	6
Far Above Average	0	0	0	0	0	2	13

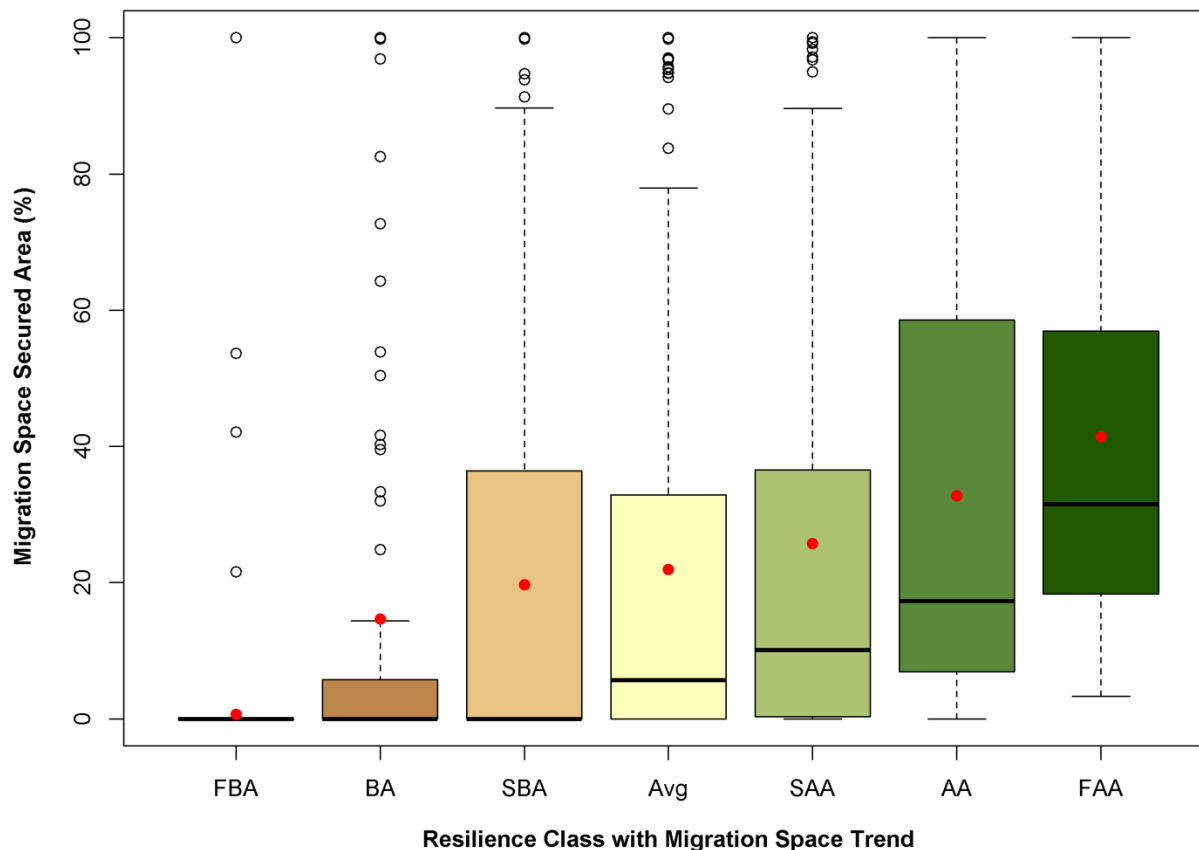
Figure 7.66. Estimated resilience class changes after incorporating migration space trend. This map shows the tidal complexes whose estimated resilience class either increased (n=191) or decreased (n=98) after incorporating the trend in migration space size for the Mid-Atlantic Coastal Lagoon CSR at the 6-foot sea level rise scenario.



Migration Space Securement

The amount of a tidal complex's total migration space that was already protected (GAP status 1-3) varied quite a bit by resilience z-score category (Figure 7.67). Tidal complex units with "far above average" resilience scores had the greatest percentage of their migration space in securement (mean=41%), followed by the "above average" class with a mean of 32% protected. The worst scoring tidal complex units had the lowest average percent protected with less than 1% (Figure 7.67), due largely to the absence of migration space for the worst scoring units.

Figure 7.67. Amount (%) of migration space in permanent protection by estimated resilience class. The boxplot shows the distribution of migration space securement (%) by resilience class. The mean percent secured is denoted by a red circle. The resilience classes are shown using our standard z-score color palette and abbreviations.



Migration Space Development and Future Development

Due to inconsistencies in spatial resolution of various datasets used in this analysis (i.e., 10-m elevation and 30-m land cover products), and how roads are inaccurately mapped in base land cover grids such as the NLCD and C-CAP products, there are cases where some development occurs within the migration space mapped at the 30-m scale. The migration space of tidal complex units with a “far above average” resilience score had an average of 12% development. The “above average” class had the lowest percentage at 11% while the “below average” class had the highest development at 24% (Figure 7.68). There are tidal complexes that have 80-100% development for the average and lower resilience classes, and this typically occurs for very small migration space areas where a single pixel of development leads to a high percentage. While the risk of future development was very similar across resilience classes (Table 7.32), the information is available for each site and could be useful for practitioners considering appropriate strategies for a specific location.

Figure 7.68. Amount (%) of migration space comprised of developed land, by estimated resilience class. The boxplot shows the distribution of migration space development (%) by resilience class with the mean denoted by a red circle. The resilience classes are shown using our standard z-score color palette and abbreviations.

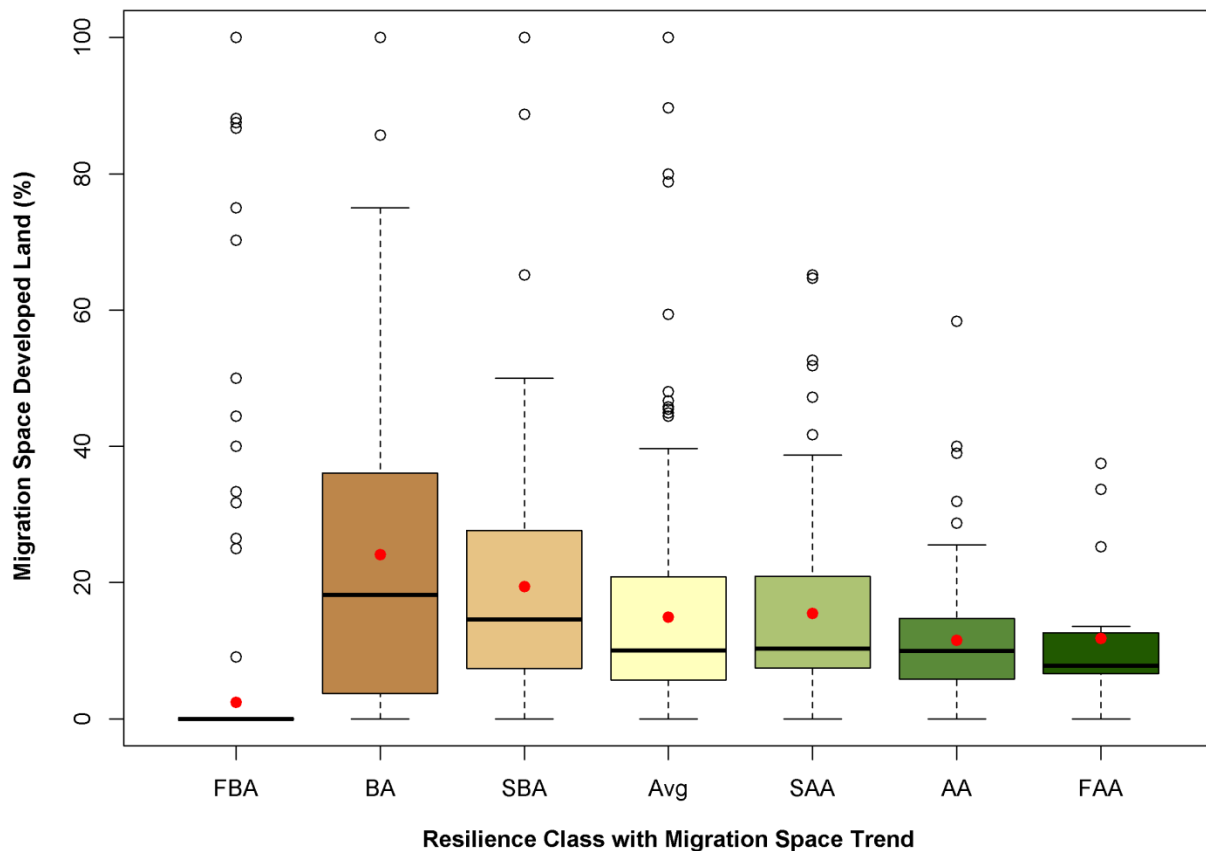
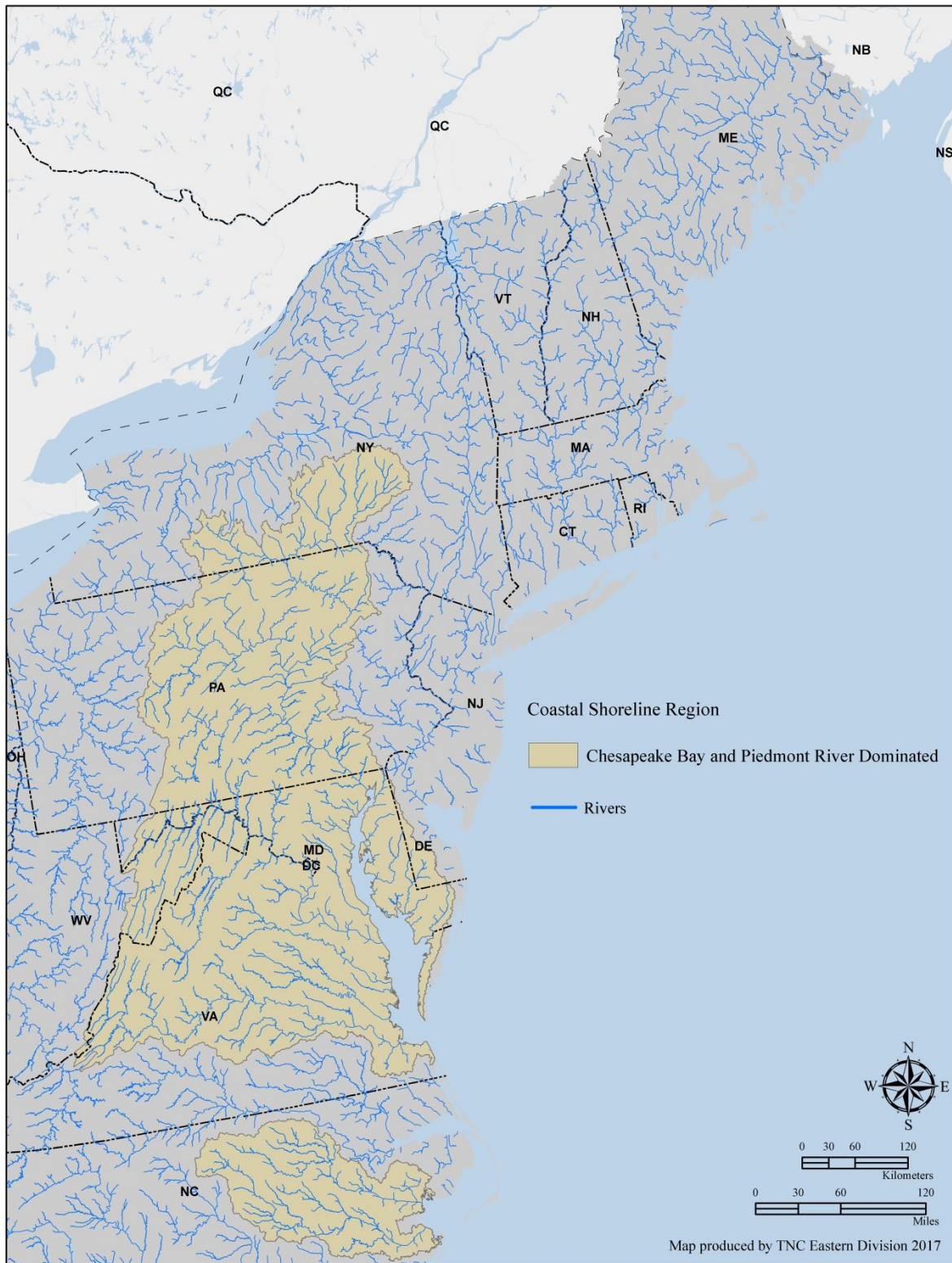


Table 7.32. Amount (%) of migration space estimated to be developed in 2100, by estimated resilience class. Summary statistics for migration space future development (%) are shown by resilience class.

Resilience Class with Migration Trend	Migration Space Future Development (%)					
	Min	1 st Quartile	Median	Mean	3 rd Quartile	Max
Far Below Average	0	0	0	0.2508		100
Below Average	0	0	0	2.39		68.78
Slightly Below Average	0	0	0	2.89		68.13
Average	0	0	0	2.11		85.71
Slightly Above Average	0	0	0	1.74	0.01	84.93
Above Average	0	0	0	0.7108	0.01	38.81
Far Above Average	0	0	0	0.9563		16.05

Chesapeake Bay and Piedmont River-Dominated CSR: Results



The **Chesapeake Bay and Piedmont River-Dominated CSR** had the most tidal complexes (5,135) of any region. The average size of complexes in this region was 54 acres with a median size of 5 acres. The largest unit in this CSR was 65,370 acres, which was also the largest unit in all five CSRs (Figures 7.69-7.70).

Figure 7.69. Distribution of tidal complex size (acres) by ten size classes in the Chesapeake Bay and Piedmont River-Dominated CSR.

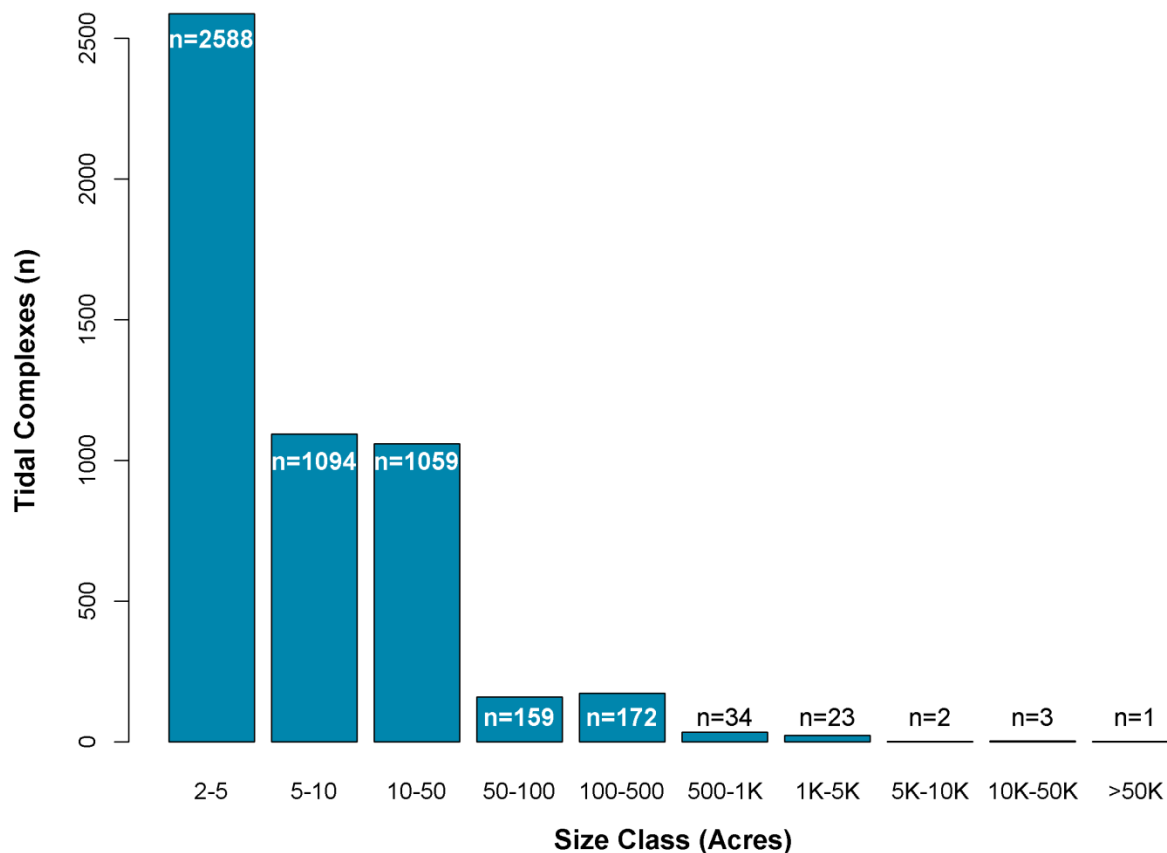
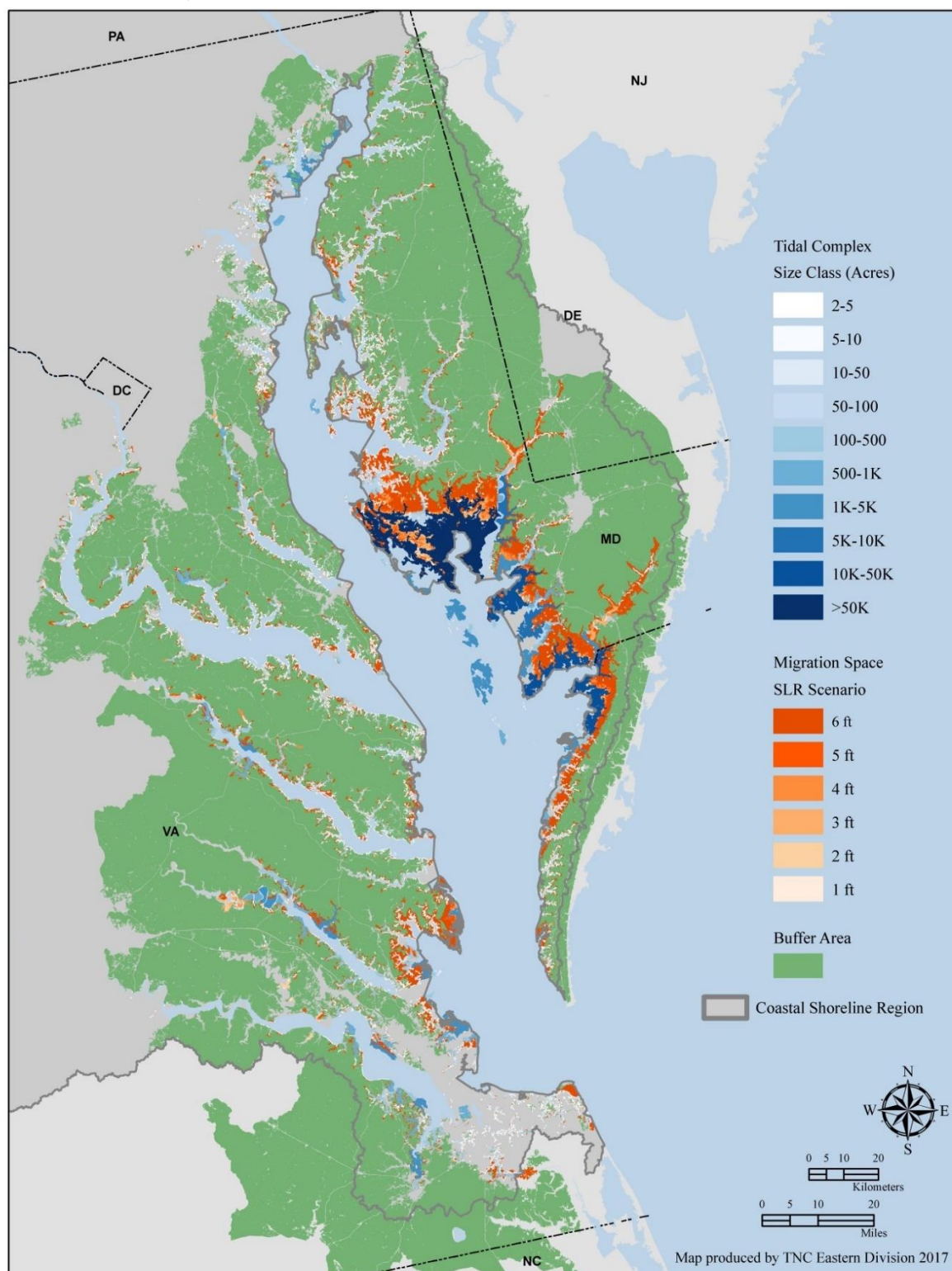
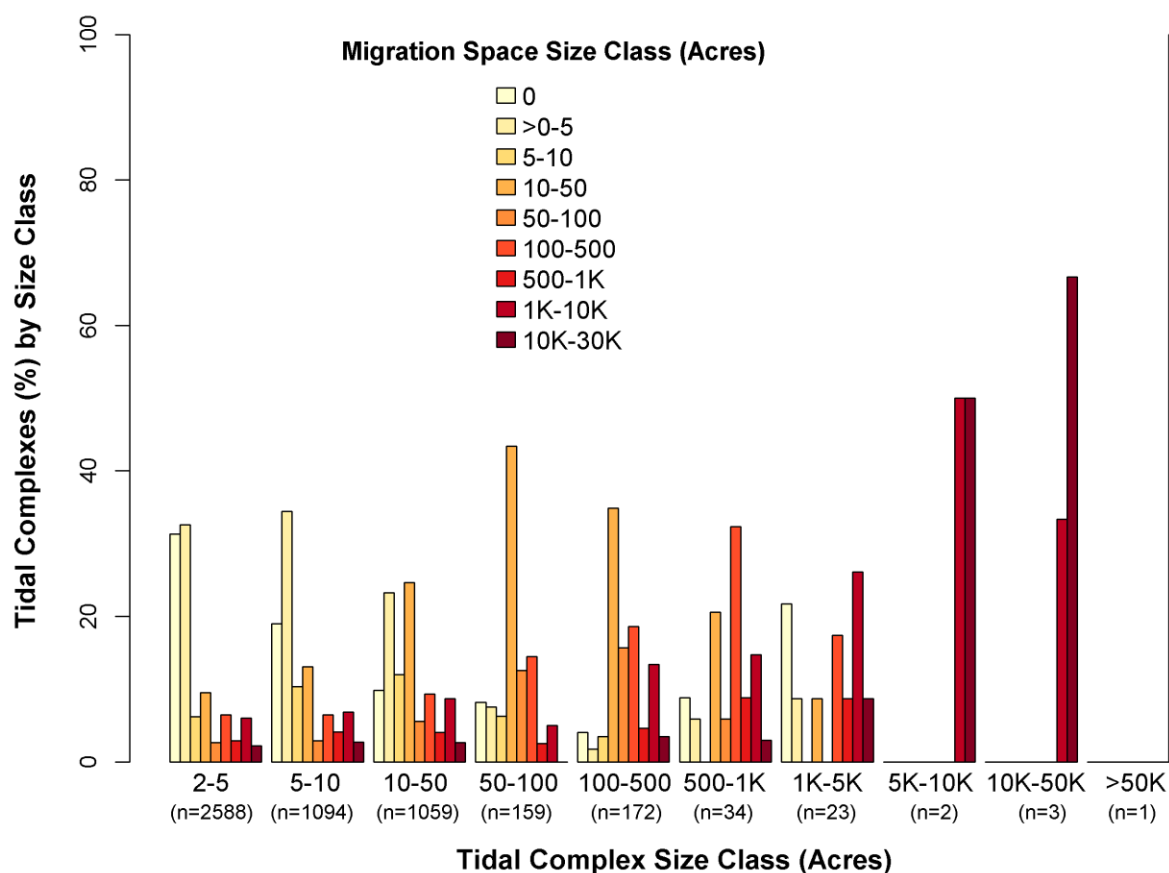


Figure 7.70. Tidal complex, migration space, and buffer area units in the Chesapeake Bay and Piedmont River-Dominated CSR. The color of the tidal complex units reflects their size class (n=10), while the color of the migration space indicates the SLR scenario (n=6).



Of the 5135 tidal complexes, 3984 or 78%, had migration space at a sea level rise of 6 feet (Figure 7.71). The average migration space size was 672 acres with a median size of 4 and a maximum size of 28,260 acres. As Figure 7.71 shows, small tidal complexes in this CSR can have little to no migration space or very large migration space areas at a sea level rise of 6ft. However, the largest tidal complexes (≥ 5000 acres) all have expansive migration space areas, reflecting the larger geophysical setting within which these tidal complexes occur.

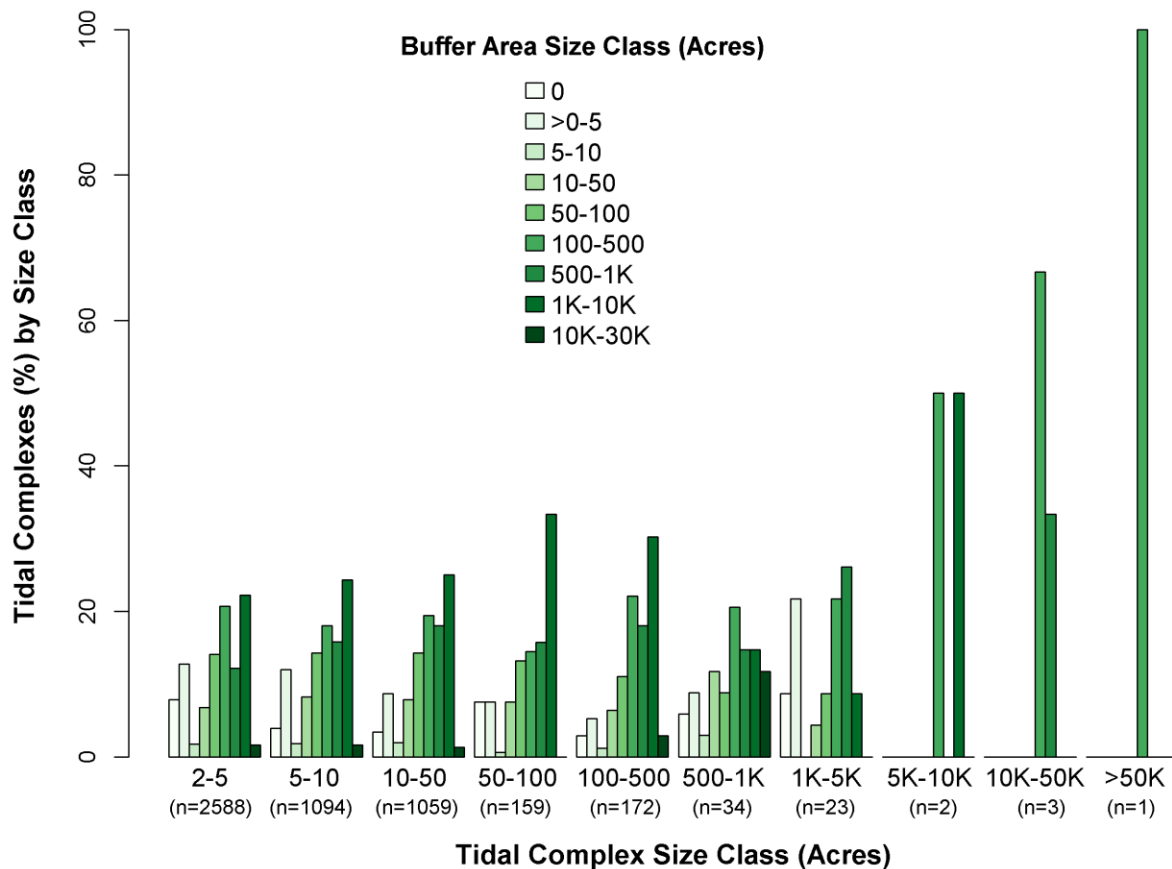
Figure 7.71. Migration space class distribution by tidal complex size class for the 6-foot sea level rise scenario. The y-axis is the percent of tidal complexes within a size class that have migration space of a particular size. Small migration space size classes are shown in light yellow shades that transition to darker oranges as the migration space size class increases.



A Spearman's rank-order correlation found the tidal complex size and migration space size were somewhat positively correlated and this relationship was statistically significant ($r_s = .31$, $p < 2.2e-16$).

Almost all the tidal complexes, 4832 or 94%, had buffer area at a sea level rise of 6 feet (Figure 7.72). The mean buffer size was 67,680 acres with the largest buffer area encompassing 485,600 acres. As Figure 7.72 illustrates, tidal complexes less than or equal to 1000 acres consistently had more of the large (100K-250K-acre) buffer areas. Regardless of tidal complex size class, the pattern of buffer space size classes skews to the right where more tidal complexes have larger buffer sizes for all size classes. This distribution results from the presence of large buffer areas that impact multiple tidal complexes. For example, the largest buffer area in this CSR provides some buffer acreage for 52 different tidal complexes. There was a very small positive relationship between tidal complex size and buffer area size ($r_s = .089$, $p = 1.725e-10$).

Figure 7.72. Buffer area class distribution by tidal complex size class for the 6-foot sea level rise scenario. The y-axis is the percent of tidal complexes within a size class that have buffer area of a particular size. Small buffer area size classes are shown in light green shades that change to darker greens as the buffer area size class increases.



Physical and Condition Scores

The estimated resilience score for a tidal complex consists of the condition and physical components, each weighted equally. Figure 7.73 shows the geographic distribution of physical scores within the CSR for a sea level rise of 6 feet. As both Figure 7.73 and Table 7.33 show, most scores fall in the average class, with the next largest category being the “far below average” category. The lowest scoring tidal complexes are predominantly those with no migration space and a less geophysically diverse buffer area. The spatial pattern of the condition scores is shown in Figure 7.74 with the numeric distribution highlighted in Table 7.33.

Figure 7.73. Estimated physical score for the Chesapeake Bay and Piedmont River-Dominated CSR. Tidal complex units in green score “above average” and have physical characteristics hypothesized to increase resilience including a large migration area with a diversity of tidal classes that are evenly distributed, a complex shoreline, and a geophysically diverse buffer area. Tidal complexes in yellow have “average” physical characteristics relative to all the units in the CSR. Tidal complexes in brown are “below average” and are estimated to respond poorly to sea level rise.

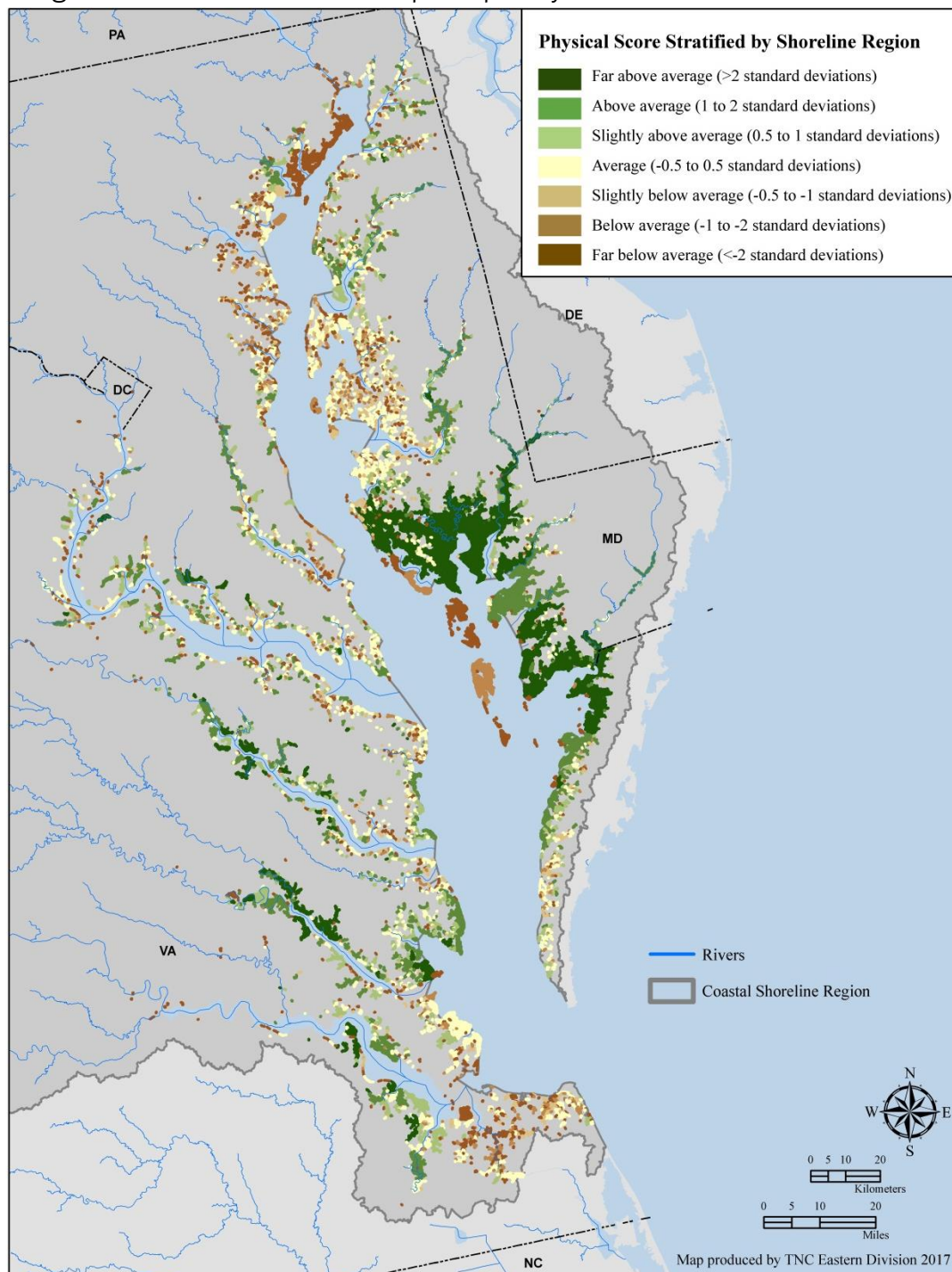


Figure 7.74. Estimated condition score for the Chesapeake Bay and Piedmont River-Dominated CSR. Tidal complex units in green score “above average” and are estimated to be in good condition based on a low percentage of hardened shoreline; good water quality and quantity, and high sediment contributions in the migration space; and a natural buffer area with highly connected wetlands. Tidal complexes in yellow are “average.” Tidal complexes in brown are “below average” and are estimated to be in poor condition.

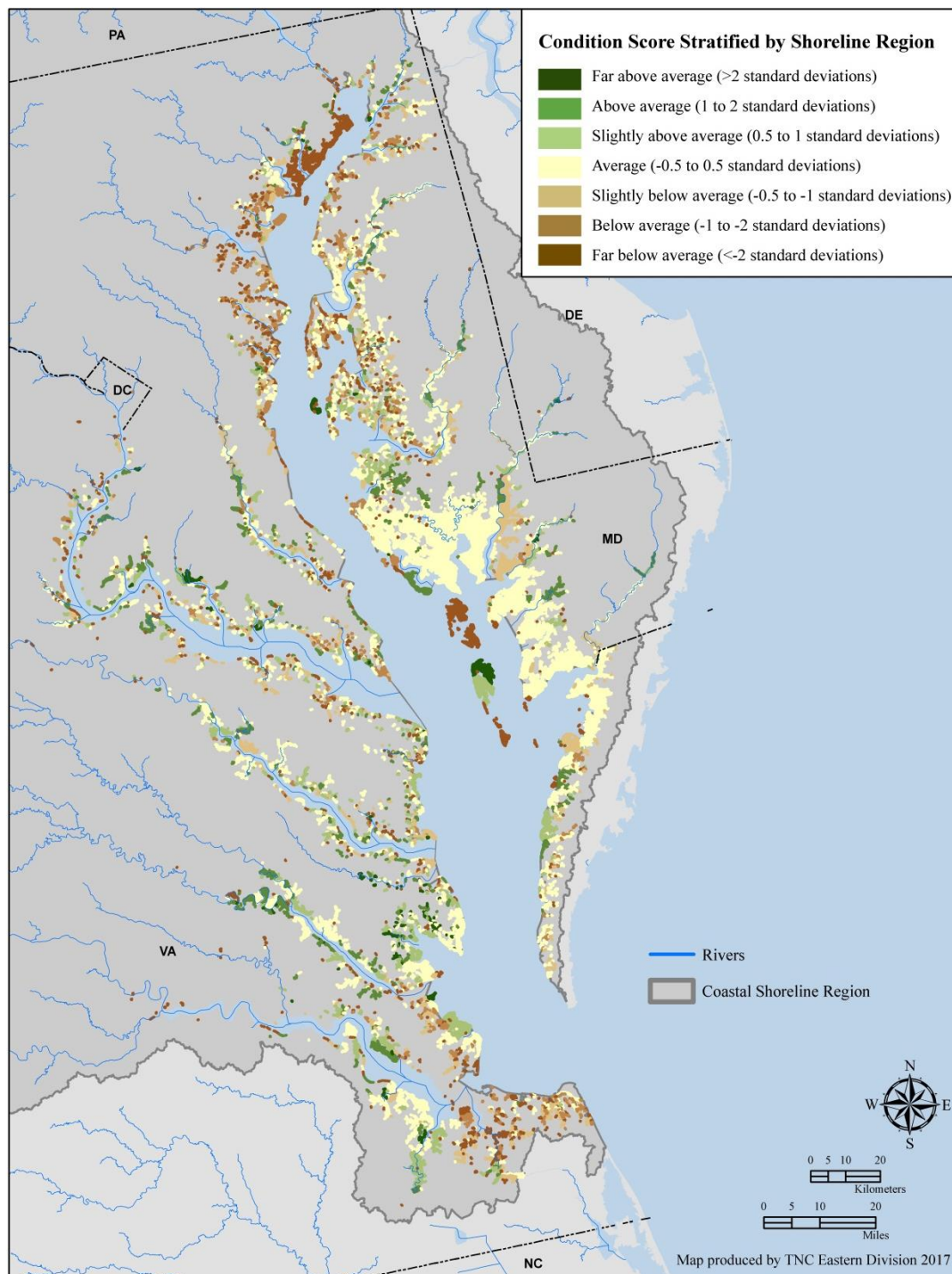


Table 7.33. Frequency of physical and condition scores in the Chesapeake Bay and Piedmont River-Dominated CSR for the 6-foot sea level rise scenario.

Z-Score Class	Tidal Complex (n)	
	Physical	Condition
Far Below Average	1217	1159
Below Average	545	553
Slightly Below Average	601	609
Average	1535	1558
Slightly Above Average	601	610
Above Average	545	552
Far Above Average	91	94

The relationship between the condition and physical scores was variable and only somewhat positively correlated ($r = .27$, $p = 2.2e-16$, Figure 7.75). A tidal complex with a high physical score does not necessarily have a high condition score as evidenced in Figures 7.75-7.76 and Table 7.34. For example, there are 17 tidal complexes that have an “above average” physical score but a “below average” condition score (Figure 7.77). Conversely, there are 10 tidal complexes that have “below average” physical scores but “far above average” condition scores (Table 7.34).

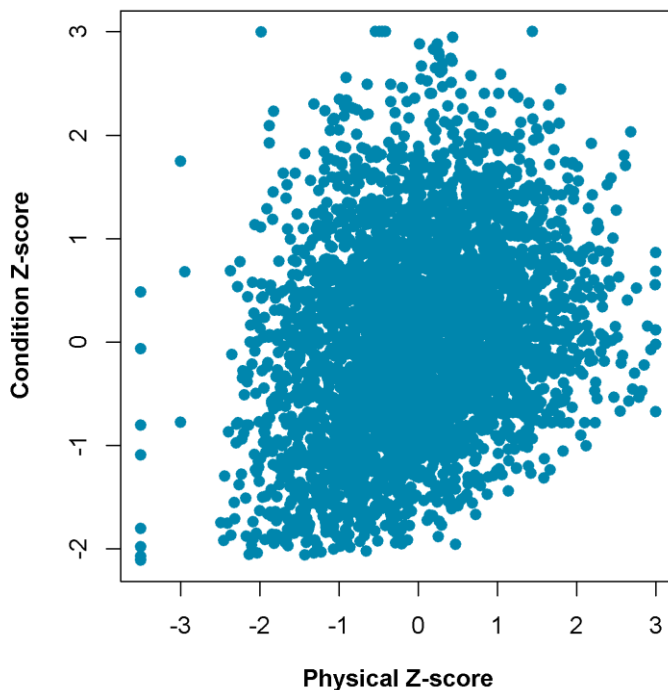
Figure 7.75. Relationship between the tidal complex units' physical and condition z-scores for the six-foot sea level rise scenario, after removing units with no migration space.

Figure 7.76. Distribution of the physical scores for each condition class at a sea level rise of 6 feet. The distribution of the physical scores is shown for each condition score class using our standard z-score color palette.

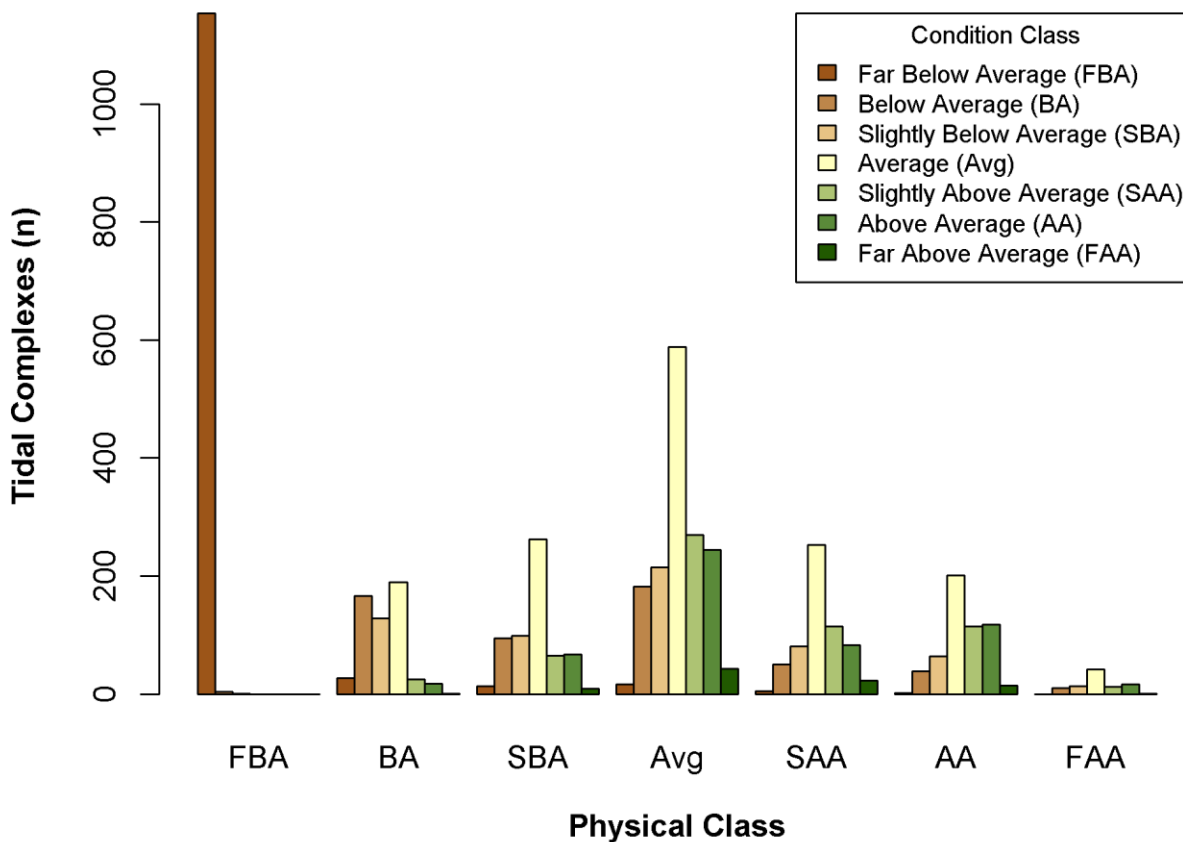


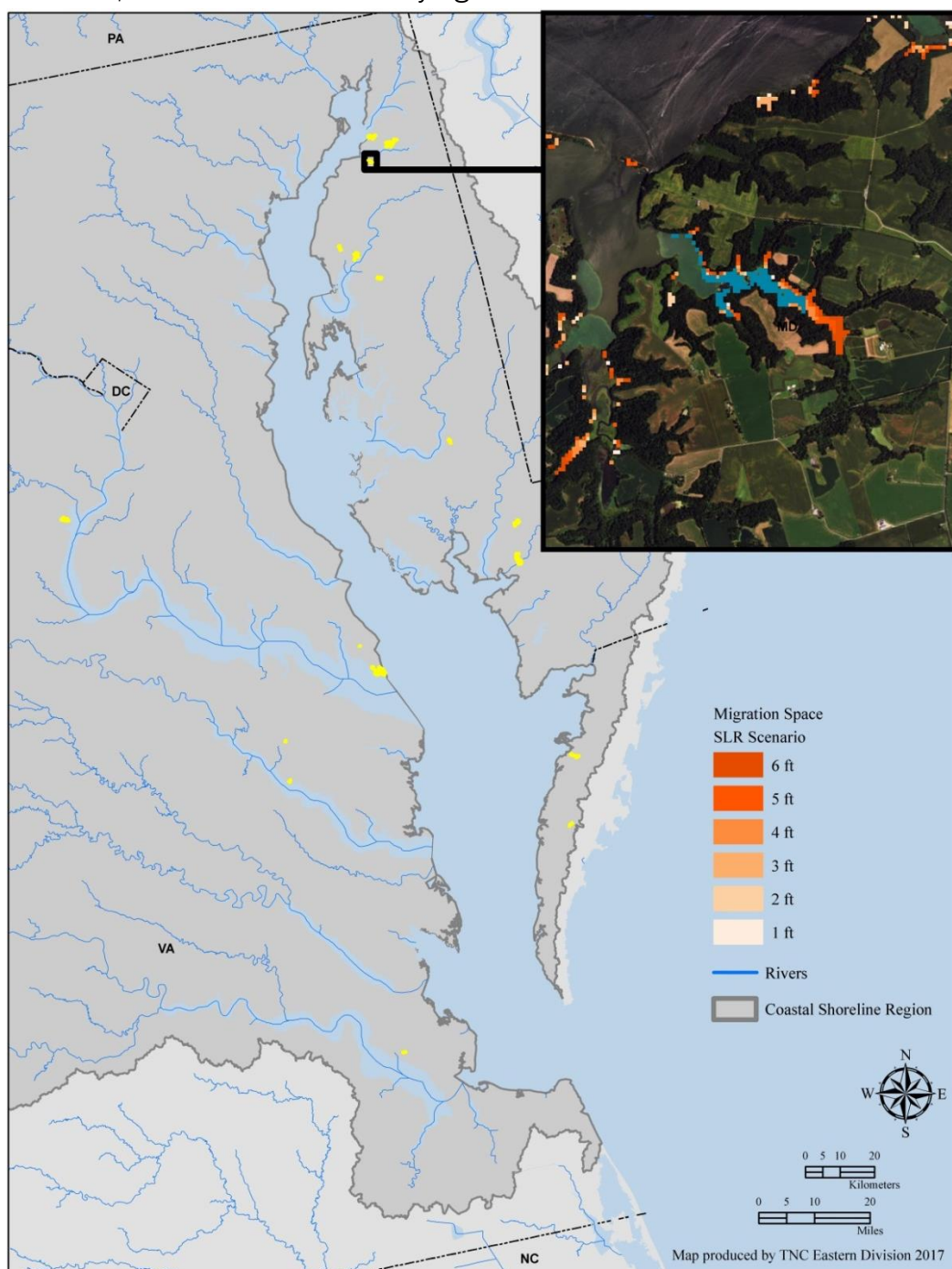
Table 7.34. The number of tidal complex units in each physical and condition score category. A two-by-two frequency table shows the count of tidal complexes occurring in each physical and condition class combination. Physical classes are by row and condition classes are by column. Boxes shaded in gray indicate tidal complexes with the same physical and condition score class. For example, only one tidal complex scored “far above average” for both physical and condition characteristics.

Physical Class	Condition Class						
	Far Below Average	Below Average	Slightly Below Average	Average	Slightly Above Average	Above Average	Far Above Average
Far Below Average	1154	27	13	16	5	2	0
Below Average	4	166	94	182	50	39	10
Slightly Below Average	1	128	99	215	81	64	13
Average	0	189	262	588	253	201	42
Slightly Above Average	0	25	65	270	115	114	12
Above Average	0	17	67	244	83	118	16
Far Above Average	0	1	9	43	23	14	1

There were 18 sites that had a low condition score (i.e., “below average” or “far below average”) and a high physical score (i.e., “above average” or “far above average”). The location of these sites is highlighted in yellow in Figure 7.77. These are potential areas for restoration as the physical template was suitable for marsh migration, but issues related to the condition of the migration space (e.g., poor water quality, hardened shoreline) would have to be addressed. The focal tidal complex in Figure 7.77 at Lloyd Creek in the Sassafras River Natural Resource Management Area of MD, had a high physical score due to the following factors: size (30 acres), relatively complex shoreline, moderately-sized migration space, high variety and evenness in tidal classes, large buffer with diverse landforms and soil classes. However, this site had poor condition characteristics including 33% hardened shoreline, high estimated nitrogen levels, and a buffer area with a high proportion of agricultural land.

Figure 7.77. Tidal complexes (n=18) with high physical scores but in poor condition.

These sites are estimated to be in poor condition (poor water quality, hardened shoreline, non-natural buffer area, etc.) but have physical characteristics hypothesized to increase resilience to sea level (large tidal complex, complex shoreline, migration space with diversity of tidal classes, etc.). The site shown in the inset, at Lloyd Creek in the Sassafras River Natural Resource Management Area of MD, had a long tidal complex with extensive migration space up the main river channel and some tributaries, but was surrounded by agricultural land.



Estimated Resilience Score

The physical and condition scores were equally weighted and combined to calculate an estimated resilience score for each tidal complex. High scoring sites were those with a large migration space, intact buffer area, and whose condition was not expected to exacerbate the impacts of sea level rise and climate change, with all these characteristics relative to other sites in the CSR. The role of some of the physical factors was evident in Figure 7.78 where high scoring tidal complexes shown in dark green have a large migration space (shown in orange shades), and very vulnerable complexes shown in dark brown had no migration space. The resilience values are in z-scores which follow a normal distribution except for the “far below average” category because tidal complexes with no migration space were manually assigned a -3.5 SD score for all migration space attributes. The relationship between the physical and condition scores and the role of that relationship in the estimated resilience score can be seen in Figure 7.79. While the patterns in the proportion of each class for the physical and condition components are relatively similar, there are some interesting nuances. For example, for both the above average and “far above average” resilience classes, the physical component had a higher proportion of the highest scores compared to the condition score distribution, indicating it was hard to score very high for both condition and physical characteristics. A “far above average” resilience score was largely comprised of above average condition and physical scores but can also occur from the following combinations:

- “average” condition and “far above average” physical,
- “slightly above average” condition and “far above average” physical,
- “far above average” condition and “above average” physical,
- “far above average” condition and “slightly above average” physical.

The ten tidal complexes with the highest estimated resilience score are shown in Figure 7.80. The average tidal complex size of this group was 189 acres with an average migration space size at a 6-foot sea level rise of 2,086 acres (min = 6, max = 17,965, SD = 5325 acres) and a large average buffer area (136,209 acres). Vulnerable sites, those having below average estimated resilience, are shown in Figure 7.81. These tidal complexes are locations with little to no migration space and whose poor condition, again relative to all other sites in the CSR, was expected to exacerbate the impacts of sea level rise and climate change. The results of a Pearson correlation analysis show the role of tidal complex size, migration space size, and buffer area size in the condition, physical, and resilience score (Table 7.36). As expected, given the weight of these attributes in the physical component score, size was significantly and positively correlated with the physical score, particularly for the migration space size. The condition score was also significantly but only somewhat positively correlated with the migration space and buffer area size, likely reflecting land use and geophysical patterns in the larger landscape whereby smaller migration spaces are in areas with greater elevation and slope and/or more developed land use.

Figure 7.78. Estimated resilience score. This map shows the estimated resilience score for the Chesapeake Bay and Piedmont River-Dominated CSR for the 6-foot sea level rise scenario. The map shows areas that are above (green) or below (brown) the mean. Areas in green score “above average” and are estimated to be more resilient based on their physical and condition characteristics. Areas in yellow are “average.” Areas in brown are “below average” and are estimated to be vulnerable to sea level rise and climate change.

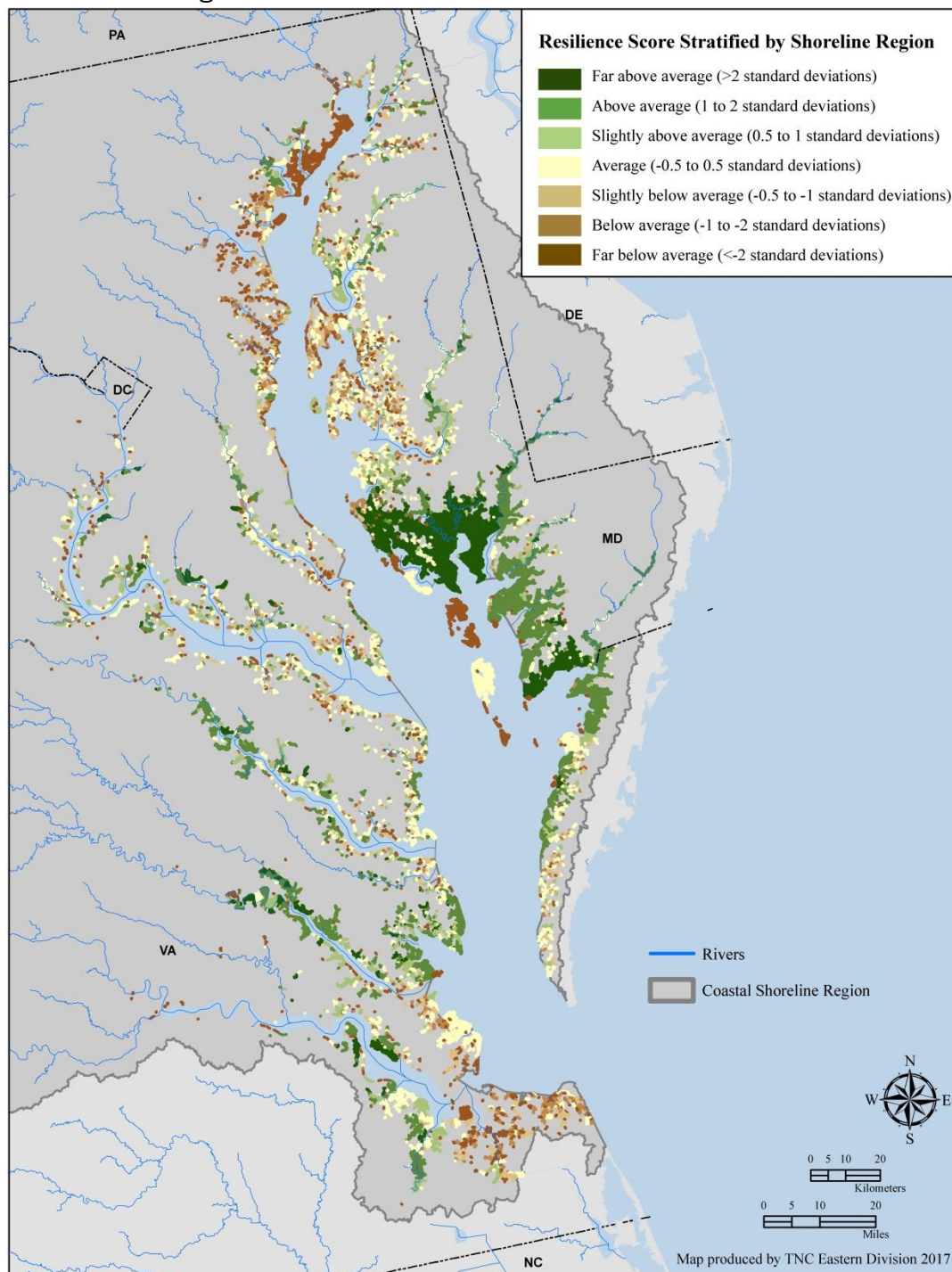


Figure 7.79. Relationship between condition and physical components for each estimated resilience class at a sea level rise of 6 feet. The physical and condition bars are split vertically based on the proportion of each score for each resilience class.

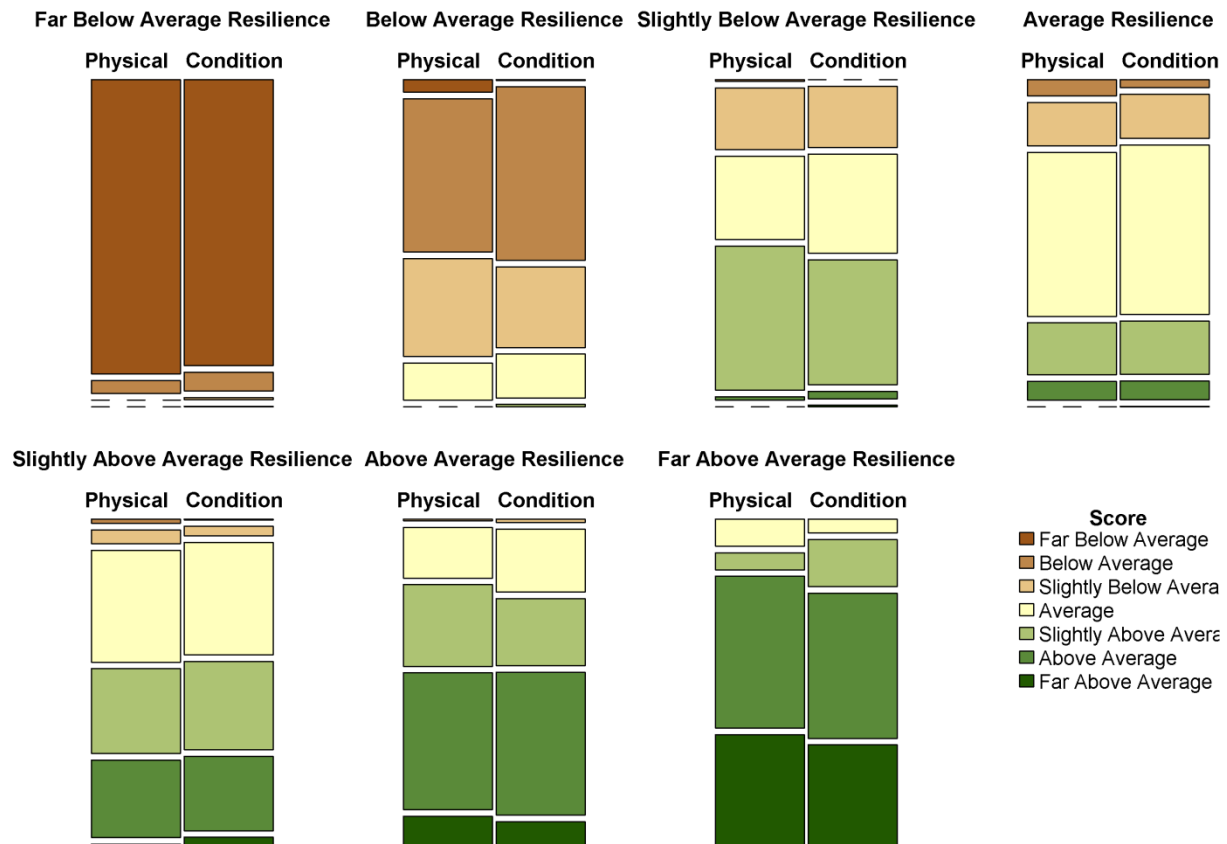


Table 7.35. Distribution of estimated resilience scores in the Chesapeake Bay and Piedmont River-Dominated CSR for the 6-foot sea level rise scenario.

Z-Score Class	Estimated Resilience	Estimated Resilience with Migration Space Trend
Far Below Average	1245	1243
Below Average	541	485
Slightly Below Average	596	543
Average	1525	1419
Slightly Above Average	596	622
Above Average	541	684
Far Above Average	91	139

Figure 7.80. The top ten highest scoring tidal complexes in the Chesapeake Bay and Piedmont River-Dominated CSR. The ten tidal complexes with the highest estimated resilience score are highlighted in yellow. The focal tidal complex shown in the inset, located at Big Annesmessex River and near Holland Neck in MD, was large (377 acres), had a complex shoreline, a large migration space (18,000 acres) that surrounded a large portion of the tidal complex (i.e., high shared edge), “average” water quality, “average” sediment inputs, and a large, intact, and diverse buffer area.

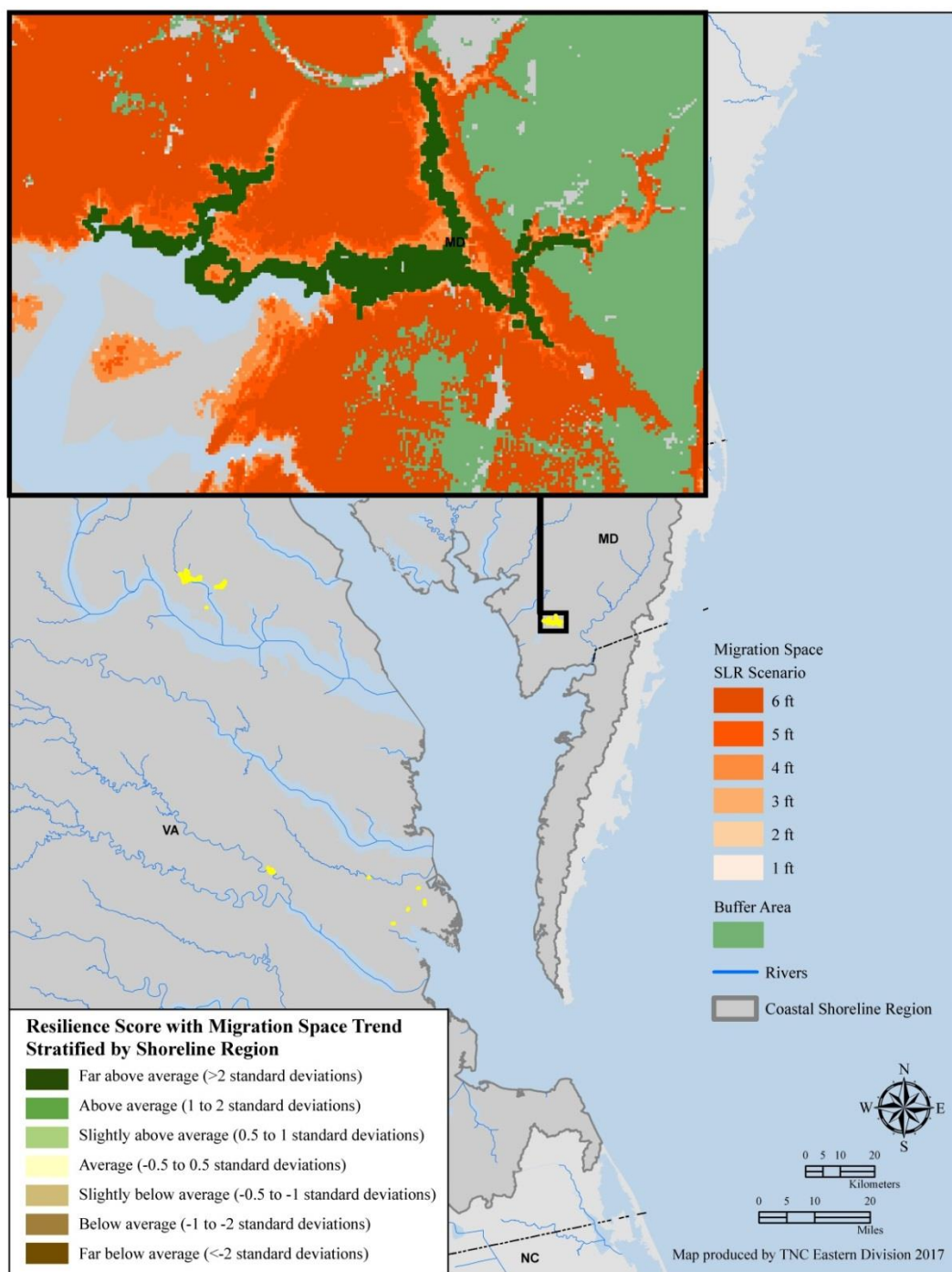


Figure 7.81. Vulnerable tidal complexes. Sites that scored below the mean are considered vulnerable. Sea level rise is expected to worsen the degradation of vulnerable sites, but these sites may still provide valuable ecosystem services (i.e., buffering storm effects, wildlife habitat, etc.).

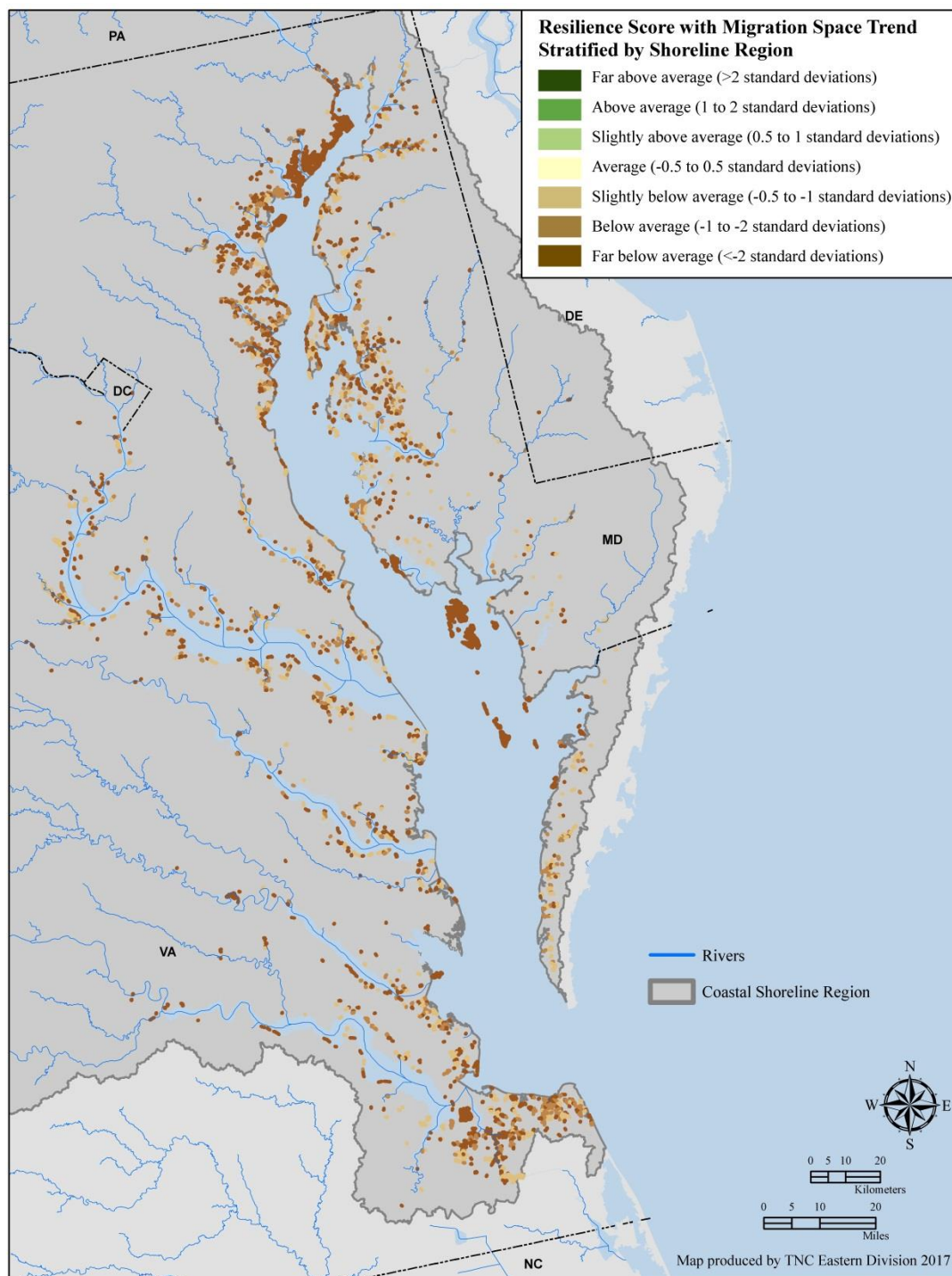


Table 7.36. Relationship between resilience components and analysis unit size.

Pearson correlation coefficients between the condition, physical, and estimated resilience scores and the size (acres) of the tidal complex, migration space, and buffer area, after removing tidal complexes with no migration space. A star indicates a significant ($p \leq .05$) relationship.

	Tidal Complex Size	Migration Space Size	Buffer Area Size
Physical Z-score	0.446*	.576*	0.467*
Condition Z-score	-0.0009	.183*	0.235*
Resilience Z-score	0.288*	0.478*	.442*

Trends in Migration Space Size

For tidal complex units in the Chesapeake Bay and Piedmont River-Dominated setting, the mean size across all migration spaces increased from a 1 to 3-foot sea level rise but then showed a decline from 3 to 6 feet (Table 7.37). Linear regressions identified 3088 tidal complex units with a statistically significant ($p \leq .05$) relationship between the latter three sea level rise scenarios (3 – 6 feet) and migration space size. Of those tidal complex units with a significant relationship, some had decreasing migration space but the majority experienced an increase in migration space (Table 7.38). The mean increase in size was 109 acres while the average decrease was 255.30 (Table 7.38). Tidal complexes with a significant migration space trend were assigned to one of three trend categories: increase, decrease, no change, and we adjusted their score to reflect the trend. The 1451 tidal complexes whose migration space showed an increasing trend were awarded an additional 0.50 SD points to their estimated resilience score. The 496 tidal complexes that experienced a decline in migration space size from the 3 to the 6-foot SLR scenario had their estimated resilience scores reduced by 0.50 SD. The resilience score of the 1141 tidal complexes with no significant change in migration space size was not impacted by the trend analysis. The map in Figure 7.82 shows the spatial distribution of the resilience scores with the trend analysis incorporated. Of the top ten highest scoring sites shown in Figure 7.80, 80% or 8, of the tidal complexes received a boost to their score from a positive migration space size trend. The other two tidal complexes had stable migration space sizes and thus had no change to their resilience score. The use of 0.50 SD to adjust the resilience score meant that no tidal complex's score could change by more than one resilience class (Table 7.39). After incorporating migration space trend, the resilience class did not change for 3892 or 76% of the tidal complexes, while 308 or 6% of sites went to the next lower class and 18% or 935 complexes moved up a class (Figure 7.83, Table 7.39).

Table 7.37. Summary statistics for migration space size by sea level rise scenario.

SLR Scenario (feet)	Migration Space (Acres)				
	1 st Quartile	Median	Mean	3 rd Quartile	Max
1	0.2224	2.224	328.6	16.01	34910
2	0.4448	3.114	627.8	28.58	52560
3	0.2224	4.448	842.8	40.7	56730
4	0.2224	4.67	837.7	46.04	42330
5	0.2224	4.67	768.6	49.15	32970
6	0.2224	4.448	672.3	51.82	28260

Table 7.38. Summary of regression coefficients for tidal complex units (n=3088) with a significant ($p \leq .05$) relationship between sea level rise scenario (≥ 3 feet) and migration space size.

Migration Space Size (acres) Change					
Trend direction	Count	Minimum	Median	Mean	Max
Decrease	496	-3588	-2.135	-255.300	-0.057
Increase	1451	0	7.256	109.00	2199
No change	1141	0	0	0	0

Figure 7.82. Estimated resilience score with migration space trend. This map shows the estimated resilience score after incorporating the trend in migration space size for the Chesapeake Bay and Piedmont River-Dominated CSR at the 6-foot sea level rise scenario. Tidal complex units whose migration space showed a significant increase ($p \leq .05$) from the 3 to 6-foot SLR received an additional 0.50 standard deviation units to their score, while the score of units with a significant decrease in migration space was reduced by 0.50 SD units.

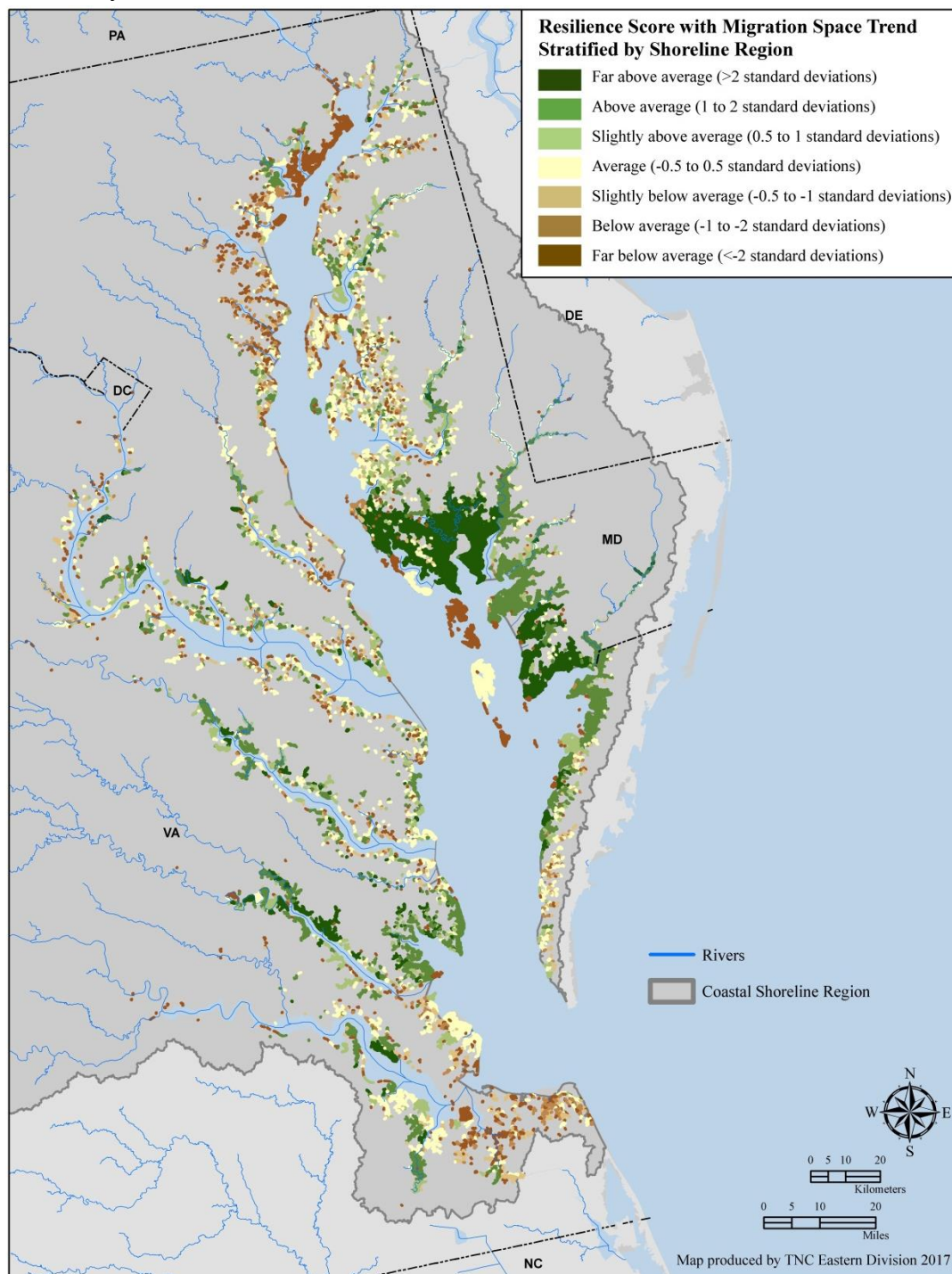
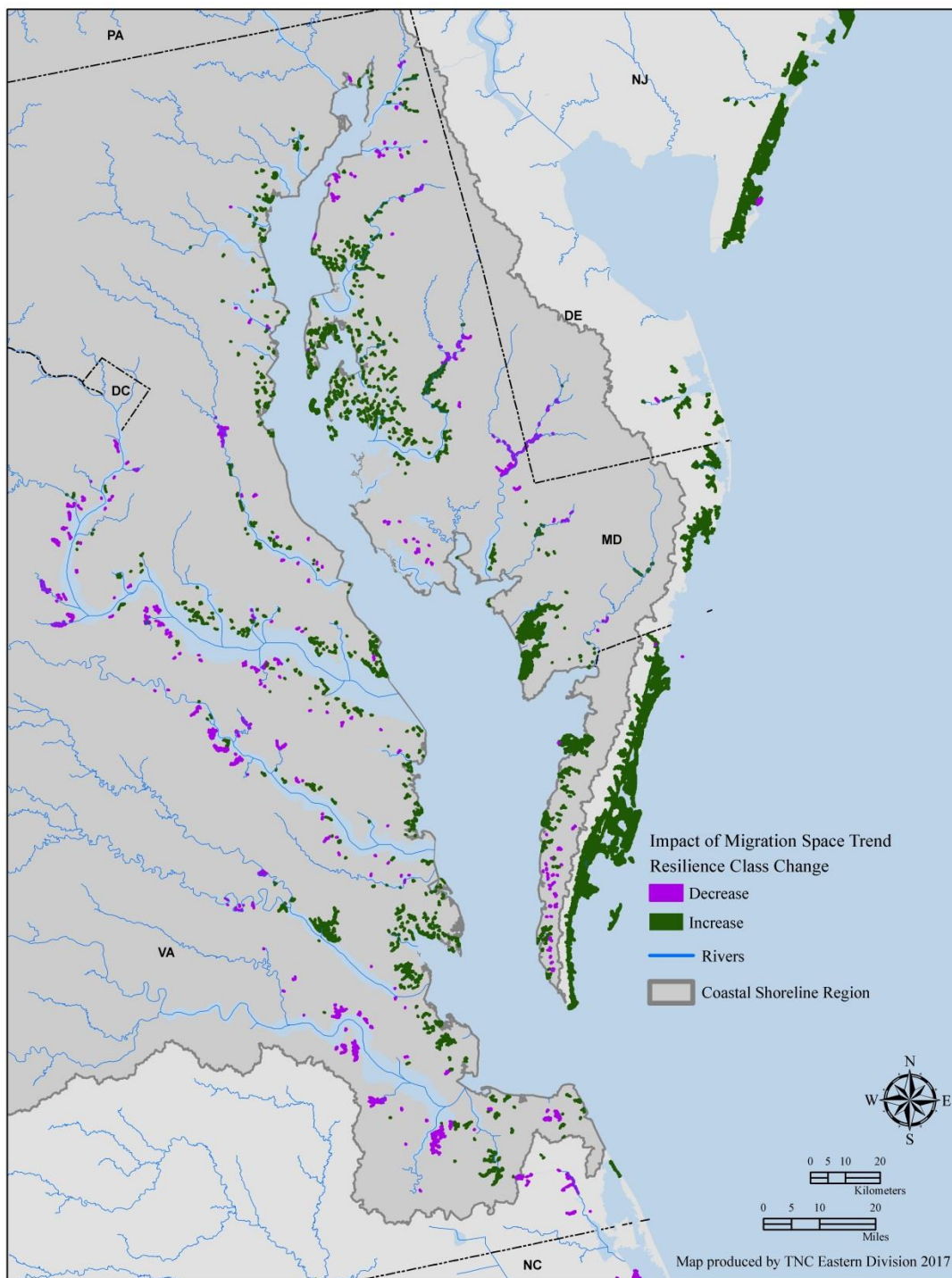


Table 7.39. The change in resilience class after incorporating the trend in migration space size. Tidal complex units whose migration space showed a significant increase ($p \leq .05$) from the 3 to 6-foot sea level rise received an additional 0.50 standard deviation units to their score, while the score of units with a significant decrease in migration space size was reduced by 0.50 SD units. The purple boxes indicate the number of tidal complex units that moved to the next lower resilience class, and the green boxes highlight the number of units whose class improved when the migration space trend was considered.

Resilience Class	Resilience class with Trend						
	Far Below Average	Below Average	Slightly Below Average	Average	Slightly Above Average	Above Average	Far Above Average
Far Below Average	1234	11	0	0	0	0	0
Below Average	9	427	105	0	0	0	0
Slightly Below Average	0	47	336	213	0	0	0
Average	0	0	102	1120	303	0	0
Slightly Above Average	0	0	0	86	269	241	0
Above Average	0	0	0	0	50	429	62
Far Above Average	0	0	0	0	0	14	77

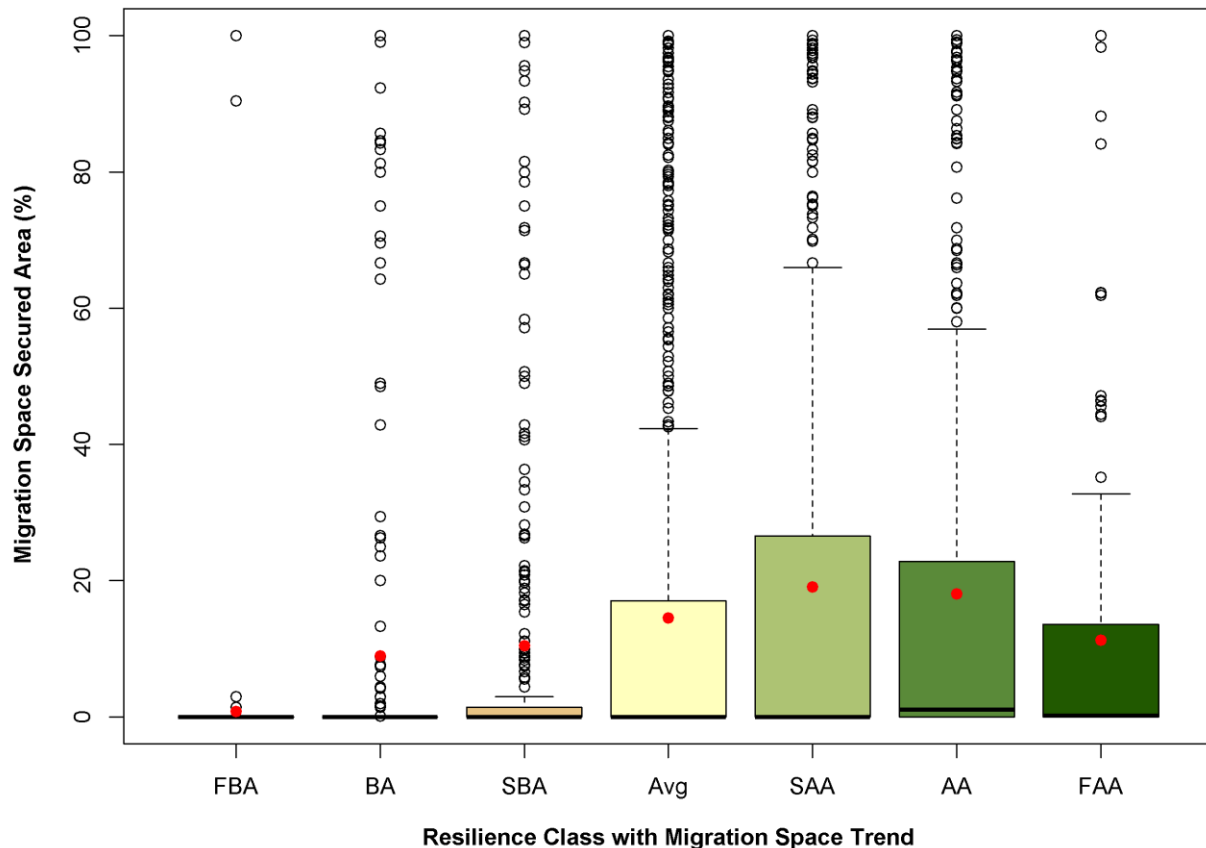
Figure 7.83. Estimated resilience class changes after incorporating migration space trend. This map shows the tidal complexes whose estimated resilience class either increased (n=935) or decreased (n=308) after incorporating the trend in migration space size for the Chesapeake Bay and Piedmont River-Dominated CSR at the 6-foot sea level rise scenario.



Migration Space Securement

The amount of a tidal complex's total migration space that was already protected (GAP status 1-3) varied substantially by resilience z-score category (Figure 7.84). Tidal complex units with "slightly above average" resilience scores had the greatest percentage of their migration space in securement (mean=19%) while the worst scoring tidal complex units had the lowest average percent protected with less than 1% (Figure 7.84), which was due largely to the fact that the worst scoring units had very little if any migration space.

Figure 7.84. Amount (%) of migration space in permanent protection by estimated resilience class. The boxplot shows the distribution of migration space securement (%) by resilience class. The mean percent secured is denoted by a red circle. The resilience classes are shown using our standard z-score color palette and abbreviations.



Migration Space Development and Future Development

Due to inconsistencies in spatial resolution of various datasets used in this analysis (i.e., 10-m elevation and 30-m land cover products), and how roads are inaccurately mapped in base land cover grids such as the NLCD and C-CAP products, there are cases where some development occurs within the migration space mapped at the 30-m scale. For all the resilience classes except “far below average,” the tidal complexes have an average of approximately 10% development (Figure 7.85). There are tidal complexes that have 80-100% development for the average and lower resilience classes, and this typically occurs for very small migration space areas where a single pixel of development leads to a high percentage. While the risk of future development was very similar across resilience classes (Table 7.40), the information provides a useful tool for practitioners considering appropriate strategies for a specific location.

Figure 7.85. Amount (%) of migration space comprised of developed land, by estimated resilience class. The boxplot shows the distribution of migration space development (%) by resilience class with the mean denoted by a red circle. The resilience classes are shown using our standard z-score color palette and abbreviations.

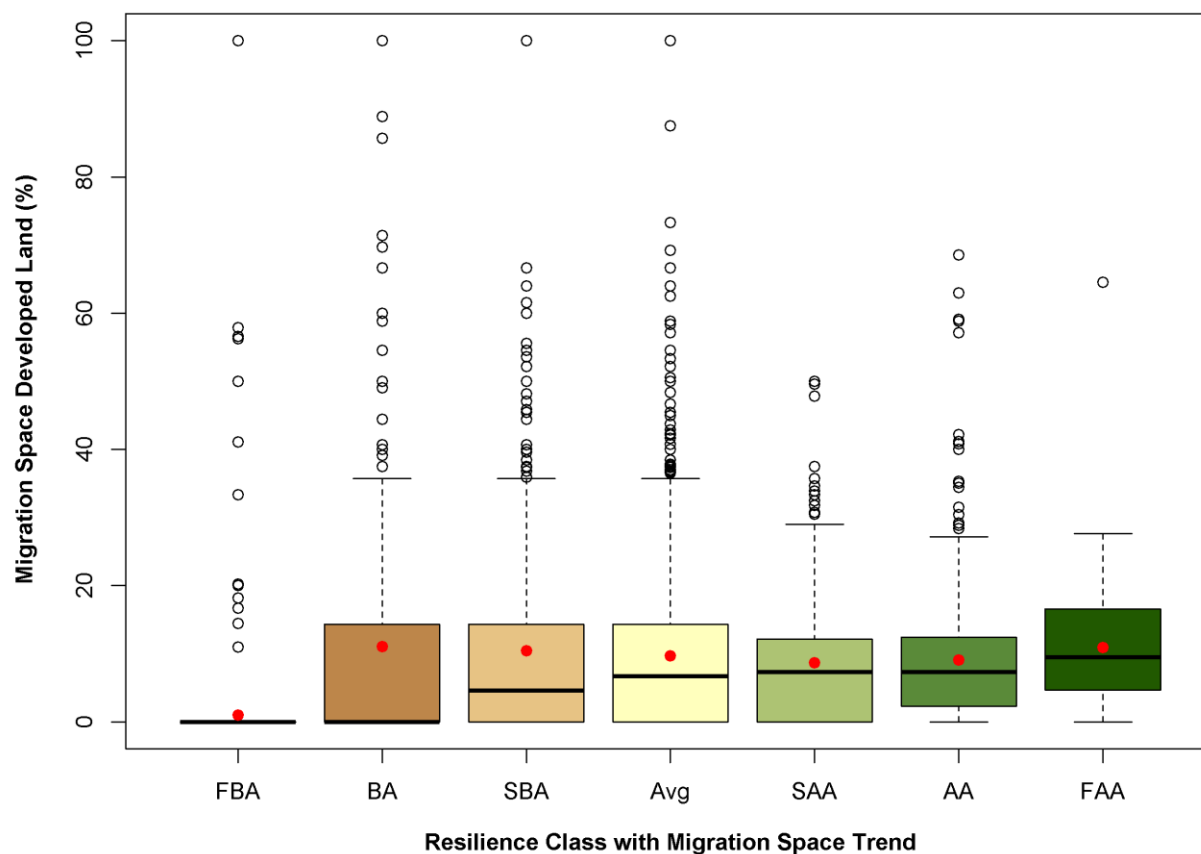
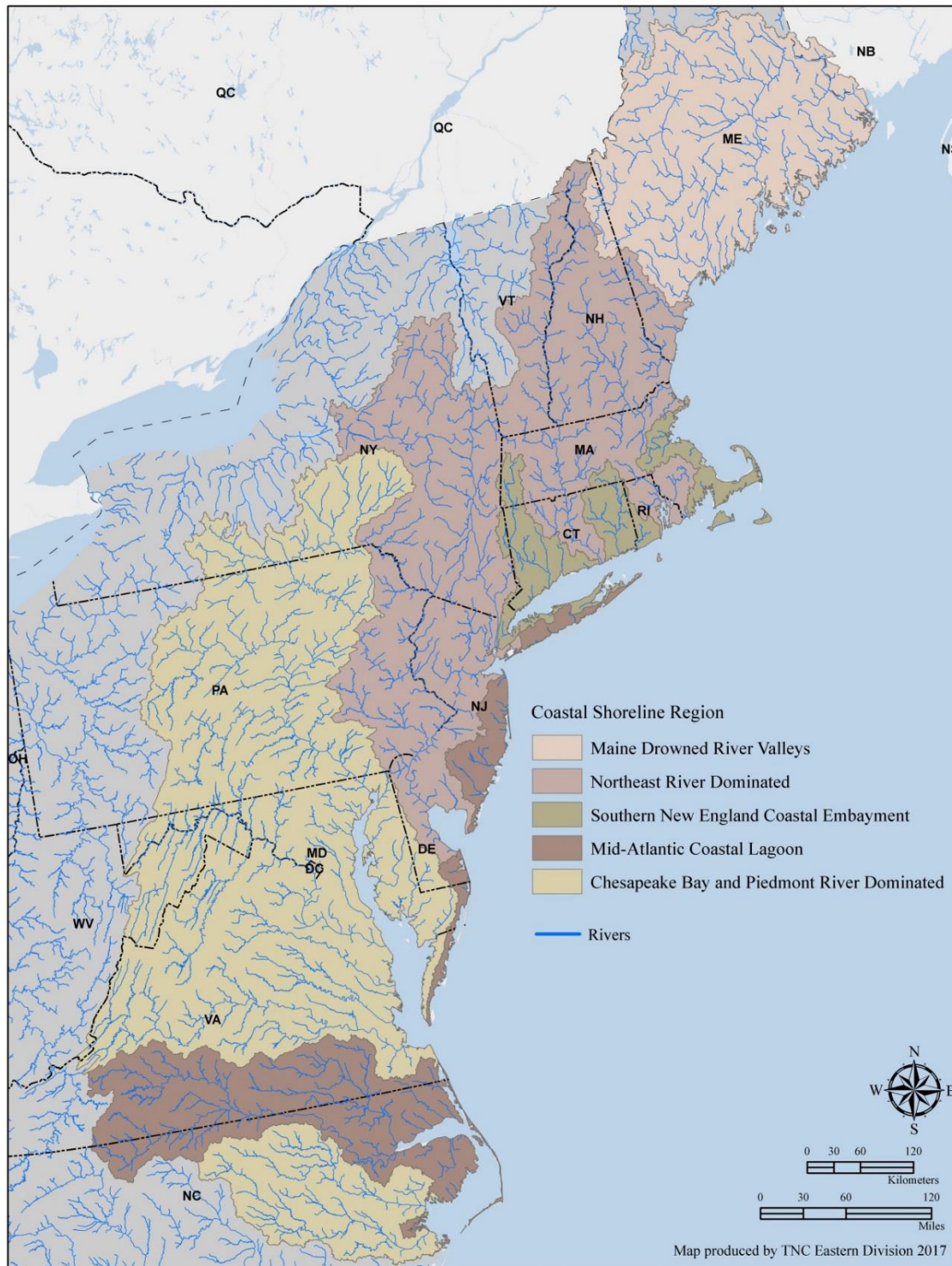


Table 7.40. Amount (%) of migration space estimated to be developed in 2100, by estimated resilience class. The summary statistics for migration space future development (%) are shown by resilience class.

Resilience Class with Migration Trend	Migration Space Future Development (%)					
	Min	1 st Quartile	Median	Mean	3 rd Quartile	Max
Far Below Average	0	0	0	0.16	0	100
Below Average	0	0	0	0.51	0	100
Slightly Below Average	0	0	0	0.044	0	16.67
Average	0	0	0	0.052	0	30
Slightly Above Average	0	0	0	0.027	0	12.68
Above Average	0	0	0	0.005	0	2.45
Far Above Average	0	0	0	0	0	0

Full Region: Results



Full Region

This project was designed to create consistent and credible results within each CSR. We focused on the shoreline regions because they are ecologically consistent and contain less heterogeneity than the arbitrary boundary of the project area. Additionally, the CSRs change dramatically from North to South in concert with the geomorphic structure and processes that maintain the tidal complexes and determine resilience. Thus, the within-CSR results identify the sites that are most resilient within a given type of shoreline, and avoid comparing, for example, a rocky drowned river valley to a sheltered lagoon. However, comparisons across shoreline regions can provide useful context for interpreting the within-CSU results, and for completeness, we include them here.

Tidal Complex Units

There were 10,736 tidal complexes in the project area that had a minimum area of two acres with at least two acres of tidal marsh. As described in the methods, the two-acre marsh threshold was used to prevent tidal complexes from being comprised entirely of unconsolidated shore. Unconsolidated shore complexes were often mapped erroneously and inconsistently, largely due to tidal variations dependent on when the underlying satellite imagery was taken. As Figure 7.86 shows, the Chesapeake Bay CSR had the largest number of tidal complexes (5135), and the Maine Drowned River Valleys had the smallest number (650). For all CSRs, the smallest tidal complex size class (2-5 acres) was the most frequent (Figure 7.86). The Chesapeake featured the largest tidal complex in the region, encompassing over 50,000 acres. The Mid-Atlantic CSR had an average tidal complex size that was significantly larger than the other CSRs (Table 7.41). The Embayment region had the smallest average size, followed by the Chesapeake. While the Chesapeake had many large complexes, it had many small complexes in the first three size classes that brought down the average size. The southern CSRs in the project area (Chesapeake and Mid-Atlantic) had more of the large tidal complex size classes than the other CSRs, reflecting both the physical setting and land use patterns within the five CSRs (Figures 7.87-7.88).

Figure 7.86. Frequency of tidal complex size class by CSR. Small size classes are shown in white and blue colors that transition to dark blues as the size increases.

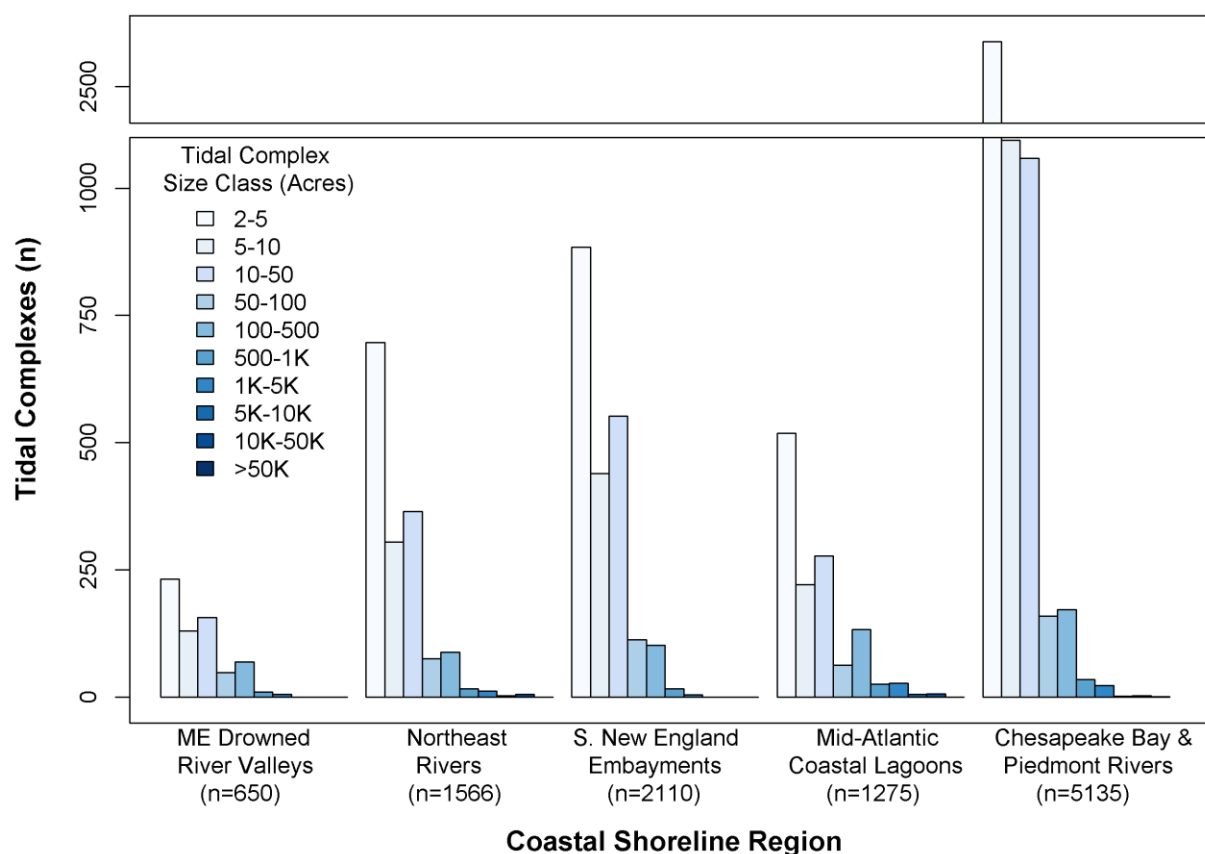


Table 7.41. Summary statistics for tidal complex size by CSR.

Coastal Shoreline Region	Tidal Complex Size (Acres)				
	1 st Quartile	Median	Mean	3 rd Quartile	Max
Chesapeake Bay & Piedmont River	2.89	4.89	54.31	11.56	65,370
ME Drowned River Valleys	3.56	8.23	62.71	30.75	4344
Mid-Atlantic Coastal Lagoon	3.34	7.12	225.6	32.8	39,040
Northeast River Dominated	3.11	5.78	135.5	17.57	40,620
S. New England Coastal Embayment	3.11	6.45	29.69	17.12	3540

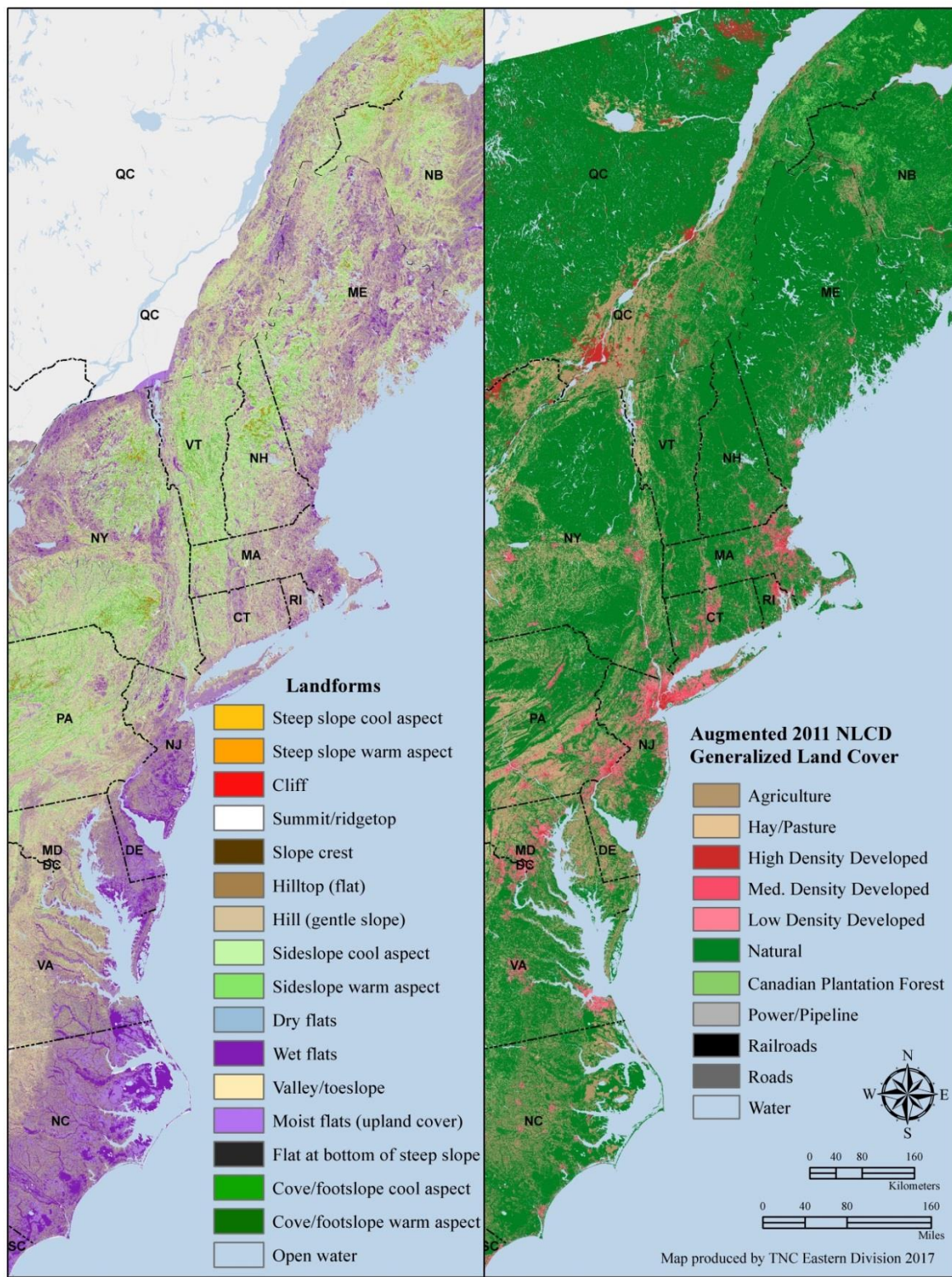
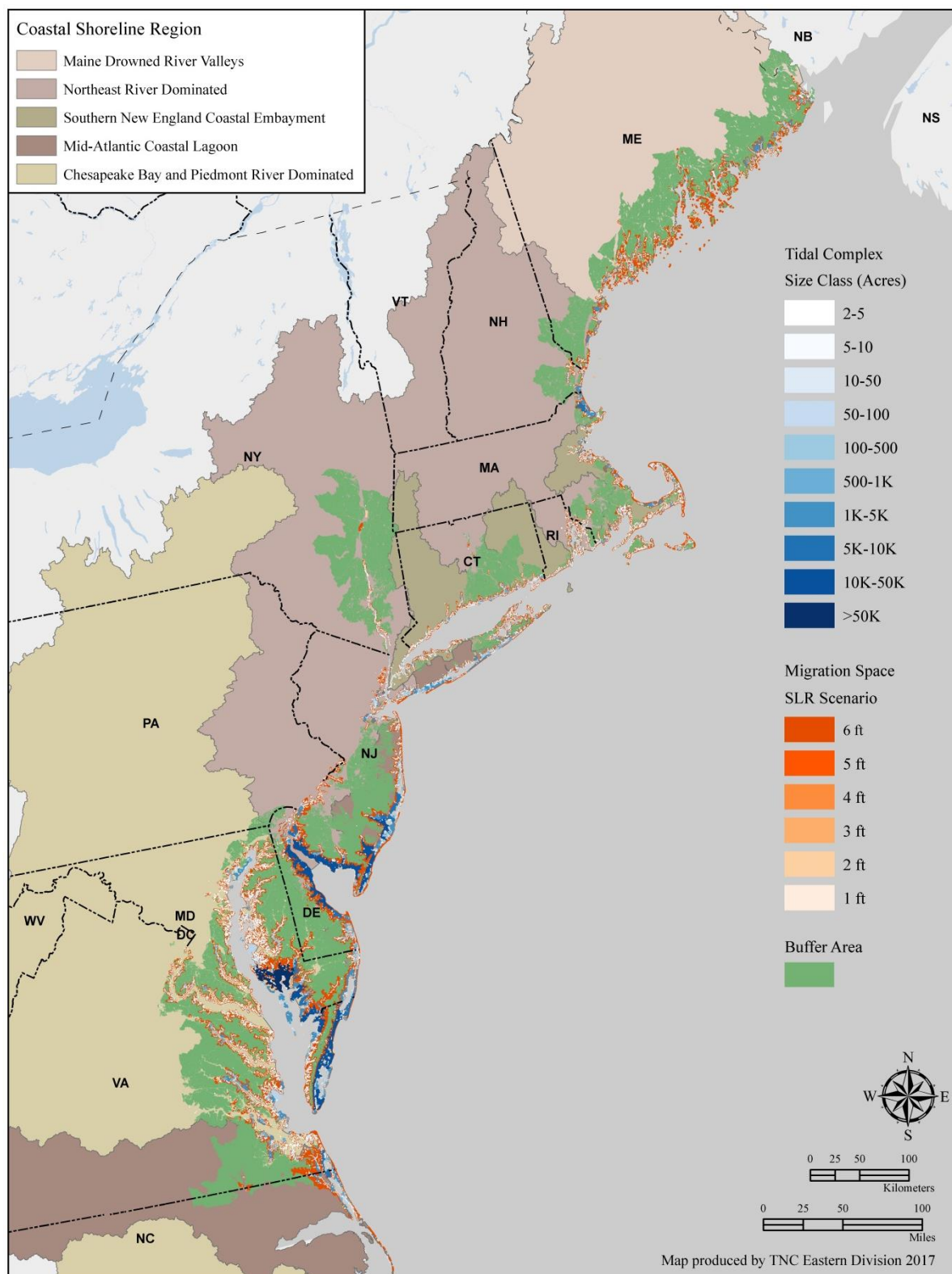
Figure 7.87. Physical settings and land use characteristics of the full region.

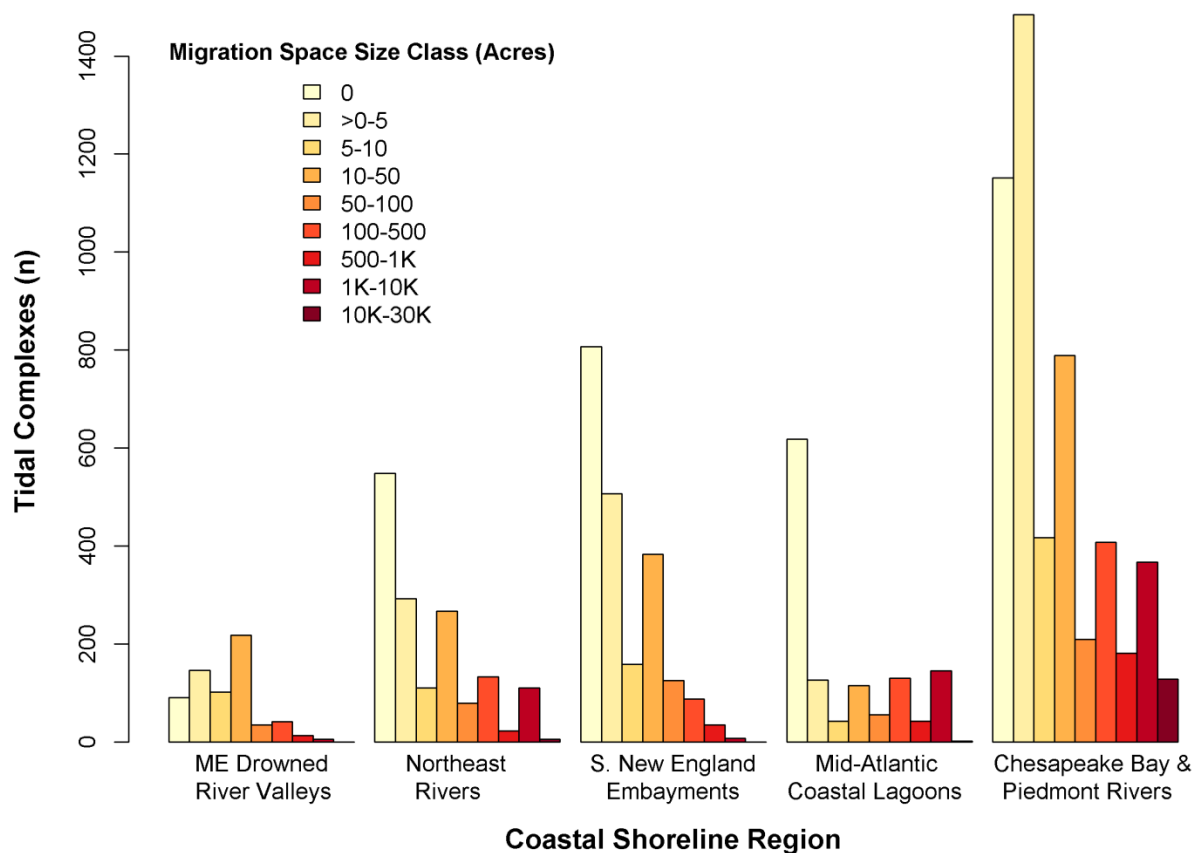
Figure 7.88. Tidal complex, migration space, and buffer area units. The color of the tidal complex units reflects their size class (n=10), while the color of the migration space indicates the SLR scenario (n=6).



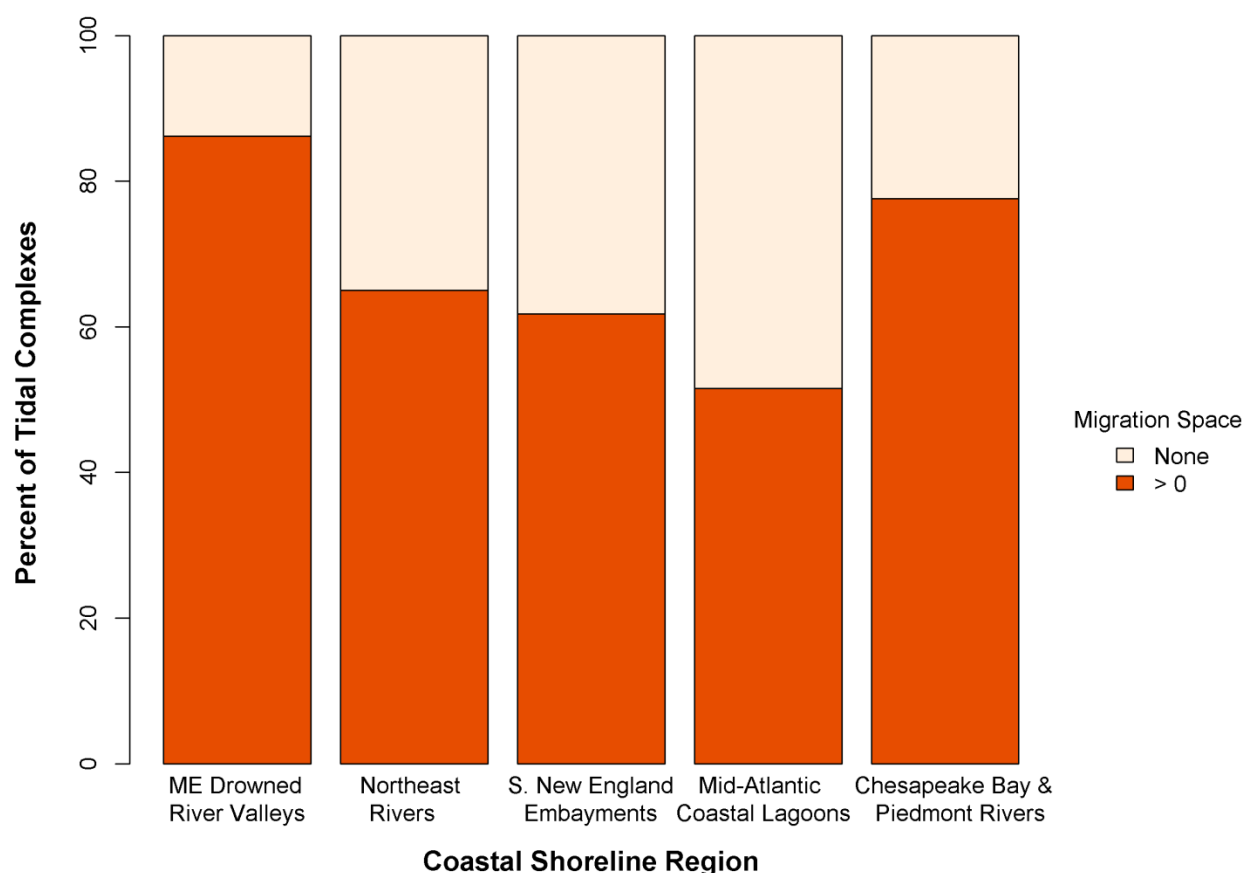
Migration Space Units

Of the 10,736 tidal complexes, 7522 (70%), had migration space at a sea level rise of 6 feet (Figure 7.89). Of the five CSRs, the Chesapeake had the greatest number of large migration space size classes, followed by the Lagoon region and then the Northeast Rivers (Figure 7.89). With the exception of the Chesapeake and Maine regions, tidal complexes with no migration space comprised the most frequent class in the CSRs.

Figure 7.89. Frequency of migration space size class by CSR. Small migration space size classes are shown in light yellow shades that transition to darker oranges as the migration space size class increases.



The percentage of tidal complexes with migration space varied substantially by CSR (Figure 7.90). The Maine Drowned River Valleys had the highest with 86%, followed by the Chesapeake Bay with 78%. In the Mid-Atlantic Lagoons, only 52% of the tidal complexes had migration space at a sea level rise of 6ft, the lowest percentage of the five CSRs.

Figure 7.90. Percent of tidal complex units with migration space by CSR.

The Chesapeake had the largest average migration space size while the Embayment region had the smallest (Table 7.42). As with the tidal complexes, the Chesapeake had the largest migration space at almost 30,000 acres. A Spearman's rank-order correlation showed tidal complex size and migration space size were somewhat positively correlated and this relationship was statistically significant ($r_s = .30$, $p < 2.2e-16$).

Table 7.42. Summary statistics for migration space size by CSR.

Coastal Shoreline Region	Migration Space (Acres)				
	1 st Quartile	Median	Mean	3 rd Quartile	Max
Chesapeake Bay & Piedmont River	0.22	4.45	672.3	51.82	28,260
ME Drowned River Valleys	2.45	9.23	56.62	26.46	2696
Mid-Atlantic Coastal Lagoon	0	0.44	538.8	99.86	18,100
Northeast River Dominated	0	3.11	329	38.97	17,430
S. New England Coastal Embayment	0	1.33	35.49	15.35	1458

Buffer Area Units

Most of the tidal complexes, 9488 (88%), had buffer area at a sea level rise of 6 feet (Figure 7.91). The buffer size pattern was quite variable by CSR. For example, the Maine region had more tidal complexes with the largest buffer area in the region than it had tidal complexes with small buffer areas, while the most frequent size class in the Mid-Atlantic region was tidal complexes with no buffer area. Tidal complexes in the Chesapeake typically had large to very large buffer areas. The Maine region had the largest mean buffer size as well as the largest buffer area for the full region (Table 7.43). There was a very small positive relationship between tidal complex size and buffer area size ($r_s = .073$, $p < 2.171e-14$).

Figure 7.91. Frequency of buffer area size class by CSR.

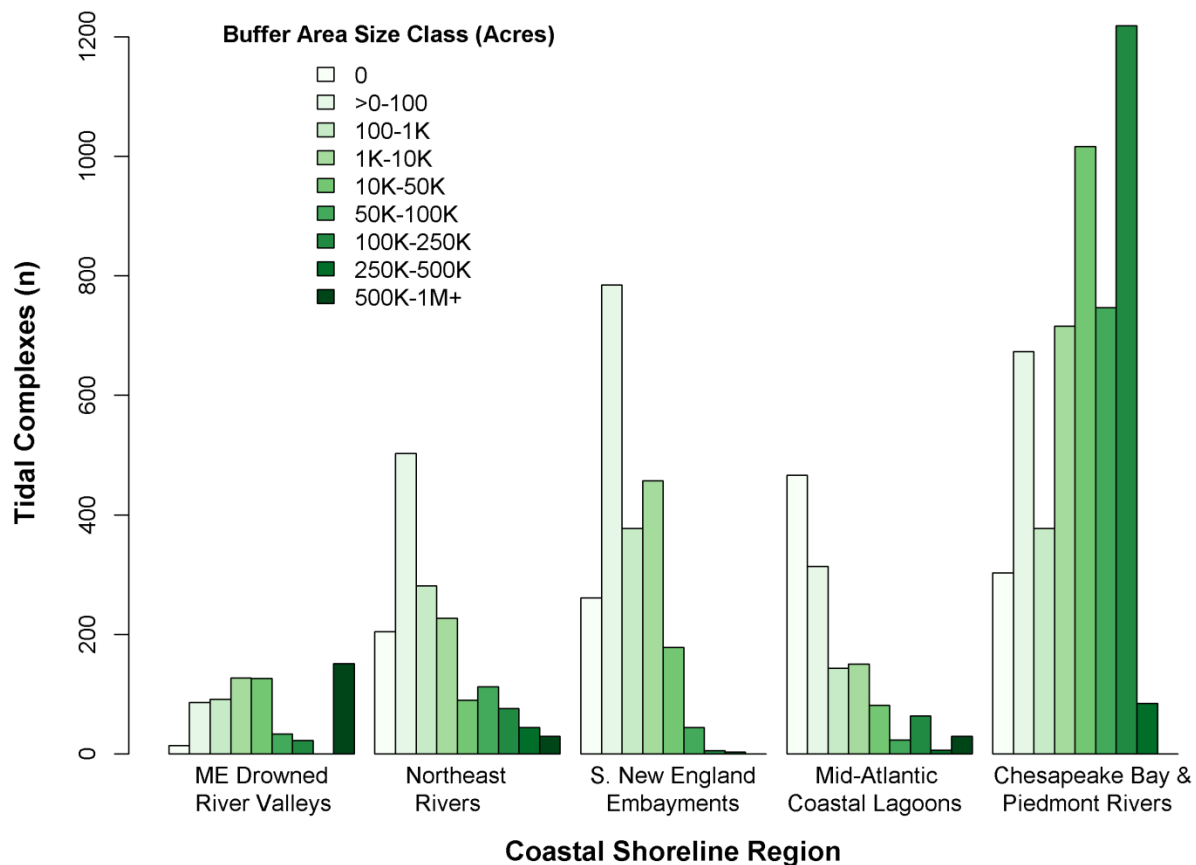


Table 7.43. Summary statistics for buffer area size by CSR.

Coastal Shoreline Region	Buffer Area (Acres)				
	1 st Quartile	Median	Mean	3 rd Quartile	Max
Chesapeake Bay & Piedmont River	644.1	27,110	68K	100K	485,600
ME Drowned River Valleys	568.1	10,130	231K	148K	1M
Mid-Atlantic Coastal Lagoon	0	7.12	26K	1742	656,200
Northeast River Dominated	3.78	161.1	44K	6892	948,000
S. New England Coastal Embayment	3.56	104.2	5262	2256	357,100

Physical and Condition Scores

The estimated resilience score for a tidal complex consists of the condition and physical components, each weighted equally. The final estimated resilience for the 6-ft SLR scenario was stratified by CSR. However, we calculated unstratified physical, condition, and resilience scores to understand the results and regional patterns. Figure 7.92 shows the geographic distribution of the unstratified physical scores and Figure 7.93 shows the top ten highest scoring sites for unstratified physical characteristics. As the regional map in Figure 7.92 shows, there was a cluster of high scoring sites in the Chesapeake Bay and Delaware Bay, reflecting an extensive flat and wet landscape that was expected to provide large areas for migration at a 6-ft SLR. There were other spatial clusters of “far above average” sites evident at the regional scale including southern New Jersey, northern Massachusetts, and northern Maine. The focal site in Figure 7.93 was the Blackwater National Wildlife Refuge (NWR) tidal complex on Maryland’s shore. The tidal complex was very large (65K acres, “far above average”) with a complex shoreline, and a “far above average” migration space size (26K acres). The tidal complex shared approximately 24% of its border with its migration space, which was “slightly above average” for the full region. The site had a moderately large buffer area for the project area, but did score “slightly below average” for soil and landform diversity. Without stratification, the Lagoon and Embayment regions had the greatest proportion of low scoring sites for physical characteristics. The Maine region had the greatest proportion of high scoring tidal complexes, followed by the Northeast and Chesapeake regions. Figure 7.94 shows the estimated physical score, after stratifying by shoreline region. Table 7.44 shows the number of tidal complexes in each stratified physical class. Stratification ensured that all tidal complexes in a shoreline region were only compared to other sites in that same region, allowing the best physical sites in each region to rise to the top. As the stratified results map shows, the sites that scored high for unstratified physical characteristics remained high (green), but new high scoring sites are visible in the Embayment and Lagoon regions.

The unstratified condition scores are shown in Figure 7.95. There are sprinkles of high scoring sites in locations across the full project area, but there was a distinct and large geographic cluster of high scoring sites in Maine, which was expected given the extensive natural land cover and low population density throughout much of this shoreline region. Figure 7.96 shows that the top eleven highest scoring sites for the full region (11 sites are shown as they all had the highest and same score) are distributed across the full geographic extent. The focal site highlighted in Figure 7.92 is a tidal complex on Atkins Bay, near Fort Baldwin, in Maine. The site had no hardened shoreline, the highest possible water quality score, “average” sediment contributions, and a completely natural buffer area. The high scoring physical sites in the Chesapeake region had some condition challenges and none scored “far above average” for unstratified condition. The stratified condition scores are shown in Figure 7.97, with the class breakdown by CSR in Table 7.45. The stratified map shows the best condition sites for all regions, even those that had low scoring sites for condition at the full regional scale.

Figure 7.92. Estimated physical score, not stratified by shoreline region. Tidal complex units in green score “above average” and have physical characteristics hypothesized to increase resilience including a large migration area with a diversity of tidal classes that are evenly distributed, a complex shoreline, and a geophysically diverse buffer area. Tidal complexes in yellow have “average” physical characteristics relative to all the units in the CSU. Tidal complexes in brown are “below average” and are estimated to respond poorly to sea level rise.

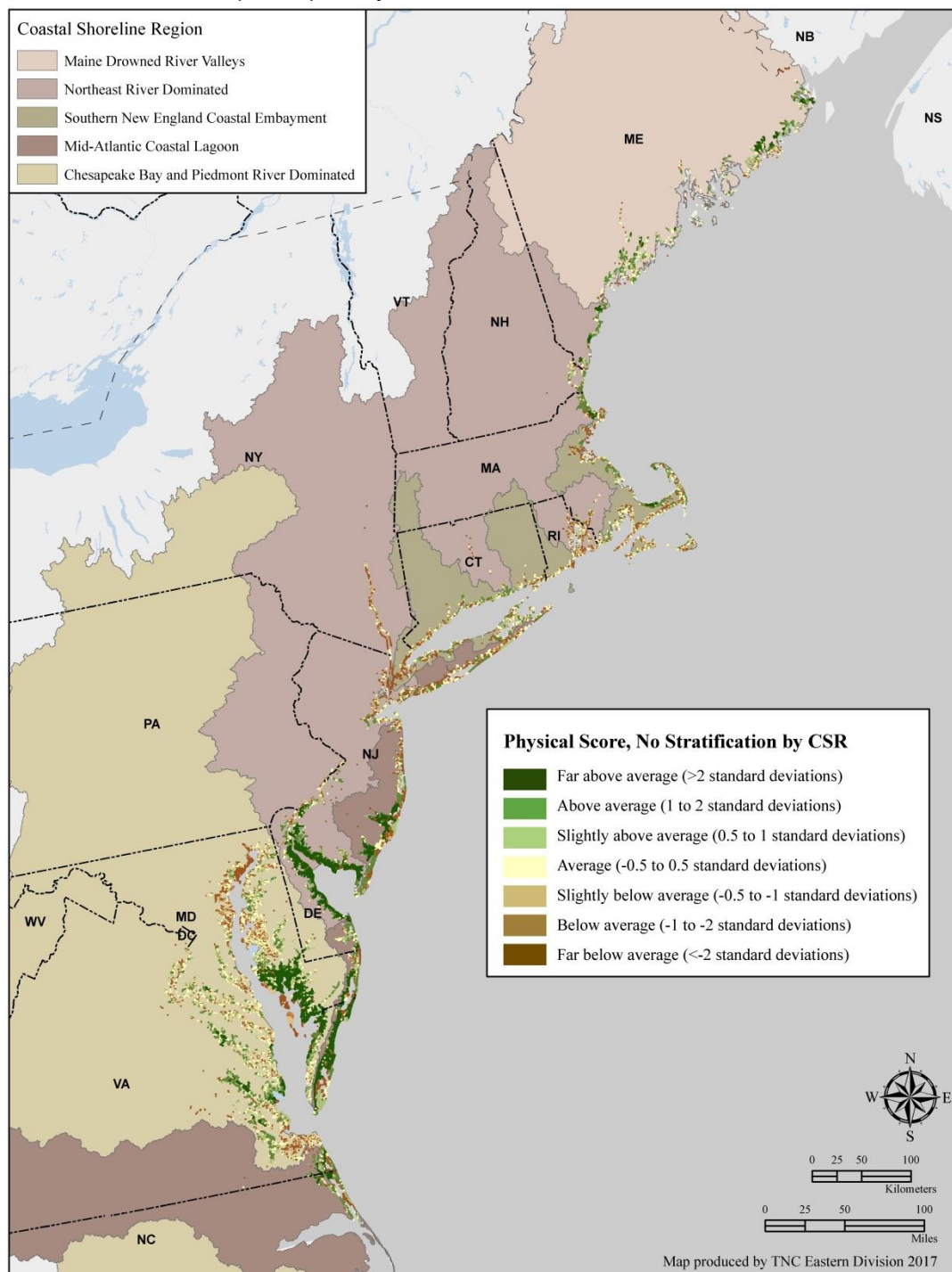


Figure 7.93. Top ten highest scoring sites for physical characteristics, not stratified by shoreline region. The Blackwater NWR tidal complex on Maryland's shore is highlighted in the map. The tidal complex was very large (65K acres) with a complex shoreline, and had a "far above average" migration space size (26K acres).

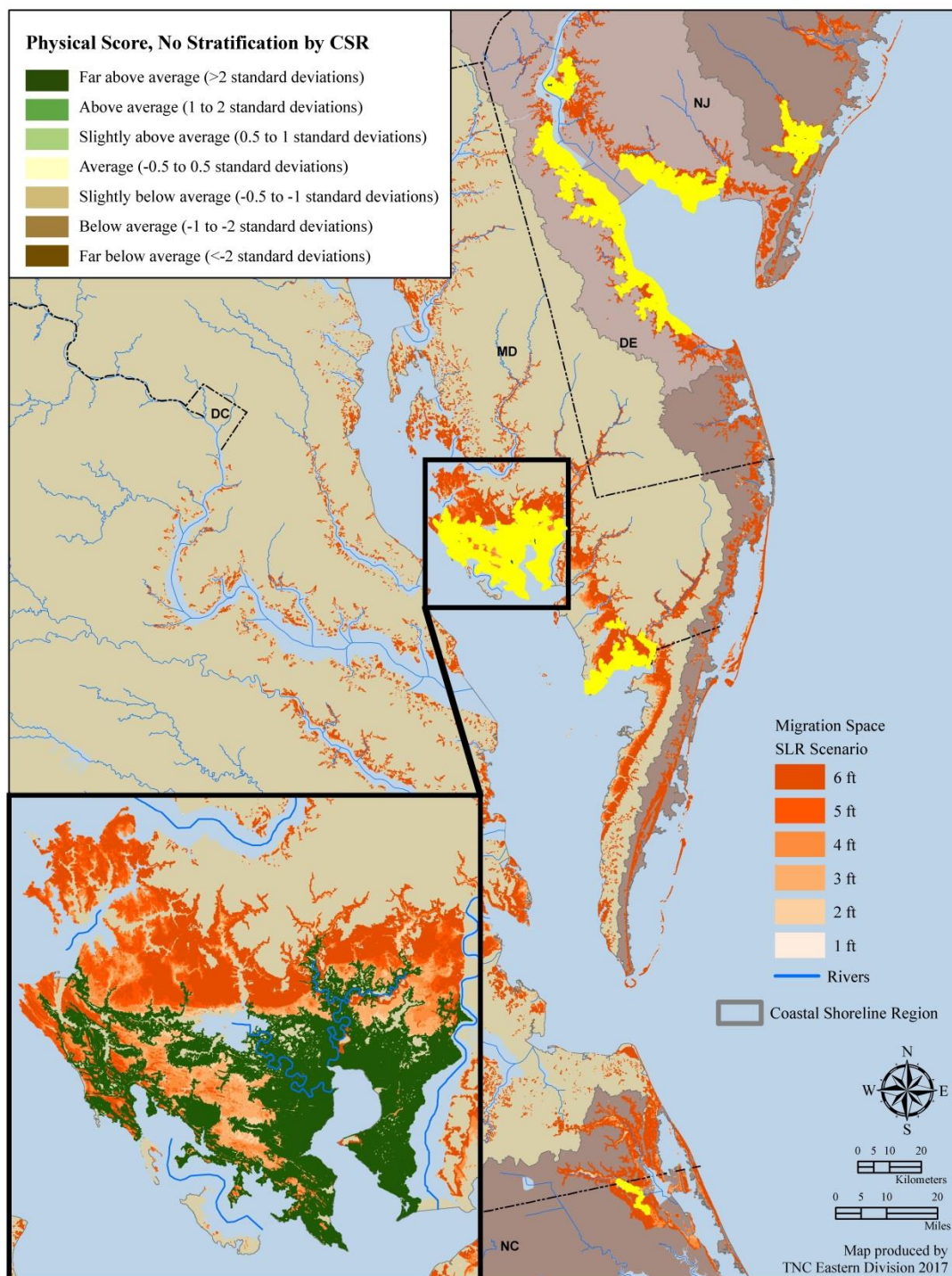


Figure 7.94. Estimated physical score, stratified by shoreline type. Tidal complex units in green score “above average” and have physical characteristics hypothesized to increase resilience including a large migration area with a diversity of tidal classes that are evenly distributed, a complex shoreline, and a geophysically diverse buffer area. Tidal complexes in yellow have average physical characteristics relative to all the units in the CSU. Tidal complexes in brown are “below average” and are estimated to respond poorly to sea level rise.

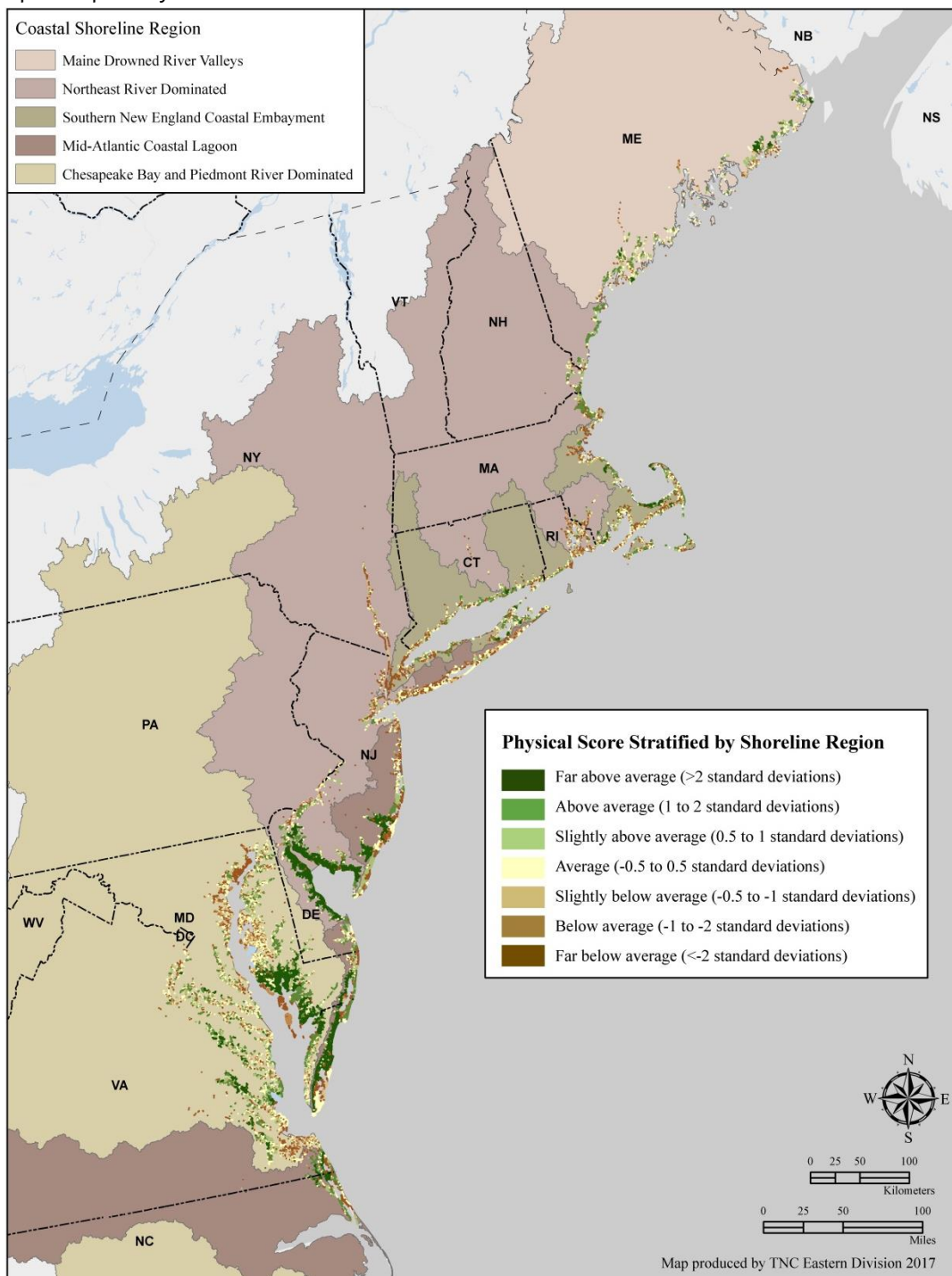


Figure 7.95. Estimated condition score, not stratified by shoreline region. Tidal complex units in green score “above average” and are estimated to be in good condition based on a low percentage of hardened shoreline; good water quality and quantity, high sediment contributions in the migration space; and a natural buffer area with highly connected wetlands. Tidal complexes in yellow are “average.” Tidal complexes in brown are “below average” and are estimated to be in poor condition.

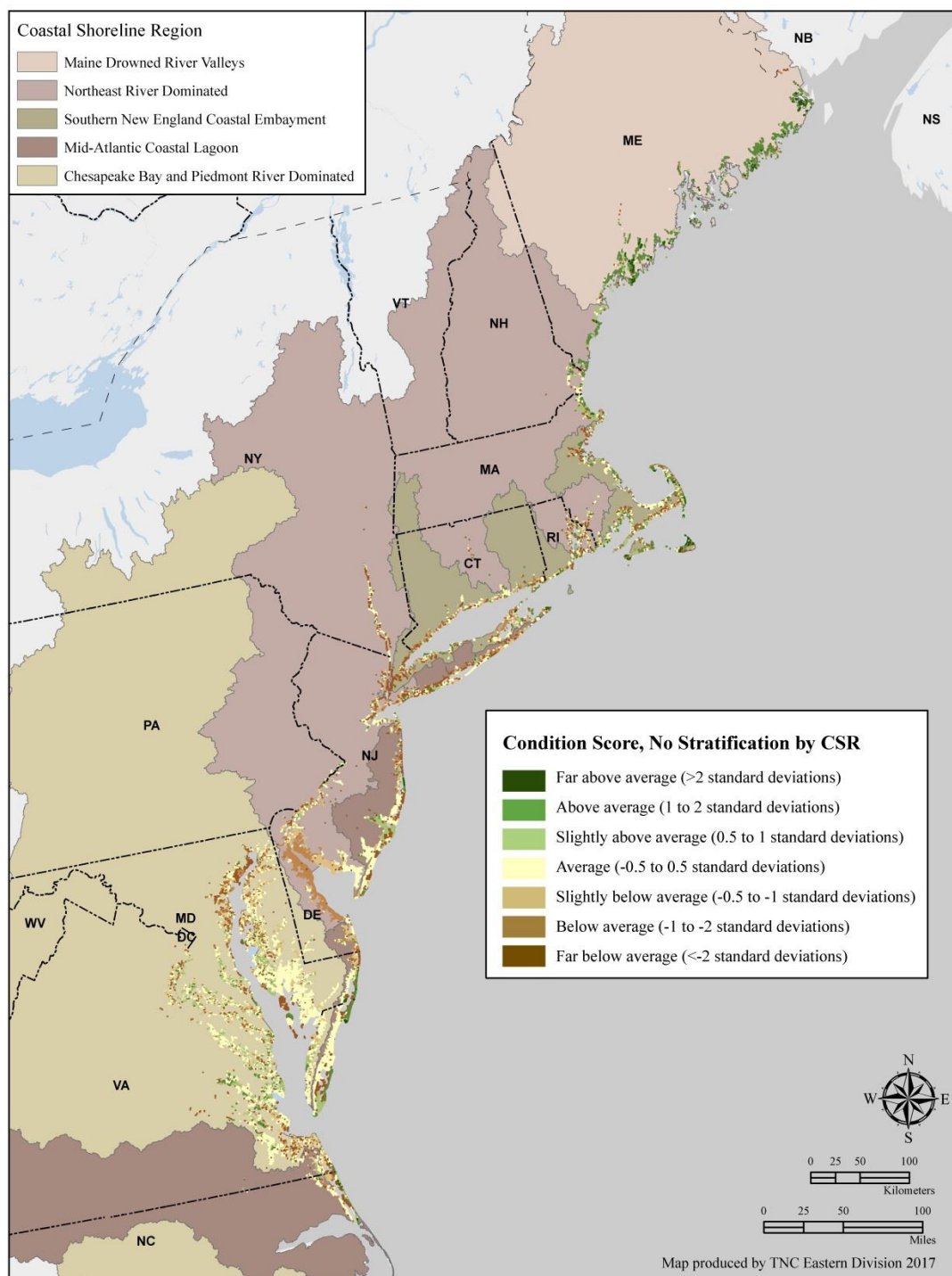


Figure 7.96. Top eleven highest scoring sites for condition characteristics, not stratified by shoreline region. The focal site in the inset is on Atkins Bay, near Fort Baldwin, in Maine. The site had no hardened shoreline, low estimated nitrogen loadings, “average” sediment contributions, and a completely natural and intact buffer area.

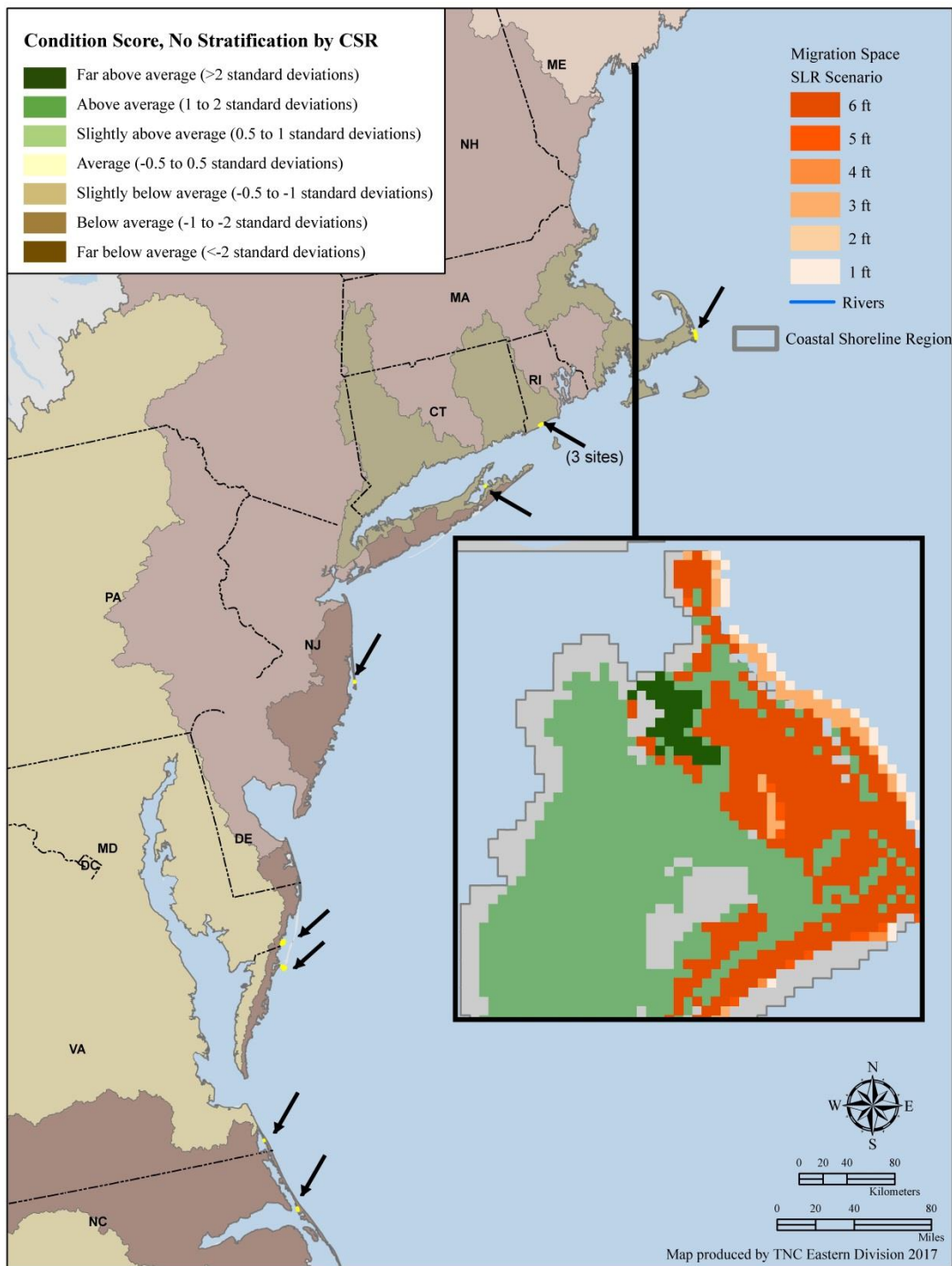


Figure 7.97. Estimated condition score, stratified by shoreline region. Tidal complex units in green score “above average” and are estimated to be in good condition based on a low percentage of hardened shoreline; good water quality and quantity, and high sediment contributions in the migration space; and a natural buffer area with highly connected wetlands. Tidal complexes in yellow are “average.” Tidal complexes in brown are “below average” and are estimated to be in poor condition.

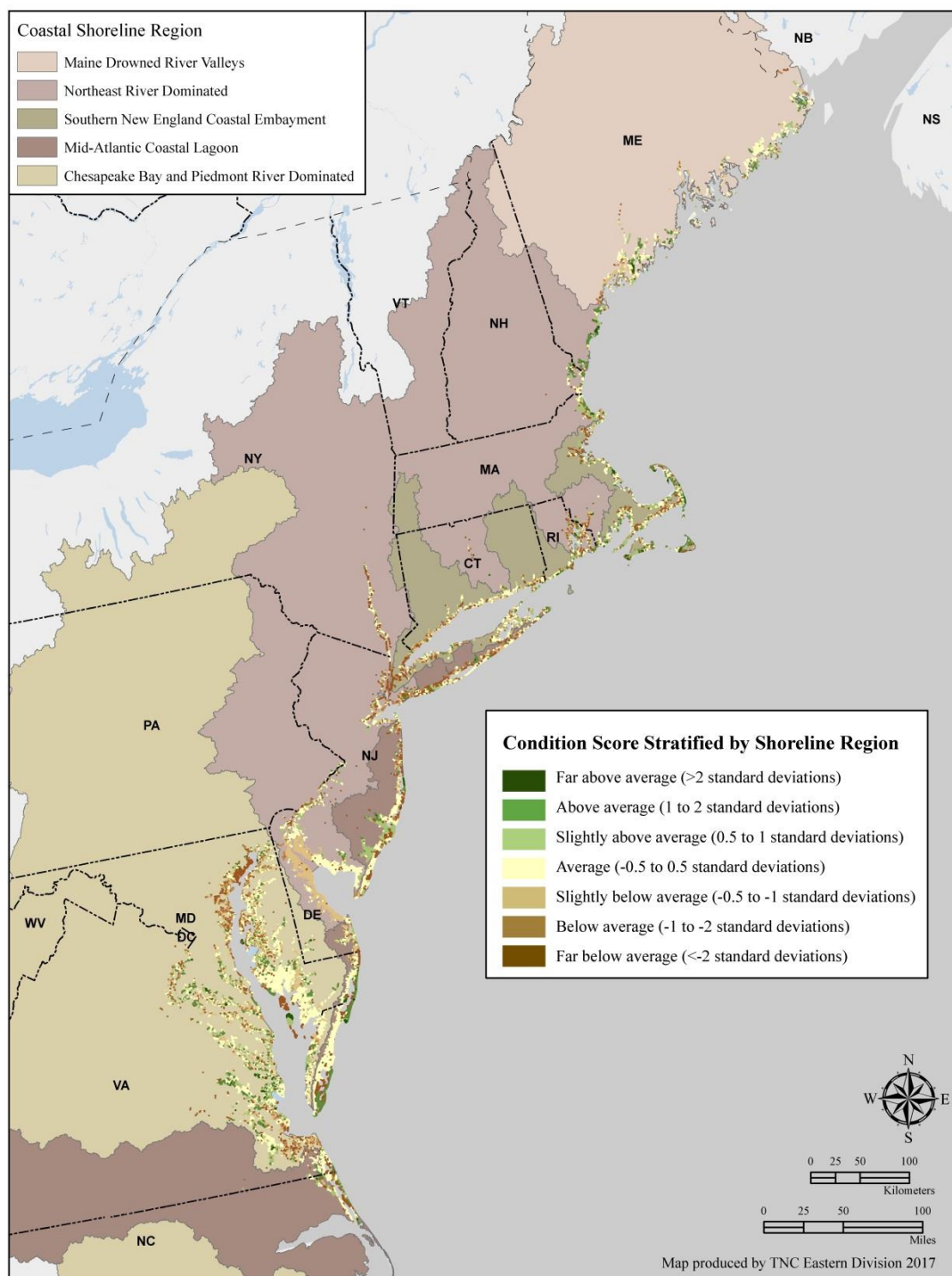


Table 7.44. Frequency of stratified physical scores for the 6-foot sea level rise scenario.

Physical Score	ME Drowned River Valleys	Northeast River Dominated	S. New England Coastal Embayment	Mid-Atlantic Coastal Lagoon	Chesapeake Bay & Piedmont River
Far Below Average	106 (16%)	571 (36%)	839 (40%)	639 (50%)	1217 (24%)
Below Average	75 (12%)	139 (9%)	176 (8%)	88 (7%)	545 (11%)
Slightly Below Average	84 (13%)	152 (10%)	195 (9%)	98 (8%)	601 (12%)
Average	213 (33%)	390 (25%)	499 (24%)	249 (20%)	1535 (30%)
Slightly Above Average	84 (13%)	152 (10%)	195 (9%)	98 (8%)	601 (12%)
Above Average	75 (12%)	139 (9%)	176 (8%)	88 (7%)	545 (11%)
Far Above Average	13 (2%)	23 (1%)	30 (1%)	15 (1%)	91 (2%)

Table 7.45. Frequency of stratified condition scores for the 6-foot sea level rise scenario. The percentage of sites in each score class by CSR is shown in parentheses.

Condition Score	ME Drowned River Valleys	Northeast River Dominated	S. New England Coastal Embayment	Mid-Atlantic Coastal Lagoon	Chesapeake Bay & Piedmont River
Far Below Average	38 (6%)	519 (33%)	646 (31%)	598 (47%)	1159 (23%)
Below Average	85 (13%)	151 (10%)	204 (10%)	94 (7%)	553 (11%)
Slightly Below Average	94 (14%)	160 (10%)	224 (11%)	104 (8%)	609 (12%)
Average	240 (37%)	407 (26%)	574 (27%)	265 (21%)	1558 (30%)
Slightly Above Average	94 (14%)	160 (10%)	224 (11%)	104 (8%)	610 (12%)
Above Average	84 (13%)	145 (9%)	203 (10%)	94 (7%)	552 (11%)
Far Above Average	15 (2%)	24 (2%)	35 (2%)	16 (1%)	94 (2%)

Table 7.45 shows that sites in the Maine region scored better for condition than sites in any other CSR as they had the smallest proportion of sites in the “far below average” category. Sites in the Lagoon region fared the worst for condition and physical attributes. Table 7.46 shows it was difficult to score “far above average” for both physical and condition sites as only six sites achieved this distinction. This association was true for the unstratified results where only nine sites scored “far above average” for both physical and condition characteristics. The relationship between the condition and physical scores was variable and only somewhat positively correlated ($r = .23$, $p < 2.210e-16$).

Table 7.46. The number of tidal complex units in each physical and condition score category, stratified. A two-by-two frequency table shows the count of tidal complexes occurring in each physical and condition class combination. Physical classes are by row and condition classes are by column. Boxes shaded in gray indicate tidal complexes with the same physical and condition score class. For example, only one tidal complex scored “far above average” for both physical and condition characteristics.

Physical Class	Condition Class						
	Far Below Average	Below Average	Slightly Below Average	Average	Slightly Above Average	Above Average	Far Above Average
Far Below Average	2942	320	46	45	13	6	0
Below Average	13	228	177	360	131	100	14
Slightly Below Average	4	178	184	452	150	136	26
Average	1	287	492	1143	477	412	74
Slightly Above Average	0	45	145	494	220	196	30
Above Average	0	28	130	465	166	200	34
Far Above Average	0	1	17	85	35	28	6

Estimated Resilience Score

The physical and condition scores were equally weighted and combined to calculate an estimated resilience score for each tidal complex. The unstratified scores for the 6-foot SLR scenario are mapped in Figure 7.98 and show that the large complexes with ample migration space in the southern portion of the project area were penalized for poor to average conditions and received above average and “slightly above average” resilience scores. The “far above average” sites were largely clustered in Maine, particularly northern Maine, where sites had “far above average” physical and condition scores. As noted in the previous section, regardless of stratification, few sites scored “far above average” for both physical and condition characteristics, with most “far above average” physical sites having “average” condition characteristics.

The ten tidal complexes with the highest unstratified resilience score are shown in Figure 7.99. The site highlighted in Figure 7.99 is Long Point along the Cape Cod National Seashore. This site featured a large tidal complex (47 acres, “above average” for the full region) with a large migration space at the 6-foot SLR (391 acres, “above average”). More than half of the tidal complex perimeter was shared with migration space. The buffer area was “average” in size (7000 acres) with “average” soil and landform variety, but was completely in natural cover (“far above average”). The average tidal complex size of the top ten highest scoring sites for unstratified resilience was 175 acres, and the complexes shared an average of 34% of their edge with migration space. Under the 6-foot sea level rise scenario, these sites had an average migration space size of 235 acres (min = 28, max = 491, SD = 189 acres), and a very

large average buffer area (825K acres). Average condition characteristics included no hardened shoreline, the best water quality class (1), “average” sediment contributions, and buffer areas mostly in natural cover (97%) with moderate local connectedness of wetlands.

The estimated resilience scores stratified by coastal shoreline region are mapped in Figure 7.100, with the distribution of resilience classes by CSR shown in Table 7.47. Comparing Figures 7.99 and 7.100, one can see how stratification forced sites to be in one of seven resilience classes in each CSR to highlight those sites likely to be the most resilient in their respective region while also identifying those likely to be the most vulnerable.

The results of a Pearson correlation analysis show the role of tidal complex size, migration space size, and buffer area size in the stratified physical, condition, and resilience scores (Table 7.48). Given the weight of the size attributes in the physical component score, it was not surprising that size was significantly and positively correlated with the physical score, particularly for the migration space size. The condition score was also significantly and mildly positively correlated with the migration space size, and moderately positively correlated with the buffer area size.

Figure 7.98. Estimated resilience score, not stratified by shoreline region. This map shows the estimated resilience score for the 6-foot sea level rise scenario. The map shows areas that are above (green) or below (brown) the mean for the project area. Areas in green score “above average” and are estimated to be more resilient based on their physical and condition characteristics. Areas in yellow are “average.” Areas in brown are “below average” and are estimated to be vulnerable to sea level rise and climate change.

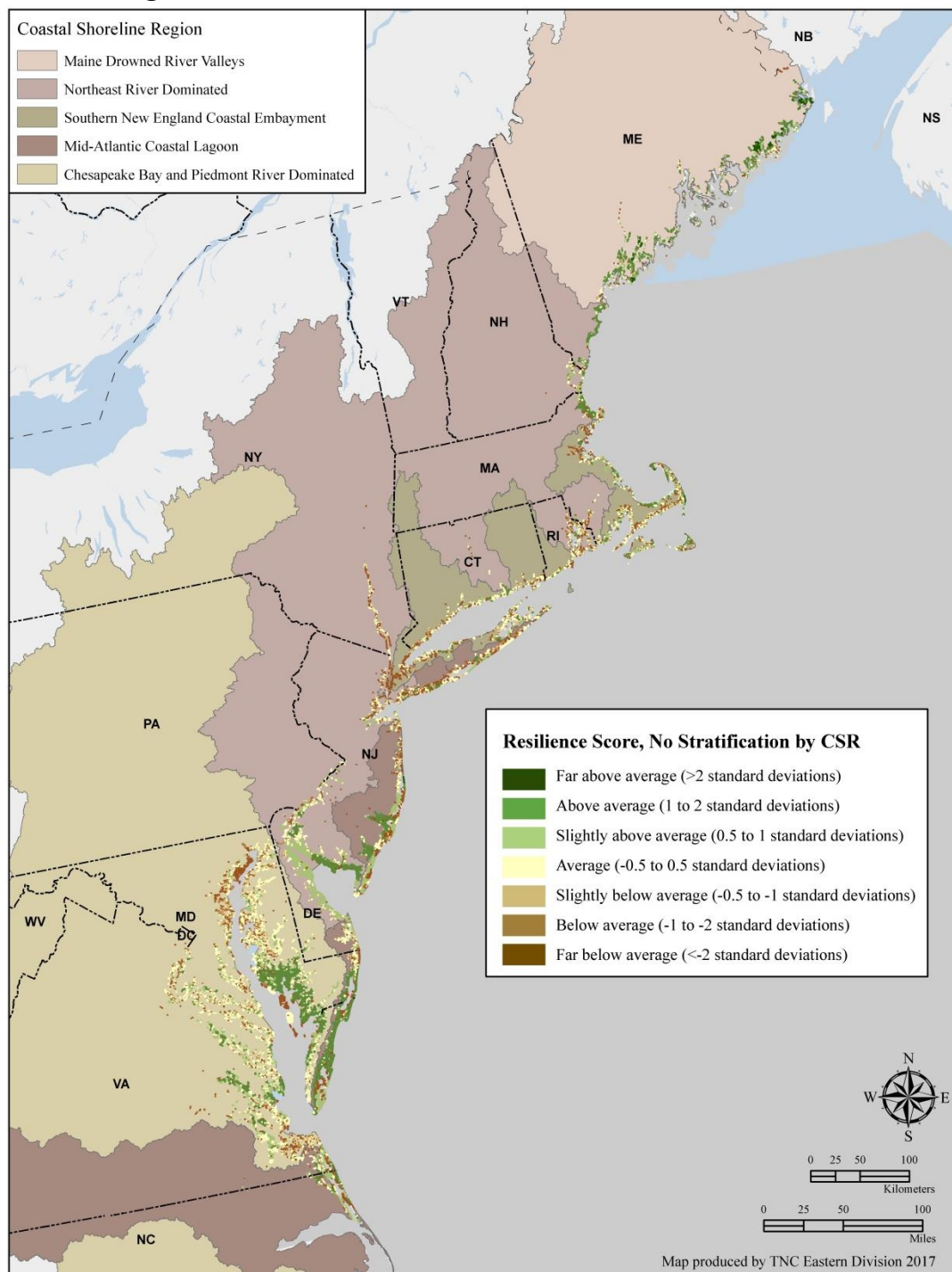


Figure 7.99. The top ten highest scoring tidal complexes in the full region, not stratified by shoreline region. The ten tidal complexes with the highest unstratified estimated resilience score in the project area are highlighted in yellow and denoted with black arrows. The Long Point site on the Cape Cod National Seashore is highlighted in the map. The tidal complex was “above average” in size at 47 acres and had more than 50% of its perimeter immediately adjacent to migration space. The migration space was also “above average” in size at 391 acres. The site had low estimated nitrogen loadings, “average” sediment contributions and no hardened shoreline. The buffer area was “average” in size but was completely natural with “average” landform and soil variety.

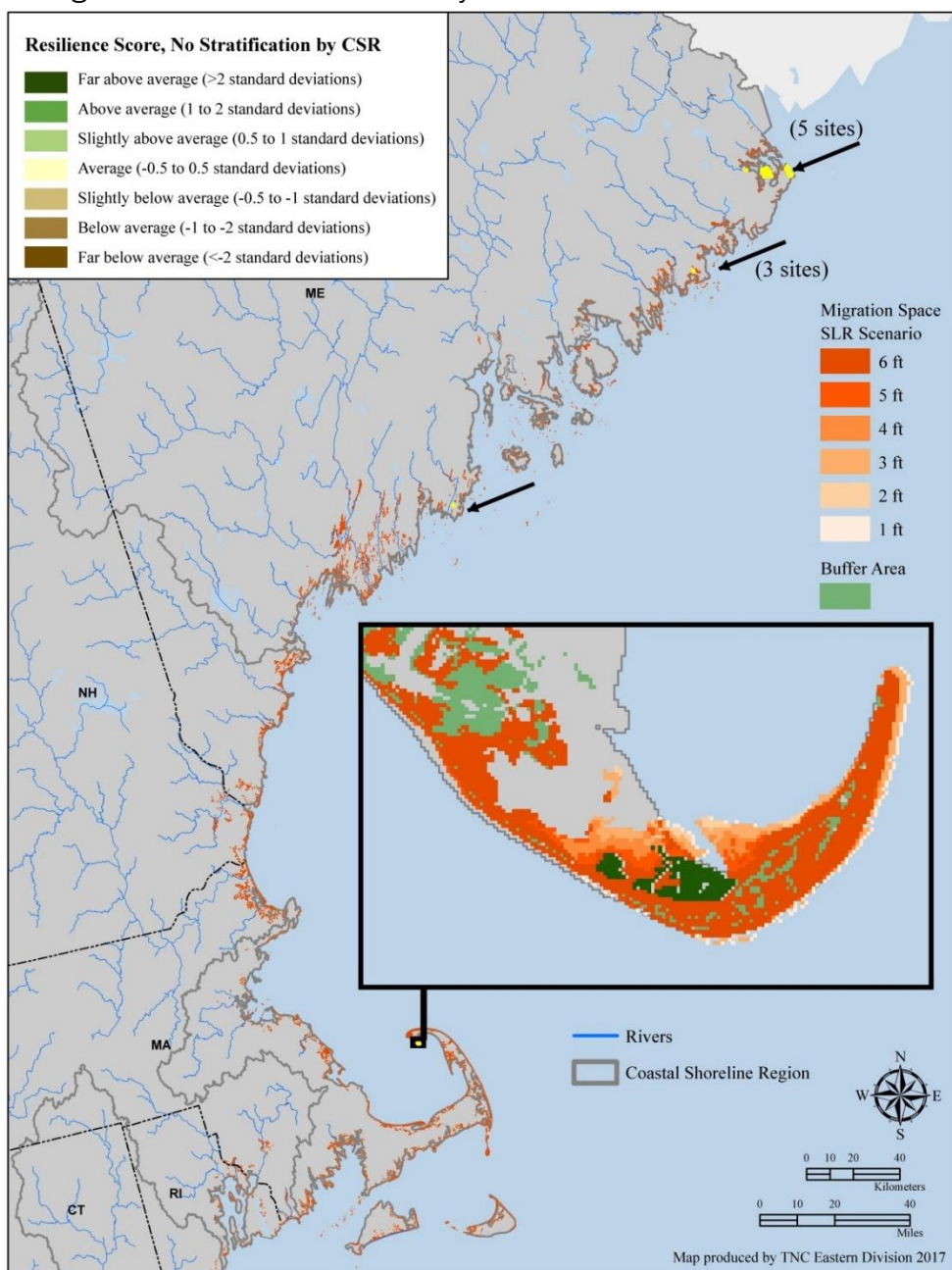


Table 7.47. Frequency of stratified resilience scores for the 6-foot sea level rise scenario.

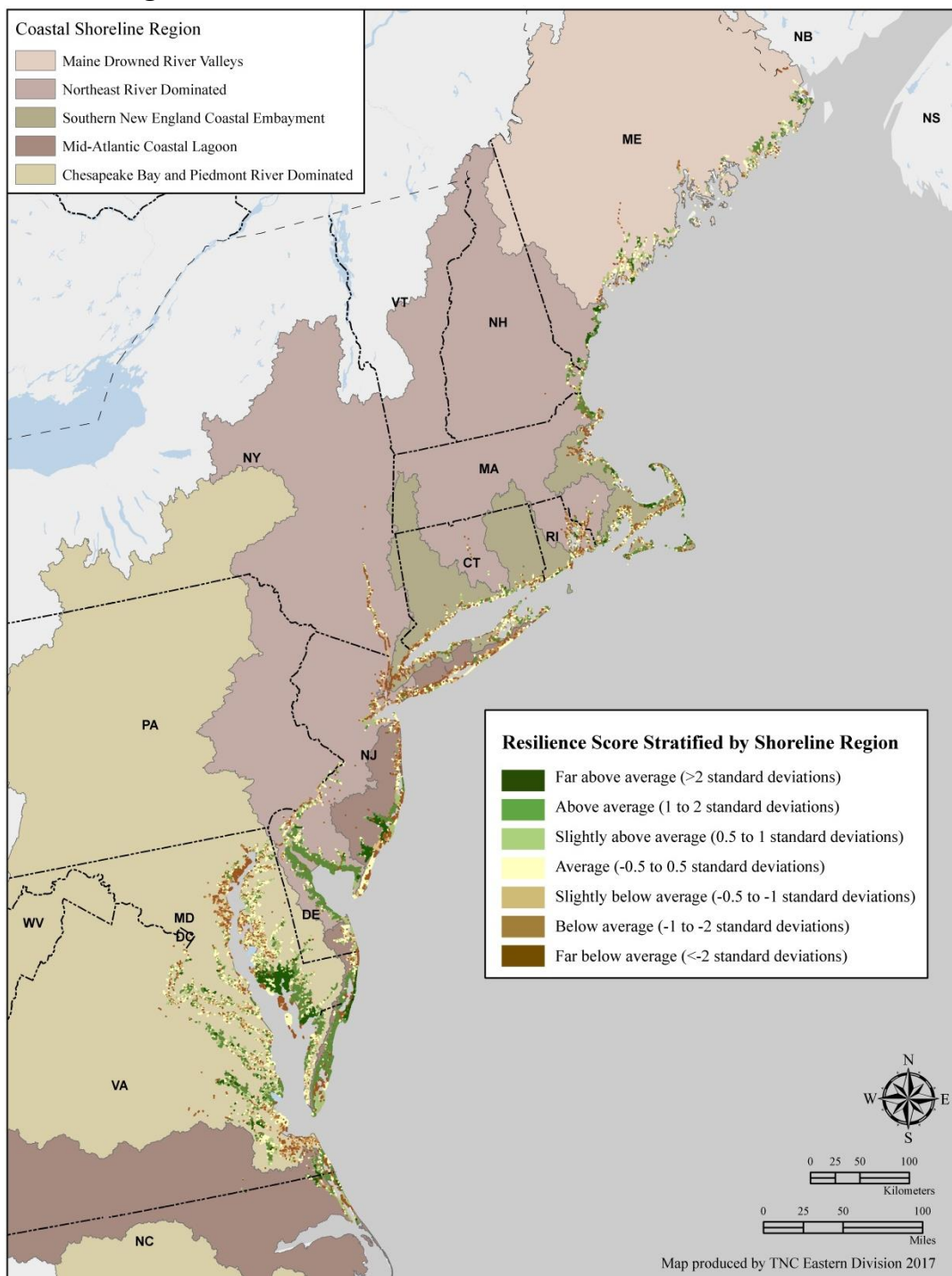
Z-Score Class	ME Drowned River Valleys	Northeast River Dominated	S. New England Coastal Embayment	Mid-Atlantic Coastal Lagoon	Chesapeake Bay & Piedmont River
Far Below Average	104	573	848	647	1245
Below Average	76	138	176	87	541
Slightly Below Average	83	152	193	96	596
Average	215	390	495	247	1525
Slightly Above Average	83	152	193	96	596
Above Average	76	138	176	87	541
Far Above Average	13	23	29	15	91

Table 7.48. Relationship between resilience components and analysis unit size.

Pearson correlation coefficients between the stratified condition, physical, and estimated resilience scores and the size (acres) of the tidal complex, migration space, and buffer area, after removing complexes with no migration space. A star indicates a significant ($p \leq .05$) relationship.

	Tidal Complex Size	Migration Space Size	Buffer Area Size
Physical Z-score	0.411*	0.677*	0.524*
Condition Z-score	0.025*	0.147*	0.268*
Resilience Z-score	0.289*	0.540*	0.512

Figure 7.100. Estimated resilience score, stratified by shoreline region. This map shows the estimated resilience score for the 6-foot sea level rise scenario. The map shows areas that are above (green) or below (brown) the mean relative to each CSR. Areas in green score “above average” and are estimated to be more resilient based on their physical and condition characteristics. Areas in yellow are “average.” Areas in brown are “below average” and are estimated to be vulnerable to sea level rise and climate change.



Trends in Migration Space Size

All of the shoreline regions experienced a decline in average migration space at a SLR of 3 feet, except for the Northeast River region, which begins to decline at the 6-foot scenario (Figure 7.101). The Maine region was the only CSR whose mean migration space increases at the 6-foot SLR, perhaps reflecting greater inundation of the more rugged and higher elevation coastline that characterizes this region. Linear regressions identified 6959 tidal complex units with a statistically significant ($p \leq .05$) relationship between the latter three sea level rise scenarios (3 – 6 feet) and migration space size. Of those tidal complex units with a significant relationship, some had decreasing migration space but the majority experienced an increase in migration space (Figure 7.102). The Chesapeake Bay had the greatest mean increase and decrease in size (-255, +109 acres, Table 7.49). Maine had the smallest mean decline in migration space size (-3 acres) while the Embayment region had the smallest mean increase (+6 acres). The magnitude of change in migration space size reflects the patterns highlighted earlier in this section (i.e., tidal complexes in the Embayment region have the smallest average migration space size so their increase or decrease was small relative to the other CSRs).

Tidal complexes with a significant migration space trend were assigned to one of three trend categories: increase, decrease, no change, and we adjusted their score to reflect the trend. The 2760 tidal complexes whose migration space showed an increasing trend were awarded an additional 0.50 SD points to their estimated resilience score. The 956 tidal complexes that experienced a decline in migration space size from the 3 to the 6-foot SLR scenario had their estimated resilience scores reduced by 0.50 SD. The resilience score of the remaining tidal complexes with no significant change in migration space size was not impacted by the trend analysis. The map in Figure 7.103 shows the spatial distribution of the stratified resilience scores with the trend analysis incorporated. The use of 0.50 SD to adjust the resilience score meant that no tidal complex's score could change by more than one resilience class (Table 7.50). After incorporating migration space trend, only 587 (5%) of sites went to the next lower class and 1763 (16%) complexes moved up a class (Figure 7.104, Table 7.50).

Figure 7.101. Mean migration space size by sea level rise scenario for each shoreline region.

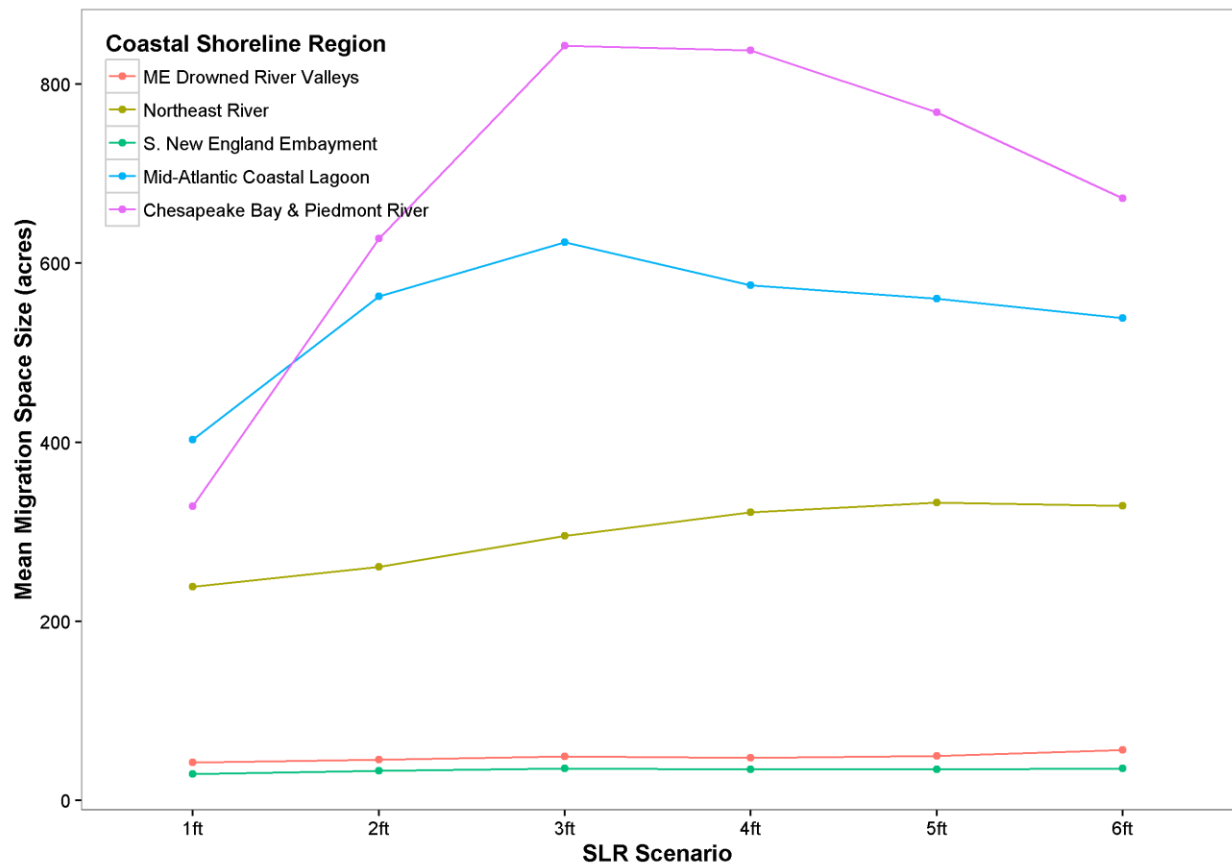


Table 7.49. Significant migration space trend by CSR. The number of tidal complexes with a significant ($p \leq .05$) relationship between sea level rise scenario (≥ 3 feet) and migration space size. The mean change in migration space size (acres) for each CSR is shown in parentheses next to the count of tidal complexes in each category.

Trend direction	ME Drowned River Valleys	Northeast River Dominated	S. New England Coastal Embayment	Mid-Atlantic Coastal Lagoon	Chesapeake Bay & Piedmont River
Decrease	34 (-3)	150 (-63)	178 (-9)	98 (-110)	496 (-255)
Increase	180 (7)	472 (68)	466 (6)	191 (78)	1451 (109)

Figure 7.102. Migration space size trend by shoreline region. The percent of tidal complexes in each CSR with an increasing or decreasing migration space trend is shown in the stacked bar plot.

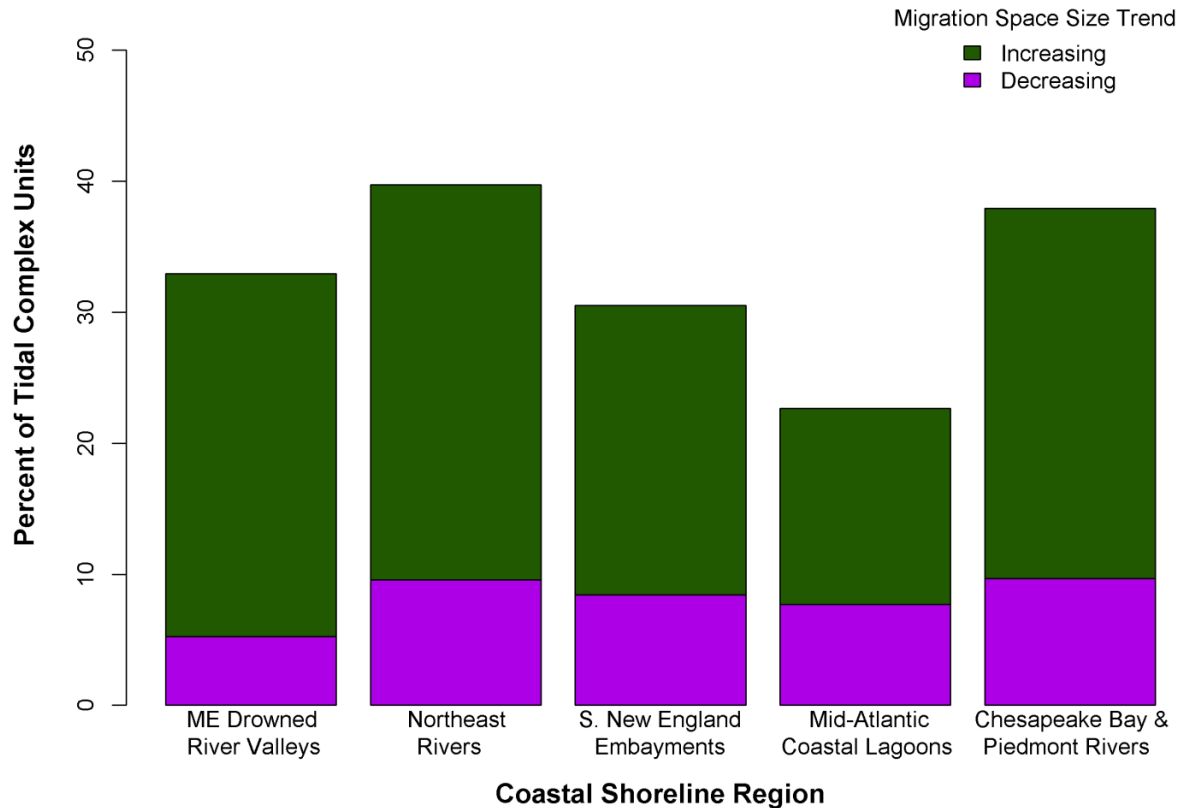


Table 7.50. The change in resilience class after incorporating the trend in migration space size. Tidal complex units whose migration space showed a significant increase ($p \leq .05$) from the three to 6-foot sea level rise received an additional 0.50 standard deviation units to their score, while the score of units with a significant decrease in migration space size was reduced by 0.50 SD units. The purple boxes indicate the number of tidal complex units that moved to the next lower resilience class, and the green boxes highlight the number of units whose class improved when the migration space trend was considered.

Resilience Class	Resilience class with Trend						
	Far Below Average	Below Average	Slightly Below Average	Average	Slightly Above Average	Above Average	Far Above Average
Far Below Average	3395	22	0	0	0	0	0
Below Average	27	791	200	0	0	0	0
Slightly Below Average	0	124	630	366	0	0	0
Average	0	0	189	2117	566	0	0
Slightly Above Average	0	0	0	138	511	471	0
Above Average	0	0	0	0	83	797	138
Far Above Average	0	0	0	0	0	26	145

Table 7.51. Frequency of stratified resilience scores with migration trend for the six-foot sea level rise scenario.

Z-Score Class	ME Drowned River Valleys	Northeast River Dominated	S. New England Coastal Embayment	Mid- Atlantic Coastal Lagoon	Chesapeake Bay & Piedmont River
Far Below Average	105	574	852	648	1243
Below Average	68	132	170	82	485
Slightly Below Average	81	135	176	84	543
Average	192	329	441	240	1419
Slightly Above Average	80	171	187	100	622
Above Average	101	174	233	102	684
Far Above Average	23	51	51	19	139

Figure 7.103. Estimated resilience score with migration space trend. This map shows the estimated resilience score after incorporating the trend in migration space size for the 6-foot sea level rise scenario. Tidal complex units whose migration space showed a significant increase ($p \leq .05$) from the three to 6-foot SLR received an additional 0.50 standard deviation units to their score, while the score of units with a significant decrease in migration space was reduced by 0.50 SD units.

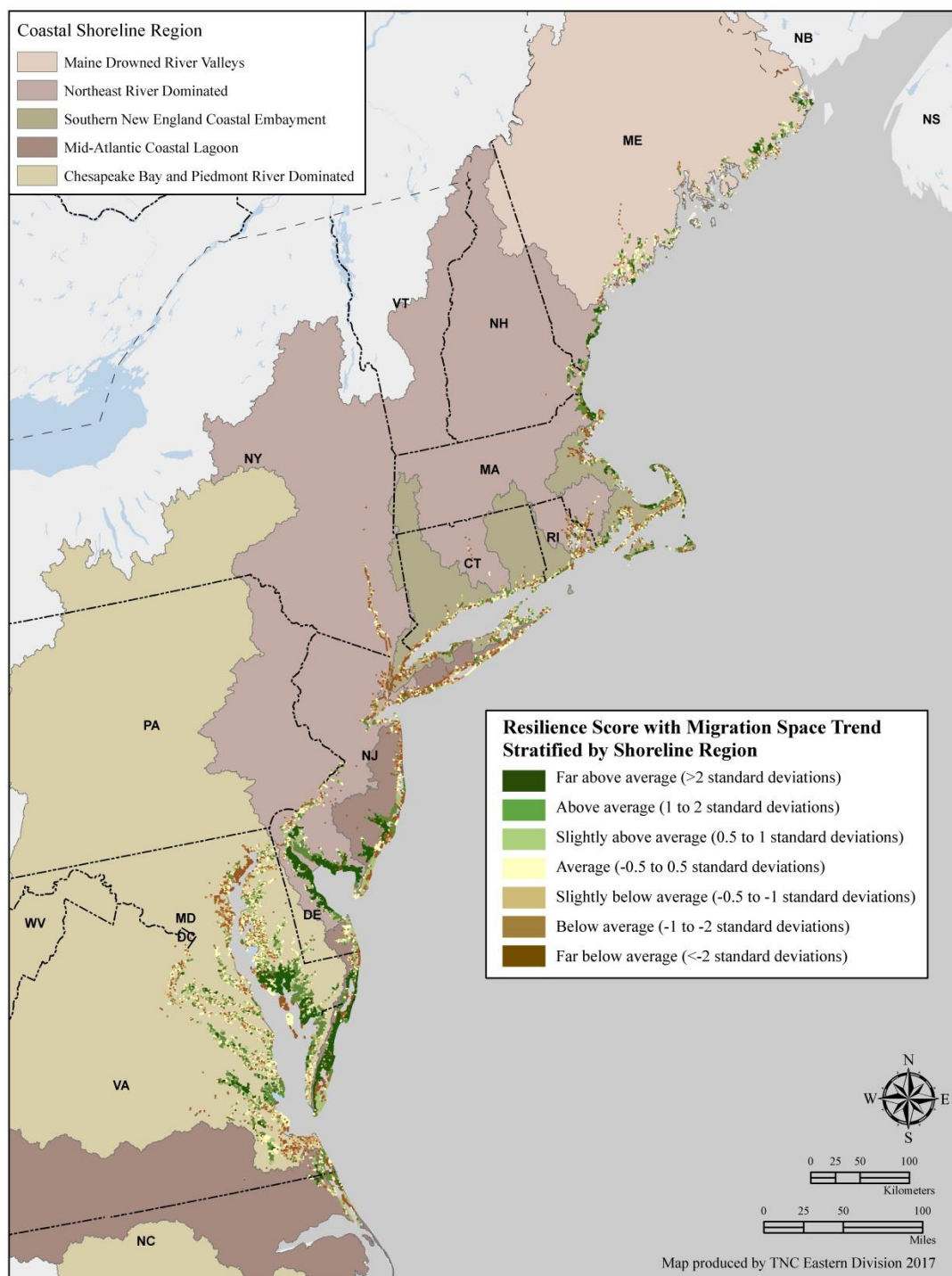
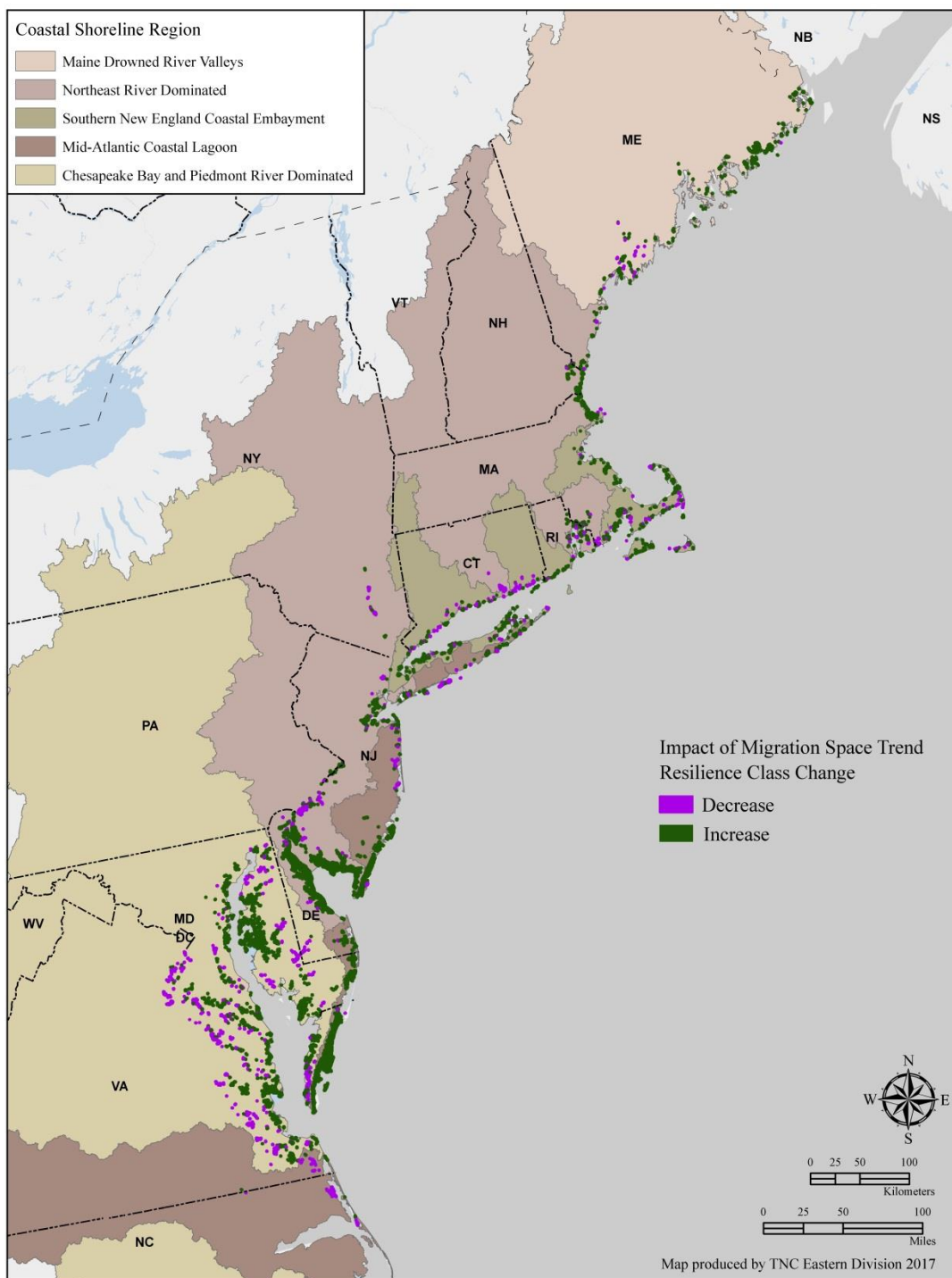


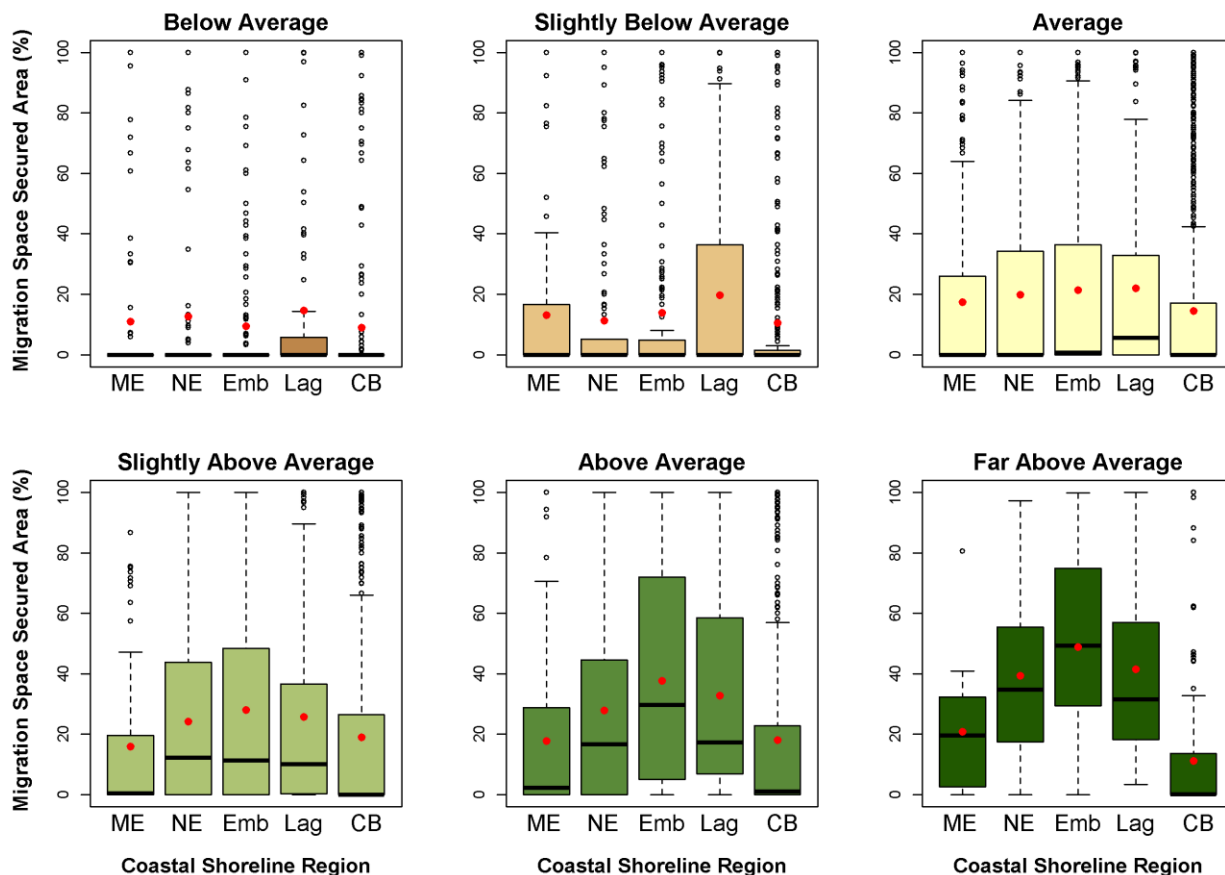
Figure 7.104. Estimated resilience class changes after incorporating migration space trend. This map shows the tidal complexes whose estimated resilience class either increased (n=1763) or decreased (n=587) after incorporating the trend in migration space size at the 6-foot sea level rise scenario.



Migration Space Securement

The amount of a tidal complex's total migration space that was already protected (GAP status 1-3) varied by CSR and resilience z-score category (Figure 7.105). Sites estimated to be highly resilient had the highest rate of securement, with the Embayment region having the highest percentage of the five coastal regions. In the Embayment region, tidal complex units with "far above average" scores had, on average, 49% of their migration space permanently protected, followed by the "above average" category with 38% secured. The worst scoring tidal complex units, "far below average," are not shown in Figure 7.105 as these sites have very little, if any, migration space so this category always had the lowest average percent protected.

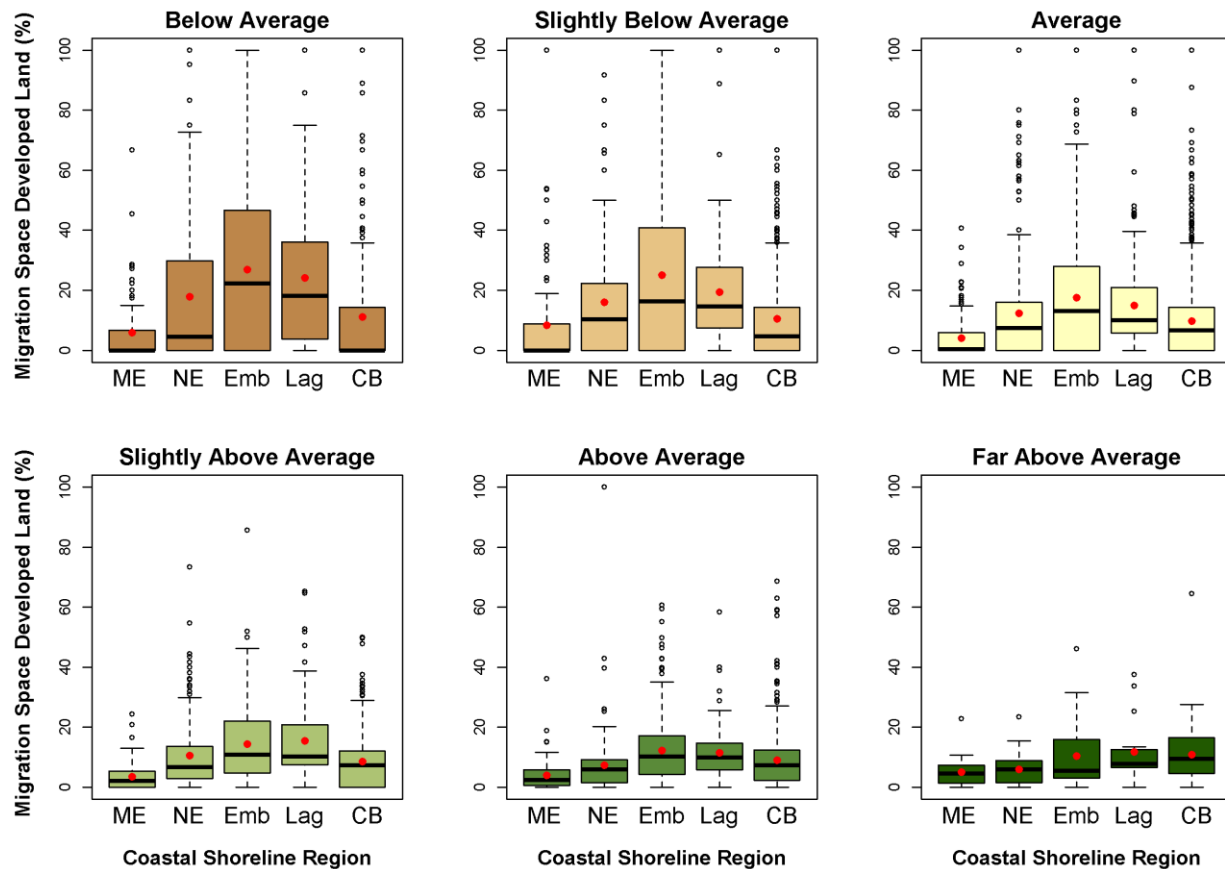
Figure 7.105. Amount (%) of migration space in permanent protection for each CSR by estimated resilience class. A boxplot with the distribution of migration space securement (%) by CSR is shown for each estimated resilience class. The mean percent secured is denoted by a red circle. The resilience classes are shown using our standard z-score color palette.



Migration Space Development and Future Development

Due to inconsistencies in the spatial resolution of various datasets used in this analysis (i.e., 10-m elevation and 30-m land cover products), and how roads are inaccurately mapped in base land cover grids such as the NLCD and C-CAP products, there are cases where some development occurs within the migration space mapped at the 30-m scale. While the percent of developed land in the migration space varied for each resilience class by CSR, there was a consistent trend where development increased with decreasing resilience score until reaching the “far below average” class, which had very little migration space and is not shown in Figure 7.106. The “below average” class had the highest amount of development followed by the “slightly below average” class. The Embayment region had the most development in the below average classes and shared this distinction with the Lagoon region for the above average resilience classes. There are tidal complexes that have 80-100% development for the “average” and lower resilience classes, and this typically occurs for very small migration space areas where a single pixel of development leads to a high percentage. Regardless of resilience score, the Embayment region had the highest average risk of future development by 2100 in the migration space, which likely reflects this region’s already urban and developed coastline, relative to other parts of the project area (Figure 7.87).

Figure 7.106. Amount (%) of migration space comprised of developed land for each CSR by estimated resilience class. A boxplot with the distribution of migration space development (%) by CSR is shown for each estimated resilience class. The boxplot shows the distribution of migration space development (%) by resilience class with the mean denoted by a red circle. The resilience classes are shown using our standard z-score color palette



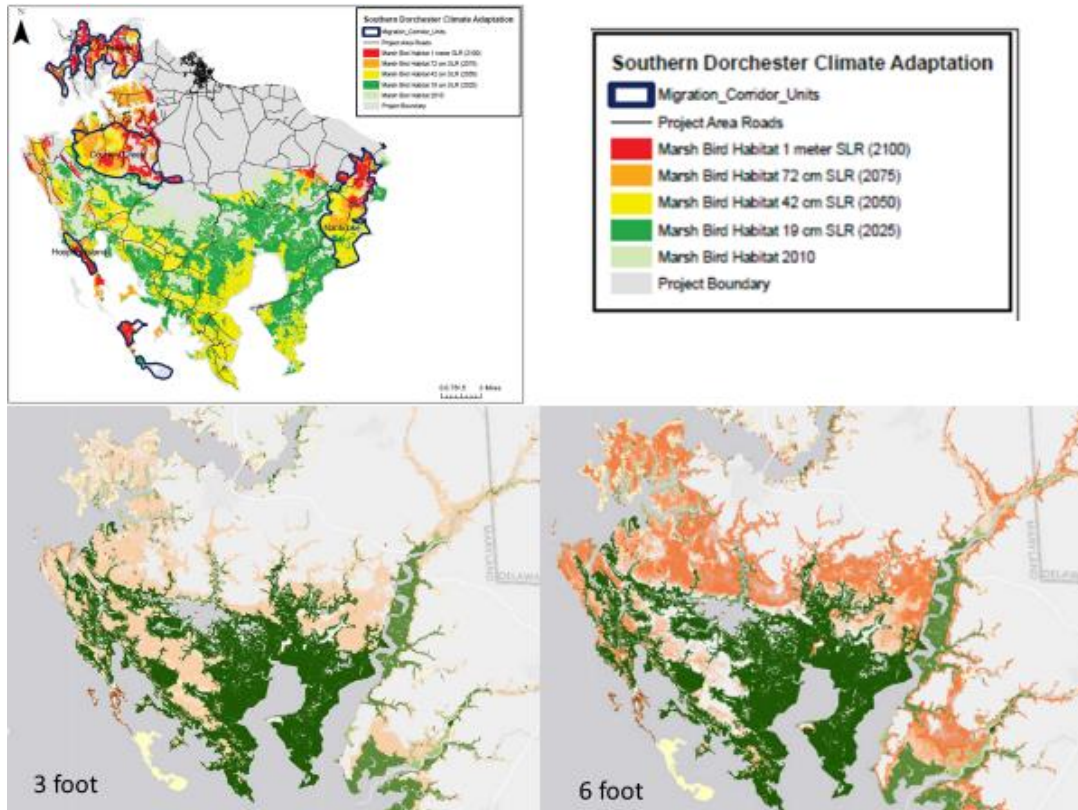
DISCUSSION

We estimated the relative resilience of 10,736 sites across five coastal shoreline regions based on the amount and quality of each site's migration space and buffer area. The results identify the places that could potentially retain species and functions under rising sea levels because they have both the physical characteristics needed to allow the tidal complex to migrate and persist, and the conditions needed to support and facilitate such migration. Specifically, we identified sites that (1) had extensive, diverse, unfragmented, and easily-accessed migration space, (2) were well supplied with high quality freshwater and sediment, and (3) were surrounded by natural buffer area. We argue that these sites offer more options for rearrangement and continued productivity (i.e., are more resilient) than sites that lack these characteristics, but we do not know the specifics of how they will adapt and transform.

Blackwater National Wildlife Refuge (Figure 8.1) is a site that offers an illustrative example of how this analysis might inform management. Tide gauges in this region show that sea level has risen by over a foot during the last century, and air-photos document a corresponding loss of 5,028 acres of tidal marsh in the refuge for the 68-year period from 1938 to 2006 (Lerner et al. 2013). The loss is partially due to inundation and partially due to nutria, an introduced rodent that consumes vegetation and creates erosion-promoting channels (Baird 2009). During the same period, the refuge gained 2,949 acres of new marsh at the upland edge, presumably through upslope migration of tidal marsh into the available migration space as sea levels rose. Although these observations confirm that the tidal complex is migrating and new tidal marsh is forming, the concern is that the emerging area of new marsh is not keeping pace with losses of existing marsh elsewhere, and could result in a net loss of both marsh habitat and associated saltmarsh-dependent birds. These observations have given rise to strategies aimed at slowing marsh loss such as eliminating nutria, and pumping thin sediment layers onto specific marsh conservation areas to increase the surface elevation and facilitate marsh accretion. The hope is that adding thin sediment will speed up marsh accretion rates which currently depend on decaying organic matter and have slowed with the decline in marsh health (Lerner et al. 2013).

Figure 8.1. Priority migration corridors for the Blackwater National Wildlife Refuge.

The priority corridors are outlined in black on the upper map, and are positioned to encompass the expected marsh bird habitat at 1 meter SLR (3.3 feet, red). The lower maps show the results from this study for two scenarios. In the 3-foot scenario, the upland migration space corresponds closely with the priority corridors, and in the 6-foot scenario the migration space expands considerably beyond the corridors.

**Table 8.1. Physical and condition scores for the Blackwater River tidal complex**

Physical		Condition	
Characteristics	Scores (high to low)	Characteristics	Scores (high to low)
Migration Space Size	Far Above Average	Wetland Local Connectedness*	Above Average
Tidal Complex Size	Far Above Average	Riverine Sediment	Slightly Above Average
Shoreline Complexity	Above Average	Hardened Shoreline	Average
Shared Edge	Slightly Above Average	Water Quality (N)	Average
Tidal Class Evenness	Slightly Below Average	Flow Alteration	Average
Buffer Area Size*	Average	Percent Natural*	Slightly Below Average
Landform Variety*	Below Average		
Soil Variety*	Below Average		
Physical Score:	Above Average	Condition Score:	Average

In our analysis, the Blackwater Refuge site is mapped as a huge interconnected tidal complex, with a smaller complex making up the northern boundary of the Blackwater River (Figure 8.1). It is in the Chesapeake coastal shoreline region and scores “above-average” for resilience compared to the region’s 5,134 other sites. The high score is based on the site’s large migration space, which totals over 28,000 acres and shares an extensive edge with the current tidal complex. The site receives an “above-average” amount of sediment and is buffered by highly connected wetlands. To a lesser extent, the site’s score reflects the large size and complexity of the existing marsh, but most of its other attributes are “average” or “below average” (Table 8.1).

Our analysis strongly supports the assertion that the Blackwater refuge is the right place to be doing conservation work, because it has high potential to rearrange and adjust to sea level rise compared to other sites. Further, the natural establishment of 2,949 acres of new marsh is evidence that parts of the marsh are already migrating. On the other hand, the nutria problem and sediment manipulations discussed above suggest that even sites with high resilience may need active management to facilitate migration and adaption. Moreover, a high resilience score does not guarantee that some saltmarsh won’t be lost. At the 6-foot SLR scenario, the total amount of migration space available is less than the current amount of existing tidal complex, so it might be inevitable that there is less marsh in the future if inundation is that severe. Of course, the actual process of transition from tidal complex to open water is hard to predict, and unanticipated events such as faster accretion due to changes in decomposition or sedimentation rates could, and often do, result in unexpected surprises. Additionally, the migration space does not show the same distribution of tidal classes as the current complex and the below-average score for tidal class evenness suggests that it might be dominated by tidal flat. Our analysis also highlights potential limitations relative to the amount of hardened shoreline in the migration space and in the low soil variety and natural cover in the buffer. These factors could interrupt the smooth transition of terrestrial land to tidal complex. Finally, to put this site in context with the other sites in this shoreline region, it scores “average” or above on all the migration space physical and condition metrics. Moreover, the size of its migration space is four times the mean for the region (672 acres, median = 4.5 acres), not including the 22% of the sites that will have no migration space at 6-feet of inundation. Thus, although there is much to monitor and manage, the resilience score of “above-average” appears to accurately reflect the potential of this site for adaptation in the Chesapeake shoreline region.

Scientists at Blackwater have also developed a map of priority corridors for marsh migration (Lerner et al 2013). They identified five key areas based on a one-meter (3.3 feet) SLR scenario, which included the Nanticoke marsh migration corridor (12,607 acres) and the Coursey’s Creek migration corridor (14,000 acres). There is a high correspondence between these migration corridors and the migration space predicted in our study based on the 3-foot scenario. These are also areas where the Lerner et al.

(2013) models predict future habitat for saltmarsh birds (Figure 8.1). While these areas continue to remain important under the 6-foot scenario, there is extensive additional migration space predicted for much of the upland margin, suggesting a further expansion of saltmarsh habitat.

Within the Maine Drowned River Valley region, comparison of our results with those of the finer-scale analysis created by the Maine Natural Heritage Program (2016) indicates a fair amount of congruence among the two studies with respect to the relative ranking of sites. For example, both studies identify the Indian River site as one of the most resilient sites in the region due to its extensive migration space, which snakes its way up the low-lying floodplain of the Indian River. Some of the differences in ranking derive from context: sites in the Maine study area are compared to other sites in Maine, whereas study sites in southern Maine are compared to other sites in the Northern Rivers region (which includes New Hampshire and Massachusetts). This highlights the importance of the coastal shoreline regions as the context for interpreting the results. Finally, although the relative rankings are similar, there are marked differences in the absolute estimates of migration space acres resulting from scale differences in the measuring tool. We expect the finer-scale study to be more precise as to actual acreages and more useful for identifying specific tracts of land to conserve.

A striking pattern in our results was that the small and medium size tidal complexes had a wide variety of sizes in their migration space, while the largest tidal complexes all had large migration spaces. This reflects the geomorphic conditions under which the large complexes have formed: extensive low-lying or subsiding continental margins. In these areas, inundation from SLR is a continuation of the processes that formed the marsh in the past. For many of these sites, the physical characteristics are in place for marsh migration but the critical elements for successful migration are found in the condition score. Often the large site scored “average” for their condition characteristics as they typically have agricultural lands in the migration space and buffer which increases sedimentation rates and decrease water quality and quantity.

Short and long-term trends in a site’s marsh migration space can often be opposing, and responses to the shallow scenarios were not indicative of responses to deeper inundation scenarios. Tidal complexes that formed within barrier islands, for example, often had ample migration spaces under the 1 to 3-foot scenario, but no migration space under the 4 to 6-foot scenarios as the islands started to shrink. In contrast, many sites with small migrations spaces under the 1 to 3-foot scenarios seem to cross an elevational threshold at deeper inundation levels and have large and expanding spaces under the 4 to 6 foot scenarios. The five coastal shoreline regions showed marked differences in responses to the scenarios (Figure 7.101). The two southern regions (Chesapeake Rivers and Mid-Atlantic Lagoons), where the coast is subsiding, showed increasing migration space up to 3 feet and then declining space from 4-6 feet. In the

Northern Rivers the migration space shows a steady increase across all scenarios. Along the rocky coast of the Maine Drowned Rivers and New England Embayments, the migration space shows no change across scenarios. It is likely these patterns reflect the same geomorphic history and structure that determined their different estuary types. Recognition of these patterns across scenarios influenced our decision to use the 6-foot threshold for our results, although we encourage users of this study to examine all six scenarios to get a complete understanding of a site's trajectory.

We emphasize that this analysis was based on site attributes that could be mapped consistently at a regional scale to allow for accurate comparisons among sites. Each individual dataset had a range of error. While we reviewed each dataset with our steering committee, there are certain mistakes in the results that are a consequence of data error. Our restriction of the results to sites with at least two acres of salt marsh eliminated many of the most egregious spatial errors, and the comparison of our inundation scenarios with other studies (Figure 3.5) can help users understand the spatial accuracy and limits of the data. There was also subjectivity in the weighting of individual factors, which was done through agreement of a team of coastal experts. Nevertheless, as we explored the sensitivity of the results to the weighting scheme and to the inclusion or exclusion of certain datasets, we found that many of the same sites continually emerged at the extreme ends of the resilience spectrum. This was because the physical and condition characteristics of these sites were so distinct (e.g., large migration space in natural setting versus no migration space and hemmed in by development) that the patterns were easily detected even with imperfect data. We expect that data errors have the most relevance to sites that score close to "average" because detecting differences among similar sites could be easily influenced by small data errors.

The results from this study can be used to identify potential sites for restoration, defined as sites that have the physical characteristics needed to accommodate migration but that score low for their condition characteristics. Users can explore the data to see if the low condition score indicates a lack of sediment, poor water quality, too much hardened shoreline, or other characteristics that could be improved by strategies aimed at the source of the problem. For example, conservationists in Long Island have made strides in improving the Sound's water quality through a partnership of businesses and individuals dedicated to reducing the nitrogen overload that is degrading saltmarshes and hard clam beds (<http://longislandcleanwaterpartnership.org//default.aspx>). Notably, in our condition model, many of the sites that flank Long Island Sound have "average" or "below average" scores for water quality.

Going forward, we plan to integrate the results of this study with our terrestrial resilience map and web tools (Anderson et al. 2016 a and b). The terrestrial study

identified climate resilient sites across Eastern North America, but did not address the 6-foot coastal zone, which was masked-out on the final maps. Both studies were designed to help users make informed decisions when facing large uncertainties about climate and SLR. However, they are not intended to replace basic conservation principles such as the importance of coastal reserves, reducing direct threats, managing land appropriately, and using natural resources in a sustainable way.

We expect the coastal sites to change dramatically over the next century with our familiar tidal marsh and tidal flats migrating onto the adjacent low lands and much of the existing marsh converting to open water. This is admittedly difficult to imagine, but identifying those places where conservation actions could succeed and managing those sites to adapt to change is a first step in sustaining the diversity and natural services of our coastal systems. We hope that this study and the accompanying tools prove useful to planners and conservationists in identifying where to focus conservation action, and what strategies to employ.

References

- Abell, R., M. Thieme, C. Revenga, M. Bryer, M. Kottelat, N. Bogutskaya, B. Coad, N. Mandrak, S. Contreras-Balderas, W. Bussing, M. L. J. Stiassny, P. Skelton, G. R. Allen, P. Unmack, A. Naseka, R. Ng, N. Sindorf, J. Robertson, E. Armijo, J. Higgins, T. J. Heibel, E. Wikramanayake, D. Olson, H. L. Lopez, R. E. d. Reis, J. G. Lundberg, M. H. Sabaj Perez, and P. Petry. 2008. Freshwater ecoregions of the world: A new map of biogeographic units for freshwater biodiversity conservation. *BioScience* 58:403-414.
- Anderson, M.G., Barnett, A., Clark, M., Prince, J., Olivero Sheldon, A. and Vickery B. 2016. Resilient and Connected Landscapes for Terrestrial Conservation. The Nature Conservancy, Eastern Conservation Science, Eastern Regional Office. Boston, MA.
- Anderson, M.G., M. Clark, and A. Olivero Sheldon. 2014. Estimating Climate Resilience for Conservation across Geophysical Settings. *Conservation Biology* DOI: 10.1111/cobi.12272
- Anderson, M.G., and C.E. Ferree. 2010. Conserving the Stage: climate change and the geophysical underpinnings of species diversity. *PLoS ONE* July (5): 7 e11554: <http://dx.plos.org/10.1371/journal.pone.0011554>
- Arkema KK, et al. 2015. Embedding ecosystem services in coastal planning leads to better outcomes for people and nature. *Proc Natl Acad Sci USA* 112:7390–7395.
- Arkema KK, et al. 2013. Coastal habitats shield people and property from sea-level rise and storms. *Nat Clim Change* 3(10):913–918
- Beier, P., Hunter, M.L., Anderson, M.G. 2015. Special Section: Conserving Nature's Stage. *Conservation Biology* 29 (3) 1523-1739. <http://dx.doi.org/10.1111/cobi.12511>.
- Bourke, P., 1993. Fractal Dimension Calculator User Manual, Online. Available: <http://paulbourke.net/fractals/fracdim/>
- Chaffee, C, Coastal policy analyst for the R.I. Coastal Resources Management Council. personal communication. April 4, 2017,

- Compton, B.W, McGarigal, K, Cushman S.A. and L.G. Gamble. 2007. A resistant-kernel model of connectivity for amphibians that breed in vernal pools. *Conservation Biology* 21: 78-799. <http://www.umasscaps.org/>
- Crist, P. J., B. Thompson, T. C. Edwards, C. J. Homer, and S. D. Bassett. 1998. Mapping and Categorizing Land Stewardship. A Handbook for Conducting Gap Analysis.
- DeConto, R.M. & D. Pollard. 2016. Contribution of Antarctica to past and future sea-level rise. *Nature* 531, 591–597 (31 March 2016) doi:10.1038/nature17145
- Deegan, L.A., Johnson, D.S., Warren, R.S., Peterson, B.J., Fleeger, J.W, Fagherazzi, S. and W. M. Wollheim. 2012. Coastal eutrophication as a driver of salt marsh loss. *Nature* 490, 388–392 (18 October 2012) doi:10.1038/nature11533
- Donnelly, J.P and M.D. Bertness. 2001. Rapid shoreward encroachment of salt marsh cordgrass in response to accelerated sea-level rise. *PNAS* 98(25) www.pnas.org/cgi/doi/10.1073/pnas.251209298
- Ganju, N.K., Defne, Z., Kirwan, M.L., Fagherazzi, S., D’Alpaos, A., & L. Carniello. 2017. Spatially integrative metrics reveal hidden vulnerability of microtidal salt marshes. *Nature Communications* 8:14156. DOI: 10.1038/ncomms14156
- Gesch, D.B., 2007, The National Elevation Dataset, in Maune, D., ed., *Digital Elevation Model Technologies and Applications: The DEM Users Manual*, 2nd Edition: Bethesda, Maryland, American Society for Photogrammetry and Remote Sensing, p. 99-118.
- Gesch, D., Oimoen, M., Greenlee, S., Nelson, C., Steuck, M., and Tyler, D., 2002, *The National Elevation Dataset: Photogrammetric Engineering and Remote Sensing*, v. 68, no. 1, p. 5-11.
- Gill, J. L., Blois, J. L., Benito, B., Dobrowski, S., Hunter, M. L. and McGuire, J. L. (2015), A 2.5-million-year perspective on coarse-filter strategies for conserving nature's stage. *Conservation Biology*, 29: 640–648. doi:10.1111/cobi.12504
- Greene, J.K., M.G. Anderson, J. Odell, and N. Steinberg, eds. 2010. *The Northwest Atlantic Marine Ecoregional Assessment: Species, Habitats and Ecosystems. Phase One*. The Nature Conservancy, Eastern U.S. Division, Boston, MA.

- Gregory, R., Failing, L., Harstone, M., Long, G., McDaniels, T., and D. Ohlson. 2012. Structured Decision Making: A Practical Guide to Environmental Management. Wiley-Blackwell, 301 pp.
- gSSURGO 2014. Gridded Soil Survey Geographic Database for the Conterminous United States. United States Department of Agriculture, Natural Resources Conservation Service. Available from the NRCS geospatial data gateway, online at <https://gdg.sc.egov.usda.gov/>
- Heller, N.E. and Zavaleta E.S. 2009. Biodiversity management in the face of climate change: A review of 22 years of recommendations. *Biological Conservation* 142; 14-32.
- Homer, C.G., Dewitz, J.A., Yang, L., Jin, S., Danielson, P., Xian, G., Coulston, J., Herold, N.D., Wickham, J.D., and Megown, K. 2015. Completion of the 2011 National Land Cover Database for the conterminous United States-Representing a decade of land cover change information. *Photogrammetric Engineering and Remote Sensing*, v. 81, no. 5, p. 345-354
- Howarth, R.W., and others. 2000. Nutrient pollution of coastal rivers, bays, and seas. *Issues Ecol.* 7: 1-15.
- IPCC, 2013: Summary for Policymakers. In: *Climate Change 2013: The Physical Science Basis. Contribution of Working Group I to the Fifth Assessment Report of the Intergovernmental Panel on Climate Change* [Stocker, T.F., D. Qin, G.-K. Plattner, M. Tignor, S.K. Allen, J. Boschung, A. Nauels, Y. Xia, V. Bex and P.M. Midgley (eds.)]. Cambridge University Press, Cambridge, United Kingdom and New York, NY, USA.
- Karegar, M.A., T.H. Dixon, and S.E. Engelhart. 2016. Subsidence along the Atlantic coast of North America: Insights from GPS and late Holocene relative sea level data. *Geophysical Research Letters*, 43, doi: 10.1002/2016GL068015.
- Krasting JP, Dunne JP, Stouffer RJ,. 2016. Enhanced Atlantic sea-level rise relative to the Pacific under high carbon emission rates. *Nature Geoscience* 9: 210-214.
- Kelley, J.T., Belknap, D.F., Jacobson, Jr, G.L., & H.A. Jacobson. 1988. The morphology and origin of salt marshes along the glaciated coastline of Maine, USA. *Journal of Coastal Research*, 4(4). 649-665, Charlottesville (Virginia). ISSN 0749-0208.

- Lawler J.J, Ackerly, D.D., Albano, C.M., Anderson, M.G., Dobrowski, S.Z., Gill, J.L., Heller, N.E., Pressey, R.L., Sanderson, E.W., Weiss, S. B. 2015. The theory behind, and challenges of, conserving nature's stage in a time of rapid change. *Conservation Biology* 29:618–629. Abstract
<http://onlinelibrary.wiley.com/doi/10.1111/cobi.12505/full>
- Lentz, E.E., Thieler, E.R., Plant, N.G., Stippa, S.R., Horton, R.M., and Gesch, D.B. 2016. Evaluation of dynamic coastal response to sea-level rise modifies inundation likelihood. *Nature Climate Change*.
- Lerner, J.A., Curson, D.R., Whitbeck, M. and Meyers, E.J., *Blackwater 2100: A strategy for salt marsh persistence in an era of climate change*. 2013. The Conservation Fund (Arlington, VA) and Audubon MD-DC (Baltimore, MD).
- Liaw, A. and M. Wiener (2002). Classification and Regression by randomForest. *R News* 2(3), 18-22.
- Lucey, K. NH Coastal Program. Personal Communication. April 4, 2017.
- Madden, C. J., K. Goodin, R. J. Allee, G. Cicchetti, C. Moses, M. Finkbeiner, and D. Bamford. 2009. Coastal and Marine Ecological Classification Standard. NOAA A and NatureServe. 107 pp.
- Maine Natural Areas Program. 2016. Coastal Resiliency Datasets, Schlawin, J and Puryear, K., project leads.
http://www.maine.gov/dacf/mnap/assistance/coastal_resiliency.html
- Marcy, D., Herold, N., Waters, K., Brooks, W., Hadley, B., Pendleton, M., Schmid, K., Sutherland, M., Dragonov, K., McCombs, J., Ryan, S. 2011. New Mapping Tool and Techniques For Visualizing Sea Level Rise And Coastal Flooding Impacts. National Oceanic and Atmospheric Administration (NOAA) Coastal Services Center. Originally published in the Proceedings of the 2011 Solutions to Coastal Disasters Conference, American Society of Civil Engineers (ASCE), and reprinted with permission of ASCE (<https://coast.noaa.gov/slr/>).
- MassDEP 2015: Wetlands (1:12,000), MassGIS Data
<http://www.mass.gov/anf/research-and-tech/it-serv-and-support/application-serv/office-of-geographic-information-massgis/datalayers/wetchange.html>

- Mastrandrea, M.D., C.B. Field, T.F. Stocker, O. Edenhofer, K.L. Ebi, D.J. Frame, H. Held, E. Kriegler, K.J. Mach, P.R. Matschoss, G.-K. Plattner, G.W. Yohe, and F.W. Zwieter, 2010: Guidance Note for Lead Authors of the IPCC Fifth Assessment Report on Consistent Treatment of Uncertainties. Intergovernmental Panel on Climate Change (IPCC). Available at <http://www.ipcc.ch/>
- Maupin, M.A., Kenny, J.F., Hutson, S.S., Lovelace, J.K., Barber, N.L., and Linsey, K.S. 2014. Estimated use of water in the United States in 2010: U.S. Geological Survey Circular 1405, 56 p., <https://pubs.usgs.gov/circ/1405/>.)
- McKay, L., Bondelid, T., Dewald, T., Johnston, J., Moore, R., and Rea, A., 2012. "NHDPlus Version 2: User Guide"
- Moore, Richard B., Craig M. Johnston, Richard A. Smith, and Bryan Milstead. 2011. Source and Delivery of Nutrients to Receiving Waters in the Northeastern and Mid-Atlantic Regions of the United States. *Journal of the American Water Resources Association (JAWRA)* 47(5):965-990. DOI: 10.1111/j.1752-1688.2011.00582.x
- National Climate Assessment 2014. U.S. Global Change Research Program. <http://nca2014.globalchange.gov/report/our-changing-climate/introduction>
- NOAA Coastal Change Analysis Program (C-CAP) Regional Land Cover Database. 2010. Data collected 1995-present. Charleston, SC: National Oceanic and Atmospheric Administration (NOAA) Office for Coastal Management. Data accessed at <http://coast.noaa.gov/landcover>.
- NOAA Coastal Services Center. May 2008. Nonpoint-Source Pollution and Erosion Comparison Tool (N-SPECT): Technical Guide. Version 1.5. (20 March 2015; www.csc.noaa.gov/digitalcoast/tools/opennspect/arccgis-versions)
- Olcott, C.A. 2001. Impacts of Nitrogen Addition on the Monthly Above- and Belowground Production of *Spartina alterniflora* in a Virginia Marsh. MS Thesis. University of Virginia.
- Olivero Sheldon, A., Barnett, A. and Anderson, M.G. 2015. A Stream Classification for the Appalachian Region. The Nature Conservancy, Eastern Conservation Science, Eastern Regional Office. Boston, MA.
- Osland, M.J., Enwright, N., and Stagg, C.L. 2014. Freshwater availability and coastal wetland foundation species: ecological transitions along a rainfall gradient. *Ecology*, 95(10) 2789–2802.

- Peterson, J, Michel, J., Zengel, S., White, M., Lord C, and C. Plank. 2002. Environmental Sensitivity Index Guidelines version 3.0. NOAA Technical Memorandum NOS OR&R 11. Hazardous Materials Response Division, Office of Response and Restoration, NOAA Ocean Service
- Raposa, K.B., et al. 2016. Assessing tidal marsh resilience to sea-level rise at broad geographic scales with multi-metric indices, *Biological Conservation*, <http://dx.doi.org/10.1016/j.biocon.2016.10.015>
- Rahmstorf, S. 2007. A Semi-Empirical Approach to Projecting Future Sea-Level Rise 56 *Science* 315, 368
- Renard, K.G., G.R. Foster, G.A. Weesies, D.K. McCool, and D.C. Yoder. 1997. Predicting Soil Erosion by Water: A Guide to Conservation Planning with the Revised Universal Soil Loss Equation (RUSLE). U.S. Department of Agriculture-Agriculture Handbook No. 703.
- R Core Team (2016). R: A language and environment for statistical computing. R Foundation for Statistical Computing, Vienna, Austria. URL <https://www.R-project.org/>.
- Saba, V. S., et al. 2016. Enhanced warming of the Northwest Atlantic Ocean under climate change, *J. Geophys. Res. Oceans*, 121, 118–132, doi:10.1002/2015JC011346.
- Sallenger, A.H., Jr., Doran, K.S., and Howd, P.A. 2012. Hotspot of accelerated sea-level rise on the Atlantic coast of North America: *Nature Climate Change*, published online June 24, 2012, doi:10.1038/nclimate1597 [<http://dx.doi.org/10.1038/nclimate1597>].
- Snedden, G.A., Cretini, K., and B. Patton. 2015. Inundation and salinity impacts to above- and belowground productivity in *Spartina patens* and *Spartina alterniflora* in the Mississippi River deltaic plain: Implications for using river diversions as restoration tools. *Ecological Engineering*, Volume 81, August 2015, Pages 133–139.

- Sharp, R., Tallis, H.T., Ricketts, T., Guerry, A.D., Wood, S.A., Chaplin-Kramer, R., Nelson, E., Ennaanay, D., Wolny, S., Olwero, N., Vigerstol, K., Pennington, D., Mendoza, G., Aukema, J., Foster, J., Forrest, J., Cameron, D., Arkema, K., Lonsdorf, E., Kennedy, C., Verutes, G., Kim, C.K., Guannel, G., Papenfus, M., Toft, J., Marsik, M., Bernhardt, J., Griffin, R., Glowinski, K., Chaumont, N., Perelman, A., Lacayo, M. Mandle, L., Hamel, P., Vogl, A.L., Rogers, L., Bierbower, W., Denu, D., and Douglass, J. 2016. InVEST +VERSION+ User's Guide. The Natural Capital Project, Stanford University, University of Minnesota, The Nature Conservancy, and World Wildlife Fund.
- Tayyebi, Amin, Burak K. Pekin, Bryan C. Pijanowski, James D. Plourde, Jarrod S. Doucette, and David Braun. 2012. Hierarchical modeling of urban growth across the conterminous USA: developing meso-scale quantity drivers for the Land Transformation Model, *Journal of Land Use Science*.
- Thieler, E.R., and Hammar-Klose, E.S. 1999. National Assessment of Coastal Vulnerability to Future Sea-Level Rise: Preliminary Results for the U.S. Atlantic Coast. U.S. Geological Survey, Open-File Report 99-593.
- US Census Bureau. 2012. TIGER Roads/Line Shapefiles. U.S. Department of Commerce, Geography Division, U.S. Census Bureau and available for download at <http://www.census.gov/geo/maps-data/data/tiger.html>
- U.S. Environmental Protection Agency (USEPA) and the U.S. Geological Survey (USGS). 2006. NHD Plus. US Environmental Protection Agency, Washington, DC (Available at: (<http://www.horizon-systems.com/nhdplus/index.php>)).
- U.S. Environmental Protection Agency (USEPA) and the U.S. Geological Survey (USGS). 2012. National Hydrography Dataset Plus – NHDPlus. Version 2.01.
- U.S. Fish and Wildlife Service. September 2012. National Wetlands Inventory website. U.S. Department of the Interior, Fish and Wildlife Service, Washington, D.C. <http://www.fws.gov/wetlands/> Accessed April 2015.
- Vogel, R.M., I. Wilson, C. Daly, 1999, Regional Regression Models of Annual Streamflow for the United States, *Journal of Irrigation and Drainage Engineering*, 125 (3), 148-157.

Warren Pinnacle Consulting, Inc. 2015. Enhancing Coastal Resilience on Virginia's Eastern Shore: Application of the Sea-Level Affecting Marshes Model. Prepared for The Nature Conservancy, Charlottesville, VA.

<http://maps.coastalresilience.org/virginia/#>

Weston, N. 2014. Declining Sediments and Rising Seas: an Unfortunate Convergence for Tidal Wetlands. *Estuaries and Coasts* 37:1–23.

Scoring Methods

Z-scores

In order to identify resilient and vulnerable sites in each Coastal Shoreline Region (CSR), we transformed each metric to standardized normalized scores (z-scores) so that each had a mean of zero and a standard deviation of one. A z-score is calculated using the following formula:

$$z = (X - \mu) / \sigma$$

where z is the z-score, X is the value of the CSR attribute, μ is the mean of the attribute for all sites in the CSR, and σ is the standard deviation of the attribute for all sites in the CSR. The resultant z-score indicates how many standard deviations a particular site is from the CSR mean for a variable. For example, a site with a z-score of 1 indicates that the value for this attribute is 1 standard deviation greater than the attribute mean of all sites in the CSR.

Rank-based Z-scores




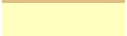



An assumption of standardized normal scores is that the data come from a normal distribution. Many of the CSR attribute values were not normally distributed and various approaches to transform the CSR attributes to a normal distribution were unsuccessful. We thus used rank-based z-scores which do not require a normal distribution. To calculate a rank-based z-score, we used the following steps:

1. Rank the attribute values from lowest to smallest
2. Compute a percentile for each attribute value in the dataset as follows:
 - a. $100(i-0.5)/n$ where i is the rank and n is the sample size
3. For each percentile, calculate the inverse of the standard normal cumulative distribution function to determine how many standard deviations from the mean that particular percentile is on a normal distribution.

The resultant rank-based z-scores are interpreted in the same manner as standard z-scores. That is, a rank-based z-score of 1 indicates that the site value for this attribute is 1 standard deviation greater than the attribute mean for all the sites in that CSR.

We assigned all z-score and all rank-based z-scores to one of seven categories (Table A-1).

Table AI-1. Z-score classes with corresponding abbreviations and colors used in the report and accompanying spatial data.

Z-score Class	Figure Color	Value Range
Far Below Average (FBA)		< -2 standard deviations
Below Average (BA)		-1 to -2 standard deviations
Slightly Below Average (SBA)		-0.5 to -1 standard deviations
Average (A)		-0.5 to 0.5 standard deviations
Slightly Above Average (SAA)		0.5 to 1 standard deviations
Above Average (AA)		1 to 2 standard deviations
Far Above Average (FAA)		> 2 standard deviations

Detailed Data Sources and Methods

SOFTWARE

- *ArcGIS 10.x*: Unless specified otherwise, all spatial analysis operations were conducted in ArcGIS 10.x.
- *R*: All statistical analyses, data aggregation, and data restructuring were conducted in R. R Core Team (2016).

CREATION OF ANALYSIS UNITS

Unit: Tidal Complex

Data Sources:

- Land Cover: NOAA 2010 Coastal Change Analysis Program (C-CAP), <https://coast.noaa.gov/ccapftp/#/>
 - March 2016: data downloaded by state
- Wetlands: National Wetland Inventory (NWI, USFWS 2012), <https://www.fws.gov/wetlands/data/State-Downloads.html>
 - April 2015: data downloaded by state, processed into single 30-m raster, and projected to NAD83 Albers

Analysis Steps:

1. Download NOAA 2010 C-CAP data by state
2. Select the following classes:
 - 16 = Estuarine Forested Wetland
 - 17 = Estuarine Scrub/Shrub Wetland
 - 18 = Estuarine Emergent Wetland
 - 19 = Unconsolidated Shore
3. Merge state selections and project to NAD83 Albers
4. Extract selected grid cells by project area mask
5. Expand classes by 1 cell
6. Region group expanded grid with 4-neighbor rule

7. Assign region group ID to the original tidal complex units (from step 4 above) using Combine and Lookup operation
8. Convert marsh units to polygons
9. Dissolve by grid code and calculate acreage of each discrete unit
10. Tabulate area of C-CAP 2010 within each tidal complex
 - Calculate % unconsolidated shore
 - Examine distribution
11. Select tidal complex units ≥ 2 acres
 - Subset to select tidal complexes with ≥ 2 acres of marsh (classes 16, 17, and 18)
 - Subset to select tidal complexes with < 2 acres of marsh (mostly unconsolidated shore)
 - Then remove those with no marsh migration space
12. Calculate standard metrics for tidal complex:
 - ID
 - Type
 - Acres
 - Perimeter (m)
13. Calculate shared edge % between tidal complex units and associated migration space units (see next page for creation of migration space units) for SLR = 1ft:
 - Intersect tidal complex units with migration space units, set line as output
 - Calculate NEW_Length field (m)
 - Summarize NEW_Length field by TC_ID
 - $(\text{shared length (m)} / \text{total length of tidal complex (m)}) * 100$
14. Calculate shared edge % between tidal complex units and buffer area units (see following pages for creation of buffer areas) for SLR = 1 ft.
 - Intersect tidal complex units with buffer area units, set line as output
 - Calculate NEW_Length field (m)
 - Summarize NEW_Length field by TC_ID
 - $(\text{shared length (m)} / \text{total length of tidal complex (m)}) * 100$
15. Calculate total shared edge %: migration space shared edge (%) + buffer area shared edge (%)
16. In R, assign NWI attribute information to units:
 - Tabulate area of each NWI attribute in the tidal complex units
 - Calculate dominant attribute (maximum % area value) for each tidal complex unit and assign from table of NWI types
 - Calculate NWI wetland variety
17. Join NWI attributes to tidal complex units
18. Calculate metrics for the tidal complex units using migration space and buffer area units (see migration space and buffer area sections on the following pages for details)

Unit: Migration Space*Data Sources:*

- Marsh Migration: NOAA Sea Level Rise (SLR) Viewer marsh data, no accretion rate, (see table below)

NOAA SLR Geography	Data Link
New England	ftp://coast.noaa.gov/temp/ccap/SLR_wetlands_revised/NewEngland/
CT	ftp://coast.noaa.gov/temp/ccap/SLR_wetlands/CT/
NY	ftp://coast.noaa.gov/temp/ccap/SLR_wetlands/NY/
DE, NJ, PA	ftp://coast.noaa.gov/temp/ccap/SLR_wetlands/DE-NJ-PA/
MD and VA	ftp://coast.noaa.gov/temp/ccap/SLR_wetlands/MD-VA/
VA North	ftp://coast.noaa.gov/temp/ccap/SLR_wetlands/MD-VA/
VA South	ftp://coast.noaa.gov/temp/ccap/SLR_wetlands/MD-VA/
NC	ftp://coast.noaa.gov/temp/ccap/SLR_wetlands_revised/NC/

- Elevation: NOAA SLR Viewer 5 and 10-m Digital Elevation Models (DEMs) by state, <https://coast.noaa.gov/slrdata/>
 - Dec. 2015: Data downloaded by state
- Stream lines: NHDPlus v2 flowlines (USEPA & USGS 2012), http://www.horizon-systems.com/NHDPlus/NHDPlusV2_data.php

Analysis Steps:

1. Download and process the 10-m and 5-m DEMs from NOAA's SLR Viewer:
 - a. Resample the 5m grids to 10m using cubic convolution
 - b. Mosaic the resampled 5m grids (n=4) and the 10m grids (n=8) using mean to address overlapping areas
 - c. Re-project to NAD83 Albers
2. Download NOAA SLR Viewer Data shown in table above
3. Combine 1, 2, 3, 4, 5, and 6-foot SLR scenarios with baseline to identify pixels that changed from baseline
 - a. Remove existing salt marsh and other tidal habitats (values 16 – 19)
 - b. Only select cells that ended up as unconsolidated shoreline (19), salt marsh (18), and brackish (transitional) marsh (17)
4. Combine all state files and project to NAD83 Albers
5. Resample to 30 m, snap to 2010 C-CAP grid

6. Combine resampled grid with tidal complex grid to identify overlapping pixels
 - a. Convert all tidal complexes to grid, coded as 100
 - b. Merge tidal complex grid on top of 30-m resampled migration space grid
 - c. Remove those overlapping pixels in the migration space by setting 100 to Null
 - d. **Note: For NC and New England migration space creation, follow same procedure as above BUT clip combined grid by NOAA 10-m DEM to avoid pixel shift issues and extract any attribute values where baseline scenario (000) starts as 0.
7. Assign SLR scenario attribute to migration space
 - a. For each SLR scenario, reclass each combined grid from Step 3 above to its corresponding value (i.e., 1 ft = 1, 3 ft = 3)
 - b. Merge each scenario for all the geographies and project to NAD83 Albers
 - c. Resample each scenario to 30 m, snap to C-CAP 2010
 - d. Extract each scenario by the migration space grid with tidal complexes removed from Step 6 above
 - e. Extract the region grouped migration space with tidal complexes removed from above by each SLR scenario grid
 - i. Note: This maintains the original region group ID of the migration space so that the connection between each tidal complex and migration space is maintained as the SLR scenario increases
 - f. Convert each scenario with its region grouped ID to polygon and dissolve by GRIDCODE (unique ID for each migration space polygon)
 - g. Calculate base attributes
 - i. ID
 - ii. Acres
 - iii. Perimeter (m)
 - iv. Type
8. For each scenario, run spatial join (one to many) between the tidal complexes and the migration space based on intersection so can use this output to calculate the total migration space acreage for each tidal complex
 - a. Start with SLR=1 to get the initial migration space ID that will carry over for each scenario. For each SLR scenario > 1, will identify other migration space polygons that come into play.
 - i. SLR = 1 ft = spatial selection
 - ii. SLR > 1 ft, R script to get MS_IDs and then do join with spatial data to select the migration space units

9. Calculate total migration space and count of migration space units for each tidal complex
 - a. Write R script to calculate the total migration space for each tidal complex at each SLR scenario using the .dbf from the one-to-many join from Step 8 above, and the relationship between each tidal complex and its connected migration space ID's at SLR = 1 ft.
10. For each SLR scenario, calculate shared edge % between migration space units and tidal complex units at SLR = 1 ft
 - a. Intersect tidal complex units with migration space units and set line as output:
 - i. In R, run shared edge script where
 1. $(\text{shared length (m)} / \text{total length of migration space (m)}) * 100$
11. For each SLR scenario, calculate shared edge % between migration space units and buffer area units
 - a. Intersect migration space units with buffer space units, line is output:
 - i. Calculate NEW_Length field (m)
 - ii. Summarize NEW_Length field by migration space ID
 - iii. $(\text{shared length (m)} / \text{total length of migration space (m)}) * 100$
12. Calculate total shared edge %: Tidal Complex Shared Edge % + Buffer Area Shared Edge %
13. Use R script to calculate migration space area weights to roll up attributes to the tidal complex based on the relationship between each tidal complex and its associated migration space units. For example, if a tidal complex had two migration space units, one covering 75% of the total migration space area and the second covering 25% of the area, the attributes of the first would be weighted by 0.75 and the characteristics of the second would be weighted by 0.25 when combined into a final score for the site .
14. Calculate drainage-area weights for the migration space units using both NHDPlus v2 flowlines and catchments
 - a. Clip NHDPlus v2 data to project area
 - b. Clip NHDPlus v2 catchments to project area
 - c. For each SLR scenario, spatial join (one to many) between migration space units and NHDPlus v2 flowlines (with cumulative drainage area (DivDASqKM))
 - d. For all the migration space units that do not intersect (Join_Cnt <>1)
 - i. spatial join (one to many) with the NHDPlus v2 catchments

Unit: Buffer Area*Data Sources:*

- Land Cover: augmented version of NLCD 2011 (Homer et al. 2015) published in Anderson et al. (2016)
 - The augmented version has more information on minor roads, railroads and transmission lines than the standard version
- Elevation: 10-m National Elevation Dataset (NED, Gesch et al. 2002, Gesch 2007)
 - Spring 2016: downloaded NED tiles and created seamless mosaic of 10-m DEM data

Analysis Steps:

1. Select the following classes from the augmented NLCD 2011 generalized land cover grid:
 - a. natural land cover (value = 5)
 - b. agricultural land cover (value = 1)
 - c. hay/pasture (value = 2)
2. Use SLR mask created from NED 10-m DEM to remove buffer area pixels that would likely be underwater in the future
 - a. Con NED 10-m DEM at 1.8288 (m = 6 ft)
3. For each SLR scenario:
 - a. merge respective migration space SLR scenario grid with the tidal complex grid, make sure the tidal complex grid is on top
 - i. Con all values to 10
 - b. Remove migration space and tidal complex units from the grid
 - i. Mosaic
 - ii. Set null (10)
 - c. Region group remaining buffer area pixels using 8 neighbor rule
 - d. Convert to polygon and dissolve by grid code (region group ID)
 - e. Select buffer units that intersect selected migration space units (those that intersected tidal complexes) and/or buffer units that intersect selected tidal complexes
4. Create fields for each buffer unit
 - a. ID
 - b. Acres
 - c. Perimeter (m)
 - d. Type
5. Relationship 1: Link buffer area units to tidal complexes via the tidal complex's migration space units
 - a. Spatial join one to many, target = buffer area, join = migration space
 - b. Spatial join one to many, target = tidal complex, join = buffer area

- c. Run R script to restructure and aggregate spatial join outputs and calculate weights to roll-up variables to the tidal complex units
- 6. Relationship 2: Link buffer units to tidal complex unit (no migration space unit to connect the tidal complex to the buffer area unit)
 - a. Spatial join between tidal complex and buffer unit, one to many
 - i. Write R script to calculate total tidal complex acreage for each buffer unit and total buffer acreage for each tidal complex
 - 1. Note that some tidal complexes have very little to no migration space but lots of buffer space
 - ii. Write R script to calculate buffer area area- weights to roll up to the tidal complex. For example, if a tidal complex had two buffer area units, one covering 75% of the total buffer area and the second covering 25% of the area, the attributes of the first would be weighted by 0.75 and the characteristics of the second would be weighted by 0.25 when combined into a final score for the site.
- 7. Calculate shared edge % between migration space and buffer units for all SLR scenarios:
 - a. Intersect migration space units with buffer space units, line is output:
 - i. Calculate NEW_Length field (m)
 - ii. Summarize NEW_Length field by Migration Space ID
 - iii. $(\text{shared length (m)} / \text{total length of migration space (m)}) * 100$
- 8. Calculate shared edge % between tidal complex and buffer units for SLR = 1 ft
 - a. Intersect tidal complex units with buffer space units, line is output:
 - i. Calculate NEW_Length field (m)
 - ii. Summarize NEW_Length field by Migration Space ID
 - iii. $(\text{shared length (m)} / \text{total length of migration space (m)}) * 100$

STRATIFICATION UNITS

Unit: Coastal Shoreline Regions (CSRs)

Data Sources:

- Coastal Regions and Types: Coastal Shoreline Units (CSUs, Greene et al. 2010)
- Freshwater Ecoregions: World Wildlife Fund (WWF) Freshwater Ecoregions of the World (Abell et al. 2008)

Analysis Steps:

1. Dissolve the 62 CSU polylines and polygons using the Coastal Marine Ecological Classification Standard (CMECS) types (Madden et al. 2005) assigned by the Environmental Protection Agency (EPA).
 - a. The CMECS types of coastal areas are 1) river dominated, 2) lagoon, 3) coastal embayment, and 4) fjord
2. After review of the stratification units and the initial analysis results, used the WWF Freshwater Ecoregions to further subdivide the river-dominated region as follows:
 - a. Chesapeake Bay and Piedmont River Dominated
 - b. Northeast River Dominated
3. After feedback from the steering committee, modified the CSR names to better reflect the dominant processes in each coastal region.

TIDAL COMPLEX PHYSICAL ATTRIBUTES

Attribute: Tidal Complex Size

- See previous section on creation of tidal complex units

Attribute: Tidal Complex Shared Edge (%) with Migration Space

- See previous section on creation of migration space and tidal complex attributes

Attribute: Shoreline Complexity

Data Source:

- Shoreline: NOAA Environmental Sensitivity Index (ESI) shoreline (Peterson et al. 2002, Greene et al. 2010), <http://response.restoration.noaa.gov/maps-and-spatial-data/download-esi-maps-and-gis-data.html>

Analysis Steps:

1. Run Euclidean allocation of the tidal complexes using tidal complex ID and a 90-m max distance (30-m resolution, snap to C-CAP 2010 dataset)
2. Convert the Euclidean allocation raster to polygon
3. From the ESI shoreline, select all non-manmade lines where the "BC_REP_TYP" <> man-made
4. Run identity of the ESI shoreline (with hardened shoreline removed) with the Euclidean allocation polygon
 - a. Select all lines where alloc <> -1 (i.e., line intersected with a polygon)
 - b. Dissolve by tidal complex ID
5. Run ET Geowizards Polyline Characteristics to calculate line characteristics:
 - a. ET_Sinous: Sinuosity (1 = straight line, higher = more bendy; 0 = closed loop)
 - b. ET_Fract: Fractal (1 = straight line, 2 = most complex line)
 - c. Use sinuosity score BUT
 - i. 176 tidal complexes had a sinuosity score of 0, use fractal score for these cases
6. For those tidal complexes that did not have shoreline data from the ESI, assign a shoreline complexity Z-score of 0 (average) which does not reward or punish a site for no data.

MIGRATION SPACE PHYSICAL ATTRIBUTES

Attribute: Migration Space Size

- See earlier section on creation of migration space units

Attribute: Tidal Height Classes Variety and Evenness

Data Source:

- Marsh migration: NOAA Sea Level Rise (SLR) Viewer marsh data, no accretion rate (see table below)

NOAA SLR Geography	Data Link
New England	ftp://coast.noaa.gov/temp/ccap/SLR_wetlands_revised/NewEngland/
CT	ftp://coast.noaa.gov/temp/ccap/SLR_wetlands/CT/
NY	ftp://coast.noaa.gov/temp/ccap/SLR_wetlands/NY/
DE, NJ, PA	ftp://coast.noaa.gov/temp/ccap/SLR_wetlands/DE-NJ-PA/
MD & VA	ftp://coast.noaa.gov/temp/ccap/SLR_wetlands/MD-VA/
VA North	ftp://coast.noaa.gov/temp/ccap/SLR_wetlands/MD-VA/
VA South	ftp://coast.noaa.gov/temp/ccap/SLR_wetlands/MD-VA/
NC	ftp://coast.noaa.gov/temp/ccap/SLR_wetlands_revised/NC/

Analysis Steps:

1. For each geography, convert NOAA SLR Viewer data to tidal height categories
 - a. For each SLR scenario and geography, reclass the .img grids as follows
 - i. LULC 13,14,15 = 4
 - ii. LULC 17 = 3
 - iii. LULC 18 = 2
 - iv. LULC 19 = 1
 - v. All other values = NoData
2. Project MD-VA grids as these were not projected
3. Merge and project all the grids together, snap to base 10-m grid
4. For each SLR scenario, tabulate area of each tidal class in the migration space units
5. For each SLR scenario, use R script to calculate proportion of each tidal height class in each migration space unit:
 - a. Square proportions and sum
 - b. Take reciprocal = Simpsons D
 - c. Evenness = $D / \text{total number of habitats}$:
 - i. 1 = equal distribution
 - ii. $\text{Min} = 1 / D_{\text{max}}$
 - d. Calculate proportion of unconsolidated shore in each migration space unit

- e. If unconsolidated proportion > .50, multiply the evenness value by (1- the unconsolidated shore proportion)
- f. If unconsolidated proportion <= .50, leave evenness value as is
6. For each SLR scenario, use the migration space area-based weights for each tidal complex to roll up the values to the tidal complex unit

Attribute: Migration Response Static Coastal Response

Data Source:

- Model: Dynamic coastal response model for the Northeastern US (Lentz et al. 2016)

Analysis Steps:

1. Download the Coastal Response Type Likelihood raster datasets from USGS at: https://woodshole.er.usgs.gov/project-pages/coastal_response/data.html
 - a. The grids provide the probability of observing either static or dynamic coastal response in the 2020s, 2030s, 2050s, and 2080s.
2. Select 2080 model results as compatible with 2100 horizon for max SLR = 6 ft.
3. Per Lentz, convert model results to IPCC probability categories (Mastrandrea et al. 2010, table below)

IPCC Term	Likelihood of the Outcome	Probability of a Dynamic Response in 2080	Dynamic Response Class Value
Virtually certain	99-100% probability	>=99 [No pixels]	7 (>=99)
Very likely	90-100% probability	90 <99%	6 (90 <99%)
Likely	66-100% probability	66 <90%	5 (66 <90%)
About as likely as not	33-66% probability	33 < 66%	4 (33 < 66%)
Unlikely	0-33% probability	10 < 33%	3 (10 < 33%)
Very unlikely	0-10% probability	1-10% [No pixels]	2 (1-10%)
Exceptionally unlikely	0-1% probability	1 [No pixels]	1

4. For each migration space SLR scenario, calculate the average coastal response probability category
5. For each SLR scenario, select all migration space units with a mean probability response class score <= 3.5 (unlikely to respond dynamically)
 - a. Assign these units a Z-score of -1 ("below average")
6. For each SLR scenario, use the migration space area-based weights for each tidal complex to roll up the values to the tidal complex unit

BUFFER AREA PHYSICAL ATTRIBUTES

Attribute: Buffer Area Size (acres)

- See earlier section on creation of buffer area units

Attribute: Landform Variety in the first 1-km Buffer Area

Data Source:

- Landforms: 30-m landform model with 17 classes for the Eastern US (Anderson et al. 2016)

Analysis Steps:

1. Select landforms compatible with coastal processes and systems:
 - a. Hilltop (flat)
 - b. Hill (gentle slope)
 - c. Dry flats
 - d. Wet flats
 - e. Valley/toeslope
 - f. Moist flats in upland land cover
 - g. Open water
2. To address correlation between landform variety and buffer size, calculate landform variety for 100-acre circular area within project area using Focal Statistics with:
 - a. Neighborhood Shape = circle
 - b. Radius = 358.908800 meters
3. Relationship 1: Migration space units and buffer area units
 - a. For each migration space SLR scenario polygon, run Euclidean distance (30 m, snap to NOAA C-CAP 2010), max distance of 1-km
 - b. For each Euclidean distance output, Con to set 0 values to Null and all other values to 1
 - c. Combine the Euclidean distance Con output with the buffer grid for each SLR scenario
 - d. Run a Lookup on the combine grid to set the raster value to the buffer ID (gridcode)
 - e. Calculate Zonal Mean of the landform variety 100-acre grid using the Lookup grid buffer ID as the zone
4. Relationship 2: Tidal complex units and buffer area units (since there were buffer units that only intersected tidal complexes (i.e., did not intersect the migration space of tidal complexes), do the following steps:
 - a. For the tidal complex polygon, run Euclidean distance (30 m, snap to NOAA 2010 C-CAP), max to 1000 m
 - b. For the Euclidean distance output, Con to set 0 values to Null and all other values to 1

- c. Combine the Euclidean distance Con output with the buffer grid for each SLR scenario
 - d. Run Lookup on the combine grid to set the raster value to the buffer ID (gridcode)
 - e. Calculate Zonal Mean of the landform variety 100-acre grid using the Lookup grid buffer ID as the zone
5. As there are two sets of landform variety means:
 - a. Run R script to combine the two sets of buffer 1-km mean values for each SLR scenario to ensure that a buffer area's relationship with a tidal complex is not counted more than once (i.e., a buffer unit that is immediately adjacent to a tidal complex but is also linked to the tidal complex via the migration space).
6. For each SLR scenario, use the buffer area units' area-based weights for each tidal complex to roll up the values to the tidal complex unit

Attribute: Soil Variety in the first 1-km of the Buffer Area

Data Source:

- Soils: 30-m Soil Texture grid with 12 classes developed for the Eastern US (Anderson et al. 2016)

Analysis Steps:

1. To address correlation between soil variety and buffer size, we calculated soil variety for a 100-acre circular area for the project area using Focal Statistics
 - a. Neighborhood Shape = Circle
 - b. Radius = 358.908800 meters
 - c. Calculate for all 12 soil texture values
2. Relationship 1: Migration space units and buffer area units
 - a. For each migration space SLR scenario polygon, run Euclidean distance (30 m, snap to NOAA C-CAP 2010), max distance of 1-km
 - b. For each Euclidean distance output, Con to set 0 values to Null and all other values to 1
 - c. Combine the Euclidean distance Con output with the buffer grid for each SLR scenario
 - d. Run a Lookup on the combine grid to set the raster value to the buffer ID (gridcode)
 - e. Calculate Zonal Mean of the soil variety 100-acre grid using the Lookup grid buffer ID as the zone
3. Relationship 2: Tidal complex units and buffer area units (since there were buffer units that only intersected tidal complexes (i.e., did not intersect the migration space of tidal complexes), do the following steps:
 - a. For the tidal complex polygon, run Euclidean distance (30 m, snap to NOAA 2010 C-CAP), max to 1000 m

- b. For the Euclidean distance output, Con to set 0 values to Null and all other values to 1
 - c. Combine the Euclidean distance Con output with the buffer grid for each SLR scenario
 - d. Run Lookup on the combine grid to set the raster value to the buffer ID (gridcode)
 - e. Calculate Zonal Mean of the soil variety 100-acre grid using the Lookup grid buffer ID as the zone
4. As there are two sets of soil variety means:
 - a. Run R script to combine the two sets of buffer 1-km mean values for each SLR scenario to ensure that a buffer area's relationship with a tidal complex is not counted more than once (i.e., a buffer unit that is immediately adjacent to a tidal complex but is also linked to the tidal complex via the migration space).
5. For each SLR scenario, use the buffer area units' area-based weights for each tidal complex to roll up the values to the tidal complex unit

PHYSICAL SCORE CALCULATIONS

Attribute Weights

- Each attribute was given a rank with respect to its importance for site resilience, and each was weighted on a numeric scale from 1 to 5 in terms of its influence and importance. The numeric weights were used as a multiplier when combining factors, with the objective of giving more weight to factors with more influence. The numeric weights were: 5 - very high, 4 - high, 3 - moderate, 2 - low, and 1 - very low.

Tidal Complex and Migration Space Physical Score:

The tidal complex and migration space physical score was calculated using one of two options:

- If a site had a value for the static coastal response metric (only a small number of sites):

$$((\text{Tidal Complex Acreage} * 2) + (\text{Tidal Complex Shoreline Complexity} * 2) + (\text{Migration Space Shared Edge (\%)} * 3) + (\text{Migration Space Acreage} * 5) + (\text{Tidal Class Evenness \& Diversity} * 3) + (\text{Static Coastal Response} * 5)) / 20$$
- If a site did not have a value for the static coastal response metric (majority of sites):

$$((\text{Tidal Complex Acreage} * 2) + (\text{Tidal Complex Shoreline Complexity} * 2) + (\text{Migration Space Shared Edge (\%)} * 3) + (\text{Migration Space Acreage} * 5) + (\text{Tidal Class Evenness \& Diversity} * 3)) / 15$$

Buffer Area Physical Score

The buffer physical score was calculated as follows:

$$((\text{Buffer Area Size} * 5) + (\text{Landform Variety} * 4) + (\text{Soil Variety} * 2)) / 11$$

Total Physical Score

The total physical score for a tidal complex was calculated as follows:

$$(.80 * \text{Tidal Complex and Migration Space Physical Score}) + (.20 * \text{Buffer Area Physical Score})$$

Each tidal complex's total physical z-score was converted to a new set of standardized normalized values (z-scores) using a z-rank procedure, after removing the very low scoring sites (essentially sites without any migration space or with very poor scores for all their physical attributes). The very low sites were manually assigned a z-score of -3.5 SD and then combined with the new set of z-scores.

TIDAL COMPLEX CONDITION ATTRIBUTES

Attribute: Percent Hardened Shoreline

Data Source:

- Shoreline: NOAA Environmental Sensitivity Index (ESI) shoreline (Peterson et al. 2002, Greene et al. 2010), <http://response.restoration.noaa.gov/maps-and-spatial-data/download-esi-maps-and-gis-data.html>

Analysis Steps:

1. Select all manmade lines from the ESI shoreline
2. Run Euclidean allocation to assign tidal complex units ID (TC_ID) to nearest cells out to 90-m max (30-m resolution, snap to C-CAP 2010 dataset)
3. Convert Euclidean allocation to polygon
4. Run identity between hardened shoreline and Euclidean allocation polygon
 - a. Select all lines with alloc (FID_tc_all <> - 1)
 - b. Dissolve by tidal complex ID
 - c. Add "Length" field and calculate length in KM
5. Run identity between NAM ESI full shoreline and allocation polygon
 - a. Select all lines with alloc <> - 1
 - b. Dissolve by tidal complex ID (GRIDCODE field in identity polygon)
 - c. Add "Length" field and calculate length in KM
 - d. Add field called "PER_HARD" to hold % hardened shoreline values
6. Join the manmade dissolved lines to the full ESI lines by GRIDCODE
7. Calculate % of the full shoreline comprised of manmade materials for each tidal complex
8. For tidal complexes with no ESI data, assign a percent hardened shoreline z-score value of 0 (average) which does not reward or punish a site for no data.

MIGRATION SPACE CONDITION ATTRIBUTES

Attribute: Water Quality / Nitrogen Inputs

Data Sources:

- Regional Nitrogen estimates: USGS SPARROW 2002 Total Nitrogen Model for the New England and Mid-Atlantic Region (Moore et al. 2011), <https://cida.usgs.gov/sparrow/map.jsp?model=51>
- Stream lines: NHDPlus v2 flowlines (USEPA & USGS 2012), http://www.horizon-systems.com/NHDPlus/NHDPlusV2_data.php
- Flowline attributes (potential predictor variables): >250 land use, hydrologic, geologic, and physical variables attributed to the NHDPlus v2 catchments and flowlines
 - Over 300 attributes for each NHDPlusV2 flowline were compiled and calculated. The attributes included a set of 50 value-added attributes pre-calculated by USGS and distributed with the NHDPlusV2, along with over 250 local and cumulative attributes calculated by TNC using available soils, geology, landforms, land cover, and other source datasets. For more details, please see the Appendices in Olivero Sheldon et al. 2015)

Analysis Steps:

1. Download 2002 Nitrogen model results attributed to the NHDPlus v1 flowlines
2. Create Nitrogen yield (kg/km²/yr) classes based on USGS results (see table below)

Nitrogen Class	Total Nitrogen Yield (Kg/km2/yr.)
1 (Low, good water quality)	< 210
2	210 – 300
3	300 – 470
4	470 – 830
5 (High, poor water quality)	> 830

3. Cross walk NHDPlus v1 reaches to v2 reaches as the full suite of potential predictor variables were already linked to the NHDPlus v2
4. Process flowline variables for use as potential predictor variables
 - a. For example, create summary land cover classes such as % forest f using the three forest cover classes in the 2001 NLCD dataset
5. Use random forest (RF) models to assess relationship between variety of predictor variables and total N yield classes based on 2001 NLCD land use data variables
 - a. R randomForest package: A. Liaw and M. Wiener (2002). Classification and Regression by randomForest. R News 2(3), 18--22.
6. Good model was found (RF total error rate = 15.8%)

7. Using best RF model, predict nitrogen classes using new predictor variables based on more current 2011 land cover variables; retain other non-land cover variables that were not updated.
8. To translate the estimated total nitrogen yield classes from the flowlines to the migration space units, use drainage area-weighted average approach for each SLR scenario
9. For each SLR scenario, use the migration space area-based weights for each tidal complex to roll up the estimated 2011 total nitrogen values to the tidal complex unit

Attribute: Freshwater Flow*Data Sources:*

- Stream lines and catchments: NHDPlus v2 flowlines and catchments (USEPA & USGS 2012), http://www.horizon-systems.com/NHDPlus/NHDPlusV2_data.php
- Cumulative drainage area (CDA): NHDPlus v2 Value Added Attribute (VAA) divergence-routed cumulative drainage area (USEPA & USGS 2012)
- Mean annual flow (MAF): NHDPlus v2 VAA Enhanced Unit Runoff Method (EROM) gage-adjusted mean annual flow estimate (McKay et al. 2012)

Analysis Steps:

1. Clip NHDPlus v2 flowlines by the project area and spatially assign to Coastal Shoreline Regions
2. Write R script to:
 - a. Join CDA and MAF attributes to the NHDPlus v2 flowlines
 - b. Select the two riverine CSR's:
 - i. Chesapeake Bay and Piedmont River Dominated
 - ii. Northeast River Dominated
 - c. Examine data distributions and log transform both CDA and MAF
 - d. Run linear regression to predict MAF using CDA by CSR (stratification by CSR improved the regression diagnostic results)
 - i. adjusted $R^2 = .9915$ ($p \leq 2.2e-16$)
 - e. Calculate average standardized residuals for each flowline
 - f. Assign standardized residuals to following flow alteration classes based on how much a stream's predicted flow deviated from expected flow (e.g., 1 SD above mean indicates the mean annual flow is one standard deviation higher than expected based on CDA)
 - i. 1: far above average alteration (> 2 SD)
 - ii. 2: above average (1 to 2 SD)
 - iii. 3: slightly above average (0.5 to 1 SD)
 - iv. 4: average (0.5 to -0.5 SD)
 - v. 5: slightly below average (- 0.5 to -1 SD)
 - vi. 6: below average (-1 to -2 SD)
 - vii. 7: far below average (< -2 SD)
 - g. For each SLR scenario, calculate average flow alteration class using the flowline drainage-area weighted average approach
3. For each SLR scenario, use the migration space area-based weights for each tidal complex to roll up the migration space flow alteration values to the tidal complex unit

Attribute: Sediment Input

Part 1: Large catchments (cumulative drainage area > 1000 km²)

Data Sources:

- Sediment model: Flow-weighted suspended sediment (FWA-SSC, Weston 2014)
- Watershed area: NHDPlus v2 cumulative drainage area (CDA)
- Land Cover: NLCD 2011 (Homer et al. 2015) for CDA. Variable linked and accumulated for NHDPlus v2 in Olivero Sheldon et al. 2015.
- Soil Erodibility: ESRI's USA Soils Erodibility Factor, created from gSSURGO 2014
 - The value for soil erosion factor was calculated from the field Kf (kffact) in the gSSURGO horizon table (chozion). Each map unit in SSURGO has one or more components and each component has one or more layers or horizons. To flatten these one-to-many relationships Esri calculated an average value of horizons weighted by thickness for each component and the average value of the components weighted by component percentage to determine the final value for each map unit.
 - <https://www.arcgis.com/home/item.html?id=93be1788338d492e8d9079abb65d5722>
- Stream lines: NHDPlus v2 flowlines (USEPA & USGS 2012), http://www.horizon-systems.com/NHDPlus/NHDPlusV2_data.php

Analysis Steps:

1. Use NHDPlus Catchment Attribute Allocation and Accumulation Tool (CA3T) ([http://www.horizon-systems.com/NHDPlus/NHDPlusV2_tools.php#NHDPlusV2 Catchment Attribute Allocation and Accumulation Tool \(CA3TV2\)](http://www.horizon-systems.com/NHDPlus/NHDPlusV2_tools.php#NHDPlusV2_Catchment_Attribute_Allocation_and_Accumulation_Tool_(CA3TV2))) to accumulate mean SSURGO k-factor for the NHDPlus v2 flowlines CDA
2. Use equation from Weston 2014 where >80% of variation in FWA-SSC was predicted for watersheds > 1000 km² in area
 - a.
$$\text{FWA-SSC} = 64.8 (\text{CDA}) + 0.71(\% \text{ agriculture}) + 87.2 (\text{SSURGO k-factor}) - 23.5$$
3. Assign the estimated FWA-SSC results to z-scores for the project area using z-rank procedure

Part 2: Small catchments (cumulative drainage area ≤ 1000 km²) estimated sediment delivery

Data Sources:

- Sediment Model: Natural Capital Integrated Valuation of Ecosystem Services and Tradeoffs (InVEST) Sediment Delivery Ratio (SDR) model (Sharp et al. 2016), <http://www.naturalcapitalproject.org/invest/>
- Stream lines: NHDPlus v2 flowlines (USEPA & USGS 2012), http://www.horizon-systems.com/NHDPlus/NHDPlusV2_data.php

- Hydrologically modified Digital Elevation Model (DEM): NHDPlus v2 DEM (USEPA & USGS 2012), http://www.horizon-systems.com/NHDPlus/NHDPlusV2_data.php
- Land Cover: augmented version of NLCD 2011 (Homer et al. 2015) published in Anderson et al. (2016)
 - The augmented version has more information on minor roads, railroads and transmission lines than the standard version
- Soil Erodibility: ESRI's USA Soils Erodibility Factor, created from gSSURGO 2014
 - The value for soil erosion factor was calculated from the field Kf (kffact) in the gSSURGO horizon table (chozion). Each map unit in SSURGO has one or more components and each component has one or more layers or horizons. To flatten these one-to-many relationships Esri calculated an average value of horizons weighted by thickness for each component and the average value of the components weighted by component percentage to determine the final value for each map unit.
 - <https://www.arcgis.com/home/item.html?id=93be1788338d492e8d9079abb65d5722>
- Rainfall Erosivity: R-factor grid (800-m resolution) for the continental US from the NOAA OpenNSPECT model data inputs/sources (Renard et al. 1997), <https://coast.noaa.gov/digitalcoast/tools/opensnspect>
- Watershed: NHDPlus v2 catchments (USEPA & USGS 2012), http://www.horizon-systems.com/NHDPlus/NHDPlusV2_data.php
- USLE cover factor for each land cover class: (NOAA 2008), www.csc.noaa.gov/digitalcoast/tools/opensnspect/arcgis-versions)
- USLE practice factor for each LULC: set to 1 (no conservation treatment)
- Stratification Units: NHDPlus v2 production units 1 (Northeast), 2 (Mid-Atlantic), and 3a (South Atlantic North)

Analysis Steps:

1. Prepare all the input data for the InVEST model and ensure grids have same resolution, projection, and are aligned
2. Run sediment delivery ratio (SDR) model by NHDPlus v2 production units, and adjust model parameters as needed
3. Extract the sediment output for each NHDPlus v2 catchment by production unit
4. Convert the values to Z-scores using z-rank procedure
5. Combine the large and small catchment Z-scores into a single dataset
6. For each SLR scenario, calculate drainage-area weighted average for each migration space unit
7. For each SLR scenario, use the migration space area-based weights for each tidal complex to roll up the migration space flow alteration values to the tidal complex unit

BUFFER AREA CONDITION METRICS

Attribute: Local Wetland Connectedness

Data Sources:

- Model: Resistant kernel analysis (Compton et al. 2007)
- Landforms: 30-m landform model with 17 classes for the Eastern US (Anderson et al. 2016)
- Land Cover: augmented version of NLCD 2011 (Homer et al. 2015) published in Anderson et al. (2016)
 - The augmented version has more information on minor roads, railroads and transmission lines than the standard version

Analysis Steps:

1. Create resistance grid where each cell is coded with a resistance weight based on the slope and land position of that cell.
 - a. Flatter areas (less slope) and/or areas that are lower (lower land position) are more likely to facilitate the connectedness of wetlands.
2. Experiment with a variety of focal distances, select 1km as it best represents flow of wetlands
3. To run the local connectedness analysis on the resistance surface, increase the grid cell size from 30 m to 90 m
4. Aggregate the 30 m cells to the 90 m cells using the average of the 30 m resistance weights (table below).
5. Output grid of 90-m cells where each cell was scored with a local connectivity value from 0 (least connected) to 100 (most connected).

Landform	code	Resistance
Steep slope (cool/warm aspect)	3/4	10
Cliff	5	10
Summit/ridgetop	11	5.5
Slope crest	13	7.5
Hilltop (flat)	21	3.5
Hill (gentle slope)	22	3.5
Sideslope (cool/warm)	23/24	5.5
Dry flats	30	1.5
Wet flats	31	1
Valley/toeslope	32	2
Moist flats	39	1.25
Flat at the bottom of a steep slope	41	1
Cove/footslope (cool/warm aspect)	43/44	3.5
Open water	50	1.5
Development		20

6. For each SLR scenario, run Zonal Mean to calculate the average local connectedness for each buffer unit
7. For each SLR scenario, use the buffer area units' area-based weights for each tidal complex to roll up the values to the tidal complex unit

Attribute: Percent Natural Cover in first 1-km of Buffer Area

Data Source:

- Land Cover: augmented version of NLCD 2011 (Homer et al. 2015) published in Anderson et al. (2016)
 - The augmented version has more information on minor roads, railroads and transmission lines than the standard version

Analysis Steps:

1. Relationship 1: Migration space units and buffer area units
 - a. For each migration space SLR scenario polygon, run Euclidean distance (30 m, snap to NOAA C-CAP 2010), max distance of 1-km
 - b. For each Euclidean distance output, Con to set 0 values to Null and all other values to 1
 - c. Combine the Euclidean distance Con output with the buffer grid for each SLR scenario
 - d. Run a Lookup on the combine grid to set the raster value to the buffer ID (gridcode)
 - e. Tabulate area of agriculture and natural land using the Lookup grid buffer ID as the zone
 - f. Using the tabulate area results, calculate percent of ag and natural land cover in the first 1-km buffer area
2. Relationship 2: Tidal complex units and buffer area units (since there were buffer units that only intersected tidal complexes (i.e., did not intersect the migration space of tidal complexes), do the following steps:
 - a. For the tidal complex polygon, run Euclidean distance (30 m, snap to NOAA 2010 C-CAP), max to 1000 m
 - b. For the Euclidean distance output, Con to set 0 values to Null and all other values to 1
 - c. Combine the Euclidean distance Con output with the buffer grid for each SLR scenario
 - d. Run Lookup on the combine grid to set the raster value to the buffer ID (gridcode)
 - e. Tabulate area of agriculture and natural land using the Lookup grid buffer ID as the zone
 - f. Using the tabulate area results, calculate percent of ag and natural land cover in the first 1-km buffer area

3. As there are two sets of percent natural values:
 - a. Run R script to combine the two sets of buffer 1-km mean values for each SLR scenario to ensure that a buffer area's relationship with a tidal complex is not counted more than once (i.e., a buffer unit that is immediately adjacent to a tidal complex but is also linked to the tidal complex via the migration space).
4. For each SLR scenario, use the buffer area units' area-based weights for each tidal complex to roll up the values to the tidal complex unit

CONDITION SCORE CALCULATIONS

Attribute Weights

- Each attribute was given a rank with respect to its importance for site resilience, and each was weighted on a numeric scale from 1 to 5 in terms of its influence and importance. The numeric weights were used as a multiplier when combining factors, with the objective of giving more weight to factors with more influence. The numeric weights were: 5 - very high, 4 - high, 3 - moderate, 2 - low, and 1 - very low.

Tidal Complex and Migration Space Condition Score:

The tidal complex and migration space condition score was calculated using one of two options:

1. River-dominated Coastal Shoreline Regions (CSRs): $((\text{Tidal Complex Percent Hardened Shoreline} * 5) + (\text{Migration Space Water Quality} * 5) + (\text{Migration Space Sediment Input} * 3) + (\text{Migration Space Flow Alteration} * 4)) / 17$
2. All other CSRs: $((\text{Tidal Complex Percent Hardened Shoreline} * 5) + (\text{Migration Space Water Quality} * 5) + (\text{Migration Space Sediment Input} * 3)) / 13$

Buffer Area Condition Score

The buffer condition score was calculated as follows:

$$((\text{Buffer Area Wetland Connectedness} * 5) + (\text{Buffer Area \% Natural Land Cover} * 3)) / 8$$

Total Condition Score

The total condition score for a tidal complex was calculated as follows:

$$(.80 * \text{Tidal Complex and Migration Space Condition Score}) + (.20 * \text{Buffer Area Condition Score})$$

Each tidal complex's total condition z-score was converted to a new set of standardized normalized values (z-scores) using a z-rank procedure, after removing the very low scoring sites (essentially those without any migration space or with very poor scores for all their condition attributes). The very low sites were assigned a z-score of -3.5 SD and then combined with the new set of z-scores.

ESTIMATED RESILIENCE CALCULATIONS

The final estimated resilience z-score was calculated as follows:

$(\text{Total Physical Score} + \text{Total Condition Score}) / 2$

Each tidal complex's estimated resilience z-score was converted to a new set of standardized normalized values (z-scores) using a z-rank procedure, after removing the very low scoring sites (essentially those without any migration space or with very poor scores for all their physical and condition attributes). The very low sites were assigned a z-score of -3.5 SD and then combined with the new set of z-scores.

ADDITIONAL MIGRATION SPACE ATTRIBUTES

Attribute: Migration Space Percent Securement

Data Source:

- Secured Lands: TNC's Eastern Conservation Science team's 2013 dataset of Secured Land (Anderson et al. 2016)

Analysis Steps:

1. Select secured lands with GAP status of 1,2, or 3
2. For each SLR scenario, tabulate area of secured lands in the migration space and calculate % of migration space in securement
3. For each SLR scenario, use the migration space area-based weights for each tidal complex to roll up the migration space percent securement values to the tidal complex unit

Attribute: Migration Space Percent Development

Data Source:

- Land Cover: augmented version of NLCD 2011 (Homer et al. 2015) published in Anderson et al. (2016)
 - The augmented version has more information on minor roads, railroads and transmission lines than the standard version

Analysis Steps:

1. Tabulate area of NLCD 2011 land cover classes for each migration space SLR scenario
2. For each SLR scenario, use R script to calculate percentage of developed lands and roads 21:24,31,100,200, and 300 in the migration space units
3. For each SLR scenario, use the migration space area-based weights for each tidal complex to roll up the migration space flow alteration values to the tidal complex unit

Attribute: Migration Space Percent Future Development (2100)

Data Sources:

- Future Land Cover: Land Transformation Model (LTM) Version 3 developed by the Human-Environment Modeling and Analysis Laboratory at Purdue (Tayyebi et al. 2013)
- Secured Lands: TNC's Eastern Conservation Science team's 2013 dataset of Secured Land (Anderson et al. 2016)

Analysis Steps:

1. Select LTM 2100 land cover data (us_2100_urbv3)
2. Convert TNC internal secured lands(GAP status 1-3) to a 30-m raster, snap to LTM 2100 grid
3. Merge TNC internal secured lands GAP 1-3 on top of the future development pixels
4. Select all future development pixels (value > 95) that do not occur on secured lands
5. For each SLR scenario, tabulate area of future development for the migration space and calculate % of migration space expected to be developed in 2100
6. For each SLR scenario, use the migration space area-based weights for each tidal complex to roll up the migration space flow alteration values to the tidal complex unit